

THERMAL RADIATION HEAT TRANSFER

(ACCESSION NUMBER) **69-35817**
 (THRU) **1**
 (PAGES) **290**
 (CODE) **33**
 (CATEGORY)
 (NASA CR OR TRX OR AD NUMBER)

FACILITY FORM 888



Volume II

Radiation Exchange
Between Surfaces and in Enclosures



NASA SP-164

THERMAL RADIATION HEAT TRANSFER

Volume II

Radiation Exchange Between Surfaces and in Enclosures

John R. Howell and Robert Siegel
Lewis Research Center
Cleveland, Ohio



Scientific and Technical Information Division
OFFICE OF TECHNOLOGY UTILIZATION
NATIONAL AERONAUTICS AND SPACE ADMINISTRATION
Washington, D.C.

1969

For Sale by the Superintendent of Documents,
U.S. Government Printing Office, Washington, D.C. 20402
Price \$1.50
Library of Congress Catalog Card Number 67-62877

CONTENTS

CHAPTER		PAGE
1	INTRODUCTORY COMMENTS	1
	1.1 ENCLOSURE THEORY.....	1
	1.1.1 Ideal Enclosures.....	2
	1.1.2 Nonideal Enclosures.....	3
	1.2 ENERGY TRANSFER BY COMBINED MODES.....	4
	1.3 NOTATION.....	4
	1.4 CONCLUDING REMARKS.....	5
	REFERENCES.....	5
2	EXCHANGE OF RADIANT ENERGY BETWEEN BLACK ISOTHERMAL SURFACES	7
	2.1 INTRODUCTION.....	7
	2.2 SYMBOLS.....	8
	2.3 RADIATIVE EXCHANGE BETWEEN TWO DIFFERENTIAL AREA ELEMENTS.....	8
	2.4 RADIATIVE GEOMETRIC CONFIGURATION FACTORS AND ENERGY EXCHANGE BETWEEN TWO SURFACES.....	12
	2.4.1 Configuration Factor for Energy Exchange Between Differ- ential Elements.....	13
	2.4.1.1 Reciprocity for differential element configuration factors...	14
	2.4.1.2 Some sample configuration factors between differential elements.....	14
	2.4.2 Configuration Factor Between a Differential Element and a Finite Area.....	19
	2.4.2.1 Reciprocity for configuration factor between differential and finite areas.....	21
	2.4.2.2 Radiation interchange between differential and finite areas.....	21
	2.4.2.3 Some sample configuration factors involving a differential and a finite area.....	22
	2.4.3 Configuration Factor for Two Finite Areas.....	26
	2.4.3.1 Reciprocity for configuration factor between finite areas.....	27
	2.4.3.2 Radiation exchange between finite areas.....	28
	2.4.4 Summary of Configuration Factor and Energy Exchange Relations.....	30
	2.5 METHODS FOR EVALUATING CONFIGURATION FACTORS..	30
	2.5.1 Configuration Factor Algebra for Pairs of Surfaces.....	30
	2.5.2 Configuration Factors in Enclosures.....	39
	2.5.3 Mathematical Techniques for the Evaluation of Configuration Factors.....	42
	2.5.3.1 Hottel's crossed-string method.....	43

THERMAL RADIATION HEAT TRANSFER

CHAPTER	PAGE
2.5.3.2	46
2.5.3.2.1	47
2.5.3.2.2	52
2.5.3.3	55
2.6	59
2.7	59
2.8	64
REFERENCES	65
3	67
RADIATION EXCHANGE IN AN ENCLOSURE COMPOSED OF DIFFUSE-GRAY SURFACES	
3.1	67
3.1.1	67
3.1.2	68
3.2	69
3.3	70
3.3.1	70
3.3.1.1	77
3.3.1.2	79
3.3.2	81
3.4	83
3.4.1	83
3.4.1.1	86
3.4.1.2	88
3.4.1.3	89
3.4.2	97
3.4.2.1	97
3.4.2.2	99
3.4.2.3	102
3.4.2.4	103
3.4.2.5	104
3.5	107
REFERENCES	107
4	109
RADIATION IN ENCLOSURES HAVING SOME SPECULARLY REFLECTING SURFACES	
4.1	109
4.2	109
4.3	110
4.3.1	110
4.3.2	115
4.3.2.1	115
4.3.2.2	117
4.3.3	123

CONTENTS

CHAPTER	PAGE
4.4	NET RADIATION METHOD IN ENCLOSURES HAVING SPECULAR AND DIFFUSE SURFACES..... 129
4.4.1	Enclosures With Plane Surfaces..... 129
4.4.2	Curved Specular Reflecting Surfaces..... 139
4.5	CONCLUDING REMARKS..... 142
	REFERENCES..... 144
5	THE EXCHANGE OF THERMAL RADIATION BE- TWEEN NONDIFFUSE NONGRAY SURFACES .. 147
5.1	INTRODUCTION..... 147
5.2	SYMBOLS..... 148
5.3	ENCLOSURE THEORY FOR DIFFUSE SURFACES WITH SPECTRALLY DEPENDENT PROPERTIES..... 149
5.4	THE BAND ENERGY APPROXIMATION..... 156
5.4.1	Multiple Bands..... 157
5.4.2	The Semigray Approximations..... 160
5.5	DIRECTIONAL-GRAY SURFACES..... 162
5.6	SURFACES WITH DIRECTIONALLY AND SPECTRALLY DEPENDENT PROPERTIES..... 169
5.7	CONCLUDING REMARKS..... 175
	REFERENCES..... 175
6	THE MONTE CARLO APPROACH TO RADIANT INTERCHANGE PROBLEMS 177
6.1	INTRODUCTION..... 177
6.1.1	Definition of Monte Carlo..... 177
6.1.2	History..... 178
6.1.3	General References..... 178
6.2	SYMBOLS..... 179
6.3	DETAILS OF THE METHOD..... 180
6.3.1	The Random Walk..... 180
6.3.2	Choosing From Probability Distributions..... 181
6.3.3	Random Numbers..... 187
6.3.3.1	Definition of random numbers..... 187
6.3.3.2	How random numbers are generated..... 187
6.3.3.3	How the numbers are made sufficiently random..... 188
6.3.4	Evaluation of Error..... 188
6.4	APPLICATION TO THERMAL RADIATIVE TRANSFER..... 190
6.4.1	Introduction..... 190
6.4.2	Model of the Radiative Exchange Process..... 191
6.4.3	Sample Problem..... 191
6.4.4	Useful Functions..... 197
6.4.5	Literature on Application to Radiation Exchange Between Surfaces..... 204
6.4.5.1	Configuration factor computation..... 204
6.4.5.2	Cavity properties..... 207
6.4.5.3	Extension to directional and spectral surfaces..... 208
6.4.6	Statistical Difficulties of Monte Carlo Technique..... 209
6.4.7	Closing Remarks..... 209
	REFERENCES..... 210

THERMAL RADIATION HEAT TRANSFER

CHAPTER		PAGE
7	RADIATION IN THE PRESENCE OF OTHER MODES OF ENERGY TRANSFER	213
7.1	INTRODUCTION.....	213
7.2	SYMBOLS.....	215
7.3	PROBLEMS INVOLVING COMBINED RADIATION AND CONDUCTION.....	217
7.3.1	Uncoupled Problems.....	217
7.3.2	Coupled Nonlinear Problems.....	218
7.4	RADIATION AND CONVECTION.....	227
7.5	RADIATION COMBINED WITH BOTH CONDUCTION AND CONVECTION.....	232
7.6	COMPUTER PROGRAMS FOR MULTIMODE ENERGY TRANSFER.....	237
7.7	CONCLUDING REMARKS.....	237
	REFERENCES.....	238
	APPENDIXES	
A	DIFFUSE CONFIGURATION FACTORS.....	241
B	ENCLOSURE ANALYSIS METHOD OF GEBHART.....	277
C	CONVERSION FACTORS.....	279
	INDEX	283

Chapter 1. Introductory Comments

The study of radiation interchange between individual surface elements in a system is required in a variety of engineering disciplines including applied optics, illumination engineering, and heat transfer. Indeed, such studies have been conducted for many years as evidenced by the publication dates of references 1 and 2. More recently the study of radiant interchange has been given impetus by technological advances that have resulted in systems where thermal radiation can be a very significant factor. Some examples are satellite temperature control, energy leakage into cryogenic vacuum systems, high-temperature phenomena in hypersonic flight, and the heat transfer in nuclear propulsion systems.

1.1 ENCLOSURE THEORY

In this volume the theory will be developed for computing thermal radiation exchanges within enclosures. First it must be understood what is meant by an enclosure. Any surface can be considered as completely surrounded by an envelope of other solid surfaces or open areas. This envelope is the enclosure for the surface; thus an enclosure accounts for all directions surrounding the surface. By considering the radiation going from the surface to all parts of the enclosure, and the radiation arriving at the surface from all parts of the enclosure, it is assured that all the radiative contributions are accounted for. In working a problem, a convenient enclosure will usually be evident from the physical configuration. An opening can be considered as a plane of zero reflectivity. It will also act as a source of radiation when radiation is entering the enclosure from the environment.

All the enclosures considered here will be subject to the assumption that the medium in the space between the surfaces is perfectly transparent and thus does not participate in the radiative interchange. For an enclosure filled with a radiating material such as a gas containing water vapor, carbon dioxide, or smoke, the theory will be treated in volume III of this series.

Reference 3, which is volume I of this series, discusses in detail the radiative properties of solid surfaces. It was demonstrated that for some materials there are substantial variations of properties with wavelength, surface temperature, and direction. For radiation computations within enclosures, the geometric effects governing how much radiation from one surface reaches another is a complication in addition to the variations

of the surface properties. For simple geometries it may be possible to account in detail for property variations without the problem becoming unduly complex. As the geometry becomes more involved, it is often necessary to invoke more idealizations of the surface properties in order that the problem can be solved with reasonable effort.

The treatment presented here could begin with the most general situation where properties vary with wavelength, temperature, and direction, and where the radiation fluxes vary arbitrarily over the enclosure surfaces. All other situations would then be simplified special cases. However, this would entail the uninitiated reader plunging into the most complex treatment, which would be very difficult to understand. Hence the development presented here will begin with the most simple situation; successive complexities will then be added to build more comprehensive treatments.

1.1.1 Ideal Enclosures

The greatest simplification is to assume that all the enclosure surfaces are black. In this instance there is no reflected radiation to be accounted for. Also, all the emitted energy is diffuse; that is, the intensity leaving a given isothermal surface is independent of direction. The exchange theory for a black enclosure is presented in chapter 2. The heat balances involve the enclosure geometry, which governs how much radiation leaving a surface will reach another surface. The geometric effects are expressed in terms of diffuse configuration factors; these factors are the fractions of radiation leaving a surface that reach another surface. The factors are derived on the basis that the directional distribution of radiation leaving a surface is diffuse and uniformly distributed, and these restrictions should be kept in mind when the factors are applied in nonblack enclosures.

The computation of configuration factors involves integration over the solid angles by which the surfaces can view each other. Since these integrations are often tedious, it is desirable to use certain useful relations that exist between configuration factors. By using these relations, the desired factor can often be obtained from factors that are already known, and the integration will not have to be performed. These relations, along with various shortcut methods that can be used to obtain configuration factors, are presented in detail in chapter 2. An appendix is also provided giving references where configuration factors can be found for approximately 150 different geometrical configurations.

After analyzing the black enclosure, the next step of complexity is an enclosure with gray surfaces that emit and reflect diffusely. It is also assumed that both the emitted and reflected energies are uniform over

each surface. For these conditions the diffuse configuration factors found for black surfaces still apply for the radiation leaving a surface. For gray surfaces, reflections between surfaces must be accounted for. This is done in chapter 3 by using a method developed by Poljak.

Another type of ideal surface is a perfect mirror reflector. The emission from this type of surface is approximated as being diffuse; hence, the emitted energy is treated by using the diffuse configuration factors. The reflected energy, however, is followed within the enclosure by using the characteristics of a mirror where the angle of reflection is equal in magnitude to the angle of incidence. The method of tracing the reflected radiation paths and deriving the necessary heat balances is treated in chapter 4.

1.1.2 Nonideal Enclosures

In some instances the black or diffuse-gray approximations are inadequate and directional and/or spectral effects must be considered. The necessity of treating spectral effects was noticed quite early in the field of radiative transfer. In the remarkable paper (ref. 4) published in 1800 by Sir William Herschel entitled "Investigation of the Powers of the Prismatic Colours to Heat and Illuminate Objects; with Remarks, that prove the Different Refrangibility of Radiant Heat to which is added, an Inquiry into the Method of Viewing the Sun Advantageously, with Telescopes of large Apertures and High Magnifying Powers." appears the following statement: "In a variety of experiments I have occasionally made, relating to the method of viewing the sun, with large telescopes, to the best advantage, I used various combinations of differently coloured darkening glasses. What appeared remarkable was, that when I used some of them, I felt a sensation of heat, though I had but little light; while others gave me much light, with scarce any sensation of heat. Now, as in these different combinations, the suns image was also differently coloured, it occurred to me, that the prismatic rays might have the power of heating bodies very unequally distributed among them. . . ." This paper was the first in which what is now called the infrared region of the spectrum was defined and the energy radiated as "heat" shown to be of different wavelengths than those for "light."

The quotation shows an awareness that in some instances spectral effects must be included in the radiative analysis. The performance of spectrally selective surfaces such as are used in satellite temperature control and for solar collector surfaces can be understood only by considering the wavelength variations of the surface properties.

A second nonideal surface property is that of strong directional dependence. In volume I of this work (ref. 3), a number of directionally

dependent surface properties were examined, and some were shown to differ considerably from the diffuse or specular approximations. A good example is the lunar surface, which has a distribution of reflected energy strongly peaked back into the direction of incident radiation. This is in a sense the opposite of a specular reflector and can certainly not be considered diffuse.

Methods for treating surfaces that are nonideal in either spectral or directional properties, or both, are examined in chapters 5 and 6. Chapter 5 continues the enclosure theory development of the previous chapters. Chapter 6 deals with an alternate approach—the Monte Carlo method. This is a general technique that involves following “bundles” of radiant energy along their paths within an enclosure. It can be applied to all types of radiation problems but is usually too detailed and costly in terms of computer time for use in simple situations. When directional and spectral effects must be considered, the Monte Carlo method is very valuable.

1.2 ENERGY TRANSFER BY COMBINED MODES

Chapter 7 deals with problems where conduction and/or convection is combined with radiative heat transfer. Since only opaque surfaces are being dealt with here, the radiative interaction with a body is considered to occur only at the surface. Thus the radiation serves only as a boundary condition with regard to the conduction process within a body. This is analogous to the convective boundary condition at a surface. When a body is undergoing a transient temperature change, the radiative terms are applied at each instant when solving the energy balances governing the temperature distribution within the body.

The heat conduction process is governed by local derivatives of the first power of the temperature. The convection process depends on local differences between the first power of the fluid and surface temperatures. Radiative exchange, however, depends approximately on differences of fourth powers of the surface temperatures and also depends on the integral of the radiation incident from all the surroundings of the surface. As a result, the energy balance for a combined convection, conduction, and radiation problem can result in an integrodifferential equation. There are few standard mathematical methods for attacking these equations, and few closed-form analytical solutions are available. Numerical methods are usually employed for multimode problems.

1.3 NOTATION

The notation employed here is the same as in volume I of this pub-

lication (ref. 3) and is now briefly reviewed. A prime denotes a directional quantity, while a λ subscript specifies that the quantity is spectral; for example, ϵ'_λ is the directional spectral emissivity. Certain quantities such as bidirectional reflectivities can depend on two directions, that is, the directions of the incoming and outgoing radiation. These bidirectional quantities are denoted by a double prime. A hemispherical quantity will not have a prime, and a total quantity will not have a λ subscript; thus ϵ is the hemispherical total emissivity. In addition a notation such as $\epsilon'_\lambda(\lambda, \beta, \theta, T)$ can be used to emphasize the functional dependencies or to state more specifically at what wavelength, angle, and surface temperature the quantity is being evaluated.

Additional notation is needed for the energy rate Q for a finite area in order to keep consistent mathematical forms for energy balances. The quantity $d^2Q'_\lambda$ is directional-spectral, and the second derivative is used to indicate that the energy is of differential order in both wavelength and solid angle. The quantities dQ' and dQ_λ are of differential order with respect to solid angle and wavelength, respectively. If a differential area is involved, the order of the derivative is correspondingly increased.

1.4 CONCLUDING REMARKS

As mentioned previously, certain restrictions to ideal surfaces and nonparticipating media are present in each of the chapters that follow. In addition, some phenomena that are rather more specialized than is the intent of this work can be of importance in certain situations. For example, effects of polarization can lead to errors in energy transfer calculations if ignored under special conditions of geometry (ref. 5). Interference effects (ref. 6), chemical and photochemical phenomena (refs. 7 to 10), and perhaps others can in some situations be the dominant mechanisms governing the radiative transfer. The reader can only be referred to the specialized literature and warned to watch for such cases.

REFERENCES

1. CHARLES, M.: *Les Manuscrits de Leonard de Vinci*, Manuscripts C, E, and K de la Bibliothèque de l'Instituté Publiés en Facsimilés Phototypiques, Ravisson-Mollien, Paris, 1888. (Referenced in Middleton, W. E. Knowles: Note on the Invention of Photometry. *Am. J. Phys.*, vol. 31, no. 3, Mar. 1963, pp. 177-181.)
2. FRANCOIS D'AGUILLON, S. J.: *Opticorum Libri Sex*. Antwerp, 1613. (Referenced in Middleton, W. E. Knowles: Note on the Invention of Photometry. *Am. J. Phys.*, vol. 31, no. 3, Mar. 1963, pp. 177-181.)
3. SIEGEL, ROBERT; AND HOWELL, JOHN R.: *Thermal Radiation Heat Transfer*. I—The Blackbody, Electromagnetic Theory, and Material Properties. NASA SP-164, 1968.
4. HERSCHEL, WILLIAM: Investigation of the Powers of the Prismatic Colours to Heat and Illuminate Objects. *Trans. Roy. Soc. (London)*, vol. 90, pt. II, 1800, pp. 255-283.

5. EDWARDS, D. K.; AND TOBIN, R. D.: Effect of Polarization on Radiant Heat Transfer through Long Passages. *J. Heat Transfer*, vol. 89, no. 2, May 1967, pp. 132-138.
6. CRAVALHO, E. G.; TIEN, C. L.; AND CAREN, R. P.: Effect of Small Spacings on Radiative Transfer between two Dielectrics. *J. Heat Transfer*, vol. 89, no. 4, Nov. 1967, pp. 351-358.
7. GARLICK, G. F. J.: Luminescence in Solids. *Sci. Prog.*, vol. 52, Jan. 1964, pp. 3-25.
8. PRINGSHEIM, PETER: Fluorescence and Phosphorescence. Interscience Publ., 1949.
9. CURIE, DANIEL (G. F. J. GARLICK, TRANS.): Luminescence in Crystals. John Wiley & Sons, Inc., 1963.
10. BOWEN, E. J.; AND GARLICK, G. F. J.: Luminescence. *Int. Sci. Tech.*, no. 56, Aug. 1966, pp. 18-29.

Chapter 2. Exchange of Radiant Energy Between Black Isothermal Surfaces

2.1 INTRODUCTION

This chapter begins the discussion of radiation exchange between surfaces and is concerned with the special situation where all the surfaces involved are black. Black surfaces are chosen to deal with first since they are perfect absorbers, and the energy exchange process is thus simplified because there is no reflected energy to be considered. Also, all black surfaces emit in a perfectly diffuse fashion where the radiation intensity leaving a surface is independent of the direction of emission. This simplifies the computation of how much of this radiation will reach another surface.

The fraction of the radiation leaving one surface that reaches another surface is defined as the geometric configuration factor between the two surfaces because it depends on the geometric orientation of the surfaces with respect to each other. The geometric dependence is discussed here for black surfaces, but the results have a wider generality as they will apply for any uniform diffuse radiation leaving a surface. This geometric dependence leads to some algebraic relations between the factors, and these relations are demonstrated in this chapter for various surface configurations. In table A-I of appendix A, a tabulation is provided of references where known configuration factors can be found in the literature. Applications of these factors to example problems of engineering interest are then examined for radiative energy exchange between two surfaces.

After the relations for exchange between two surfaces have been developed, the relations can be applied to any number of surfaces arranged to form an enclosure of black surfaces each at a different temperature. The general set of equations governing the exchange within such an enclosure is developed, and some illustrative examples are provided.

In chapter 3 the concepts developed in this chapter are extended for use in systems with diffuse-gray surfaces, and succeeding chapters introduce more and more complex systems. The concepts of the present chapter are discussed at some length because they are fundamental to the succeeding material dealing with less ideal surfaces.

2.2 SYMBOLS

A	area
e	emissive power
f	function defined by eq. (2-49b)
F	configuration factor
i	intensity
l, m, n	direction cosines, eq. (2-49a)
N	number of surfaces in an enclosure
P, Q, R	functions in contour integration used in section 2.5.3.2
Q	energy per unit time
r	radius
S	distance between two differential elements
T	temperature
U	number of unknowns in equations describing an N-sided enclosure
x, y, z	Cartesian coordinate positions
α, γ, δ	angles in direction cosines
β	angle from normal
λ	wavelength
σ	Stefan-Boltzmann constant
ω	solid angle

Subscripts:

b	blackbody
$d1, d2$	evaluated at differential element $d1$ or $d2$
i	inner
j, k	j^{th} or k^{th} surface
N	N^{th} surface
<i>ring</i>	ring area
s	Sun
<i>strip</i>	elemental strip
λ	wavelength dependent
1, 2	at area 1 or 2

Superscript:

denotes quantity is in one direction

2.3 RADIATIVE EXCHANGE BETWEEN TWO DIFFERENTIAL AREA ELEMENTS

The relations describing radiative exchange between differential elements are considered first as they will be used in the succeeding sections to derive the relations for exchange between areas of finite size. Consider two differential black area elements as shown in figure 2-1. The elements

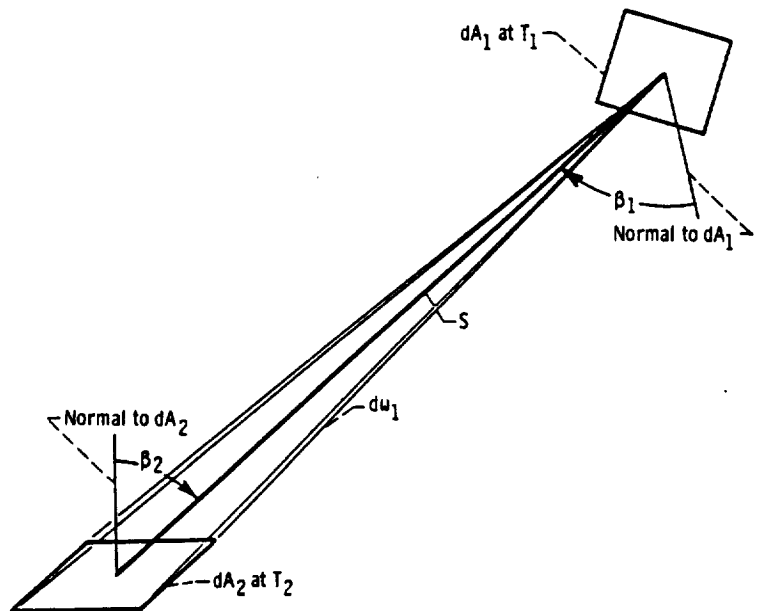


FIGURE 2-1. — Radiative interchange between two black differential area elements.

dA_1 and dA_2 are isothermal at temperatures T_1 and T_2 , respectively, are arbitrarily oriented, and have their normals at angles β_1 and β_2 to the line of length S joining them.

Using the notation of reference 1 (which will be referred to from this point as Vol. I), the total energy per unit time leaving dA_1 and incident upon dA_2 is

$$d^2Q'_{d_1-d_2} = i'_{b,1} dA_1 \cos \beta_1 d\omega_1 \quad (2-1)$$

where $d\omega_1$ is the solid angle subtended by dA_2 when viewed from dA_1 . Equation (2-1) follows directly from the definition of $i'_{b,1}$, the total black-body intensity of surface 1, as the total energy emitted by surface 1 per unit time, per unit of area dA_1 projected normal to S , and per unit of solid angle. As in Vol. I, the prime indicates a quantity applied in a single direction. The quantity d^2Q' is a second differential to denote the dependence upon two differential quantities, dA_1 and $d\omega_1$.

Equation (2-1) can also be written for radiation at only one wavelength

$$d^3Q'_{\lambda, d_1-d_2} = i'_{\lambda b, 1}(\lambda) d\lambda dA_1 \cos \beta_1 d\omega_1$$

The total radiation quantities are then found by integrating over all wavelengths

$$d^2Q'_{d_1-d_2} = \int_{\lambda=0}^{\infty} d^3Q'_{\lambda, d_1-d_2} = dA_1 \cos \beta_1 d\omega_1 \int_0^{\infty} i'_{\lambda b, 1}(\lambda) d\lambda$$

For a black surface $i'_{\lambda b}(\lambda)$ does not depend on direction; hence, all the geometric factors can be removed from under the integral sign, and the integration over wavelength is independent of any geometrical considerations. Thus the geometric configuration factors that follow apply for both spectral and total quantities. For simplicity in not having to carry the λ notation, the discussion will be carried out for total quantities.

The solid angle $d\omega_1$ is related to the projected area of dA_2 and the distance between the differential elements by the relation

$$d\omega_1 = \frac{dA_2 \cos \beta_2}{S^2} \quad (2-2)$$

Substituting this relation into equation (2-1) gives the following equation for the total energy per unit time leaving dA_1 that is incident upon dA_2 :

$$d^2Q'_{d_1-d_2} = \frac{i'_{b,1} dA_1 \cos \beta_1 dA_2 \cos \beta_2}{S^2} \quad (2-3)$$

An analogous derivation for the radiation leaving dA_2 that arrives at dA_1 results in

$$d^2Q'_{d_2-d_1} = \frac{i'_{b,2} dA_2 \cos \beta_2 dA_1 \cos \beta_1}{S^2} \quad (2-4)$$

For later use, d^2Q' has been defined in equations (2-3) and (2-4) as the energy emitted by one element that is *incident* upon the second element. For the special case of a black receiving element, all incident energy is absorbed so that equations (2-3) and (2-4) in this case give the energy from one element that is *absorbed* by the second. As will be seen, the more general definition of d^2Q' allows the configuration factors derived here for black surfaces to be used in certain other cases. These will be examined at length in chapters 3 and 4.

The *net* energy per unit time $d^2Q'_{d_1 \rightleftharpoons d_2}$ exchanged from black element dA_1 to dA_2 along path S is then the difference of $d^2Q'_{d_1-d_2}$ and $d^2Q'_{d_2-d_1}$, or from equations (2-3) and (2-4)

$$d^2Q'_{d_1 \rightleftharpoons d_2} = d^2Q'_{d_1-d_2} - d^2Q'_{d_2-d_1} = (i'_{b,1} - i'_{b,2}) \frac{\cos \beta_1 \cos \beta_2}{S^2} dA_1 dA_2 \quad (2-5)$$

From equation (2-21) of Vol. I, the blackbody total intensity is related to the blackbody total hemispherical emissive power by

$$i'_b = \frac{e_b}{\pi} = \frac{\sigma T^4}{\pi} \quad (2-6)$$

so that equation (2-5) can be written as

$$d^2Q'_{d_1 \rightarrow d_2} = \sigma(T_1^4 - T_2^4) \frac{\cos \beta_1 \cos \beta_2}{\pi S^2} dA_1 dA_2 \quad (2-7)$$

EXAMPLE 2-1: The Sun emits energy at a rate that can be approximated by that of a blackbody at temperature 10 400° R. A blackbody area element in orbit around the Sun at the mean radius of the Earth's orbit (92.9×10^6 mi) is oriented normal to the line connecting the centers of the area element and Sun. If the Sun's radius is 4.32×10^5 miles, what energy flux is incident upon the element?

To the element in orbit, the Sun appears as an isothermal disk element of area

$$dA_1 = \pi r_s^2 = \pi(4.32 \times 10^5)^2 = 5.86 \times 10^{11} \text{ mi}^2$$

From equation (2-3), the incident energy flux on the element in orbit is

$$\begin{aligned} \frac{d^2Q'_{d_1 \rightarrow d_2}}{dA_2} &= i'_{b,1} dA_1 \frac{\cos \beta_1 \cos \beta_2}{S^2} = \frac{\sigma T_s^4}{\pi} \frac{dA_1}{S^2} \\ &= \frac{0.173 \times 10^{-8} (1.04 \times 10^4)^4}{\pi} \frac{5.86 \times 10^{11}}{(92.9 \times 10^6)^2} = 437 \text{ Btu/(hr)(ft}^2\text{)} \end{aligned}$$

This value is consistent with the range of measured values of the mean solar constant, 420 to 454 Btu/(hr)(ft²).

EXAMPLE 2-2: As shown in figure 2-2, a black square of side 0.1 inch is at temperature 1500° F and is near a tube 0.1 inch in diameter. The opening of the tube acts as a black surface, and the tube is at 800° F. What is the net radiation exchange along the connecting path S between the square and the tube opening?

From equation (2-7)

$$d^2Q'_{d_1 \rightarrow d_2} = \sigma(T_1^4 - T_2^4) \frac{\cos \beta_1 \cos \beta_2}{\pi S^2} dA_1 dA_2$$

The value of $\cos \beta_1$ is found from the known sides of the right triangle $dA_2 - 0 - dA_1$ as

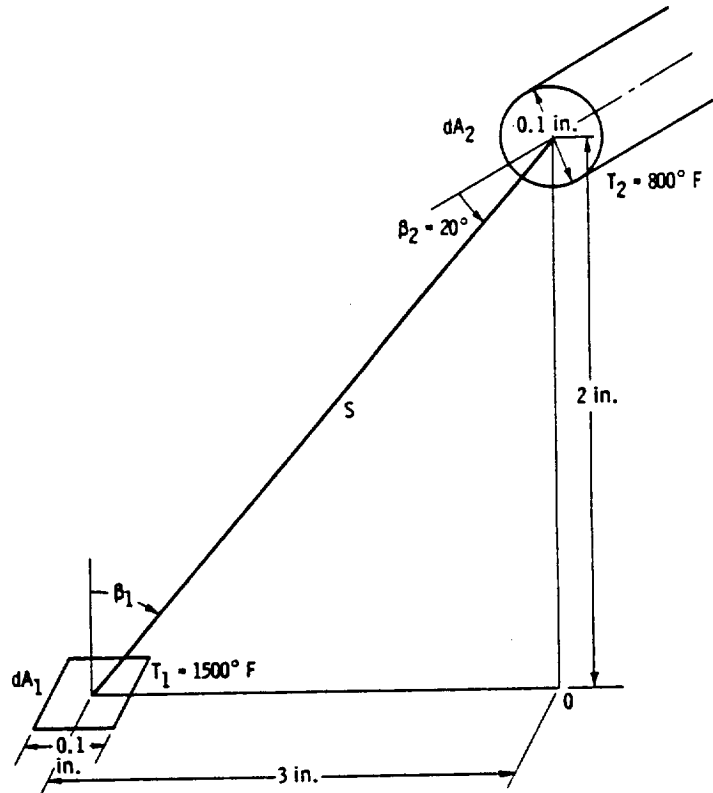


FIGURE 2-2.—Radiative exchange between square element and circular tube opening.

$$\cos \beta_1 = 2 / [(3)^2 + (2)^2]^{1/2} = 2 / (13)^{1/2}$$

The other factors in the energy exchange equation are given, and substituting them gives

$$\begin{aligned} d^2 Q'_{d_1 \rightarrow d_2} &= 0.173 \times 10^{-8} [(1960)^4 - (1260)^4] \frac{2}{(13)^{1/2}} \frac{\cos 20^\circ}{\pi(13/144)} \\ &\times \left[\frac{(0.1)^2}{144} \right] \left[\frac{\pi(0.1)^2}{4 \times 144} \right] \\ &= 1.48 \times 10^{-4} \text{ Btu/hr} \end{aligned}$$

2.4 RADIATIVE GEOMETRIC CONFIGURATION FACTORS AND ENERGY EXCHANGE BETWEEN TWO SURFACES

One of the chief mathematical complexities in treating radiative transfer between surfaces is accounting for the geometric relations

involved in how the surfaces view each other. These effects result mathematically in integrations of the radiative interchange over the finite areas involved in the exchange process. It would be helpful to have, as much as possible, handbook results to account for these geometric relations for often-encountered geometries. In this way repetitions of the tedious integrations could be avoided.

In this section, a method of accounting for the geometry is introduced in the form of a quantity called the *geometric configuration factor*. Such factors allow computation of radiative transfer in many systems by referring to formulas or tabulated data which have been previously obtained for the geometric relations between various surfaces. This removes what is often the most time-consuming and error-prone portion of the analysis.

2.4.1 Configuration Factor for Energy Exchange Between Differential Elements

The *fraction* of energy leaving black surface element dA_1 that arrives at black element dA_2 is defined as the *geometric configuration factor* $dF_{d_1-d_2}$. (Either the total or spectral energy could be considered as discussed with regard to equation (2-1), and the same results for dF would be obtained. The total energy is used here for convenience in not carrying the λ notation.) Using equations (2-3) and (2-6), the previous definition gives

$$\begin{aligned} dF_{d_1-d_2} &= \frac{d^2 Q'_{d_1-d_2}}{\sigma T_1^4 dA_1} = \frac{\sigma T_1^4 \frac{\cos \beta_1 \cos \beta_2}{\pi S^2} dA_1 dA_2}{\sigma T_1^4 dA_1} \\ &= \frac{\cos \beta_1 \cos \beta_2}{\pi S^2} dA_2 \end{aligned} \quad (2-8)$$

where $\sigma T_1^4 dA_1$ is the total energy leaving dA_1 within the entire hemispherical solid angle over dA_1 . Equation (2-8) shows that $dF_{d_1-d_2}$ depends only upon the size of dA_2 and its orientation with respect to dA_1 . By substituting equation (2-2), equation (2-8) can also be written in the form

$$dF_{d_1-d_2} = \frac{\cos \beta_1 d\omega_1}{\pi} \quad (2-9)$$

Consequently, all elements dA_2 have the same configuration factor if they subtend the same solid angle $d\omega_1$ when viewed from dA_1 and are positioned along a path at angle β_1 with respect to the normal of dA_1 .

The factor $dF_{d_1-d_2}$ has a variety of names, being called the view, angle, shape, interchange, exchange, or configuration factor. The last seems

most specific, implying a dependence upon both orientation and shape, the latter variable entering when finite areas are involved.

The notation used here for configuration factors is based on subscript designation for the types of areas involved in the energy exchange and a derivative notation consistent with the mathematical meaning of the configuration factor. For the subscript notation, $d1$, $d2$, and so forth will indicate differential area elements, while 1, 2, and so forth will indicate areas of finite size. Thus dF_{d1-d2} indicates a factor between two differential elements, as in equation (2-8). The notation dF_{1-d2} indicates a configuration factor from finite area A_1 to differential area dA_2 .

The derivative notation dF indicates that the configuration factor is for energy transfer to a differential element, as in equation (2-8). This is redundant with the subscript notation, but keeps the mathematical form of equations (such as eq. (2-8)) consistent in that a differential quantity appears on both sides (i.e., the expression for dF contains a differential area). A configuration factor F denotes a factor to a finite area. Thus F_{d1-2} is the configuration factor from differential element dA_1 to finite area A_2 .

2.4.1.1 *Reciprocity for differential element configuration factors.*— By a derivation similar to that used in obtaining equation (2-8), the configuration factor needed for calculating energy exchange from element dA_2 to dA_1 is

$$dF_{d2-d1} = \frac{\cos \beta_1 \cos \beta_2}{\pi S^2} dA_1 \quad (2-10)$$

Dividing equation (2-8) by equation (2-10) gives the *general reciprocity relation*

$$dF_{d1-d2} dA_1 = dF_{d2-d1} dA_2 = \frac{\cos \beta_1 \cos \beta_2}{\pi S^2} dA_1 dA_2 \quad (2-11)$$

Finally, equation (2-7) for energy exchange along the path between two black elements can be written by using equation (2-11); the result is

$$d^2 Q'_{d1-d2} = \sigma (T_1^4 - T_2^4) dF_{d1-d2} dA_1 = \sigma (T_1^4 - T_2^4) dF_{d2-d1} dA_2 \quad (2-12)$$

2.4.1.2 *Some sample configuration factors between differential elements.*— To this point, a series of algebraic manipulations has allowed a reduction of the equation for the net radiative transfer along the path between two black isothermal area elements to the apparently simple form of equation (2-12). This was done by introduction of the configuration factor dF which encompasses the geometric complexities.

The derivation of configuration factors will now be illustrated by considering some sample cases.

EXAMPLE 2-3: The two elemental areas shown in figure 2-3 are located on strips that have parallel generating lines. Derive an expression for the configuration factor between dA_1 and dA_2 .

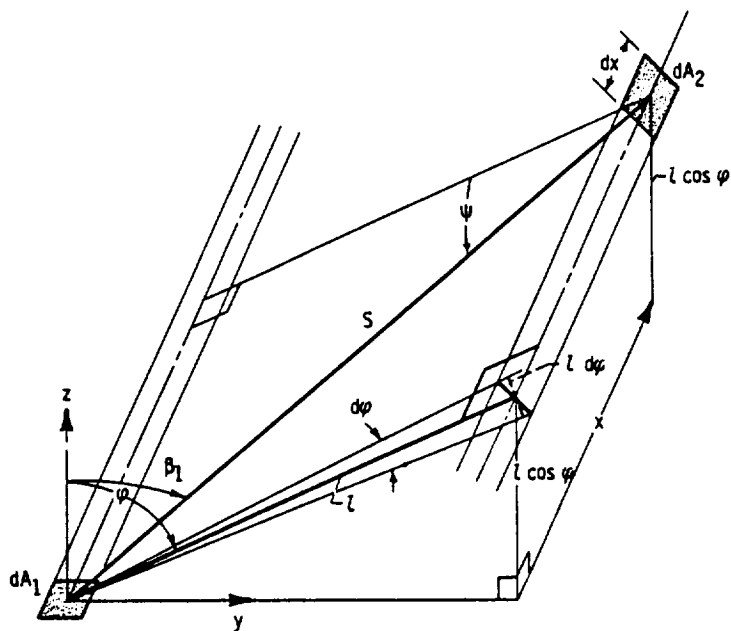


FIGURE 2-3.—Geometry for configuration factor between elements on strips formed by parallel generating lines.

The distance S can be expressed as

$$S^2 = l^2 + x^2$$

and $\cos \beta_1$ is then

$$\cos \beta_1 = \frac{l \cos \varphi}{S} = \frac{l \cos \varphi}{(l^2 + x^2)^{1/2}}$$

The solid angle subtended by dA_2 , when viewed from dA_1 , is

$$\begin{aligned}
 d\omega_1 &= \frac{(\text{projected area of } dA_2)}{S^2} \\
 &= \frac{(\text{projected width of } dA_2)(\text{projected length of } dA_2)}{S^2} \\
 &= \frac{(l \, d\varphi)(dx \cos \psi)}{S^2} = \frac{l \, d\varphi \, dx}{S^2} \frac{l}{S}
 \end{aligned}$$

Substituting into equation (2-9) gives

$$\begin{aligned}
 dF_{a_1-a_2} &= \frac{\cos \beta_1 \, d\omega_1}{\pi} = \frac{l \cos \varphi}{(l^2 + x^2)^{1/2}} \frac{1}{\pi} \frac{l^2 \, d\varphi \, dx}{(l^2 + x^2)^{3/2}} \\
 &= \frac{l^3 \cos \varphi \, d\varphi \, dx}{\pi(l^2 + x^2)^2}
 \end{aligned}$$

which is the desired configuration factor between dA_1 and dA_2 .

EXAMPLE 2-4: Find the configuration factor between an elemental area and an infinitely long strip of differential width oriented as in

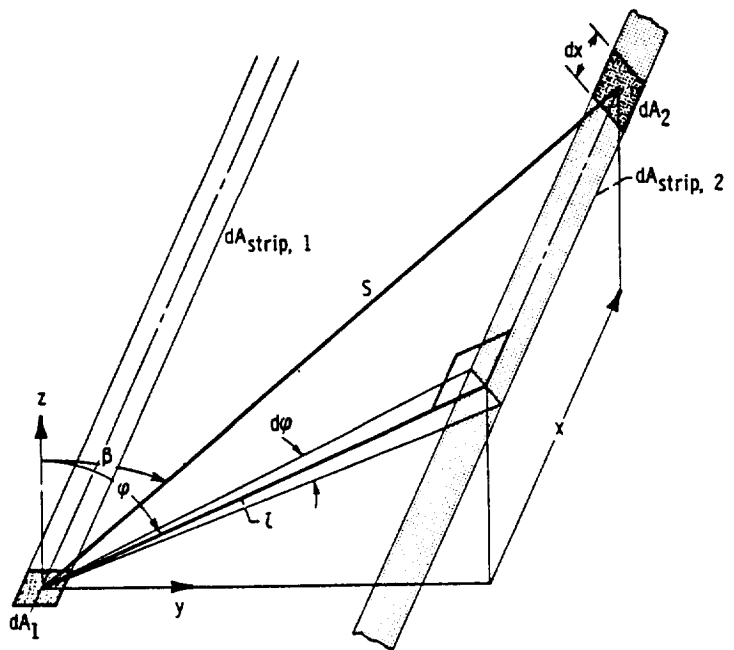


FIGURE 2-4.—Geometry for configuration factor between elemental area and infinitely long strip of differential width; area and strip are on parallel generating lines.

figure 2-4, so that the generating lines of dA_1 and $dA_{strip, 2}$ are parallel.

Example 2-3 gave the configuration factor between differential element dA_1 and area element dA_2 of length dx as

$$dF_{d1-d2} = \frac{l^3 \cos \varphi d\varphi dx}{\pi(l^2 + x^2)^2}$$

To find the factor when dA_2 becomes an infinite strip as in figure 2-4, integrate over all x to obtain

$$\begin{aligned} dF_{d1-strip, 2} &= \frac{l^3 \cos \varphi d\varphi}{\pi} \int_{-\infty}^{\infty} \frac{dx}{(l^2 + x^2)^2} \\ &= \frac{l^3 \cos \varphi d\varphi}{\pi} \left[\frac{x}{2l^2(l^2 + x^2)} + \frac{1}{2l^3} \tan^{-1} \left(\frac{x}{l} \right) \right]_{-\infty}^{\infty} \\ &= \frac{\cos \varphi d\varphi}{2} = \frac{1}{2} d(\sin \varphi) \end{aligned}$$

where the angle φ is in the $y-z$ plane. This useful configuration factor relation will be used in later examples.

Figure 2-4 also shows that, if element dA_1 lies on an infinite strip $dA_{strip, 1}$ with elements parallel to $dA_{strip, 2}$, the configuration factor

$$dF_{d1-strip, 2} = \frac{1}{2} d(\sin \varphi)$$

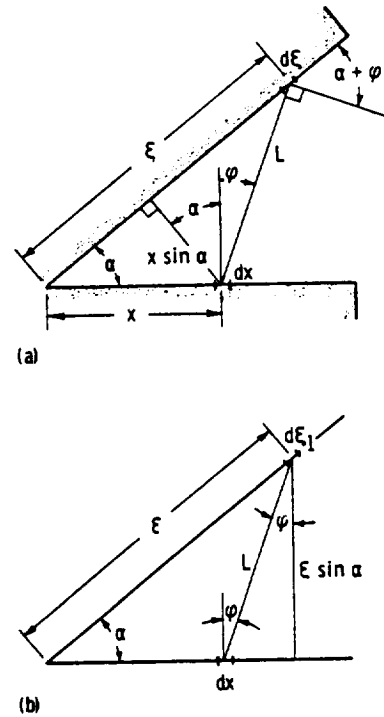
will be valid for dA_1 , regardless of where dA_1 lies on $dA_{strip, 1}$. Then, since any element dA_1 on $dA_{strip, 1}$ has the same fraction of its energy reaching $dA_{strip, 2}$, it follows that the fraction of energy from the *entire* $dA_{strip, 1}$ that reaches $dA_{strip, 2}$ is the same as the fraction for each element dA_1 . Thus, the configuration factor between two infinitely long strips of differential width and having parallel generating lines must also be the same as for element dA_1 to $dA_{strip, 2}$, or $\frac{1}{2}d(\sin \varphi)$. The angle φ is always in a plane normal to the generating lines of both strips.

EXAMPLE 2-5: Consider an infinitely long wedge-shaped groove as shown in cross section in figure 2-5. Determine the configuration factor between the differential strips dx and $d\xi$ in terms of x , ξ , and α .

As discussed in example 2-4, the configuration factor is given by

$$dF_{dx-d\xi} = \frac{1}{2} d(\sin \varphi) = \frac{1}{2} \cos \varphi d\varphi$$

From the construction in figure 2-5(b)



(a) Wedge-shaped groove geometry.
 (b) Auxiliary construction.

FIGURE 2-5. — Configuration factor between two strips on sides of wedge groove.

$$\cos \varphi = \frac{\xi \sin \alpha}{L}$$

The quantity $d\varphi$ is the angle subtended by the projection of $d\xi$ normal to L , that is,

$$d\varphi = \frac{d\xi \cos(\alpha + \varphi)}{L} = \frac{d\xi x \sin \alpha}{L L}$$

From the law of cosines

$$L^2 = x^2 + \xi^2 - 2x\xi \cos \alpha$$

Then

$$dF_{dA_1-dA_2} = \frac{1}{2} \cos \varphi d\varphi = \frac{1}{2} \frac{x\xi \sin^2 \alpha}{L^3} d\xi$$

$$= \frac{1}{2} \frac{x\xi \sin^2 \alpha}{(x^2 + \xi^2 - 2x\xi \cos \alpha)^{3/2}} d\xi$$

2.4.2 Configuration Factor Between a Differential Element and a Finite Area

Consider now an isothermal black element dA_1 at temperature T_1 exchanging energy with a surface of finite area A_2 that is isothermal at temperature T_2 as shown in figure 2-6. The relations developed for exchange between differential elements must be extended to permit A_2 to be finite. Figure 2-6 shows (compare the solid and dashed cases) that the angle β_2 will be different for different positions on A_2 and that β_1 and S will also vary as different differential elements on A_2 are viewed from dA_1 .

There are two configuration factors to be considered. The factor $F_{dA_1-A_2}$ is from the differential area dA_1 to the finite area A_2 , and $dF_{A_2-dA_1}$ is from A_2 to dA_1 . Each of these will be considered by using the definition of configuration factor as the fraction of energy leaving one surface that

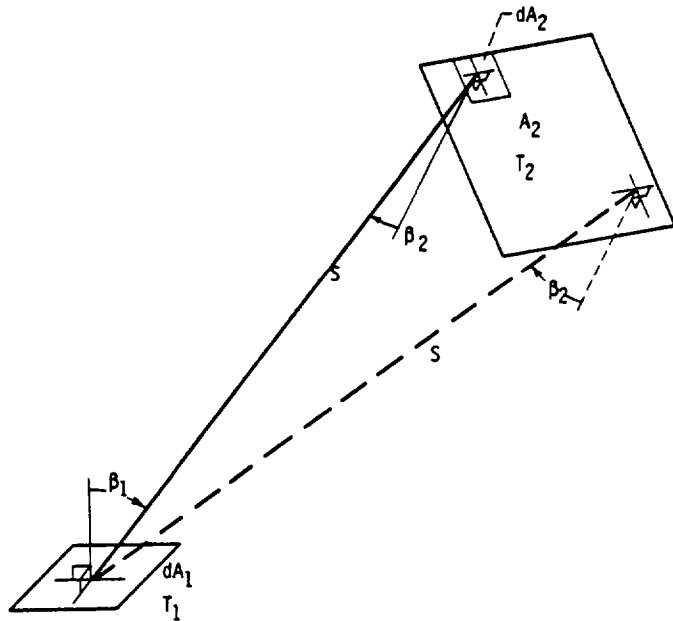


FIGURE 2-6. — Radiant interchange between differential element and finite area.

reaches the second surface. To derive F_{d1-2} , note that the total energy radiated from the black surface element dA_1 is $dQ_1 = \sigma T_1^4 dA_1$. The energy reaching dA_2 located on A_2 is

$$d^2Q'_{d1-d2} = \sigma T_1^4 \frac{\cos \beta_1 \cos \beta_2}{\pi S^2} dA_1 dA_2$$

Then integrating over A_2 to obtain the energy reaching all of A_2 , and dividing by the total energy leaving dA_1 result in

$$\begin{aligned} F_{d1-2} &= \frac{\int_{A_2} d^2Q'_{d1-d2}}{dQ_1} = \frac{\int_{A_2} \sigma T_1^4 \frac{\cos \beta_1 \cos \beta_2 dA_1}{\pi S^2} dA_2}{\sigma T_1^4 dA_1} \\ &= \int_{A_2} \frac{\cos \beta_1 \cos \beta_2}{\pi S^2} dA_2 \end{aligned} \quad (2-13)$$

where the integration limits on A_2 extend over only the portion that can be viewed by dA_1 . From equation (2-8) the quantity inside the integral of equation (2-13) is dF_{d1-d2} , so that F_{d1-2} can also be written as

$$F_{d1-2} = \int_{A_2} dF_{d1-d2} \quad (2-14)$$

This merely expresses the fact that the fraction of the energy reaching A_2 is the sum of the fractions that reach all of the parts of A_2 .

Now consider the configuration factor from the finite area A_2 to the elemental area dA_1 . The energy reaching an elemental area dA_1 from a finite area A_2 is, by integrating equation (2-4) over A_2 ,

$$dQ_{2-d1} = dA_1 \int_{A_2} i_{b,2} \frac{\cos \beta_1 \cos \beta_2}{S^2} dA_2 = dA_1 \int_{A_2} \sigma T_2^4 \frac{\cos \beta_1 \cos \beta_2}{\pi S^2} dA_2 \quad (2-15)$$

The total hemispherical energy leaving A_2 is

$$Q_2 = \int_{A_2} \sigma T_2^4 dA_2 \quad (2-16)$$

The configuration factor dF_{2-d1} is then the ratio of dQ_{2-d1} to Q_2 or

$$dF_{2-d1} = \frac{dA_1 \int_{A_2} \sigma T_2^4 \frac{\cos \beta_1 \cos \beta_2}{\pi S^2} dA_2}{\int_{A_2} \sigma T_2^4 dA_2}$$

$$= \frac{dA_1}{A_2} \int_{A_2} \frac{\cos \beta_1 \cos \beta_2}{\pi S^2} dA_2 \quad (2-17)$$

The last integral on the right was obtained subject to the imposed condition that A_2 is isothermal. From equation (2-8) the quantity under the integral in equation (2-17) is dF_{d1-d2} so the following alternate form is obtained:

$$dF_{2-d1} = \frac{dA_1}{A_2} \int_{A_2} dF_{d1-d2} \quad (2-18)$$

2.4.2.1 *Reciprocity for configuration factor between differential and finite areas.*—By use of equation (2-14) the factor dF_{2-d1} , as given by equation (2-18), can be written as

$$dF_{2-d1} = \frac{dA_1}{A_2} F_{d1-2}$$

or

$$A_2 dF_{2-d1} = dA_1 F_{d1-2} \quad (2-19)$$

which is a useful reciprocity relation.

2.4.2.2 *Radiation interchange between differential and finite areas.*—The energy radiated from dA_1 that reaches A_2 is from the definition of the configuration factor

$$dQ_{d1-2} = \sigma T_1^4 dA_1 F_{d1-2}$$

Similarly, that radiated by A_2 and reaching dA_1 is

$$dQ_{2-d1} = \sigma T_2^4 A_2 dF_{2-d1}$$

The net exchange from dA_1 to A_2 is

$$dQ_{d1 \rightleftharpoons 2} = dQ_{d1-2} - dQ_{2-d1}$$

$$= \sigma T_1^4 dA_1 F_{d1-2} - \sigma T_2^4 A_2 dF_{2-d1} \quad (2-20)$$

By use of the reciprocity relation in equation (2-19), the exchange can be expressed in the alternate forms

$$dQ_{d1 \leftrightarrow 2} = \sigma(T_1^4 - T_2^4) dA_1 F_{d1-2} \quad (2-21a)$$

$$dQ_{d1 \leftrightarrow 2} = \sigma(T_1^4 - T_2^4) A_2 dF_{2-d1} \quad (2-21b)$$

2.4.2.3 *Some sample configuration factors involving a differential and a finite area.*—Certain geometries have configuration factors that can be represented by a simple closed-form algebraic solution, while others require numerical integration of equation (2-13). Configuration factors can be tabulated for common geometries so that they need not be computed each time they are used. A list of references for available configuration factors is given in table I of appendix A.

Two geometries possessing closed-form configuration factors are given in the next examples which also serve to illustrate the method of obtaining these factors.

EXAMPLE 2-6: An elemental area dA_1 is oriented perpendicular to a circular disk of finite area A_2 and outer radius r as shown in figure 2-7(a). Find an equation describing the configuration factor F_{d1-2} for this system in terms of the appropriate parameters h , l , and r .

The first step in this problem is to find expressions for the quantities inside the integral of equation (2-13) in terms of known quantities so that the integration can be carried out. The elemental area dA_2 is known in terms of the local radius on the disk and the angle θ as

$$dA_2 = \rho \, d\rho \, d\theta$$

Because the integral in equation (2-13) must be carried out over all ρ and θ , the other quantities in the integral must be put in terms of these two variables; this is done by using auxiliary constructions. Figure 2-7(b) is drawn to evaluate $\cos \beta_1$ and $\cos \beta_2$, which are seen to be

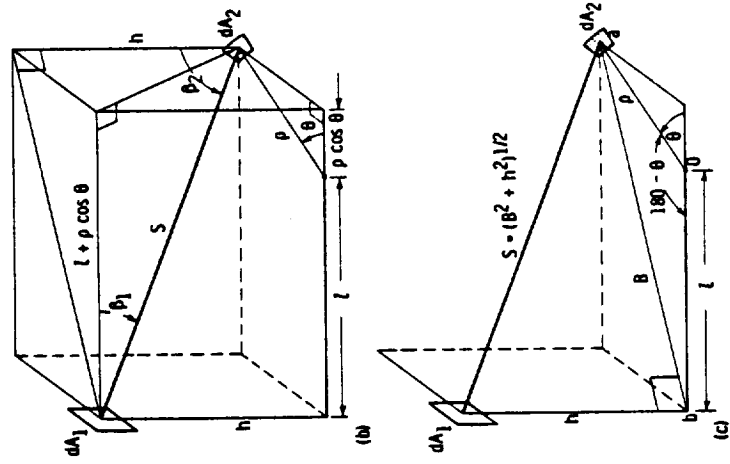
$$\cos \beta_1 = \frac{l + \rho \cos \theta}{S}$$

and

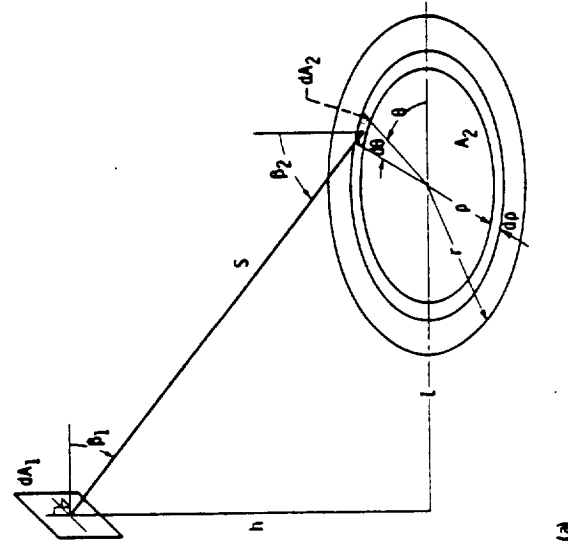
$$\cos \beta_2 = \frac{h}{S}$$

Figure 2-7(c) allows evaluation of the remaining unknown, S , as

$$S^2 = h^2 + B^2$$



(b) Auxiliary construction for determining $\cos \beta_1$ and $\cos \beta_2$.
 (c) Auxiliary construction for determining S .



(a) Geometry of problem.

FIGURE 2-7. — Geometry for radiative exchange between differential area and circular disk.

where B^2 can be evaluated by using the geometric law of cosines on triangle aOb . This gives

$$B^2 = l^2 + \rho^2 - 2l\rho \cos (180 - \theta) = l^2 + \rho^2 + 2l\rho \cos \theta$$

Substituting these relations into equation (2-13) results in

$$\begin{aligned} F_{d1-2} &= \int_{A_1} \frac{\cos \beta_1 \cos \beta_2}{\pi S^2} dA_2 = \int_{A_1} \frac{h(l + \rho \cos \theta)}{\pi S^4} \rho d\rho d\theta \\ &= \frac{h}{\pi} \int_{\rho=0}^r \int_{\theta=0}^{2\pi} \frac{\rho(l + \rho \cos \theta)}{(h^2 + l^2 + \rho^2 + 2\rho l \cos \theta)^2} d\theta d\rho \end{aligned}$$

This integration is carried out using the symmetry of the configuration and is nondimensionalized to give, after considerable manipulation,

$$\begin{aligned} F_{d1-2} &= \frac{2h}{\pi} \int_{\rho=0}^r \int_{\theta=0}^{\pi} \frac{\rho(l + \rho \cos \theta)}{(h^2 + \rho^2 + l^2 + 2\rho l \cos \theta)^2} d\theta d\rho \\ &= \frac{2H}{\pi} \int_{\xi=0}^R \int_{\theta=0}^{\pi} \frac{\xi(1 + \xi \cos \theta)}{(H^2 + \xi^2 + 1 + 2\xi \cos \theta)^2} d\theta d\xi \\ &= \frac{H}{2} \left\{ \frac{H^2 + R^2 + 1}{[(H^2 + R^2 + 1)^2 - 4R^2]^{1/2}} - 1 \right\} \end{aligned}$$

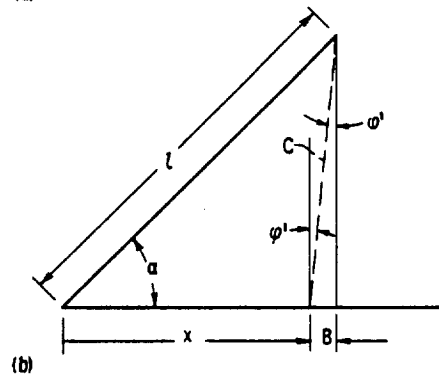
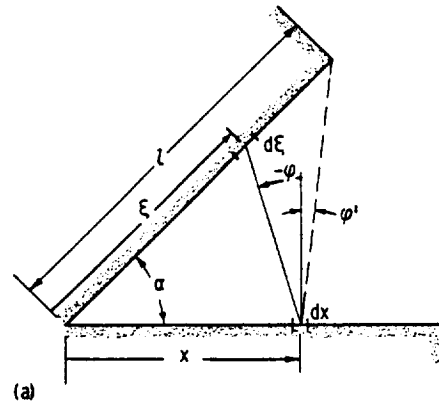
The nondimensionalization has been done by dividing numerator and denominator by l^4 and by letting $H = h/l$, $R = r/l$, and $\xi = \rho/l$. To find the net exchange of energy between two surfaces in the configuration of figure 2-7, F_{d1-2} is evaluated by the previous expression, and dQ_{d1-2} is evaluated by using equation (2-21a).

EXAMPLE 2-7: An infinitely long two-dimensional wedge cavity has an opening angle α . Derive an expression for the configuration factor from one wall of the wedge to a strip element of width dx on the other wall at a distance x from the wedge vertex as shown in figure 2-8(a). (Such configurations approximate the geometries of long fins and ribs used in space radiators.)

From example problem 2-4, the configuration factor between two infinitely long strip elements having parallel generating lines is

$$dF_{dx-d\xi} = \frac{1}{2} d(\sin \varphi)$$

where φ is in a plane containing the normals of both strips. Note that



(a) Wedge cavity geometry.

(b) Auxiliary construction to determine $\sin \varphi'$

FIGURE 2-8. — Configuration factor between one wall and strip on other wall of infinitely long wedge cavity.

φ is measured clockwise from the normal of dx ; equation (2-14) then gives

$$\begin{aligned}
 F_{dx-l} &= \int_{\xi=0}^l dF_{dx-d\xi} = \int_{\varphi=-\pi/2}^0 \frac{1}{2} d(\sin \varphi) + \int_0^{\varphi'} \frac{1}{2} d(\sin \varphi) \\
 &= \frac{\sin \varphi}{2} \Big|_{\varphi=-\pi/2}^0 + \frac{\sin \varphi}{2} \Big|_{\varphi=0}^{\varphi'} \\
 &= \frac{1}{2} + \frac{\sin \varphi'}{2}
 \end{aligned}$$

The function $\sin \varphi'$ can be found by the auxiliary construction of figure 2-8(b) to be

$$\sin \phi' = \frac{B}{C} = \frac{l \cos \alpha - x}{(x^2 + l^2 - 2xl \cos \alpha)^{1/2}}$$

Then

$$F_{dx-l} = \frac{1}{2} + \frac{l \cos \alpha - x}{2(x^2 + l^2 - 2xl \cos \alpha)^{1/2}}$$

However, the problem statement asked for dF_{l-dx} . Using the reciprocal relation of equation (2-19) gives

$$dF_{l-dx} = \frac{dx}{l} F_{dx-l} = dx \left[\frac{1}{2l} + \frac{\cos \alpha - \frac{x}{l}}{2(x^2 + l^2 - 2xl \cos \alpha)^{1/2}} \right]$$

By letting $X = x/l$, this can be placed in dimensionless form

$$dF_{l-dx} = dX \left[\frac{1}{2} + \frac{\cos \alpha - X}{2(X^2 + 1 - 2X \cos \alpha)^{1/2}} \right]$$

The only variables are the opening angle of the wedge and the dimensionless position from the vertex.

2.4.3 Configuration Factor for Two Finite Areas

Consider the configuration factor for radiation emitted from an isothermal surface A_1 shown in figure 2-9 and reaching A_2 . By definition, F_{1-2} is the fraction of the energy leaving A_1 that arrives at A_2 . The total energy leaving the black surface A_1 is $\sigma T_1^4 A_1$ since A_1 is isothermal at T_1 . The radiation leaving an element dA_1 that reaches dA_2 was given previously by

$$\sigma T_1^4 \frac{\cos \beta_1 \cos \beta_2}{\pi S^2} dA_1 dA_2$$

If this is integrated over both A_1 and A_2 , then the result will be the energy leaving A_1 that reaches A_2 . The configuration factor is then found as

$$F_{1-2} = \frac{\int_{A_1} \int_{A_2} \frac{\sigma T_1^4 \cos \beta_1 \cos \beta_2}{\pi S^2} dA_2 dA_1}{\sigma T_1^4 A_1}$$

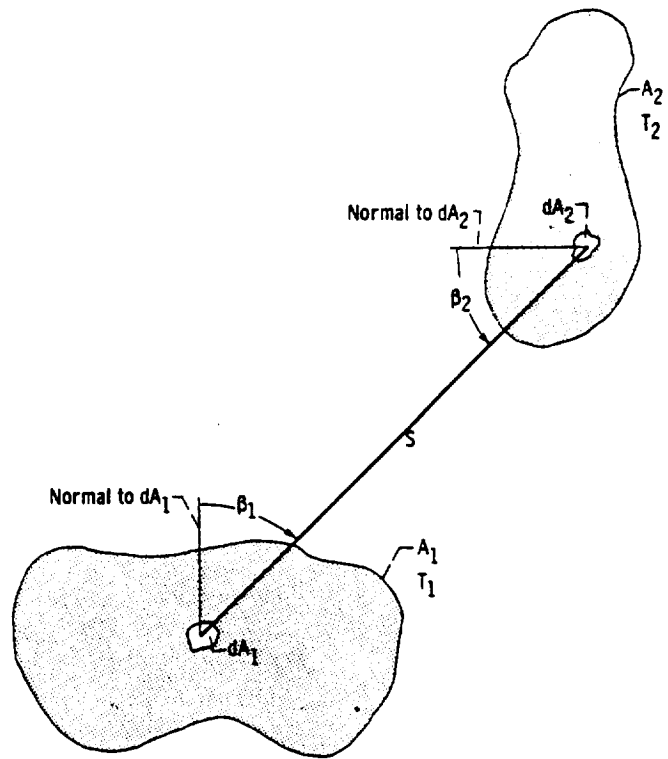


FIGURE 2-9. — Geometry for energy exchange between finite areas.

$$F_{1-2} = \frac{1}{A_1} \int_{A_1} \int_{A_2} \frac{\cos \beta_1 \cos \beta_2}{\pi S^2} dA_2 dA_1 \quad (2-22)$$

This can be written in terms of the configuration factors involving differential areas as

$$F_{1-2} = \frac{1}{A_1} \int_{A_1} \int_{A_2} dF_{d1-d2} dA_1 = \frac{1}{A_1} \int_{A_1} F_{d1-2} dA_1 \quad (2-23)$$

In a similar manner to the derivation of equation (2-22), the configuration factor from \$A_2\$ to \$A_1\$ is found to be

$$F_{2-1} = \frac{1}{A_2} \int_{A_1} \int_{A_2} \frac{\cos \beta_1 \cos \beta_2}{\pi S^2} dA_2 dA_1 \quad (2-24)$$

2.4.3.1 *Reciprocity for configuration factor between finite areas.* — The double integrals in equations (2-22) and (2-24) are identical. Hence, the reciprocity relation results

$$A_1 F_{1-2} = A_2 F_{2-1} \quad (2-25)$$

Further interrelations between configuration factors can be found by using equation (2-23) in conjunction with the reciprocity relations of equations (2-25) and (2-19), that is,

$$F_{2-1} = \frac{A_1}{A_2} F_{1-2} = \left(\frac{A_1}{A_2}\right) \frac{1}{A_1} \int_{A_1} F_{d1-2} dA_1 = \frac{1}{A_2} \int_{A_1} dF_{2-d1} A_2 = \int_{A_1} dF_{2-d1} \quad (2-26)$$

2.4.3.2 *Radiation exchange between finite areas.* — The energy radiated from A_1 that reaches A_2 is from the definition of the configuration factor

$$Q_{1-2} = \sigma T_1^4 A_1 F_{1-2}$$

Similarly, that radiated from A_2 which reaches A_1 is

$$Q_{2-1} = \sigma T_2^4 A_2 F_{2-1}$$

The net exchange from A_1 to A_2 is

$$Q_{1 \rightleftharpoons 2} = Q_{1-2} - Q_{2-1} = \sigma T_1^4 A_1 F_{1-2} - \sigma T_2^4 A_2 F_{2-1} \quad (2-27)$$

By use of equation (2-25) this can be written in the two forms

$$Q_{1 \rightleftharpoons 2} = \sigma (T_1^4 - T_2^4) A_1 F_{1-2} \quad (2-28a)$$

$$Q_{1 \rightleftharpoons 2} = \sigma (T_1^4 - T_2^4) A_2 F_{2-1} \quad (2-28b)$$

EXAMPLE 2-8: Two isothermal plates of the same finite width and of infinite length are joined along one edge at angle α as shown in figure 2-8. Using the same nondimensional parameters as in example 2-7, derive the configuration factor between the plates.

Example 2-7 gives the configuration factor between one plate and an infinite strip on the other plate as

$$dF_{l-dx} = \left[\frac{1}{2l} + \frac{\cos \alpha - \frac{x}{l}}{2(x^2 + l^2 - 2xl \cos \alpha)^{1/2}} \right] dx$$

Substituting into equation (2-26) gives

$$F_{l-l^*} = \int_{x=0}^{l^*} dF_{l-dx} = \int_0^{l^*} \left[\frac{1}{2l} + \frac{\cos \alpha - \frac{x}{l}}{2(x^2 + l^2 - 2xl \cos \alpha)^{1/2}} \right] dx$$

where, for convenience in labeling, the width of the side in figure 2-8 having element dx is specified as l^* . Using the dimensionless variable $X = x/l$ and the fact that $l^* = l$, this becomes

$$F_{l-l^*} = \int_0^1 \left[\frac{1}{2} + \frac{\cos \alpha - X}{2(X^2 + 1 - 2X \cos \alpha)^{1/2}} \right] dX$$

Carrying out the integration yields

$$F_{l-l^*} = 1 - \left(\frac{1 - \cos \alpha}{2} \right)^{1/2} = 1 - \sin \frac{\alpha}{2}$$

For the present case where the two plate widths are equal, the only parameter is the angle α . Also, because the areas of the two sides are equal, the reciprocity relation (eq. (2-25)) gives, as expected from symmetry,

$$F_{l-l^*} = F_{l^*-l}$$

TABLE 2-1.—SUMMARY OF CONFIGURATION FACTOR AND ENERGY EXCHANGE RELATIONS

Geometry	Energy exchange	Configuration factor	Reciprocity
Elemental area to elemental area	$d^2Q_{d1} = \epsilon$ $= \sigma(T_1^4 - T_2^4) dA_1 dF_{d1-d2}$	dF_{d1-d2} $= \frac{\cos \beta_1 \cos \beta_2}{\pi S^2} dA_2$	$dA_1 dF_{d1-d2}$ $= dA_2 dF_{d2-d1}$
Elemental area to finite area	$dQ_{d1} = \epsilon$ $= \sigma(T_1^4 - T_2^4) dA_1 F_{d1-2}$	F_{d1-2} $= \int_{A_2} \frac{\cos \beta_1 \cos \beta_2}{\pi S^2} dA_2$	$dA_1 F_{d1-2}$ $= A_2 dF_{2-d1}$
Finite area to finite area	Q_{1-2} $= \sigma(T_1^4 - T_2^4) A_1 F_{1-2}$	F_{1-2} $= \frac{1}{A_1} \int_{A_1} \int_{A_2} \frac{\cos \beta_1 \cos \beta_2}{\pi S^2} dA_2 dA_1$	$A_1 F_{1-2} = A_2 F_{2-1}$

2.4.4 Summary of Configuration Factor and Energy Exchange Relations

In table 2-I, there are summarized the energy exchange equations, integral definitions of the configuration factors, and the configuration factor reciprocity relations.

2.5 METHODS FOR EVALUATING CONFIGURATION FACTORS

2.5.1 Configuration Factor Algebra for Pairs of Surfaces

Because of the difficulty involved in directly computing configuration factors from the integral definitions in table 2-I for many geometries, it is desirable to utilize shortcut methods whenever possible. Such shortcuts can be obtained by using two concepts that have been developed in preceding sections: (1) the definition of configuration factor in terms of fractional intercepted energy and (2) the reciprocal relations. This section will show how these two concepts can be used to derive configuration factors for certain geometries from known configuration factors of other geometries. The interrelation between configuration factors is termed "configuration-factor algebra."

Consider an arbitrary isothermal black area A_1 in figure 2-10 ex-

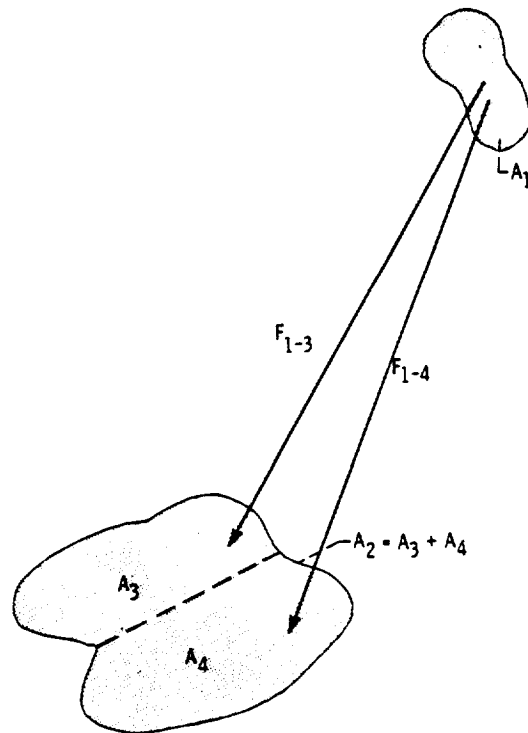


FIGURE 2-10.—Energy exchange between finite areas with one area subdivided.
 $F_{1-3} + F_{1-4} = F_{1-2}$.

changing energy with a second area A_2 . The configuration factor F_{1-2} is the fraction of the total energy emitted by A_1 that is incident upon A_2 . If A_2 is divided into two parts, A_3 and A_4 , the fraction of the total energy leaving A_1 that is incident on A_3 and the fraction incident on A_4 must total to F_{1-2} . As a consequence, the following can be written:

$$F_{1-2} = F_{1-(3+4)} = F_{1-3} + F_{1-4} \quad (2-29)$$

Suppose then that F_{1-2} and F_{1-4} are known, but configuration factor F_{3-1} is desired. Then

$$F_{1-3} = F_{1-2} - F_{1-4} \quad (2-30)$$

By using the reciprocity relation (eq. (2-25)),

$$F_{3-1} = \frac{A_1}{A_3} F_{1-3} = \frac{A_1}{A_3} (F_{1-2} - F_{1-4}) \quad (2-31)$$

This is a powerful tool for obtaining new configuration factors from those previously computed. This method will be further examined by use of some examples.

EXAMPLE 2-9: An elemental area dA_1 is oriented perpendicular to a

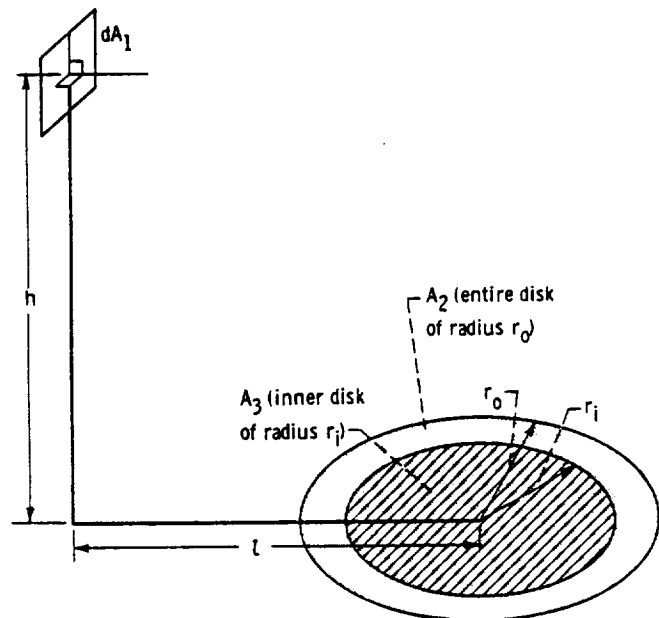


FIGURE 2-11.—Interchange between elemental area and finite ring.

ring of outer radius r_o and inner radius r_i as shown in figure 2-11. Derive an expression for the configuration factor $F_{d1-ring}$.

From example 2-6, the configuration factor between element dA_1 and the entire disk of area A_2 and outer radius r_o was found to be

$$F_{d1-2} = \frac{H}{2} \left\{ \frac{H^2 + R_o^2 + 1}{[(H^2 + R_o^2 + 1)^2 - 4R_o^2]^{1/2}} - 1 \right\}$$

where $H = h/l$ and $R_o = r_o/l$. The configuration factor to the inner disk of area A_3 and radius r_i is similarly

$$F_{d1-3} = \frac{H}{2} \left\{ \frac{H^2 + R_i^2 + 1}{[(H^2 + R_i^2 + 1)^2 - 4R_i^2]^{1/2}} - 1 \right\}$$

where $R_i = r_i/l$. Using configuration-factor algebra, the desired configuration factor from dA_1 to the ring $A_2 - A_3$ is

$$F_{d1-ring} = F_{d1-2} - F_{d1-3} = \frac{H}{2} \left\{ \frac{H^2 + R_o^2 + 1}{[(H^2 + R_o^2 + 1)^2 - 4R_o^2]^{1/2}} - \frac{H^2 + R_i^2 + 1}{[(H^2 + R_i^2 + 1)^2 - 4R_i^2]^{1/2}} \right\}$$

EXAMPLE 2-10: Suppose that the configuration factor is known between two parallel disks of arbitrary size whose centers lie on the same axis. From this, derive the configuration factor between the two rings A_2 and A_3 of figure 2-12. Give the answer in terms of known disk-to-disk factors from disk areas on the lower surface to disk areas on the upper surface.

The factor desired is F_{2-3} . From configuration factor algebra, F_{2-3} is equal to

$$F_{2-3} = F_{2-(3+4)} - F_{2-4}$$

The factor $F_{2-(3+4)}$ can be found from the reciprocal relation

$$A_2 F_{2-(3+4)} = (A_3 + A_4) F_{(3+4)-2}$$

Applying configuration algebra to the right-hand side results in

$$\begin{aligned} A_2 F_{2-(3+4)} &= (A_3 + A_4) [F_{(3+4)-(1+2)} - F_{(3+4)-1}] \\ &= (A_3 + A_4) F_{(3+4)-(1+2)} - (A_3 + A_4) F_{(3+4)-1} \end{aligned}$$

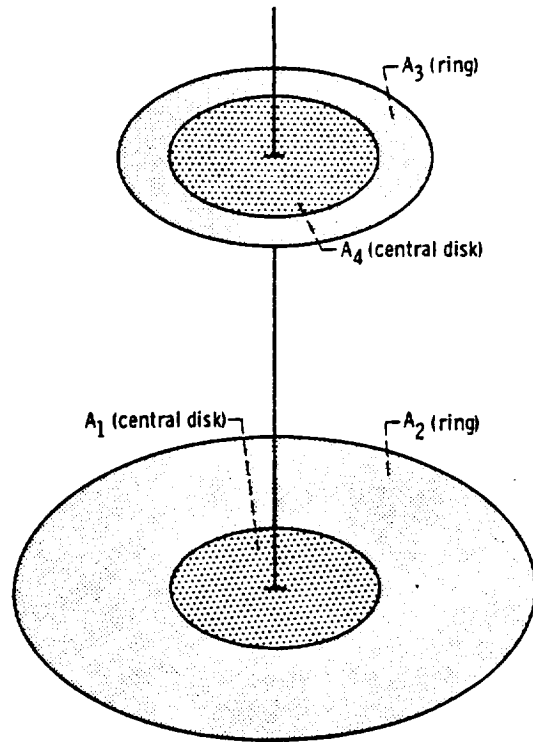


FIGURE 2-12. — Interchange between parallel ring areas having common axis.

Applying reciprocity to the right side gives

$$A_2 F_{2-(3+4)} = (A_1 + A_2) F_{(1+2)-(3+4)} - A_1 F_{1-(3+4)}$$

where the F factors on the right are both disk-to-disk factors from the lower surface to the upper.

Now the factor F_{2-4} remains to be determined. Again, apply the reciprocal relations and configuration factor algebra to find

$$\begin{aligned} F_{2-4} &= \frac{A_4}{A_2} F_{4-2} = \frac{A_4}{A_2} [F_{4-(1+2)} - F_{4-1}] \\ &= \frac{1}{A_2} [(A_1 + A_2) F_{(1+2)-4} - A_1 F_{1-4}] \end{aligned}$$

Substituting the relations for F_{2-4} and $F_{2-(3+4)}$ in the first equation gives

$$F_{2-3} = \frac{A_1 + A_2}{A_2} [F_{(1+2)-(3+4)} - F_{(1+2)-4}] - \frac{A_1}{A_2} [F_{1-(3+4)} - F_{1-4}]$$

and all configuration factors on the right-hand side of this equation are for exchange between two disks in the direction from disks on the lower surface to disks on the upper surface. The problem is now solved.

Because of the small differences of large numbers that can occur when obtaining an F factor by use of configuration-factor algebra (as might occur on the right side of the last equation of the preceding example), care must be taken that a sufficient number of significant figures are retained to ensure acceptable accuracy. Feingold (ref. 2) gives one example in which an error of 0.05 percent in a known factor causes an error of 57 percent in another factor computed from it by means of angle-factor algebra.

EXAMPLE 2-11: The internal surface of a hollow circular cylinder of radius R is radiating to a disk A_1 of radius r as shown in figure 2-13. Express the configuration factor from the cylindrical side A_3 to the disk in terms of disk-to-disk factors for the case of r less than R .

From any position on A_1 the solid angle subtended when viewing

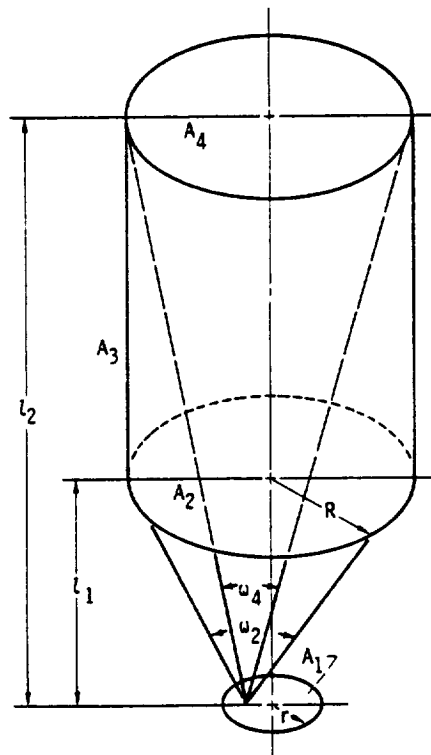


FIGURE 2-13. — Internal surface of cylindrical cavity radiating to circular disk A_1 for $r < R$.

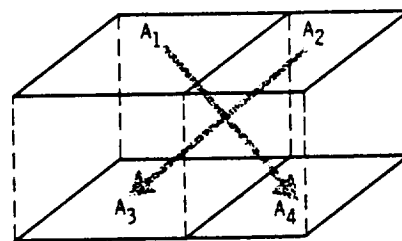
A_3 is the difference between the solid angle when viewing A_2 , $d\omega_2$, and that viewing A_4 , $d\omega_4$. This gives the F factor from an area element dA_1 on A_1 to area A_3 as $F_{d1-3} = F_{d1-2} - F_{d1-4}$. By integrating over A_1 and using equation (2-23), this can be written for the entire area A_1

$$F_{1-3} = F_{1-2} - F_{1-4}$$

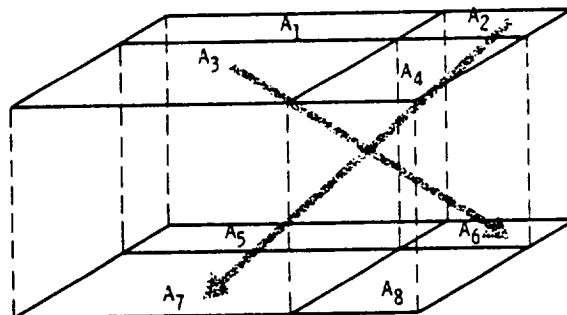
The factors on the right are between parallel disks. The final result for F from the cylindrical side A_3 to the disk A_1 is

$$F_{3-1} = \frac{A_1}{A_3} (F_{1-2} - F_{1-4})$$

There is a reciprocity relation that can be derived from the symmetry of a geometry. Consider the opposing areas in figure 2-14(a). From the symmetry it is evident that $A_2 = A_4$ and $F_{2-3} = F_{4-1}$, so that $A_2 F_{2-3} = A_4 F_{4-1}$. From reciprocity $A_4 F_{4-1} = A_1 F_{1-4}$. Hence, there is the derived relation



(a)



(b)

(a) Two pairs of opposing rectangles. $A_1 F_{1-4} = A_2 F_{2-3}$.

(b) Four pairs of opposing rectangles. $A_2 F_{2-7} = A_3 F_{3-6}$.

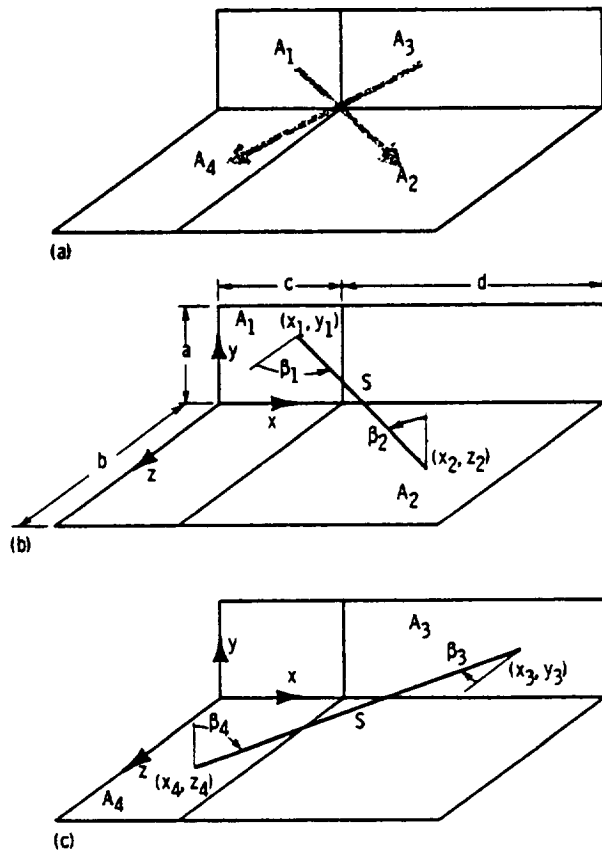
FIGURE 2-14. —Geometry for reciprocity between opposing rectangles.

$$A_2 F_{2-3} = A_1 F_{1-4}$$

which relates the diagonal directions shown by the arrows on the figure. Similarly, the symmetry of figure 2-14(b) yields

$$A_2 F_{2-7} = A_3 F_{3-6}$$

Figure 2-15(a) shows four areas on two perpendicular rectangles having a common edge. Since all of these areas are of unequal size, there is no apparent symmetry relation. However, it will be shown that the relation is valid that



(a) Representation of reciprocity, $A_1 F_{1-2} = A_3 F_{3-4}$.

(b) Construction for F_{1-2} .

(c) Construction for F_{3-4} .

FIGURE 2-15. — Reciprocity for diagonally opposite pairs of rectangles on two perpendicular planes having common edge.

$$A_1 F_{1-2} = A_3 F_{3-4} \quad (2-32)$$

To prove this, begin with the basic definition (eq. (2-22)); thus

$$A_1 F_{1-2} = \frac{1}{\pi} \int_{A_1} \int_{A_2} \frac{\cos \beta_1 \cos \beta_2}{S^2} dA_2 dA_1$$

From figure 2-15(b), $S^2 = (x_2 - x_1)^2 + y_1^2 + z_2^2$, $\cos \beta_1 = z_2/S$, and $\cos \beta_2 = y_1/S$. Then

$$A_1 F_{1-2} = \frac{1}{\pi} \int_{x_1=0}^c \int_{y_1=0}^a \int_{x_2=c}^{c+d} \int_{z_2=0}^b \frac{y_1 z_2}{[(x_2 - x_1)^2 + y_1^2 + z_2^2]^2} dx_2 dy_1 dx_1 dz_2 \quad (2-33a)$$

Similarly, referring to figure 2-15(c) reveals that

$$\begin{aligned} A_3 F_{3-4} &= \frac{1}{\pi} \int_{A_3} \int_{A_4} \frac{\cos \beta_3 \cos \beta_4}{S^2} dA_4 dA_3 \\ &= \frac{1}{\pi} \int_{x_3=c}^{c+d} \int_{y_3=0}^a \int_{x_4=0}^c \int_{z_4=0}^b \frac{y_3 z_4}{[(x_3 - x_4)^2 + y_3^2 + z_4^2]^2} dx_4 dy_3 dx_3 dz_4 \end{aligned} \quad (2-33b)$$

By interchanging the dummy integration variables x_1 , y_1 , x_2 , and z_2 for x_4 , y_3 , x_3 , and z_4 , it is found that the integrals in equations (2-33a) and (2-33b) are identical, thus proving equation (2-32).

EXAMPLE 2-12: If the configuration factor is known for two perpendicular rectangles with a common edge as shown in figure 2-16(a), derive the configuration factor F_{1-6} for figure 2-16(b).

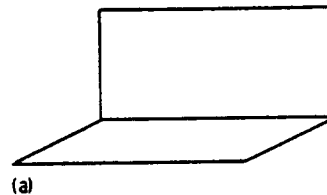
First, consider the geometry in figure 2-16(c) and derive the factor F_{7-6} as follows:

$$F_{(5+6)-(7+8)} = F_{(5+6)-7} + F_{(5+6)-8} = \frac{A_7}{A_5 + A_6} F_{7-(5+6)} + \frac{A_8}{A_5 + A_6} F_{8-(5+6)}$$

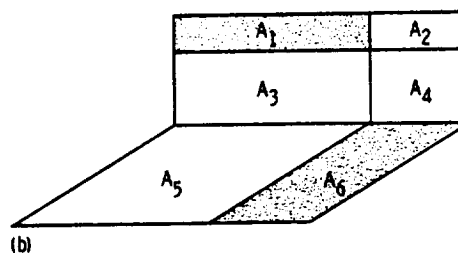
$$F_{(5+6)-(7+8)} = \frac{A_7}{A_5 + A_6} (F_{7-5} + F_{7-6}) + \frac{A_8}{A_5 + A_6} (F_{8-5} + F_{8-6})$$

Substitute $A_7 F_{7-6}$ for $A_8 F_{8-5}$ and solve the resulting relation for F_{7-6} to obtain

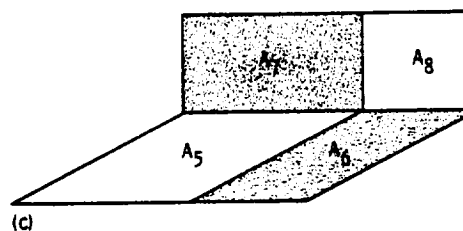
$$F_{7-6} = \frac{1}{2A_7} [(A_5 + A_6) F_{(5+6)-(7+8)} - A_7 F_{7-5} - A_8 F_{8-6}]$$



(a)



(b)



(c)

(a) Perpendicular rectangles with one common edge.

(b) Geometry for F_{1-6} .

(c) Auxiliary geometry.

FIGURE 2-16. — Orientation of areas for example 2-12.

Returning now to figure 2-16(b)

$$F_{1-6} = \frac{A_6}{A_1} F_{6-1} = \frac{A_6}{A_1} F_{6-(1+3)} - \frac{A_6}{A_1} F_{6-3}$$

The factors $F_{6-(1+3)}$ and F_{6-3} are of the same type as F_{7-6} so that F_{1-6} can finally be written as

$$F_{1-6} = \frac{A_6}{A_1} \left\{ \frac{1}{2A_6} [(A_1 + A_2 + A_3 + A_4)F_{(1+2+3+4)-(5+6)} - A_6F_{6-(2+4)} - A_5F_{5-(1+3)}] - \frac{1}{2A_6} [(A_3 + A_4)F_{(3+4)-(5+6)} - A_6F_{6-4} - A_5F_{5-3}] \right\}$$

All of the F factors on the right side are for two rectangles having one common edge as in figure 2-16(a).

When formulating relations between configuration factors, it is sometimes useful to think in terms of energy quantities rather than fractions of energy leaving a surface that reach another surface. For example, in figure 2-10 the energy leaving A_2 that arrives at A_1 is proportional to A_2F_{2-1} and is equivalent to the sums of the energies from A_3 and A_4 that arrive at A_1 . Thus

$$(A_3 + A_4)F_{(3+4)-1} = A_3F_{3-1} + A_4F_{4-1} \quad (2-34)$$

This can also be proved by using reciprocity laws as follows:

$$(A_3 + A_4)F_{(3+4)-1} = A_1F_{1-(3+4)} = A_1F_{1-3} + A_1F_{1-4} = A_3F_{3-1} + A_4F_{4-1}$$

2.5.2 Configuration Factors in Enclosures

To this point, only the radiation exchange between two black isothermal isolated surfaces has been considered, although subdivision of one or both of the surfaces into smaller portions has been examined. Consider the very useful class of problems in which the configuration factors are between black surfaces that form a complete enclosure. These configuration factors will later have a wider utility when nonblack diffuse enclosures are analyzed.

For an enclosure of N surfaces, such as shown in figure 2-17 (where $N=8$ as an example), the entire energy leaving any surface inside the enclosure, for example surface A_k , must be incident on all the surfaces making up the enclosure. Thus all the fractions of energy leaving one

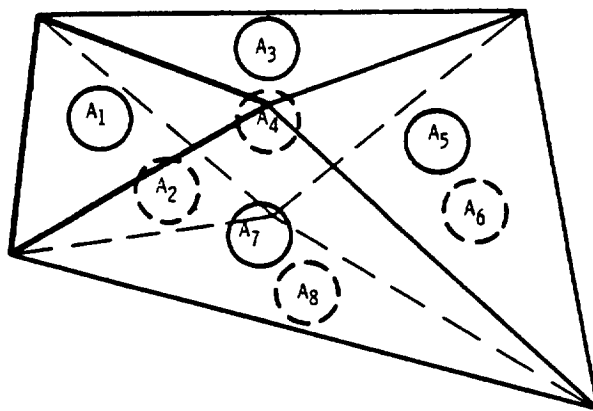


FIGURE 2-17. — Isothermal enclosure composed of black surfaces.

surface and reaching the surfaces of the enclosure must total to unity; that is,

$$F_{k-1} + F_{k-2} + F_{k-3} + \dots + F_{k-k} + \dots + F_{k-N} = \sum_{j=1}^N F_{k-j} = 1 \quad (2-35)$$

The factor F_{k-k} is included because when A_k is concave, it will intercept a portion of its own emitted energy.

EXAMPLE 2-13: Two black isothermal concentric spheres are exchanging energy. Find all the configuration factors for this geometry if the surface area of the inner sphere is A_1 and the area of the outer sphere is A_2 .

All energy leaving A_1 is incident upon A_2 , so the following is known immediately:

$$F_{1-2} = 1$$

Using the reciprocal relation reveals further that

$$F_{2-1} = \frac{A_1 F_{1-2}}{A_2} = \frac{A_1}{A_2}$$

Also, from equation (2-35),

$$F_{2-1} + F_{2-2} = 1$$

or

$$F_{2-2} = 1 - F_{2-1} = \frac{A_2 - A_1}{A_2}$$

EXAMPLE 2-14: An isothermal cavity of internal area A_1 has a plane opening of area A_2 . Derive an expression for the configuration factor of the internal surface of the cavity to itself.

Assume that a black plane surface A_2 replaces the cavity opening. Then $F_{2-1} = 1$ and

$$F_{1-2} = \frac{A_2 F_{2-1}}{A_1} = \frac{A_2}{A_1}$$

Since A_1 and A_2 form an enclosure,

$$F_{1-1} = 1 - F_{1-2} = \frac{(A_1 - A_2)}{A_1}$$

which is the desired F factor.

EXAMPLE 2-15: An enclosure of triangular cross section is made up of three plane plates each of finite width and infinite length (thus forming an infinitely long triangular prism). Derive an expression for the configuration factor between any two of the plates in terms of the plate widths, L_1 , L_2 , and L_3 .

For plate 1, $F_{1-2} + F_{1-3} = 1$. Using similar relations for each plate and multiplying through by the respective plate areas result in

$$A_1 F_{1-2} + A_1 F_{1-3} = A_1$$

$$A_2 F_{2-1} + A_2 F_{2-3} = A_2$$

and

$$A_3 F_{3-1} + A_3 F_{3-2} = A_3$$

By applying the reciprocal relations to some of the terms, these three equations become

$$A_1 F_{1-2} + A_1 F_{1-3} = A_1$$

$$A_1 F_{1-2} + A_2 F_{2-3} = A_2$$

and

$$A_1 F_{1-3} + A_2 F_{2-3} = A_3$$

thus giving three equations for the three unknown F factors. Subtracting the third from the second and adding the first give

$$F_{1-2} = \frac{A_1 + A_2 - A_3}{2A_1} = \frac{L_1 + L_2 - L_3}{2L_1}$$

For the special case of $L_1 = L_2$, this should reduce to the factor between infinitely long adjoint plates of equal width separated by an angle α as given in example 2-8. For $L_1 = L_2$,

$$F_{1-2} = \frac{2L_1 - L_3}{2L_1} = 1 - \frac{L_3}{L_1} = 1 - \sin \frac{\alpha}{2}$$

which agrees with example 2-8.

The set of three simultaneous equations from which the final result was derived in example 2-15 will now be examined more closely. The first equation involves two unknowns, F_{1-2} and F_{1-3} ; the second equation has one additional unknown, F_{2-3} ; and the final equation has no additional unknowns. Generalizing the procedure for a three surface enclosure to any N -sided enclosure made up of plane or convex surfaces shows that of N simultaneous equations, the first would involve $N-1$ unknowns, the second $N-2$ unknowns, and so forth. The total number of unknowns U is then

$$U = (N-1) + (N-2) + (N-3) + \dots + 1 = N^2 - \sum_{j=1}^N j \quad (2-36)$$

Thus, for a four-sided enclosure made up of planar or convex surfaces of known area, four equations relating $(4)^2 - \sum_{j=1}^4 j$ or six unknown configuration factors can be written. Specifying any two of these factors allows calculation of the rest by solving the set of four simultaneous equations.

If all the surfaces can see themselves, then the factor F_{k-k} must be included in each of the equations. Analyzing this situation, as previously done, shows that an N -sided enclosure allows writing N equations in $N^2 - \sum_{j=1}^{N-1} j$ unknowns. For a four-sided enclosure, four equations involving 10 unknown F factors could be written. The specification of six factors would be required, and then the simultaneous relations could be solved to determine the remaining four factors.

2.5.3 Mathematical Techniques for the Evaluation of Configuration Factors

As shown by the summary of relations in table 2-I, the evaluation of the configuration factors F_{d1-2} and F_{1-2} requires integration over the finite areas involved. There are a number of mathematical methods that are useful in evaluating certain configuration factors when the straightforward analytical integration methods become too cumbersome. These methods can encompass all techniques that are used in the evaluation of integrals, including numerical approaches.

A few methods that are especially valuable in dealing with configuration factors will be discussed here.

2.5.3.1 *Hottel's crossed-string method.*—Consider the class of configurations, such as long grooves, in which all surfaces are assumed to extend infinitely far along one coordinate. Such surfaces can be generated by moving a straight line through space in such a way that it always remains parallel to its original position.

A typical configuration of this type is shown in cross section in figure 2-18. Suppose that the configuration factor is needed between A_1 and A_2 when some blockage of radiant transfer occurs because of the presence of other surfaces A_3 and A_4 . To obtain F_{1-2} , first consider that A_1 may be concave. In this case draw the dashed line agf across A_1 . Then draw in the dotted lines ad and abc to complete the enclosure $abcfga$ which has three sides that are either convex or planar. The relation found in example 2-15 for enclosures of this type can be written as

$$A_{agf}F_{agf-abc} = \frac{A_{agf} + A_{abc} - A_{cf}}{2} \quad (2-37)$$

For the three-sided enclosure $adefga$, similar reasoning gives

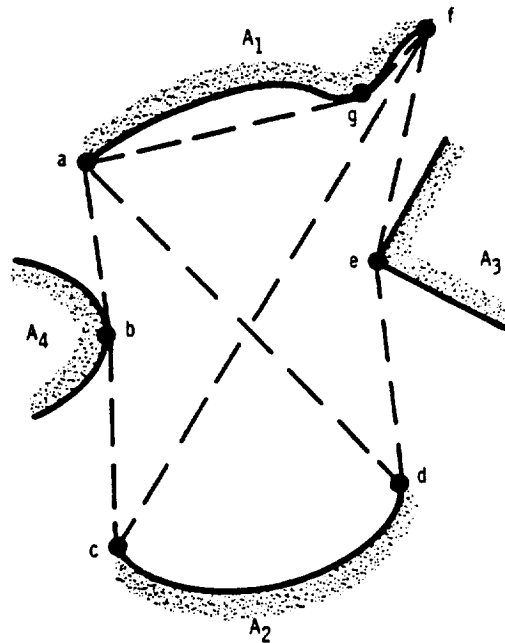


FIGURE 2-18.—Hottel's crossed-string method for configuration factor determination.

$$A_{agf}F_{agf-def} = \frac{A_{agf} + A_{def} - A_{ad}}{2} \quad (2-38)$$

Further, note that

$$F_{agf-abc} + F_{agf-2} + F_{agf-def} = 1 \quad (2-39)$$

Substituting equations (2-37) and (2-38) into equation (2-39) results in

$$\begin{aligned} A_{agf}F_{agf-2} &= A_{agf}(1 - F_{agf-abc} - F_{agf-def}) \\ &= \frac{A_{cf} + A_{ad} - A_{abc} - A_{def}}{2} \end{aligned} \quad (2-40)$$

Now $F_{2-agf} = F_{2-1}$ since A_{agf} and A_1 subtend the same solid angle when viewed from A_2 . Then with the additional use of reciprocity, the left side of equation (2-40) can be written as

$$A_{agf}F_{agf-2} = A_2F_{2-agf} = A_2F_{2-1} = A_1F_{1-2} \quad (2-41)$$

Substituting equation (2-41) into equation (2-40) results in

$$A_1F_{1-2} = \frac{A_{cf} + A_{ad} - A_{abc} - A_{def}}{2} \quad (2-42)$$

If the dashed lines in figure 2-18 are imagined as being lengths of strings stretched tightly between the outer edges of the surfaces, then the term on the right of equation (2-42) is interpreted as one-half of the total quantity formed by the sum of the lengths of the crossed strings connecting the outer edges of A_1 and A_2 minus the sum of the lengths of the uncrossed strings. This is a convenient way of determining configuration factors *in this type of two-dimensional geometry* and was first pointed out by Hottel (ref. 3).

EXAMPLE 2-16: Two infinitely long semicylinders of radius R are separated by a minimum distance D as shown in figure 2-19. Derive the configuration factor F_{1-2} for this case.

The length of crossed string $abcde$ will be denoted as L_1 , and of uncrossed string ef as L_2 . From the symmetry of the problem, equation (2-42) may be written

$$F_{1-2} = \frac{2L_1 - 2L_2}{2A_1} = \frac{L_1 - L_2}{\pi R}$$

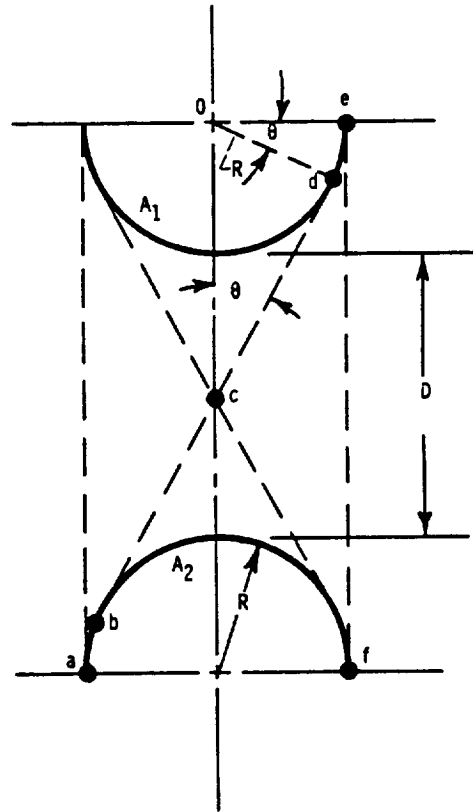


FIGURE 2-19.—Configuration factor between infinitely long semicylinders by crossed-string method.

The length L_2 is given by

$$L_2 = D + 2R$$

The length of L_1 is twice the length cde . The segment of L_1 from c to d is found from right triangle Ocd to be

$$L_{1, c-d} = \left[\left(\frac{D}{2} + R \right)^2 - R^2 \right]^{1/2} = \left[D \left(\frac{D}{4} + R \right) \right]^{1/2}$$

and the segment of L_1 from d to e is

$$L_{1, d-e} = R\theta$$

From triangle Ocd , the angle θ is given by

$$\theta = \sin^{-1} \left(\frac{R}{\frac{D}{2} + R} \right)$$

Combining the known relations results in

$$\begin{aligned} F_{1-2} &= \frac{L_1 - L_2}{\pi R} = \frac{2(L_{1,c-d} + L_{1,d-e}) - L_2}{\pi R} \\ &= \frac{\left[4D \left(\frac{D}{4} + R \right) \right]^{1/2} + 2R \sin^{-1} \left(\frac{R}{\frac{D}{2} + R} \right) - D - 2R}{\pi R} \end{aligned}$$

Letting $X = 1 + (D/2R)$ gives

$$F_{1-2} = \frac{2}{\pi} \left[(X^2 - 1)^{1/2} + \sin^{-1} \left(\frac{1}{X} \right) - X \right] \quad (2-43)$$

This can also be put in the form

$$F_{1-2} = \frac{2}{\pi} \left[(X^2 - 1)^{1/2} + \frac{\pi}{2} - \cos^{-1} \left(\frac{1}{X} \right) - X \right] \quad (2-44)$$

which agrees with the result in reference 5.

2.5.3.2 Contour integration.—Another tool that is useful in the evaluation of configuration factors is the application of Stokes' theorem for reduction of the multiple integration over a surface area to a single integration around the boundary of the area. This method is treated at some length by Moon (ref. 4), Sparrow and Cess (ref. 5), and Sparrow (ref. 6). Consider a surface area A as shown in figure 2-20 with its boundary designated as C (where C is piecewise continuous). The location of an arbitrary point on the area is at coordinate position x, y, z . At this point the normal to A is constructed and the angles between this normal and the x -, y -, and z -axes are designated as α, γ , and δ . Let the functions P, Q , and R be any twice differentiable functions of x, y , and z . Stokes' theorem in three dimensions provides the following relation between an integral of P, Q , and R around the boundary C of the area and an integral over the surface A of the area:

$$\begin{aligned} \oint_C (P dx + Q dy + R dz) \\ = \int_A \left[\left(\frac{\partial R}{\partial y} - \frac{\partial Q}{\partial z} \right) \cos \alpha + \left(\frac{\partial P}{\partial z} - \frac{\partial R}{\partial x} \right) \cos \gamma + \left(\frac{\partial Q}{\partial x} - \frac{\partial P}{\partial y} \right) \cos \delta \right] dA \end{aligned} \quad (2-45)$$

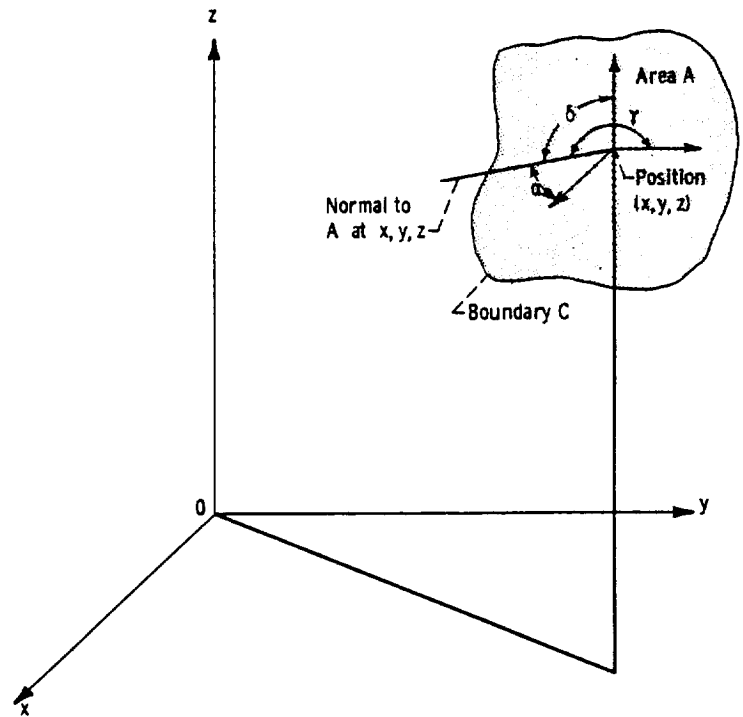


FIGURE 2-20. — Geometry for quantities used in Stokes' theorem.

Now this relation will be applied to express area integrals in configuration factor computations in terms of integrals around the boundaries of the areas.

2.5.3.2.1 Configuration factor between a differential and a finite area: The integrand in the configuration factor F_{d1-2} is

$$\frac{\cos \beta_1 \cos \beta_2}{\pi S^2} dA_2$$

as shown in table 2-I. In general, for the two cosines the following can be written (fig. 2-21):

$$\cos \beta_1 = \left(\frac{x_2 - x_1}{S}\right) \cos \alpha_1 + \left(\frac{y_2 - y_1}{S}\right) \cos \gamma_1 + \left(\frac{z_2 - z_1}{S}\right) \cos \delta_1 \tag{2-46}$$

$$\cos \beta_2 = \left(\frac{x_1 - x_2}{S}\right) \cos \alpha_2 + \left(\frac{y_1 - y_2}{S}\right) \cos \gamma_2 + \left(\frac{z_1 - z_2}{S}\right) \cos \delta_2 \tag{2-47}$$

This follows from the relation that, for two vectors \vec{V}_1 and \vec{V}_2 having

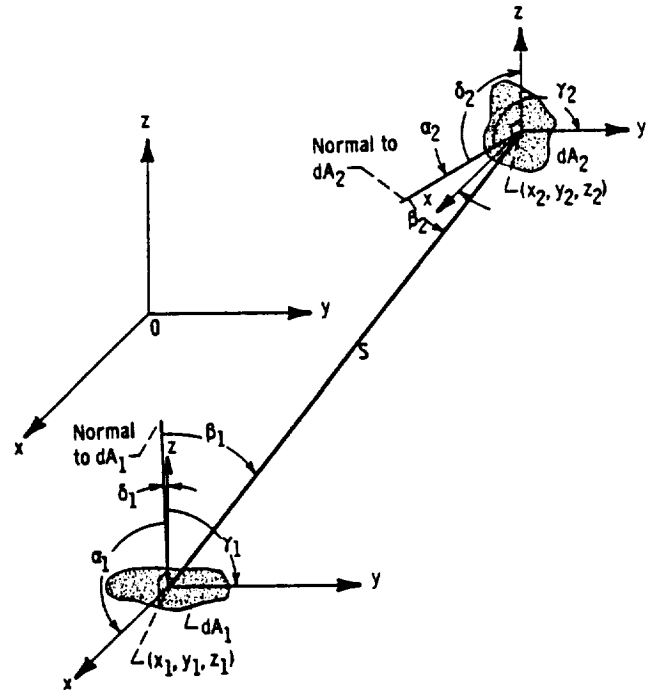


FIGURE 2-21. - Geometry for contour integration.

direction cosines (l_1, m_1, n_1) and (l_2, m_2, n_2) , the cosine of the angle between the vectors is given by $l_1 l_2 + m_1 m_2 + n_1 n_2$.

Substituting equations (2-46) and (2-47) into the integral relation for a configuration factor between a differential element and a finite area gives

$$\begin{aligned}
 F_{d1-2} &= \int_{A_2} \frac{\cos \beta_1 \cos \beta_2}{\pi S^2} dA_2 \\
 &= \frac{1}{\pi} \int_{A_2} \frac{[(x_2 - x_1) \cos \alpha_1 + (y_2 - y_1) \cos \gamma_1 + (z_2 - z_1) \cos \delta_1]}{S^4} \\
 &\quad \times [(x_1 - x_2) \cos \alpha_2 + (y_1 - y_2) \cos \gamma_2 + (z_1 - z_2) \cos \delta_2] dA_2 \quad (2-48)
 \end{aligned}$$

Now let

$$\left. \begin{aligned}
 l &= \cos \alpha \\
 m &= \cos \gamma \\
 n &= \cos \delta
 \end{aligned} \right\} \quad (2-49a)$$

and

$$f = \frac{(x_2 - x_1)l_1 + (y_2 - y_1)m_1 + (z_2 - z_1)n_1}{\pi S^4} \quad (2-49b)$$

Equation (2-48) can then be written in the abbreviated form

$$F_{d1-2} = \int_{A_2} [(x_1 - x_2)fl_2 + (y_1 - y_2)fm_2 + (z_1 - z_2)fn_2] dA_2 \quad (2-50)$$

Comparison of equation (2-50) with the right side of equation (2-45) shows that Stokes' theorem can be applied if

$$\frac{\partial R}{\partial y_2} - \frac{\partial Q}{\partial z_2} = (x_1 - x_2)f \quad (2-51a)$$

$$\frac{\partial P}{\partial z_2} - \frac{\partial R}{\partial x_2} = (y_1 - y_2)f \quad (2-51b)$$

and

$$\frac{\partial Q}{\partial x_2} - \frac{\partial P}{\partial y_2} = (z_1 - z_2)f \quad (2-51c)$$

Sparrow indicates (ref. 6) that useful solutions to these three equations are of the form

$$P = \frac{-m_1(z_2 - z_1) + n_1(y_2 - y_1)}{2\pi S^2} \quad (2-52a)$$

$$Q = \frac{l_1(z_2 - z_1) - n_1(x_2 - x_1)}{2\pi S^2} \quad (2-52b)$$

$$R = \frac{-l_1(y_2 - y_1) + m_1(x_2 - x_1)}{2\pi S^2} \quad (2-52c)$$

Equation (2-45) is used to express F_{d1-2} in equation (2-50) as a contour integral; that is,

$$F_{d1-2} = \oint_{C_2} (P dx_2 + Q dy_2 + R dz_2) \quad (2-53a)$$

Then P , Q , and R are substituted from equations (2-52), and the result is rearranged to obtain

$$\begin{aligned}
 F_{d1-2} = & \frac{l_1}{2\pi} \oint_{C_2} \frac{(z_2 - z_1) dy_2 - (y_2 - y_1) dz_2}{S^2} \\
 & + \frac{m_1}{2\pi} \oint_{C_3} \frac{(x_2 - x_1) dz_2 - (z_2 - z_1) dx_2}{S^2} \\
 & + \frac{n_1}{2\pi} \oint_{C_3} \frac{(y_2 - y_1) dx_2 - (x_2 - x_1) dy_2}{S^2} \quad (2-53b)
 \end{aligned}$$

The double integration over area A_2 has been replaced by a set of three line integrals for determination of F_{d1-2} . Sparrow (ref. 6) discusses the superposition properties of equation (2-50) that allow addition of the configuration factors of elements aligned parallel to the x -, y -, and z -axes to obtain the factors for arbitrary orientation.

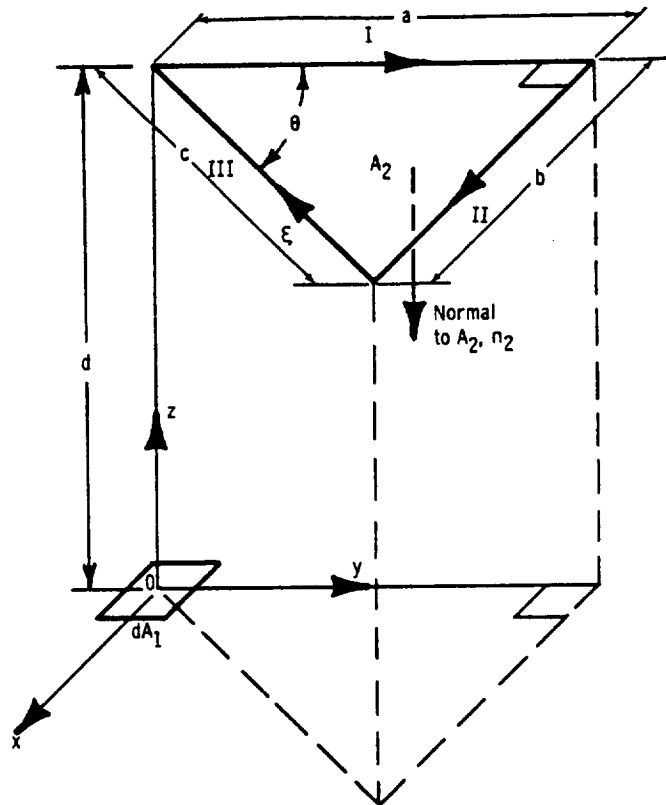


FIGURE 2-22. — Configuration factor between plane area element and right triangle in parallel plane.

EXAMPLE 2-17: Determine the configuration factor F_{d1-2} from an element dA_1 to a right triangle as shown in figure 2-22.

The normal to dA_1 is perpendicular to both the x - and y -axes and is thus parallel to z . The direction cosines for dA_1 are then

$$\cos \alpha_1 = l_1 = 0$$

$$\cos \gamma_1 = m_1 = 0$$

and

$$\cos \delta_1 = n_1 = 1$$

and equation (2-53b) becomes

$$F_{d1-2} = \frac{1}{2\pi} \oint_{C_2} \frac{(y_2 - y_1)dx_2 - (x_2 - x_1)dy_2}{S^2}$$

Since dA_1 is situated at the origin of the coordinate system, $x_1 = y_1 = 0$ and F_{d1-2} further reduces to

$$F_{d1-2} = \frac{1}{2\pi} \oint_{C_2} \frac{y_2 dx_2 - x_2 dy_2}{S^2}$$

The distance S between dA_1 and any point (x_2, y_2, z_2) on A_2 is

$$S^2 = x_2^2 + y_2^2 + z_2^2 = x_2^2 + y_2^2 + d^2$$

The contour integration of the configuration factor equation must now be carried out around the three sides of the right triangle. To keep the sign of F_{d1-2} positive, the integration is performed by traveling around the boundary lines I, II, and III in a particular direction. The correct direction is that of a person walking around the boundary with his head in the direction of the normal n_2 and always keeping A_2 to his left. Along boundary line I, $x_2 = 0$, $dx_2 = 0$, and $0 \leq y_2 \leq a$. On boundary II, $y_2 = a$, $dy_2 = 0$, $0 \leq x_2 \leq b$. On boundary III, the integration is from $\xi = 0$ to c where ξ is a coordinate along the hypotenuse of the triangle so that

$$x_2 = (c - \xi) \sin \theta$$

$$y_2 = (c - \xi) \cos \theta$$

and

$$dx_2 = -\sin \theta d\xi$$

$$dy_2 = -\cos \theta d\xi$$

Substituting these quantities into the integral for F_{d1-2} gives

$$\begin{aligned} 2\pi F_{d1-2} &= \oint_{C_1} \frac{y_2 dx_2 - x_2 dy_2}{S^2} \\ &= \oint_{I, II, III} \frac{y_2 dx_2 - x_2 dy_2}{x_2^2 + y_2^2 + d^2} \end{aligned}$$

$$\begin{aligned} 2\pi F_{d1-2} &= 0 + \int_{x_2=0}^b \frac{-a dx_2}{x_2^2 + a^2 + d^2} \\ &\quad + \int_{\xi=0}^c \frac{-(c-\xi) \cos \theta \sin \theta d\xi + (c-\xi) \sin \theta \cos \theta d\xi}{(c-\xi)^2 \sin^2 \theta + (c-\xi)^2 \cos^2 \theta + d^2} \end{aligned}$$

or

$$2\pi F_{d1-2} = \int_0^b \frac{a dx_2}{x_2^2 + a^2 + d^2}$$

Use of the integral tables gives

$$F_{d1-2} = \frac{a}{2\pi(a^2 + d^2)^{1/2}} \tan^{-1} \left[\frac{b}{(a^2 + d^2)^{1/2}} \right]$$

or, in dimensionless variables,

$$F_{d1-2} = \frac{X}{2\pi(1 + X^2)^{1/2}} \tan^{-1} \left[\frac{X \tan \theta}{(1 + X^2)^{1/2}} \right]$$

where $X = a/d$ and $\tan \theta = b/a$.

2.5.3.2.2 Configuration factor between finite areas: For configuration factors between two finite areas, substitute equation (2-53b) into equation (2-23) which gives

$$\begin{aligned}
A_1 F_{1-2} = A_2 F_{2-1} &= \int_{A_1} F_{d1-2} dA_1 \\
&= \frac{1}{2\pi} \oint_{C_2} \left[\int_{A_1} \frac{(y_2 - y_1)n_1 - (z_2 - z_1)m_1}{S^2} dA_1 \right] dx_2 \\
&+ \frac{1}{2\pi} \oint_{C_3} \left[\int_{A_1} \frac{(z_2 - z_1)l_1 - (x_2 - x_1)n_1}{S^2} dA_1 \right] dy_2 \\
&+ \frac{1}{2\pi} \oint_{C_3} \left[\int_{A_1} \frac{(x_2 - x_1)m_1 - (y_2 - y_1)l_1}{S^2} dA_1 \right] dz_2 \quad (2-54)
\end{aligned}$$

where the integrals have been rearranged and the dx_2 , dy_2 , and dz_2 factored out since these are independent of the area integration over A_1 .

Stokes' theorem is applied in turn to each of the three area integrals. Consider the first of the integrals

$$\int_{A_1} \frac{(y_2 - y_1)n_1 - (z_2 - z_1)m_1}{S^2} dA_1$$

and compare it with the area integral in Stokes' theorem equation (2-45). This gives

$$\begin{aligned}
\frac{\partial R}{\partial y_1} - \frac{\partial Q}{\partial z_1} &= 0 \\
\frac{\partial P}{\partial z_1} - \frac{\partial R}{\partial x_1} &= \frac{-(z_2 - z_1)}{S^2} \\
\frac{\partial Q}{\partial x_1} - \frac{\partial P}{\partial y_1} &= \frac{(y_2 - y_1)}{S^2}
\end{aligned}$$

A solution to this set of partial differential equations (ref. 6) is $P = \ln S$, $Q = 0$, and $R = 0$; and the area integral becomes, by use of equation (2-45) to convert it into a surface integral,

$$\int_{A_1} \frac{(y_2 - y_1)n_1 - (z_2 - z_1)m_1}{S^2} dA_1 = \oint_{C_1} \ln S dx_1$$

By applying Stokes' theorem in a similar fashion to the other two integrals in equation (2-54), it can be written as

$$A_1 F_{1-2} = \frac{1}{2\pi} \oint_{C_2} \left(\oint_{C_1} \ln S dx_1 \right) dx_2 + \frac{1}{2\pi} \oint_{C_2} \left(\oint_{C_1} \ln S dy_1 \right) dy_2 + \frac{1}{2\pi} \oint_{C_2} \left(\oint_{C_1} \ln S dz_1 \right) dz_2$$

or, more compactly,

$$F_{1-2} = \frac{1}{2\pi A_1} \oint_{C_1} \oint_{C_2} (\ln S dx_2 dx_1 + \ln S dy_2 dy_1 + \ln S dz_2 dz_1) \quad (2-55)$$

Thus the integrations over two areas which would involve integrating over four variables have been replaced by integrations over the two surface boundaries. This allows considerable computational savings when numerical evaluations must be carried out, and can sometimes result in analytical integration being possible where it could not be carried out for the quadruple integral over the areas.

EXAMPLE 2-18: Using the contour integration method, formulate the configuration factor for parallel rectangles as shown in figure 2-23.

Note that on both surfaces dz will be zero. First, integrate equation (2-55) around the boundary C_2 . The value of S to be used in equation (2-55) is measured from an arbitrary point $(x_1, y_1, 0)$ on A_1 to a point on the portion of the boundary C_2 being considered. This gives

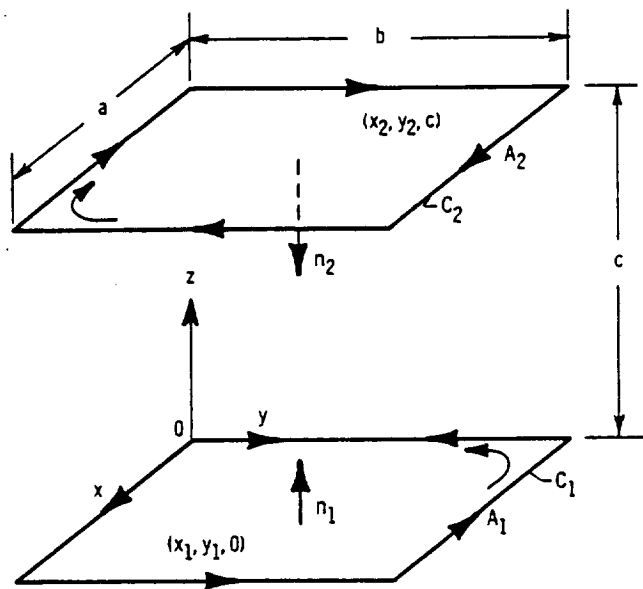


FIGURE 2-23.—Contour integration to determine configuration between two parallel plates.

$$\begin{aligned}
F_{1-2} = & \frac{1}{2\pi ab} \oint_{C_1} \left\{ \int_{y_2=0}^b \ln [x_1^2 + (y_2 - y_1)^2 + c^2]^{1/2} dy_2 \right. \\
& + \left. \int_{y_2=b}^0 \ln [(a - x_1)^2 + (y_2 - y_1)^2 + c^2]^{1/2} dy_2 \right\} dy_1 \\
& + \frac{1}{2\pi ab} \oint_{C_1} \left\{ \int_{x_2=0}^a \ln [(x_2 - x_1)^2 + (b - y_1)^2 + c^2]^{1/2} dx_2 \right. \\
& \left. + \int_{x_2=a}^0 \ln [(x_2 - x_1)^2 + y_1^2 + c^2]^{1/2} dx_2 \right\} dx_1
\end{aligned}$$

Then, carrying the integration out over C_1 gives, in this case, eight integrals. The first four, corresponding to the first two integrals of the previous equation, are written out as

$$\begin{aligned}
2\pi ab F_{1-2} = & \int_{y_1=0}^b \int_{y_2=0}^b \ln [a^2 + (y_2 - y_1)^2 + c^2]^{1/2} dy_2 dy_1 \\
& + \int_{y_1=b}^0 \int_{y_2=0}^b \ln [(y_2 - y_1)^2 + c^2]^{1/2} dy_2 dy_1 \\
& + \int_{y_1=0}^b \int_{y_2=b}^0 \ln [(y_2 - y_1)^2 + c^2]^{1/2} dy_2 dy_1 \\
& + \int_{y_1=b}^0 \int_{y_2=b}^0 \ln [a^2 + (y_2 - y_1)^2 + c^2]^{1/2} dy_2 dy_1 \\
& + (4 \text{ integral terms in } x) \\
= & \int_{y_1=0}^b \int_{y_2=0}^b \ln \left[\frac{a^2 + (y_2 - y_1)^2 + c^2}{(y_2 - y_1)^2 + c^2} \right] dy_2 dy_1 \\
& + \int_{x_1=0}^a \int_{x_2=0}^a \ln \left[\frac{(x_2 - x_1)^2 + b^2 + c^2}{(x_2 - x_1)^2 + c^2} \right] dx_2 dx_1
\end{aligned}$$

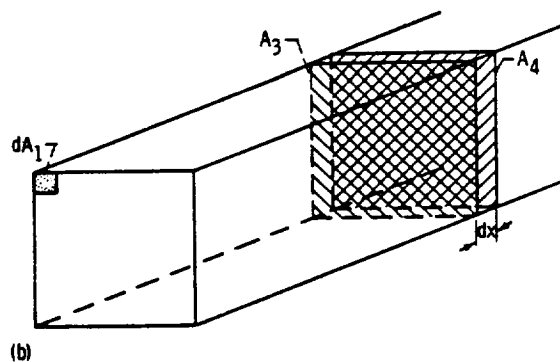
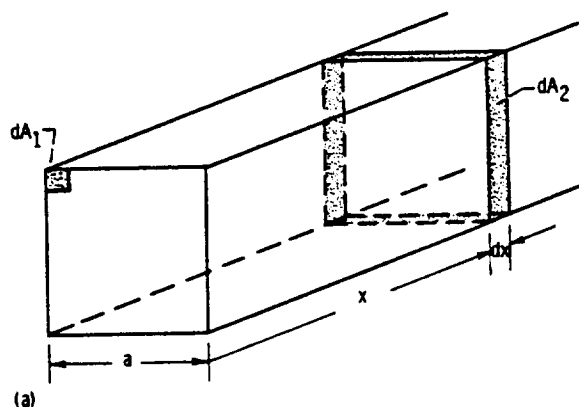
and the configuration factor is now given by the sum of two integrals. These can be integrated analytically by factoring the quadratic terms and using the relations governing log functions. This procedure results in a lengthy algebraic expression which will not be given here.

2.5.3.3 *Differentiation of known factors.*—A further extension of configuration factor algebra is the generation of configuration factors between differential elements by differentiating known factors between finite elements. This technique is very valuable in certain cases, and is best demonstrated by the use of an example problem.

EXAMPLE 2-19: As part of the determination of radiative exchange in a square channel whose temperature varies longitudinally, it is desired to find the configuration factor dF_{d1-d2} between an element dA_1 at one corner of the channel end and a differential length of wall section dA_2 as shown in figure 2-24(a).

Configuration factor algebra plus differentiation can be used to find the required factor. Refer to figure 2-24(b). Since the fraction of energy leaving dA_1 that reaches dA_2 is the difference between the fractions reaching the squares A_3 and A_4 , the factor dF_{d1-d2} is the difference between F_{d1-3} and F_{d1-4} . Then

$$dF_{d1-d2} = F_{d1-3} - F_{d1-4} = -\frac{\Delta F_{d1-4}}{\Delta x} \Delta x \Big|_{\Delta x \rightarrow 0} = -\frac{\partial F_{d1-4}}{\partial x} dx$$



(a) Configuration factor between dA_1 and differential length of channel wall dA_2 .

(b) Configuration factor between dA_1 and squares A_3 and A_4 .

FIGURE 2-24.—Derivation of configuration factor between differential length of square channel and element at corner of channel end.

Thus, if the configuration factor $F_{d_1-\square}$ between a corner element and a square in a parallel plane were known, the derivative of this factor with respect to the separation distance can be used to give the required factor.

From example 2-17, the configuration factor between a corner element and a parallel isosceles right triangle is given by setting $\tan \theta = 1$ in the expression derived for a general right triangle. This yields (for the present case where the distance $d = x$)

$$F_{d_1-\Delta} = \frac{a}{2\pi(a^2 + x^2)^{1/2}} \tan^{-1} \left[\frac{a}{(a^2 + x^2)^{1/2}} \right]$$

Inspection shows that, by symmetry, the factor between a corner element and a square is twice the factor $F_{d_1-\Delta}$. The required factor $dF_{d_1-d_2}$ is then

$$\begin{aligned} dF_{d_1-d_2} &= -\frac{\partial F_{d_1-\square}}{\partial x} dx = -\frac{adx}{\pi} \frac{\partial}{\partial x} \left\{ \frac{1}{(a^2 + x^2)^{1/2}} \tan^{-1} \left[\frac{a}{(a^2 + x^2)^{1/2}} \right] \right\} \\ &= \frac{ax dx}{\pi(a^2 + x^2)^{3/2}} \left\{ \tan^{-1} \left[\frac{a}{(a^2 + x^2)^{1/2}} \right] + \frac{a(a^2 + x^2)^{1/2}}{x^2 + 2a^2} \right\} \\ &= \frac{X dX}{\pi(1 + X^2)^{3/2}} \left\{ \tan^{-1} \left[\frac{1}{(1 + X^2)^{1/2}} \right] + \frac{(1 + X^2)^{1/2}}{2 + X^2} \right\} \end{aligned}$$

where $X = x/a$.

More generally, start with the configuration factor F_{1-2} for two parallel areas A_1 and A_2 that are cross sections of a cylindrical channel of arbitrary cross-sectional shape (fig. 2-25(a)). This factor depends on the spacing $|x_2 - x_1|$ between the two areas and includes blockage due to the channel wall (i.e., it is the factor by which A_2 is viewed from A_1 with the channel wall present). Note that for simple geometries, such as a circular tube or rectangular channel, the wall blockage is zero. The factor between A_1 and dA_2 in figure 2-25(b) is then given by

$$dF_{1-d_2} = -\frac{\partial F_{1-2}}{\partial x_2} dx_2 \quad (2-56)$$

as in example 2-19. Equation (2-56) will now be used to obtain $dF_{d_1-d_2}$, the configuration factor between the two differential area elements in figure 2-25(c).

By reciprocity

$$F_{d_2-1} = \frac{-A_1}{dA_2} \frac{\partial F_{1-2}}{\partial x_2} dx_2$$

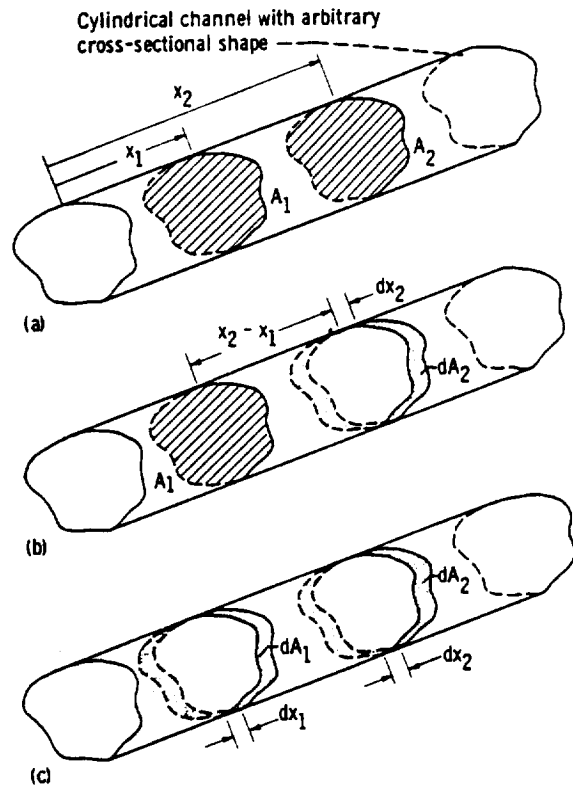


FIGURE 2-25. — Configuration factors for differential areas as derived by differentiation of factor for finite areas.

Then in a fashion similar to the derivation of equation (2-56)

$$dF_{a2-d1} = \frac{\partial F_{a2-d1}}{\partial x_1} dx_1$$

Substituting F_{a2-d1} results in

$$dF_{a2-d1} = -\frac{A_1}{dA_2} \frac{\partial^2 F_{1-2}}{\partial x_1 \partial x_2} dx_2 dx_1 \quad (2-57a)$$

or after using reciprocity

$$dF_{d1-d2} = -\frac{A_1}{dA_1} \frac{\partial^2 F_{1-2}}{\partial x_1 \partial x_2} dx_2 dx_1 \quad (2-57b)$$

Hence, by two differentiations the factor dF_{d1-d2} can be found from F_{1-2} for the cylindrical configuration under consideration.

2.6 COMPILATION OF REFERENCES FOR KNOWN CONFIGURATION FACTORS

Many configuration factors have been tabulated for specific geometries, and these tabulations are spread throughout the literature. Rather than attempt to gather the factors here, a feat that would require a separate volume of size equal to the present one, another course has been followed. In table I of appendix A, a list of geometries for which configuration factors are available and a reference list to aid in finding these factors are given. This provides a more useful general compilation than gathering only a limited number of factors here.

2.7 RADIATION EXCHANGE IN A BLACK ENCLOSURE

In the preceding parts of this chapter, the energy exchange between two separate surfaces or surface elements has been examined, and the concept of the configuration factor has been introduced. In this section, these ideas are generalized to consider the energy exchange within an enclosure composed of black surfaces that are individually isothermal.

In practice, the interior walls of a black enclosure, such as a furnace, may not be isothermal. In such a case, the various nonisothermal surfaces are subdivided into smaller portions that can be considered individually isothermal. The theory for a black enclosure, which is an ideal case, will serve as an introduction to less restrictive theory in succeeding chapters.

Perform a heat balance on a typical surface A_k (fig. 2-26). The energy supplied to A_k from an external source in order to maintain A_k at T_k is Q_k . The emission from A_k is $\sigma T_k^4 A_k$. The energy received by A_k from another surface A_j is $\sigma T_j^4 A_j F_{j-k}$. The heat balance is then

$$Q_k = \sigma T_k^4 A_k - \sum_{j=1}^N \sigma T_j^4 A_j F_{j-k} \quad (2-58)$$

where the summation includes energy arriving from all surfaces of the enclosure including A_k if A_k is concave. Equation (2-58) can be written in some alternate forms. Applying reciprocity to the terms in the summation results in

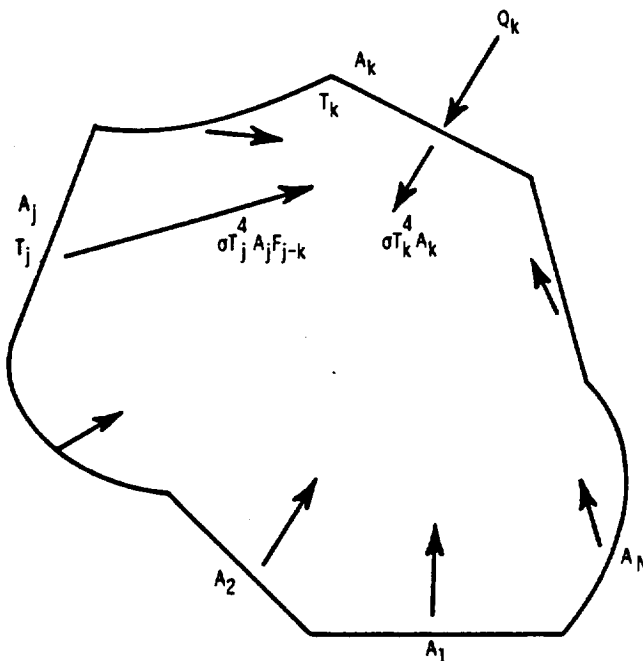


FIGURE 2-26. — Enclosure composed of N black isothermal surfaces (shown in cross section for simplicity).

$$Q_k = \sigma T_k^4 A_k - \sum_{j=1}^N \sigma T_j^4 A_k F_{k-j} \quad (2-59)$$

Also, for a complete enclosure, from equation (2-35)

$$\sum_{j=1}^N F_{k-j} = 1$$

so that

$$\begin{aligned} Q_k &= \sigma T_k^4 A_k \sum_{j=1}^N F_{k-j} - \sigma A_k \sum_{j=1}^N T_j^4 F_{k-j} \\ &= \sigma A_k \sum_{j=1}^N (T_k^4 - T_j^4) F_{k-j} \end{aligned} \quad (2-60)$$

This is in the form of a sum of exchanges between A_k and each surface.

EXAMPLE 2-20: The three-sided black enclosure of example 2-15 has its surfaces maintained at temperatures T_1 , T_2 , and T_3 , respectively. Determine the amount of energy that must be supplied to each surface per unit time in order to maintain these temperatures—this is also the net radiative loss from each surface.

Equation (2-60) is written for each surface as

$$Q_1 = A_1 F_{1-2} \sigma (T_1^4 - T_2^4) + A_1 F_{1-3} \sigma (T_1^4 - T_3^4)$$

$$Q_2 = A_2 F_{2-1} \sigma (T_2^4 - T_1^4) + A_2 F_{2-3} \sigma (T_2^4 - T_3^4)$$

$$Q_3 = A_3 F_{3-1} \sigma (T_3^4 - T_1^4) + A_3 F_{3-2} \sigma (T_3^4 - T_2^4)$$

The configuration factors have been found for this geometry in example 2-15. Thus all factors on the right of this set of equations are known, and the Q values may be computed directly.

A check for a numerical computation is that from overall energy conservation, the net Q added to the entire enclosure must be zero in order to maintain steady-state temperatures. This is also shown by using reciprocal relations on the set of Q equations to obtain

$$\begin{aligned} \sum_{k=1}^3 Q_k &= [A_1 F_{1-2} \sigma (T_1^4 - T_2^4) + A_1 F_{1-3} \sigma (T_1^4 - T_3^4)] \\ &\quad + [A_1 F_{1-2} \sigma (T_2^4 - T_1^4) + A_2 F_{2-3} \sigma (T_2^4 - T_3^4)] \\ &\quad + [A_1 F_{1-3} \sigma (T_3^4 - T_1^4) + A_2 F_{2-3} \sigma (T_3^4 - T_2^4)] \\ &= 0 \end{aligned}$$

EXAMPLE 2-21: The enclosure of example 2-15 has two of its sides maintained at temperatures T_1 and T_2 , respectively. The third side is an insulated (adiabatic) surface, $Q_3 = 0$. Determine Q_1 , Q_2 , and T_3 .

Again equation (2-60) can be written for each surface as

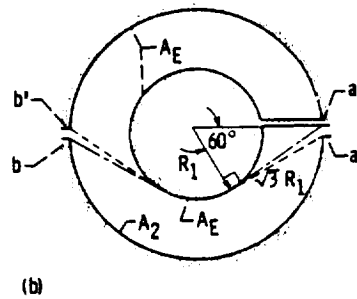
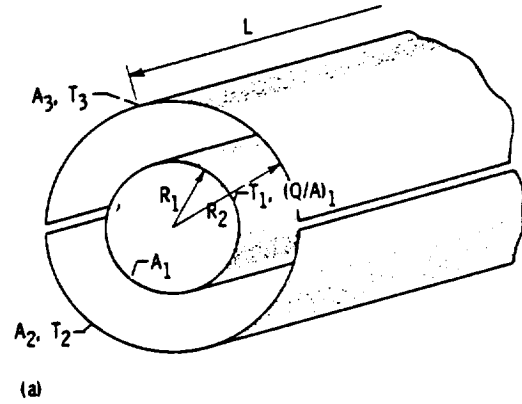
$$Q_1 = A_1 F_{1-2} \sigma (T_1^4 - T_2^4) + A_1 F_{1-3} \sigma (T_1^4 - T_3^4)$$

$$Q_2 = A_2 F_{2-1} \sigma (T_2^4 - T_1^4) + A_2 F_{2-3} \sigma (T_2^4 - T_3^4)$$

$$0 = A_3 F_{3-1} \sigma (T_3^4 - T_1^4) + A_3 F_{3-2} \sigma (T_3^4 - T_2^4)$$

The final equation is solved for T_3 , the only unknown in that equation. This T_3 is then inserted into the first two equations to give Q_1 and Q_2 .

EXAMPLE 2-22: A very long black heated tube A_1 of length L is enclosed by a concentric black split cylinder as shown in figure 2-27. The diameter of the split cylinder is twice that of the heated tube, and one-half as much energy *flux* is to be removed from the upper area A_3 of the split cylinder as from the lower area A_2 . If $T_1 = 3000^\circ \text{R}$ and a



(a) Geometry of enclosure.

(b) Auxiliary construction to determine F_{2-1} .FIGURE 2-27. — Radiant energy exchange in split-circular cylinder configuration, $L \gg R_2$.

heat flux $Q_1/A_1 = 10^5$ Btu/(hr)(sq ft) is supplied to the heated tube, what are the values of T_2 , T_3 , Q_2 , and Q_3 ? Neglect the effect of the tube ends.

Writing equation (2-60) for each surface gives

$$Q_1 = A_1 F_{1-2} \sigma (T_1^4 - T_2^4) + A_1 F_{1-3} \sigma (T_1^4 - T_3^4)$$

$$Q_2 = A_2 F_{2-1} \sigma (T_2^4 - T_1^4) + A_2 F_{2-3} \sigma (T_2^4 - T_3^4)$$

$$Q_3 = A_3 F_{3-1} \sigma (T_3^4 - T_1^4) + A_3 F_{3-2} \sigma (T_3^4 - T_2^4)$$

From the geometry

$$\frac{A_1}{A_3} = \frac{A_1}{A_2} = \frac{\pi D_1 L}{\frac{1}{2} \pi D_2 L} = 1$$

since $D_2 = 2D_1$. From an energy balance

$$Q_1 + Q_2 + Q_3 = 0$$

and, since $A_1 = A_2 = A_3$,

$$\frac{Q_1}{A_1} + \frac{Q_2}{A_2} + \frac{Q_3}{A_3} = 0$$

From the statement of the problem,

$$\frac{Q_3}{A_3} = \frac{1}{2} \frac{Q_2}{A_2}$$

and this yields

$$\frac{Q_2}{A_2} = -\frac{2}{3} \frac{Q_1}{A_1} = -0.667 \times 10^5 \text{ Btu/(hr)(sq ft)}$$

$$\frac{Q_3}{A_3} = -\frac{1}{3} \frac{Q_1}{A_1} = -0.333 \times 10^5 \text{ Btu/(hr)(sq ft)}$$

From the symmetry of the geometry and configuration factor algebra, it is known that

$$F_{1-2} = F_{1-3} = \frac{1}{2}$$

$$F_{2-1} = F_{3-1} = \frac{A_1 F_{1-3}}{A_3} = \frac{1}{2}$$

and

$$F_{2-3} = F_{3-2}$$

To determine F_{2-3} it is known that

$$F_{2-1} + F_{2-2} + F_{2-3} = 1$$

Using $F_{2-1} = 1/2$ gives

$$F_{2-3} = \frac{1}{2} - F_{2-2}$$

In the auxiliary construction of figure 2-27(b)

$$F_{2-2} = 1 - F_{2-E}$$

The effective area A_E has been drawn in to leave unchanged the view of surface 2 to itself and to simplify the geometry so that the crossed string method can be used to determine F_{2-E} . The uncrossed strings extending from $a-a'$ and $b-b'$ have zero length. The crossed strings extend from $a-b'$ and $a'-b$, and each has the length $2\sqrt{3}R_1 + (\pi R_1/3)$. Then, from section 2.5.3.1 and the fact that $A_2 = A_1 = 2\pi R_1$,

$$F_{2-E} = \frac{2\sqrt{3}R_1 + \frac{\pi R_1}{3}}{2\pi R_1} = \frac{\sqrt{3}}{\pi} + \frac{1}{6}$$

It then follows

$$F_{2-3} = \frac{1}{2} - F_{2-2} = \frac{1}{2} - (1 - F_{2-E}) = \frac{\sqrt{3}}{\pi} - \frac{1}{3} = 0.218$$

With this information, the energy exchange equations can now be written as

$$\begin{aligned} 10^8 &= \frac{\sigma}{2} (3000^4 - T_2^4) + \frac{\sigma}{2} (3000^4 - T_3^4) \\ -0.667 \times 10^8 &= \frac{\sigma}{2} (T_2^4 - 3000^4) + 0.218\sigma (T_2^4 - T_3^4) \\ -0.333 \times 10^8 &= \frac{\sigma}{2} (T_3^4 - 3000^4) + 0.218\sigma (T_3^4 - T_2^4) \end{aligned}$$

Adding the second and third equations results in the first, so only two of the equations are independent. Solving the first and second equations gives $T_2 = 1890^\circ \text{R}$ and $T_3 = 2400^\circ \text{R}$.

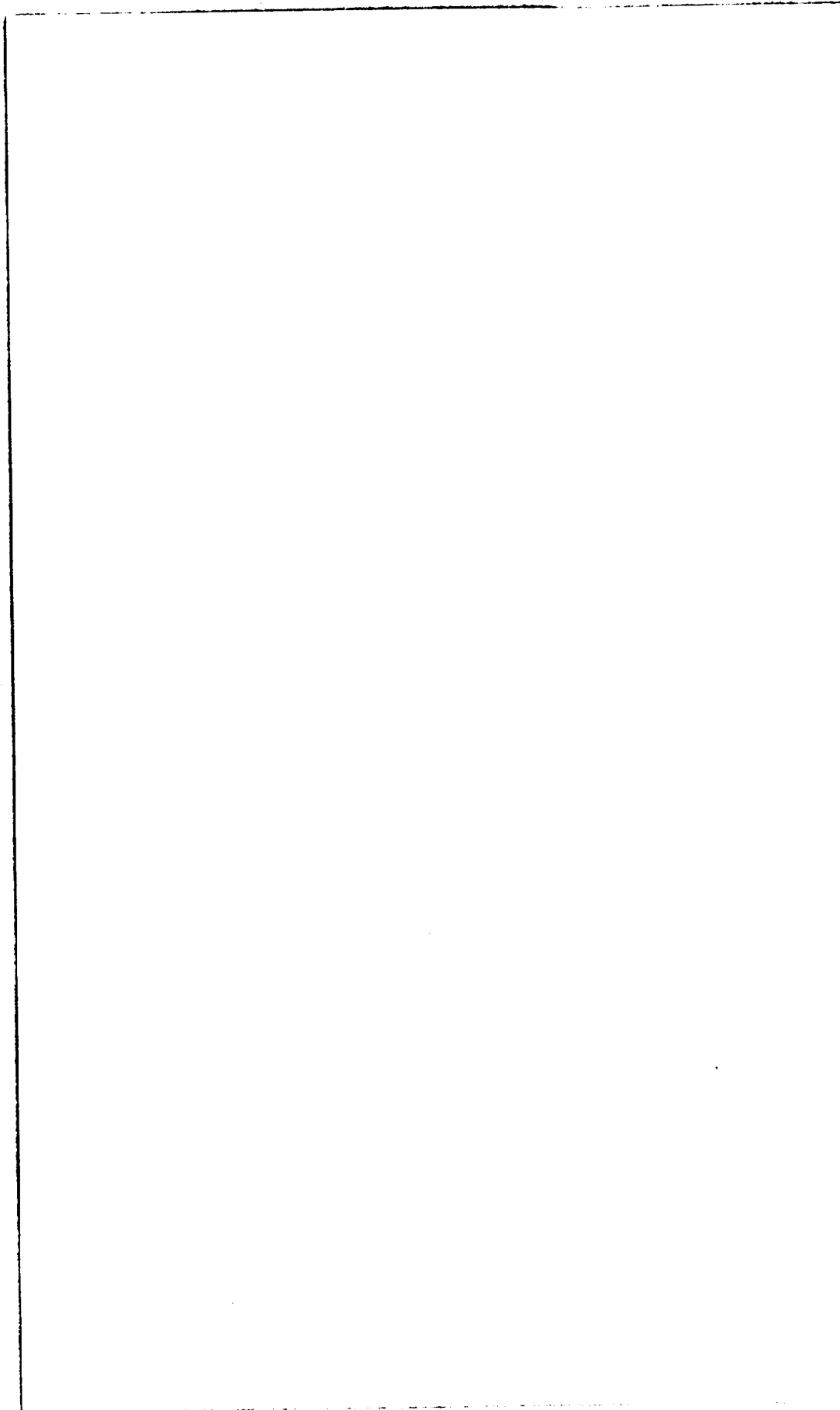
2.8 CONCLUDING REMARKS

In this chapter, methods have been introduced and developed for the computation of energy exchange between isothermal black surfaces and in enclosures consisting of individual isothermal black surfaces. The radiant interchange between individual isothermal black surfaces can be treated by reasonably straightforward techniques. The chief difficulties in such problems are not in the concepts involved, but are rather in the geometrical and algebraic manipulations plus the integrations that must be carried out to determine the configuration factors for specific geometries. These difficulties are minimized by the availability in the literature of fairly extensive formulas, graphs, and tabulations of configuration factors that have already been calculated. References to the sources of these factors are given in table A-I of appendix A.

For practical radiation computations, the assumption of black surfaces is quite restrictive. Hence, the results given here have limited direct application; there may be some instances, such as within certain furnaces, where a black computation will yield reasonable results. The black computation theory, in spite of its limitations, serves two important functions. First, it is a limiting case with which nonblack performance and computations can be compared. It provides a good numerical check for problems in which a parametric study is being made wherein the radiation properties are varied over a range of values. The second function is that the black case provides a foundation for more general exchange and enclosure theories. In succeeding chapters, the approach used in this chapter will be adapted and extended for problems that deal with more complicated effects such as nonblack and nonisothermal surfaces.

REFERENCES

1. SIEGEL, ROBERT; AND HOWELL, JOHN R.: Thermal Radiation Heat Transfer. I—The Blackbody, Electromagnetic Theory, and Material Properties. NASA SP-164, 1968.
2. FEINGOLD, A.: Radiation-Interchange Configuration Factors Between Various Selected Plane Surfaces. Proc. Roy. Soc., Ser. A, vol. 292, no. 1428, May 3, 1966, pp. 51-60.
3. HOTTEL, H. C.: Radiant Heat Transmission. Heat Transmission. Third ed., William H. McAdams, McGraw-Hill Book Co., Inc., 1954, ch. 4.
4. MOON, PARRY: The Scientific Basis of Illuminating Engineering. Rev. ed., Dover Publications, Inc., 1961.
5. SPARROW, E. M.; AND CESS, R. D.: Radiation Heat Transfer. Brooks/Cole Publishing Co., 1966.
6. SPARROW, E. M.: A New and Simpler Formulation for Radiative Angle Factors. J. Heat Transfer, vol. 85, no. 2, May 1963, pp. 81-88.



PRECEDING PAGE BLANK NOT FILMED.

Chapter 3. Radiation Exchange in an Enclosure Composed of Diffuse-Gray Surfaces

3.1 INTRODUCTION

3.1.1 Restrictions in the Analysis

In the previous chapter an enclosure composed of black surfaces was considered. As a next step in building toward more complex treatments that can account for the real property behavior of surfaces, the surfaces of the enclosure will now be taken as both *diffuse and gray*. In chapter 3 of Vol. I, the relations between emissivity and absorptivity are discussed. By definition, when a surface is diffuse-gray, the directional spectral emissivity and absorptivity do not depend on either angle or wavelength, but can depend on surface temperature. As a result of this definition, at any surface temperature T_A the hemispherical total absorptivity and emissivity are equal and depend only on T_A ; that is, $\alpha(T_A) = \epsilon(T_A)$. Even though this behavior is approached by only a limited number of real materials, the diffuse-gray approximation is often made to simplify greatly the enclosure theory.

Some comment is warranted as to what is meant by the individual "surfaces" or "areas" that comprise the total enclosure boundary. Usually, the geometry will tend to divide the enclosure into natural surface areas, such as the individual sides of a rectangular prism enclosure. In addition, it may be necessary to specify surface areas on the basis of heating conditions; for example, if one side of an enclosure is partly at one temperature and partly at a second temperature, the side would be divided into two separate areas so that this difference in boundary condition could be accounted for. Hence, the "surfaces" or "areas" discussed in the radiation analysis are simply each separate portion of the enclosure boundary for which a heat balance is formed. These portions are selected on the basis of geometry and imposed heating conditions. A further consideration is the accuracy of the solution. If too few areas are designated, the accuracy will be poor; too many areas will require excessive computational time. Thus some engineering judgment is required in selecting both the shape of the surfaces and their number.

Surfaces of the enclosure can have various thermal boundary conditions imposed upon them. A given surface can be held at a specified temperature, have a specified imposed heat input, or be perfectly insulated (i.e., specified heat input = 0). It is a restriction in the present analysis

that, whatever conditions are imposed, each separate surface of the enclosure must be at a uniform temperature. If the imposed heating conditions are such that the temperature would vary markedly over an area, the area should be subdivided into smaller more nearly isothermal portions; these portions can be of differential size if necessary. As a consequence of this isothermal area requirement, the emitted energy is taken to be uniform over each surface of the enclosure.

Because a gray surface is not a perfect absorber (i.e., its absorptivity is less than unity rather than unity, as for the black case considered in chapter 2), part of the energy incident on a surface is reflected. With regard to the reflected energy, two assumptions are made: (1) the reflected energy is diffuse, that is, the reflected intensity at each position on the boundary is uniform for all directions and (2) the reflected energy is uniform over each surface of the enclosure. If the reflected energy is expected to vary over an area, the area should be subdivided into smaller areas over which the reflected energy will not vary too much. With these restrictions reasonably met, the reflected energy for each surface has the same diffuse and uniformly distributed character as the emitted energy. Hence, the reflected and emitted energy can be combined into a single energy quantity leaving the surface.

When a surface is both diffusely emitting and reflecting, the intensity of all the energy leaving the surface does not vary with angular direction. As a result, the geometric configuration factors (F factors) derived for black surfaces can be used for the present enclosure theory. It is well to emphasize that the derivation of the F factors in chapter 2 for black surfaces was based on the condition of a diffuse uniform intensity leaving the surface; this diffuse-uniform condition must be true for both the emitted and reflected energies in order to use the F factors for a nonblack surface.

Most of the problems encountered in practice are at steady state. However, the radiative heat balances considered here are not limited to steady-state conditions. The radiative balances can be directly applied to situations where transient temperature changes are occurring. Instantaneously, the heat flux q that will be computed in the enclosure theory that follows can be considered as the net radiative loss from the location being considered on the enclosure boundary. For example, if a solid body is cooling by radiation, q provides the boundary condition for the transient heat conduction solution for the temperature distribution within the solid.

3.1.2 Summary of Restrictions

The assumptions for the present chapter are now summarized. The enclosure boundary is divided into areas so that over each of these areas the following restrictions are met:

- (1) The temperature is uniform.
- (2) The ϵ'_λ , α'_λ , and ρ'_λ are independent of wavelength and direction so that $\epsilon(T_A) = \alpha(T_A) = 1 - \rho(T_A)$ where ρ is the reflectivity.
- (3) All energy is emitted and reflected diffusely.
- (4) The incident, and hence reflected energy flux, is uniform over each individual area.

In some instances an analysis assuming diffuse-gray surfaces cannot yield good results. For example, if the temperatures of the individual surfaces of the enclosure differ considerably from each other, then a surface will be emitting predominantly in the range of wavelengths characteristic of its temperature while receiving energy predominantly in a different wavelength region. If the spectral emissivity varies with wavelength, the fact that the incident radiation has a different spectral distribution than the emitted energy will make the gray assumption invalid, that is, $\epsilon(T_A) \neq \alpha(T_A)$. When polished (specular) surfaces are present, the diffuse reflecting assumption will be invalid, and the directional paths of the reflected energy must be considered. The treatment of specular and other more general surfaces are the subjects of chapters 4, 5, and 6.

3.2 SYMBOLS

A	area
\mathcal{A}	inverse matrix coefficients, eq. (3-29)
dA^*	differential element on same surface area as dA
a_{kj}	matrix elements defined by eq. (3-25)
a^{-1}	inverse matrix
C_{kj}	matrix elements defined by eq. (3-25)
D	diameter of tube or hole
F	configuration factor
G	function in integral eq. (3-57)
J	auxiliary variational function, eq. (3-58)
j, k	indices denoting individual surfaces
K	kernel of integral equation
L	length of surface
l	dimensionless length
M_{kj}	minor of matrix element a_{kj}
N	number of surfaces in enclosure
Q	energy per unit time
q	energy flux; energy per unit area and time
R	radius of sphere
\bar{r}	direction vector
S	distance between areas
T	absolute temperature

x, y, z	coordinates
α	absorptivity
β	cone angle; angle from normal of surface
γ	polynomial coefficients, eq. (3-59)
δ	Kronecker delta
ϵ	emissivity
ξ, η	dimensionless coordinates
ρ	reflectivity
σ	Stefan-Boltzmann constant
φ	dependent variable in integral equation, eq. (3-57)

Subscripts:

A	area
a	apparent value
<i>black</i>	blackbody property
e	external radiation entering through opening; environment
i	incoming
j, k	property of surface j or k
o	outgoing
s	sphere
λ	spectrally (wavelength) dependent
1, 2	surface 1 or 2

Superscript:

quantity in one direction

3.3 RADIATION BETWEEN FINITE AREAS

3.3.1 Net Radiation Method

Consider an enclosure composed of N discrete surface areas as shown in figure 3-1. The objectives of the analysis will be to analyze the radiation exchange between the surface areas for problems involving two types of boundary conditions: (1) the required energy supplied to a surface is to be determined when the surface temperature is specified, and (2) the temperature that a surface will achieve is to be found when a known heat input is imposed.

There is a complex radiative exchange occurring inside the enclosure as radiation leaves a surface, travels to the other surfaces, is partially reflected, and is then rereflected many times within the enclosure with partial absorption at each contact with a surface. It would be very complicated to follow the beams of radiation as they undergo this process; fortunately, it is not necessary to do this. An analysis can be formulated in a convenient manner by using the "net radiation method." This method was first devised by Hottel (ref. 1) and later presented in a different man-

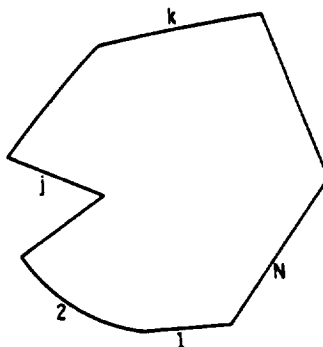


FIGURE 3-1. — Enclosure composed of N discrete surface areas with typical surfaces j and k (shown in cross section for simplicity).

ner by Poljak (refs. 2 and 3). An alternate approach was given by Gebhart (ref. 4). All of the methods are basically equivalent (as demonstrated in ref. 5); the Poljak approach, which the present authors generally prefer, will be given in this chapter. The Gebhart method is briefly presented in appendix B.

Consider the k th surface having area A_k of the enclosure shown in figures 3-1 and 3-2. The quantities q_i and q_o are the rates of incoming and outgoing radiant energy per unit surface area, respectively. The quantity q is the energy flux supplied by some external means to the surface to make up for the net radiative loss and thereby maintain the specified surface temperature. A heat balance at the surface provides the relation

$$Q_k = q_k A_k = (q_{o,k} - q_{i,k}) A_k \quad (3-1)$$

A second equation results from the fact that the energy flux leaving

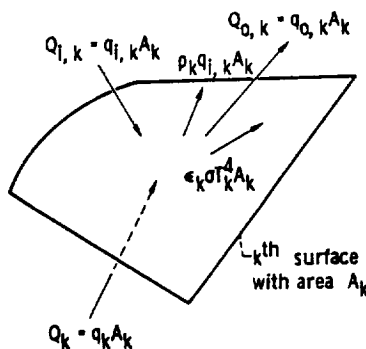


FIGURE 3-2. — Energy quantities incident upon and leaving typical surface of enclosure.

the surface is composed of directly emitted plus reflected energy. This gives

$$\begin{aligned} q_{o,k} &= \epsilon_k \sigma T_k^4 + \rho_k q_{i,k} \\ &= \epsilon_k \sigma T_k^4 + (1 - \epsilon_k) q_{i,k} \end{aligned} \quad (3-2)$$

where the relations $\rho_k = 1 - \alpha_k = 1 - \epsilon_k$ have been used for opaque gray surfaces. The term "radiosity" is often used for the quantity q_o . The incident flux $q_{i,k}$ is derived from the portions of the energy leaving the surfaces of the enclosure that arrive at the k th surface. If the k th surface can view itself (is concave), a portion of its outgoing flux will contribute directly to its incident flux. The incident energy is then equal to

$$\begin{aligned} A_k q_{i,k} &= A_1 q_{o,1} F_{1-k} + A_2 q_{o,2} F_{2-k} + \dots + A_j q_{o,j} F_{j-k} \\ &+ \dots + A_k q_{o,k} F_{k-k} + \dots + A_N q_{o,N} F_{N-k} \end{aligned} \quad (3-3)$$

From the configuration factor reciprocity relation (eq. (2-25)),

$$\left. \begin{aligned} A_1 F_{1-k} &= A_k F_{k-1} \\ A_2 F_{2-k} &= A_k F_{k-2} \\ \dots &\dots \dots \dots \\ A_N F_{N-k} &= A_k F_{k-N} \end{aligned} \right\} \quad (3-4)$$

Then equation (3-3) can be written so that the only area appearing is A_k

$$\begin{aligned} A_k q_{i,k} &= A_k F_{k-1} q_{o,1} + A_k F_{k-2} q_{o,2} + \dots + A_k F_{k-j} q_{o,j} \\ &+ \dots + A_k F_{k-k} q_{o,k} + \dots + A_k F_{k-N} q_{o,N} \end{aligned} \quad (3-5a)$$

or

$$q_{i,k} = \sum_{j=1}^N F_{k-j} q_{o,j} \quad (3-5b)$$

Equations (3-2) and (3-5) provide two different expressions for $q_{i,k}$. These are each substituted into equation (3-1) to eliminate $q_{i,k}$ and provide these two basic heat balance equations for Q_k in terms of $q_{o,k}$,

$$Q_k = A_k \frac{\epsilon_k}{1 - \epsilon_k} (\sigma T_k^4 - q_{o,k}) \quad (3-6)$$

$$Q_k = A_k \left(q_{o,k} - \sum_{j=1}^N F_{k-j} q_{o,j} \right) \quad (3-7)$$

where Q_k can be regarded as either the energy supplied to the surface k by external means or the net radiative loss from surface k .

As a first step in becoming familiar with this radiation analysis, consider that equations (3-6) and (3-7) can be written for each of the N surfaces in the enclosure. This provides $2N$ equations for $2N$ unknowns. The q_o 's will be N of the unknowns. The remaining unknowns will consist of Q 's and T 's depending on what boundary quantities are specified. As will be shown later, the q_o 's can be eliminated giving N equations relating the N unknown Q 's and T 's.

Some examples will now be given to illustrate the use of equations (3-6) and (3-7) as a system of simultaneous equations.

EXAMPLE 3-1: Derive the expression for heat exchange between two infinite parallel flat plates in terms of their temperatures T_1 and T_2 ($T_1 > T_2$) (fig. 3-3).

Since all the radiation leaving one plate will arrive at the other plate, the configuration factors are $F_{1-2} = F_{2-1} = 1$. Equations (3-6) and (3-7) are then written for each plate

$$\frac{Q_1}{A_1} = q_1 = \frac{\epsilon_1}{1 - \epsilon_1} (\sigma T_1^4 - q_{o,1}) \quad (3-8a)$$

$$\frac{Q_1}{A_1} = q_1 = q_{o,1} - q_{o,2} \quad (3-8b)$$

$$\frac{Q_2}{A_2} = q_2 = \frac{\epsilon_2}{1 - \epsilon_2} (\sigma T_2^4 - q_{o,2}) \quad (3-9a)$$

$$\frac{Q_2}{A_2} = q_2 = q_{o,2} - q_{o,1} \quad (3-9b)$$

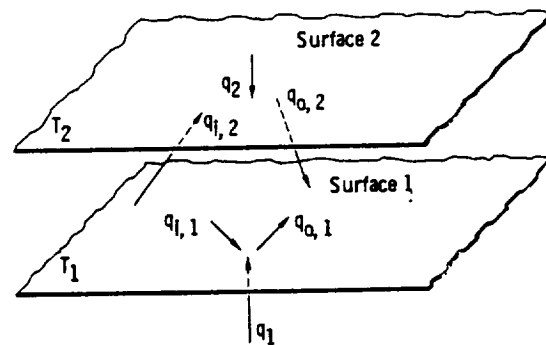


FIGURE 3-3. — Heat fluxes for radiant interchange between infinite parallel flat plates.

By comparing equations (3-8b) and (3-9b), it is evident that $q_1 = -q_2$ so that the heat added to surface 1 is removed from surface 2. The flux q_1 is thus the net heat exchange from 1 to 2 requested in the problem statement. Equation (3-8a) is solved for $q_{o,1}$

$$q_{o,1} = \sigma T_1^4 - \frac{(1 - \epsilon_1)}{\epsilon_1} q_1$$

Similarly, from equation (3-9a)

$$q_{o,2} = \sigma T_2^4 - \frac{(1 - \epsilon_2)}{\epsilon_2} q_2 = \sigma T_2^4 + \frac{(1 - \epsilon_2)}{\epsilon_2} q_1$$

These are substituted into equation (3-8b) and the result solved for q_1

$$q_1 = -q_2 = \frac{\sigma(T_1^4 - T_2^4)}{\frac{1}{\epsilon_1(T_1)} + \frac{1}{\epsilon_2(T_2)} - 1} \quad (3-10)$$

The functional notation $\epsilon(T)$ has been introduced to emphasize that ϵ_1 and ϵ_2 can be functions of temperature. Since T_1 and T_2 are specified, the ϵ_1 and ϵ_2 can be evaluated at their proper temperatures and q_1 directly calculated.

EXAMPLE 3-2: For the parallel plate geometry of the previous example, what temperature will surface 1 reach for a given heat input q_1 while T_2 is held at a specified value?

Equation (3-10) still applies and when solved for T_1 gives

$$T_1 = \left\{ \frac{q_1}{\sigma} \left[\frac{1}{\epsilon_1(T_1)} + \frac{1}{\epsilon_2(T_2)} - 1 \right] + T_2^4 \right\}^{1/4} \quad (3-11)$$

Since the emissivity $\epsilon_1(T_1)$ is a function of T_1 which is unknown, an iterative solution is necessary. A trial T_1 is selected, and then ϵ_1 is chosen at this value. Equation (3-11) is then solved for T_1 , and this value is used to select ϵ_1 for the next approximation. The process is continued until $\epsilon_1(T_1)$ and T_1 no longer change with further iterations.

EXAMPLE 3-3: Derive an expression for the radiation exchange between two uniform temperature concentric diffuse-gray spheres as shown in figure 3-4.

This situation is more complicated than the parallel plate geometry as the two surfaces have unequal areas and surface 2 can partially view itself. The configuration factors for this case were derived in example

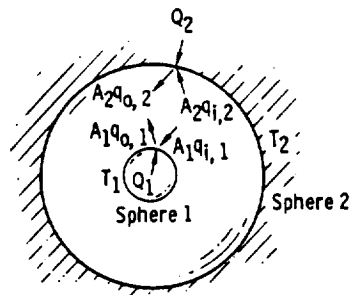


FIGURE 3-4.—Energy quantities for radiant interchange between two concentric spheres.

2-13 and were found to be $F_{1-2} = 1$, $F_{2-1} = A_1/A_2$, and $F_{2-2} = 1 - (A_1/A_2)$. The basic heat balance equations (eqs. (3-6) and (3-7)) are now written for each of the two sphere surfaces

$$Q_1 = A_1 \frac{\epsilon_1}{1 - \epsilon_1} (\sigma T_1^4 - q_{o,1}) \quad (3-12a)$$

$$Q_1 = A_1 (q_{o,1} - q_{o,2}) \quad (3-12b)$$

$$Q_2 = A_2 \frac{\epsilon_2}{1 - \epsilon_2} (\sigma T_2^4 - q_{o,2}) \quad (3-13a)$$

$$\begin{aligned} Q_2 &= A_2 \left[q_{o,2} - \frac{A_1}{A_2} q_{o,1} - \left(1 - \frac{A_1}{A_2} \right) q_{o,2} \right] \\ &= A_1 (-q_{o,1} + q_{o,2}) \end{aligned} \quad (3-13b)$$

Comparing equations (3-12b) and (3-13b) reveals that $Q_1 = -Q_2$, as would be expected from an overall heat balance on the system. The four equations (3-12) and (3-13) can be solved for the four unknowns $q_{o,1}$, $q_{o,2}$, Q_1 , and Q_2 . This yields the net heat exchange (supplied to surface 1 and removed at surface 2)

$$Q_1 = \frac{A_1 \sigma (T_1^4 - T_2^4)}{\frac{1}{\epsilon_1(T_1)} + \frac{A_1}{A_2} \left[\frac{1}{\epsilon_2(T_2)} - 1 \right]} \quad (3-14)$$

For a case when the spheres in example 3-3 are not concentric, all the radiation leaving surface 1 is still incident on surface 2. The view factor F_{1-2} is again 1 and with the use of the same assumptions, the analysis would follow as before, leading to equation (3-14). However, when sphere 1 is relatively small (e.g., one-half the diameter of sphere 2)

and the eccentricity is large, the geometric appearance of the system is so different from the concentric case that using equation (3-14) would seem intuitively incorrect. The error in using equation (3-14) is that it was derived on the basis that q , q_i , and q_o are uniform over each of A_1 and A_2 . These conditions are exactly met only for the concentric case.

EXAMPLE 3-4: Consider a long enclosure made up of three surfaces as shown in figure 3-5. The enclosure is long enough so that the ends can be neglected in the radiative heat balances. How much heat has to

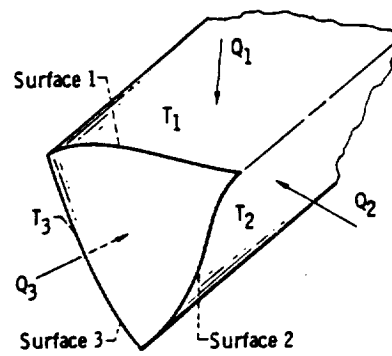


FIGURE 3-5.—Long enclosure composed of three surfaces (ends neglected).

be supplied to each surface (equal to the net radiative heat loss from each surface) to maintain the surfaces at temperatures T_1 , T_2 , and T_3 ?

To solve this problem, write equations (3-6) and (3-7) for each of the three surfaces

$$\frac{Q_1}{A_1} = \frac{\epsilon_1}{1 - \epsilon_1} (\sigma T_1^4 - q_{o,1}) \quad (3-15a)$$

$$\frac{Q_1}{A_1} = q_{o,1} - F_{1-1}q_{o,1} - F_{1-2}q_{o,2} - F_{1-3}q_{o,3} \quad (3-15b)$$

$$\frac{Q_2}{A_2} = \frac{\epsilon_2}{1 - \epsilon_2} (\sigma T_2^4 - q_{o,2}) \quad (3-16a)$$

$$\frac{Q_2}{A_2} = q_{o,2} - F_{2-1}q_{o,1} - F_{2-2}q_{o,2} - F_{2-3}q_{o,3} \quad (3-16b)$$

$$\frac{Q_3}{A_3} = \frac{\epsilon_3}{1 - \epsilon_3} (\sigma T_3^4 - q_{o,3}) \quad (3-17a)$$

$$\frac{Q_3}{A_3} = q_{o,3} - F_{3-1}q_{o,1} - F_{3-2}q_{o,2} - F_{3-3}q_{o,3} \quad (3-17b)$$

The first equation of each of these three pairs of equations can be solved for q_o in terms of T and Q . These q_o 's are then substituted into the second equation of each pair to obtain

$$\frac{Q_1}{A_1} \left(\frac{1}{\epsilon_1} - F_{1-1} \frac{1-\epsilon_1}{\epsilon_1} \right) - \frac{Q_2}{A_2} F_{1-2} \frac{1-\epsilon_2}{\epsilon_2} - \frac{Q_3}{A_3} F_{1-3} \frac{1-\epsilon_3}{\epsilon_3} \\ = (1 - F_{1-1})\sigma T_1^4 - F_{1-2}\sigma T_2^4 - F_{1-3}\sigma T_3^4 \quad (3-18a)$$

$$-\frac{Q_1}{A_1} F_{2-1} \frac{1-\epsilon_1}{\epsilon_1} + \frac{Q_2}{A_2} \left(\frac{1}{\epsilon_2} - F_{2-2} \frac{1-\epsilon_2}{\epsilon_2} \right) - \frac{Q_3}{A_3} F_{2-3} \frac{1-\epsilon_3}{\epsilon_3} \\ = -F_{2-1}\sigma T_1^4 + (1 - F_{2-2})\sigma T_2^4 - F_{2-3}\sigma T_3^4 \quad (3-18b)$$

$$-\frac{Q_1}{A_1} F_{3-1} \frac{1-\epsilon_1}{\epsilon_1} - \frac{Q_2}{A_2} F_{3-2} \frac{1-\epsilon_2}{\epsilon_2} + \frac{Q_3}{A_3} \left(\frac{1}{\epsilon_3} - F_{3-3} \frac{1-\epsilon_3}{\epsilon_3} \right) \\ = -F_{3-1}\sigma T_1^4 - F_{3-2}\sigma T_2^4 + (1 - F_{3-3})\sigma T_3^4 \quad (3-18c)$$

Since the T 's are known, the ϵ 's can be specified from surface property data at their appropriate T values and these three simultaneous equations solved for the desired Q values supplied to each surface. Note that the solutions are only first approximations, because the radiosity leaving each surface is not uniform as assumed. This is because the reflected flux is not uniform. Greater accuracy can be obtained by dividing each of the three sides into more surface elements.

Now that some familiarity with the radiant energy exchange equations has been achieved by looking at a few simple examples, the system of equations will be written in a generalized form for an enclosure of N surfaces.

3.3.1.1 *System of equations relating surface heating Q and surface temperature T .*—The form of equations (3-18) indicates that the Q 's and T 's for an enclosure of N surfaces can be related in a general system of N equations. Equation (3-6) is solved for $q_{o,k}$, and this is substituted into equation (3-7). (Note that $q_{o,j}$ is found by simply changing the subscript in the relation for $q_{o,k}$.) This results in the following form for the k th surface, a result which is also evident from equations (3-18):

$$\begin{aligned}
& -\frac{Q_1}{A_1} F_{k-1} \frac{1-\epsilon_1}{\epsilon_1} - \frac{Q_2}{A_2} F_{k-2} \frac{1-\epsilon_2}{\epsilon_2} - \dots + \frac{Q_k}{A_k} \left(\frac{1}{\epsilon_k} - F_{k-k} \frac{1-\epsilon_k}{\epsilon_k} \right) \\
& - \dots - \frac{Q_N}{A_N} F_{k-N} \frac{1-\epsilon_N}{\epsilon_N} = -F_{k-1} \sigma T_1^4 - F_{k-2} \sigma T_2^4 - \dots \\
& \qquad \qquad \qquad + (1-F_{k-k}) \sigma T_k^4 - \dots - F_{k-N} \sigma T_N^4
\end{aligned}$$

A summation notation can be used to write this as

$$\sum_{j=1}^N \left(\frac{\delta_{kj}}{\epsilon_j} - F_{k-j} \frac{1-\epsilon_j}{\epsilon_j} \right) \frac{Q_j}{A_j} = \sum_{j=1}^N (\delta_{kj} - F_{k-j}) \sigma T_j^4 \quad (3-19)$$

where corresponding to each surface, k takes on one of the values 1, 2, . . . , N and δ_{kj} is the Kronecker delta defined as

$$\delta_{kj} = \begin{cases} 1 & \text{when } k = j \\ 0 & \text{when } k \neq j \end{cases}$$

When the surface temperatures are specified, the right side of equation (3-19) is known, and there are N simultaneous equations for the unknown Q 's.

In general, the heat input to some of the surfaces may be specified, and the temperature of these surfaces is to be determined. There are still a total of N unknown Q 's and T 's, and equation (3-19) provides the necessary number of relations. Since the values of ϵ depend on temperature, it is necessary to guess initially the unknown T 's. Then the ϵ values can be chosen, and the system of equations can be solved. The resulting T values can be used to select new ϵ 's, and the process can be repeated until the T and ϵ values no longer change upon further iteration. Again, note that the results by this method will be approximate because the uniform radiosity assumption is not perfectly fulfilled over each finite area.

EXAMPLE 3-5: Consider an enclosure of three sides, as shown in figure 3-5. Side 1 is held at T_1 , side 2 is uniformly heated with a flux q_2 , and the third side is insulated. What are the equations to determine Q_1 , T_2 , and T_3 ?

The conditions of the problem give $Q_2/A_2 = q_2$ and $Q_3 = 0$. Then equation (3-19) yields the following three equations where the unknowns have been gathered on the left side:

$$\frac{Q_1}{A_1} \left(\frac{1}{\epsilon_1} - F_{1-1} \frac{1-\epsilon_1}{\epsilon_1} \right) + F_{1-2} \sigma T_2^4 + F_{1-3} \sigma T_3^4 = (1 - F_{1-1}) \sigma T_1^4 + q_2 F_{1-2} \frac{1-\epsilon_2}{\epsilon_2} \quad (3-20a)$$

$$-\frac{Q_1}{A_1} F_{2-1} \frac{1-\epsilon_1}{\epsilon_1} - (1 - F_{2-2}) \sigma T_2^4 + F_{2-3} \sigma T_3^4 = -F_{2-1} \sigma T_1^4 - q_2 \left(\frac{1}{\epsilon_2} - F_{2-2} \frac{1-\epsilon_2}{\epsilon_2} \right) \quad (3-20b)$$

$$-\frac{Q_1}{A_1} F_{3-1} \frac{1-\epsilon_1}{\epsilon_1} + F_{3-2} \sigma T_2^4 - (1 - F_{3-3}) \sigma T_3^4 = -F_{3-1} \sigma T_1^4 + q_2 F_{3-2} \frac{1-\epsilon_2}{\epsilon_2} \quad (3-20c)$$

If ϵ_2 depends on temperature, an iterative procedure is needed where a T_2 is chosen; then $\epsilon_2(T_2)$ is specified, the equations are solved for T_2 , and the iteration is continued until $\epsilon_2(T_2)$ and T_2 no longer change.

3.3.1.2 *Solution method in terms of outgoing radiative flux q_o .*—An alternate approach for computing the radiative exchange within an enclosure involves first solving for q_o for each surface and then computing the Q 's or T 's. When sighting a surface with a radiation detector, it is q_o that is intercepted, that is, the sum of both emitted and reflected radiation. For this reason, it is desirable in some instances to determine the q_o values as primary quantities. Of course, in the previous formulation (section 3.3.1.1), the q_o 's can be found from Q 's and T 's by using equation (3-6).

When the surface temperatures are all specified, the set of simultaneous equations for q_o 's is obtained by eliminating Q_k 's from equations (3-6) and (3-7). This yields the following equation for the k th surface:

$$q_{o,k} - (1 - \epsilon_k) \sum_{j=1}^N F_{k-j} q_{o,j} = \epsilon_k \sigma T_k^4 \quad (3-21)$$

To illustrate, for a system of two surfaces, equation (3-21) becomes

$$q_{o,1} - (1 - \epsilon_1) F_{1-1} q_{o,1} - (1 - \epsilon_1) F_{1-2} q_{o,2} = \epsilon_1 \sigma T_1^4 \quad (3-22a)$$

$$q_{o,2} - (1 - \epsilon_2) F_{2-1} q_{o,1} - (1 - \epsilon_2) F_{2-2} q_{o,2} = \epsilon_2 \sigma T_2^4 \quad (3-22b)$$

An alternate form of equation (3-21) is

$$\sum_{j=1}^N [\delta_{kj} - (1 - \epsilon_k) F_{k-j}] q_{o,j} = \epsilon_k \sigma T_k^4 \quad (3-23)$$

With the T 's given, the q_o 's can be found from equation (3-23). Then, if desired, equation (3-6) can be used to compute Q for each surface.

When Q is specified for some surfaces and T for others, equation (3-23) is used for the surfaces with known T in conjunction with equation (3-7) for the surfaces with known Q , to obtain the set of simultaneous equations for the unknown q_o 's. Once q_o is obtained for a surface, it can be combined with the given Q (or T) and equation (3-6) can be used to determine the unknown T (or Q). In a general form, if an enclosure has surfaces 1, 2, . . . , m with specified temperature and the remaining surfaces $m+1$, $m+2$, . . . , N with specified heat input, the system of equations for the q_o 's is from equations (3-23) and (3-7)

$$\sum_{j=1}^N [\delta_{kj} - (1 - \epsilon_k) F_{k-j}] q_{o,j} = \epsilon_k \sigma T_k^4 \quad 1 \leq k \leq m \quad (3-24a)$$

$$\sum_{j=1}^N (\delta_{kj} - F_{k-j}) q_{o,j} = \frac{Q_k}{A_k} \quad m+1 \leq k \leq N \quad (3-24b)$$

Note that, for a black surface with T_k specified, equation (3-24a) gives $q_{o,k} = \sigma T_k^4$ so that the $q_{o,k}$ is known, and the number of simultaneous equations can be immediately reduced by one.

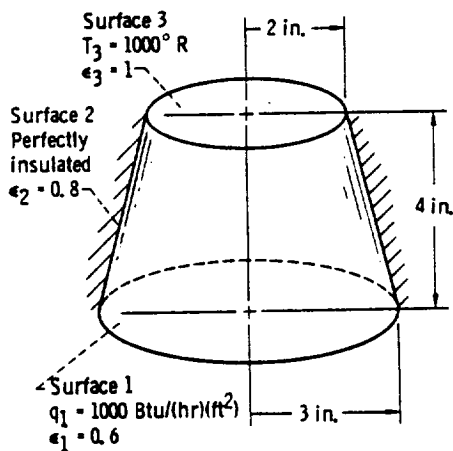


FIGURE 3-6. — Enclosure used in example 3-6.

EXAMPLE 3-6: A frustum of a cone has its base heated, as shown in figure 3-6. The top is held at 1000°R while the side is perfectly insulated. Surfaces 1 and 2 are assumed gray and diffuse while surface 3 is black. What is the temperature of side 1? How important is the value of ϵ_2 ?

By using the configuration factor for two parallel disks (see table A-1 in appendix A as a source for the F factor), it is found that $F_{3-1} = 0.33$. Then $F_{3-2} = 1 - F_{3-1} = 0.67$. From reciprocity $A_1F_{1-3} = A_3F_{3-1}$ and $A_2F_{2-3} = A_3F_{3-2}$, it is found that $F_{1-3} = 0.147$ and $F_{2-3} = 0.13$. Then $F_{1-2} = 1 - F_{1-3} = 0.853$. From $A_1F_{1-2} = A_2F_{2-1}$, $F_{2-1} = 0.372$. Finally, $F_{2-2} = 1 - F_{2-1} - F_{2-3} = 0.498$. From equation (3-19) and by noting that $Q_2 = 0$ and $1 - \epsilon_3 = 0$, the three equations can be written as

$$\begin{aligned} \frac{1000}{0.6} &= \sigma [T_1^4 - 0.853T_2^4 - 0.147(1000)^4] \\ -1000(0.372) \frac{(1-0.6)}{0.6} &= \sigma [-0.372T_1^4 + (1-0.498)T_2^4 - 0.13(1000)^4] \\ -1000(0.33) \frac{(1-0.6)}{0.6} + \frac{Q_3}{A_3} &= \sigma [-0.33T_1^4 - 0.67T_2^4 + (1000)^4] \end{aligned}$$

These three equations can be solved for the unknowns T_1 , T_2 , and Q_3 . The result requested in the problem is $T_1 = 1310^\circ\text{R}$. Since $Q_2 = 0$, all of the terms involving ϵ_2 were zero so that ϵ_2 does not appear in the simultaneous equations; hence, for this gray-diffuse analysis the emissivity of the insulated surface is of no importance.

3.3.2 Matrix Inversion

When many surfaces are present in an enclosure, a large set of simultaneous equations such as equation (3-19) or (3-24) will result. These equations can be solved using a digital computer along with standard computer programs that can accommodate several hundred simultaneous equations.

A set of equations such as equations (3-24) can be written in a shorter form. Let the known quantities on the right side be C_k and the quantities in brackets on the left side be a_{kj} . Then the k equations can be written as

$$\sum_{j=1}^N a_{kj} q_{0,j} = C_k \quad (3-25a)$$

where

$$a_{kj} = \begin{cases} \delta_{kj} - (1 - \epsilon_k)F_{k-j} \\ \delta_{kj} - F_{k-j} \end{cases} \quad C_k = \begin{cases} \epsilon_k \sigma T_k^4 & 1 \leq k \leq m \\ \frac{Q_k}{A_k} & m+1 \leq k \leq N \end{cases} \quad (3-25b)$$

For an enclosure of N surfaces, the set of equations then has the form

$$\left. \begin{aligned} a_{11}q_{0,1} + a_{12}q_{0,2} + \dots + a_{1j}q_{0,j} + \dots + a_{1N}q_{0,N} &= C_1 \\ a_{21}q_{0,1} + a_{22}q_{0,2} + \dots + a_{2j}q_{0,j} + \dots + a_{2N}q_{0,N} &= C_2 \\ \dots & \dots \\ a_{k1}q_{0,1} + a_{k2}q_{0,2} + \dots + a_{kj}q_{0,j} + \dots + a_{kN}q_{0,N} &= C_k \\ \dots & \dots \\ a_{N1}q_{0,1} + a_{N2}q_{0,2} + \dots + a_{Nj}q_{0,j} + \dots + a_{NN}q_{0,N} &= C_N \end{aligned} \right\} \quad (3-26)$$

The array of a_{kj} coefficients is termed the matrix of coefficients and is often designated by a bracket notation

$$\text{matrix } a \equiv [a_{kj}] \equiv \begin{bmatrix} a_{11} & a_{12} & \dots & a_{1j} & \dots & a_{1N} \\ a_{21} & a_{22} & \dots & a_{2j} & \dots & a_{2N} \\ \dots & \dots & \dots & \dots & \dots & \dots \\ a_{k1} & a_{k2} & \dots & a_{kj} & \dots & a_{kN} \\ \dots & \dots & \dots & \dots & \dots & \dots \\ a_{N1} & a_{N2} & \dots & a_{Nj} & \dots & a_{NN} \end{bmatrix} \quad (3-27)$$

A method of solving a set of equations such as equations (3-26) is to obtain a second matrix a^{-1} , which is called the inverse of matrix a , that is,

$$\text{matrix } a^{-1} \equiv [\mathcal{A}_{kj}] \equiv \begin{bmatrix} \mathcal{A}_{11} & \mathcal{A}_{12} & \dots & \mathcal{A}_{1j} & \dots & \mathcal{A}_{1N} \\ \mathcal{A}_{21} & \mathcal{A}_{22} & \dots & \mathcal{A}_{2j} & \dots & \mathcal{A}_{2N} \\ \dots & \dots & \dots & \dots & \dots & \dots \\ \mathcal{A}_{k1} & \mathcal{A}_{k2} & \dots & \mathcal{A}_{kj} & \dots & \mathcal{A}_{kN} \\ \dots & \dots & \dots & \dots & \dots & \dots \\ \mathcal{A}_{N1} & \mathcal{A}_{N2} & \dots & \mathcal{A}_{Nj} & \dots & \mathcal{A}_{NN} \end{bmatrix} \quad (3-28)$$

In the inverse matrix there is a term \mathcal{A}_{kj} corresponding to each a_{kj} in the original matrix. The \mathcal{A} 's are found by operating on the a 's in a way

briefly described as follows: If the k th row and j th column that contain element a_{kj} in a square matrix a are deleted, the determinant of the remaining square array is called the minor of element a_{kj} and is denoted by M_{kj} . The cofactor of a_{kj} is defined as $(-1)^{k+j}M_{kj}$. To obtain the inverse of a square matrix $[a_{kj}]$, each element a_{kj} is first replaced by its cofactor. The rows and columns of the resulting matrix are then interchanged. The elements of the matrix thus obtained are then each divided by the determinant $|a_{kj}|$ of the original matrix $[a_{kj}]$. The elements obtained in this fashion are the \mathcal{A}_{kj} . For more detailed information on matrix inversion, the reader should refer to a mathematics text such as reference 6. There are standard digital computer programs that will numerically obtain the inverse coefficients \mathcal{A}_{kj} from a matrix of a_{kj} values.

After the inverse coefficients have been obtained, the unknown q_0 values in equations (3-26) are found as the sum of products of \mathcal{A} 's and C 's

$$\begin{aligned} q_{0,1} &= \mathcal{A}_{11}C_1 + \mathcal{A}_{12}C_2 + \dots + \mathcal{A}_{1j}C_j + \dots + \mathcal{A}_{1N}C_N \\ q_{0,2} &= \mathcal{A}_{21}C_1 + \mathcal{A}_{22}C_2 + \dots + \mathcal{A}_{2j}C_j + \dots + \mathcal{A}_{2N}C_N \\ &\dots \dots \dots \end{aligned} \tag{3-29a}$$

or

$$q_{0,k} = \mathcal{A}_{k1}C_1 + \mathcal{A}_{k2}C_2 + \dots + \mathcal{A}_{kj}C_j + \dots + \mathcal{A}_{kN}C_N \tag{3-29b}$$

$$q_{0,k} = \sum_{j=1}^N \mathcal{A}_{kj}C_j$$

Therefore, the solution for each $q_{0,k}$ is in the form of a sum of $\epsilon\sigma T^4$ and Q/A that the C 's represent, each weighted by an \mathcal{A} coefficient.

For a given enclosure the configuration factors F_{k-j} in equation (3-25b) remain fixed. If, in addition, the ϵ_k 's are constant, then the elements a_{kj} , and hence the inverse elements \mathcal{A}_{kj} , remain fixed for the enclosure. The fact that the \mathcal{A}_{kj} remain fixed has utility when it is desired to compute the radiation quantities within an enclosure for many different values of the T 's and Q 's at the surfaces. The matrix need be inverted only once; then equation (3-29b) can be applied for different values of the C 's. These comments also apply to the system of equations given by equation (3-19). After the inverse is taken, the Q 's can be found as a weighted sum of the T 's.

3.4 RADIATION BETWEEN INFINITESIMAL AREAS

3.4.1 Generalized Net Radiation Method for Infinitesimal Areas

In the previous section the enclosure was divided into finite areas. The accuracy of the results is limited by the assumptions in the analysis

that the temperature, and energy incident on and leaving each surface, are uniform over that surface. If these quantities are nonuniform over part of the enclosure boundary, the boundary surface must be subdivided until the variation over each area used in the analysis is not too large. It may be necessary to carry out several calculations in which successively smaller areas (and hence more simultaneous equations) are used until the solution no longer changes significantly when the area sizes are further diminished. In the limit, the enclosure boundary or a portion of it can be divided into infinitesimal parts; this will allow large variations in T , q , q_i , and q_o to be accounted for.

The formulation in terms of infinitesimal areas leads to heat balances in the form of a set of integral equations. By using both exact and approximate mathematical techniques that have been developed for integral equations, it is sometimes possible to obtain a closed-form analytical solution. When it is not possible to obtain an analytical solution, the integral equations can be solved numerically. In the case of a numerical solution, the solution method is similar to that used in the previous discussion dealing with finite areas.

Consider, as before, an enclosure composed of N finite areas. These areas would generally be the major geometric divisions of the enclosure or the areas on which a specified boundary condition is held constant.

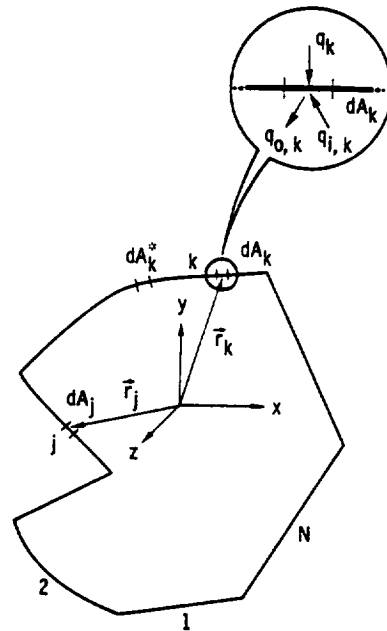


FIGURE 3-7.—Enclosure composed of N discrete surface areas with areas subdivided into infinitesimal elements.

Each of these areas is further subdivided into differential area elements, as shown for two typical areas in figure 3-7. As before, throughout the following analysis *the surfaces will be considered diffuse gray. The additional restriction is now made that the radiative properties are independent of temperature.*

A heat balance on element dA_k located at position \vec{r}_k gives

$$q_k(\vec{r}_k) = q_{o, k}(\vec{r}_k) - q_{i, k}(\vec{r}_k) \quad (3-30)$$

The outgoing flux is composed of emitted and reflected energy

$$q_{o, k}(\vec{r}_k) = \epsilon_k \sigma T_k^4(\vec{r}_k) + (1 - \epsilon_k) q_{i, k}(\vec{r}_k) \quad (3-31)$$

The incoming flux in equation (3-31) is composed of portions of the outgoing fluxes from the other area elements of the enclosure. This is a generalization of equation (3-3) in the respect that over each finite surface, an integration is performed to determine the total contribution that the local flux leaving that surface makes to the quantity $q_{i, k}$

$$\begin{aligned} dA_k q_{i, k}(\vec{r}_k) = & \int_{A_1} q_{o, 1}(\vec{r}_1) dF_{d1-dk}(\vec{r}_1, \vec{r}_k) dA_1 \\ & + \dots + \int_{A_k} q_{o, k}(\vec{r}_k^*) dF_{dk^*-dk}(\vec{r}_k^*, \vec{r}_k) dA_k^* \\ & + \dots + \int_{A_N} q_{o, N}(\vec{r}_N) dF_{dN-dk}(\vec{r}_N, \vec{r}_k) dA_N \end{aligned} \quad (3-32)$$

The second integral on the right is the contribution that other differential elements dA_k^* on surface A_k make to the incident energy at dA_k .

By using reciprocity $dA_j dF_{dj-dk} = dA_k dF_{dk-dj}$, a typical integral in equation (3-32) can be transformed to give

$$\int_{A_j} q_{o, j}(\vec{r}_j) dF_{dj-dk}(\vec{r}_j, \vec{r}_k) dA_j = \int_{A_j} q_{o, j}(\vec{r}_j) dF_{dk-dj}(\vec{r}_j, \vec{r}_k) dA_k$$

By operating on all the integrals in equation (3-32) in this manner, the dA_k will divide out of the equation, and the result becomes

$$q_{i, k}(\vec{r}_k) = \sum_{j=1}^N \int_{A_j} q_{o, j}(\vec{r}_j) dF_{dk-dj}(\vec{r}_j, \vec{r}_k) \quad (3-33)$$

Equations (3-31) and (3-33) provide two different expressions for $q_{i, k}(\vec{r}_k)$. These are each substituted into equation (3-30) to provide two expressions for $q_k(\vec{r}_k)$ comparable to equations (3-6) and (3-7)

$$q_k(\bar{r}_k) = \frac{\epsilon_k}{1 - \epsilon_k} [\sigma T_k^4(\bar{r}_k) - q_{o,k}(\bar{r}_k)] \quad (3-34)$$

$$q_k(\bar{r}_k) = q_{o,k}(\bar{r}_k) - \sum_{j=1}^N \int_{A_j} q_{o,j}(\bar{r}_j) dF_{dk-dj}(\bar{r}_j, \bar{r}_k) \quad (3-35)$$

As shown by equation (2-10), the differential configuration factor dF_{dk-dj} contains the differential area dA_j . To place equation (3-35) in a more standard form where the variable of integration is explicitly shown, it is convenient to define a quantity $K(\bar{r}_j, \bar{r}_k)$ by

$$K(\bar{r}_j, \bar{r}_k) \equiv \frac{dF_{dk-dj}(\bar{r}_j, \bar{r}_k)}{dA_j} \quad (3-36)$$

Then equation (3-35) becomes the integral equation

$$q_k(\bar{r}_k) = q_{o,k}(\bar{r}_k) - \sum_{j=1}^N \int_{A_j} q_{o,j}(\bar{r}_j) K(\bar{r}_j, \bar{r}_k) dA_j \quad (3-37)$$

The quantity $K(\bar{r}_j, \bar{r}_k)$ that appears under the integral sign with the dependent variable, such as in equation (3-37), is called the kernel of the integral equation.

As in the previous discussion for finite areas, there are two paths that can now be followed:

(1) When the temperatures and imposed heat fluxes are important, equations (3-34) and (3-35) can be combined to eliminate the variables q_o . This gives a set of simultaneous relations directly relating the surface temperatures T and the imposed heat fluxes q . Along each surface area, either the T or the q will be specified by the boundary conditions. The remaining unknown T 's and q 's can then be found by solving the simultaneous relations.

(2) Alternately, when q_o is an important quantity, the unknown q 's can be eliminated by combining equations (3-34) and (3-35) for each surface that does not have its q specified as a boundary condition. For a surface where q is known, equation (3-35) can be used to relate the q_o 's to each other directly. This yields a set of simultaneous relations for the q_o 's in terms of the known q 's and T 's that are specified by the boundary conditions. After solving for the q_o 's, equations (3-34) can be used, if desired, to relate the q 's and T 's where either the q or T will be known at each surface from the boundary conditions.

Each of these procedures will now be examined.

3.4.1.1 *Relations between surface temperature T and surface heating q .* — To eliminate the q_o in the first method of solution, equation (3-34) is solved for $q_{o,k}(\bar{r}_k)$, giving

$$q_{o, k}(\bar{r}_k) = \sigma T_k^4(\bar{r}_k) - \frac{1 - \epsilon_k}{\epsilon_k} q_k(\bar{r}_k) \quad (3-38)$$

Equation (3-38) in the form shown and also with k changed to j is then substituted into equation (3-35) to eliminate $q_{o, k}$ and $q_{o, j}$, which yields

$$\frac{q_k(\bar{r}_k)}{\epsilon_k} - \sum_{j=1}^N \frac{1 - \epsilon_j}{\epsilon_j} \int_{A_j} q_j(\bar{r}_j) dF_{dk-dj}(\bar{r}_j, \bar{r}_k) = \sigma T_k^4(\bar{r}_k) - \sum_{j=1}^N \int_{A_j} \sigma T_j^4(\bar{r}_j) dF_{dk-dj}(\bar{r}_j, \bar{r}_k) \quad (3-39)$$

Equation (3-39) directly relates the surface temperatures to the heat fluxes supplied to the surfaces.

EXAMPLE 3-7: An enclosure of the general type in figure 3-5 is composed of three plane surfaces, and for simplicity is infinitely long so that the heat transfer quantities do not vary with length. Surface 1 is heated uniformly and surface 2 is at a uniform temperature. Surface 3 is black and at zero temperature. What are the governing equations needed to determine the temperature distribution over the perimeter of surface 1?

With $T_3 = 0$, $\epsilon_3 = 1$, and the self-view factors $dF_{d_j-d_j} = 0$, equation (3-39) can be written for the two plane surfaces 1 and 2 having uniform q_1 and T_2 as

$$\frac{q_1}{\epsilon_1} - \frac{1 - \epsilon_2}{\epsilon_2} \int_{A_2} q_2(\bar{r}_2) dF_{d1-d2}(\bar{r}_2, \bar{r}_1) = \sigma T_1^4(\bar{r}_1) - \sigma T_2^4 \int_{A_2} dF_{d1-d2}(\bar{r}_2, \bar{r}_1) \quad (3-40a)$$

$$\frac{q_2(\bar{r}_2)}{\epsilon_2} - q_1 \frac{1 - \epsilon_1}{\epsilon_1} \int_{A_1} dF_{d2-d1}(\bar{r}_1, \bar{r}_2) = \sigma T_2^4 - \int_{A_1} \sigma T_1^4(\bar{r}_1) dF_{d2-d1}(\bar{r}_1, \bar{r}_2) \quad (3-40b)$$

A similar equation for surface 3 is not needed since equations (3-40) do not involve the unknown $q_3(\bar{r}_3)$ as a consequence of $\epsilon_3 = 1$ and $T_3 = 0$. From the definitions of F factors,

$$\int_{A_2} dF_{d1-d2} = F_{d1-2} \quad \text{and} \quad \int_{A_1} dF_{d2-d1} = F_{d2-1}$$

equations (3-40) simplify to the following relations where the unknowns have been placed on the left:

$$\sigma T_1^4(\bar{r}_1) + \frac{1 - \epsilon_2}{\epsilon_2} \int_{A_2} q_2(\bar{r}_2) dF_{d1-d2}(\bar{r}_2, \bar{r}_1) = \sigma T_2^4 F_{d1-2} + \frac{q_1}{\epsilon_1} \quad (3-41a)$$

$$\int_{A_1} \sigma T_1^4(\bar{r}_1) dF_{d2-d1}(\bar{r}_1, \bar{r}_2) + \frac{q_2(\bar{r}_2)}{\epsilon_2} = \sigma T_2^4 + q_1 \frac{1 - \epsilon_1}{\epsilon_1} F_{d2-1} \quad (3-41b)$$

Equations (3-41) can be solved simultaneously for the unknown distributions $T_1(\bar{r}_1)$ and $q_2(\bar{r}_2)$. Some methods for solving such a set of integral equations will be discussed in section 3.4.2.

3.4.1.2 *Solution method in terms of outgoing radiative flux q_o .* — A second method of solution results from eliminating the $q_k(\bar{r}_k)$ terms from equations (3-34) and (3-35) for the surfaces where $q_k(\bar{r}_k)$ is unknown. This provides a relation between q_o and the T variation specified along a surface

$$q_{o,k}(\bar{r}_k) = \epsilon_k \sigma T_k^4(\bar{r}_k) + (1 - \epsilon_k) \sum_{j=1}^N \int_{A_j} q_{o,j}(\bar{r}_j) dF_{dk-dj}(\bar{r}_j, \bar{r}_k) \quad (3-42)$$

When the heat supplied to surface k , $q_k(\bar{r}_k)$, is known, equation (3-35) can be used directly to relate q_k and q_o . The combination of equations (3-42) and (3-35) thus provides a complete set of relations for the unknown q_o 's in terms of known T 's and q 's.

This set of equations for the q_o 's will now be formulated more explicitly. In general, an enclosure can have surfaces 1, 2, . . . , m with specified temperature distributions. For these surfaces, equation (3-42) is utilized. The remaining $N - m$ surfaces $m + 1, m + 2, . . . , N$ have an imposed heat flux distribution specified. For these surfaces equation (3-35) is applied. This results in a set of N equations for the unknown q_o distributions

$$q_{o,k}(\bar{r}_k) - (1 - \epsilon_k) \sum_{j=1}^N \int_{A_j} q_{o,j}(\bar{r}_j) dF_{dk-dj}(\bar{r}_j, \bar{r}_k) = \epsilon_k \sigma T_k^4(\bar{r}_k) \quad 1 \leq k \leq m \quad (3-43a)$$

$$q_{o,k}(\bar{r}_k) - \sum_{j=1}^N \int_{A_j} q_{o,j}(\bar{r}_j) dF_{dk-dj}(\bar{r}_j, \bar{r}_k) = q_k(\bar{r}_k) \quad m + 1 \leq k \leq N \quad (3-43b)$$

After the q_o 's are found, equation (3-34) is applied to determine the unknown q or T distributions,

$$q_k(\vec{r}_k) = \frac{\epsilon_k}{1 - \epsilon_k} [\sigma T_k^4(\vec{r}_k) - q_{o,k}(\vec{r}_k)] \quad 1 \leq k \leq m \quad (3-44a)$$

$$\sigma T_k^4(\vec{r}_k) = \frac{1 - \epsilon_k}{\epsilon_k} q_k(\vec{r}_k) + q_{o,k}(\vec{r}_k) \quad m + 1 \leq k \leq m \quad (3-44b)$$

3.4.1.3 *Special case when imposed heating q is specified for all surfaces.*— There is an interesting special case when the imposed energy flux q is specified for all surfaces of the enclosure and it is desired to determine the surface temperature distributions. For this case the use of the method of the previous section, where the q_o 's are first determined (section 3.4.1.2), has an advantage over the method given by equation (3-39) where the T 's are directly determined from the specified q 's (section 3.4.1.1). This advantage arises from the fact that equation (3-43b) is independent of the radiative properties of the surfaces. This means that for a given set of q 's the q_o 's need be determined only once by writing equation (3-43b) for each of the surfaces. The temperature distributions are then found from equation (3-44b), which introduces the emissivity dependence. This would have an advantage when it is desired to examine the temperature variations for various emissivity values when there is a fixed set of q 's.

In the case when the surfaces are all black, then $\epsilon_k = 1$ and equation (3-44b) becomes

$$\sigma T_k^4(\vec{r}_k)_{black} = q_{o,k}(\vec{r}_k)$$

Since the $q_{o,k}$'s are independent of the emissivities, these $q_{o,k}$'s are also valid for surfaces where $\epsilon_k \neq 1$. The solution in equation (3-44b) can then be written as

$$\sigma T_k^4(\vec{r}_k) = \frac{1 - \epsilon_k}{\epsilon_k} q_k(\vec{r}_k) + \sigma T_k^4(\vec{r}_k)_{black} \quad (3-45)$$

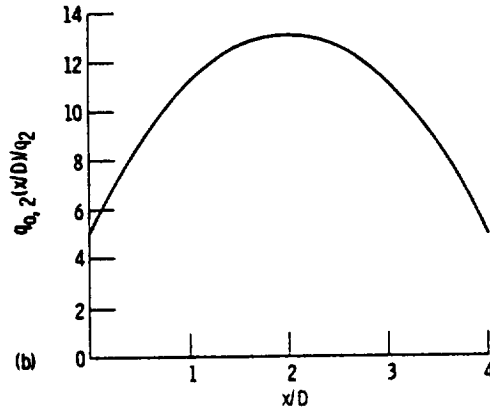
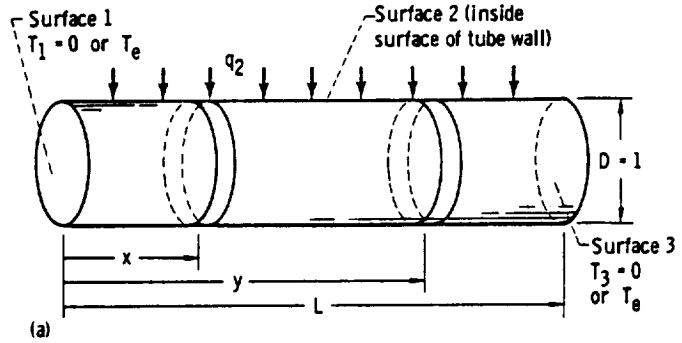
This relates the temperature distributions in an enclosure for $\epsilon_k \neq 1$ to the temperature distributions in a black enclosure having the same imposed heat fluxes. Thus, once the temperature distributions have been found for the black case, the fourth-power temperature distribution $\sigma T_k^4(\vec{r}_k)$ for gray surfaces are found by simply adding the term $[(1 - \epsilon_k)/\epsilon_k]q_k(\vec{r}_k)$.

To this point, a number of formulations of the governing equations of radiation interchange within an enclosure have been made. In table 3-1 the relations that have been derived for finding quantities of interest, such as Q , T , and q_o on various surfaces in terms of given quantities, are summarized for convenience.

TABLE 3-1.—RELATIONS BETWEEN ENERGY FLUX AND TEMPERATURE IN DIFFUSE-GRAY ENCLOSURES

Boundary conditions		Desired quantities	Equation
Finite areas	T_k on all surfaces $1 \leq k \leq N$	Q_k	(3-19)
		$q_{o,k}$	(3-23)
	Q_k on all surfaces $1 \leq k \leq N$	T_k	(3-19)
		T_k for $1 \leq k \leq m$ Q_k for $m+1 \leq k \leq N$	Q_k for $1 \leq k \leq m$ T_k for $m+1 \leq k \leq N$
$q_{o,k}$	(3-24)		
Infinitesimal areas	T_k on all surfaces $1 \leq k \leq N$	q_k	(3-39)
		$q_{o,k}$	(3-42)
	q_k on all surfaces $1 \leq k \leq N$	T_k	(3-35) and (3-44b)
		$q_{o,k}$	(3-35)
	T_k for $1 \leq k \leq m$ q_k for $m+1 \leq k \leq N$	q_k for $1 \leq k \leq m$ T_k for $m+1 \leq k \leq N$	(3-39) or (3-43) and (3-44)
		$q_{o,k}$	(3-43a) and (3-43b)
$q_{o,k}$ for $1 \leq k \leq N$ T_k for $1 \leq k \leq m$ q_k for $m+1 \leq k \leq N$	q_k for $1 \leq k \leq m$ T_k for $m+1 \leq k \leq N$	(3-44a) (3-44b)	

EXAMPLE 3-8: A relatively simple example of a heated enclosure is a circular tube shown in figure 3-8 open at both ends and insulated on the outside surface (ref. 7). (1) For a uniform heat addition along the tube wall and a surrounding environment temperature of 0° R , what is the



(a) Geometry and coordinate system.
 (b) Distribution of q_o on inside of tube for $L/D = 4$.

FIGURE 3-8. — Uniformly heated tube insulated on outside and open to environment at both ends.

temperature distribution along the tube? (2) If the surroundings are at temperature T_e , how does this influence the temperature distribution?

(1) Since the open ends of the tube are nonreflecting, they can be assumed to act as black disks at a specified temperature of 0° R . Equation (3-44b) is then used for these two disks to find their q_o . With $\epsilon_1 = \epsilon_3 = 1$, equation (3-44b) gives

$$q_{o,1} = q_{o,3} = \sigma T_1^4 = \sigma T_3^4 = 0$$

Consequently, the summation in equation (3-43b) will provide only radiation from surface 2 to itself. Since the tube is axisymmetric, the two differential areas dA_k and dA_k^* can be taken as rings, and they are located at x and y , respectively. For convenience, all lengths are non-dimensionalized with respect to the tube diameter; then equation (3-43b) yields

$$q_{o,2}(\xi) - \int_{\eta=0}^{\eta=l} q_{o,2}(\eta) dF_{d\xi-d\eta}(|\eta-\xi|) = q_2 \quad (3-46a)$$

where $\xi = x/D$, $\eta = y/D$, $l = L/D$, and $dF_{d\xi-d\eta}(|\eta-\xi|)$ is the configuration factor for two rings a distance $|\eta-\xi|$ apart and is given by (for source see table A-1 in appendix A)

$$dF_{d\xi-d\eta}(|\eta-\xi|) = \left\{ 1 - \frac{|\eta-\xi|^3 + \frac{3}{2}|\eta-\xi|}{[(\eta-\xi)^2 + 1]^{3/2}} \right\} d\eta \quad (3-46b)$$

Absolute value signs are used on $\eta-\xi$ because the configuration factor depends only on the magnitude of the separation distance between the rings. When $|\eta-\xi|=0$, $dF=d\eta$, and this represents the view factor from a differential ring to itself. Equation (3-46a) can be divided by the constant q_2 , and the solution for the dimensionless quantity $q_{o,2}(\xi)/q_2$ can be found by numerical or approximate methods for solving linear integral equations. A discussion of these methods will be given in section 3.4.2. The resulting $q_{o,2}(\xi)/q_2$ distribution is shown in figure 3-8(b) for a tube 4 diameters in length. From equation (3-44b), the distribution of temperature to the fourth power along the tube is given by

$$\sigma T_2^4(\xi) = \frac{1-\epsilon_2}{\epsilon_2} q_2 + q_{o,2}(\xi)$$

Since q_2 is a constant, the distribution $T_2^4(\xi)$ has the same shape as the distribution $q_{o,2}(\xi)$. The wall temperature is high in the central region of the tube and low near the end openings, where heat can be radiated easily to the low-temperature environment.

(2) Now consider the case where the environment is at T_e rather than at zero. The open ends of the cylindrical enclosure can be regarded as perfectly absorbing disks at T_e . The integral equation (3-43b) now yields

$$q_{o,2}(\xi) - \int_{\eta=0}^l q_{o,2}(\eta) dF_{d\xi-d\eta}(|\eta-\xi|) - \sigma T_e^4 F_{d\xi-1}(\xi) - \sigma T_e^4 F_{d\xi-3}(l-\xi) = q_2$$

where $F_{d\xi-1}(\xi)$ is the configuration factor from a ring element at ξ to

disk 1 at $\xi = 0$, that is,

$$F_{d\xi-1}(\xi) = \frac{\xi^2 + \frac{1}{2}}{(\xi^2 + 1)^{1/2}} \xi$$

Since the integral equation is linear in the variable $q_{0,2}(\xi)$, let a trial solution be in the form of a sum of two parts where for each part either $T_e = 0$ or $q_2 = 0$

$$q_{0,2}(\xi) = q_{0,2}(\xi)|_{T_e=0} + q_{0,2}(\xi)|_{q_2=0}$$

Substitute the trial solution into the integral equation to get

$$\begin{aligned} q_{0,2}(\xi)|_{T_e=0} + q_{0,2}(\xi)|_{q_2=0} - \int_{\eta=0}^l q_{0,2}(\eta)|_{T_e=0} dF_{d\xi-\sigma\eta}(|\eta-\xi|) \\ - \int_{\eta=0}^l q_{0,2}(\eta)|_{q_2=0} dF_{d\xi-\sigma\eta}(|\eta-\xi|) - \sigma T_e^4 F_{d\xi-1}(\xi) - \sigma T_2^4 F_{d\xi-3}(l-\xi) = q_2 \end{aligned}$$

For $T_e = 0$, equation (3-46a) applies; subtract this equation to give

$$\begin{aligned} q_{0,2}(\xi)|_{q_2=0} - \int_{\eta=0}^l q_{0,2}(\eta)|_{q_2=0} dF_{d\xi-\sigma\eta}(|\eta-\xi|) \\ - \sigma T_2^4 F_{d\xi-1}(\xi) - \sigma T_2^4 F_{d\xi-3}(l-\xi) = 0 \end{aligned}$$

As can be verified by direct substitution and then integrating, the solution is

$$q_{0,2}|_{q_2=0} = \sigma T_2^4$$

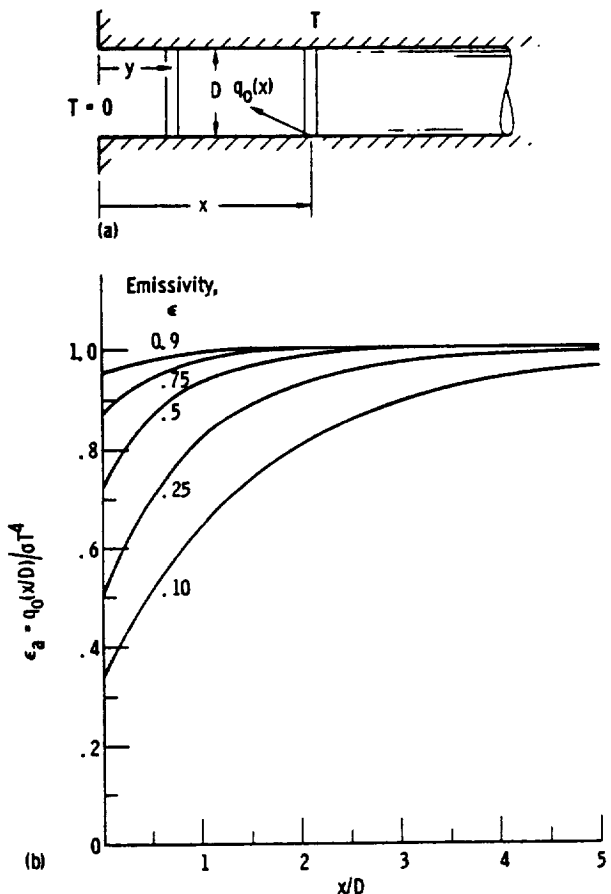
This would be expected physically for an unheated surface in a uniform temperature environment. The temperature distribution along the tube is found from equation (3-44b) as

$$\sigma T_2^4(\xi) = \frac{1-\epsilon_2}{\epsilon_2} q_2 + q_{0,2}(\xi)|_{T_e=0} + q_{0,2}(\xi)|_{q_2=0}$$

$$\sigma T_2^4(\xi) = \frac{1-\epsilon_2}{\epsilon_2} q_2 + q_{0,2}(\xi)|_{T_e=0} + \sigma T_2^4$$

where $q_{0,2}(\xi)|_{T_e=0}$ was found in part (1) of this example. The superposition of an environment temperature has thus added a σT_2^4 term to the solution for $\sigma T_2^4(\xi)$ found previously for $T_e = 0$.

EXAMPLE 3-9: This example will consider the emission from a long cylindrical hole drilled into a material that is all at uniform temperature T (fig. 3-9). The hole is assumed sufficiently long that the surface at the bottom end of the hole can be neglected in the radiative heat balances. The environment outside the hole is taken to be at 0°R . If a position is viewed at x on the cylindrical side wall of the hole, the energy leaving the wall is composed of the direct emission plus the reflected energy, the total being the quantity $q_o(x)$. An apparent emissivity is defined as $\epsilon_a(x) = q_o(x)/\sigma T^4$. The objective of this analysis will be to determine how $\epsilon_a(x)$ is related to the actual surface emissivity ϵ where ϵ is constant over the side of the hole. The integral equation governing the radiation exchange within the hole was first derived by Buckley (refs. 8 and 9) and



(a) Geometry and coordinate system.
 (b) Apparent emissivity of cylinder wall.

FIGURE 3-9.—Radiant emission from cylindrical hole at uniform temperature.

later by Eckert (ref. 10); both investigators obtained approximate analytical solutions. The results were later carried out numerically to greater accuracy by Sparrow and Albers with a digital computer (ref. 11).

The opening of the hole can be approximated by a perfectly absorbing (i.e., black) disk at zero temperature; then from equation (3-44b) (because $\epsilon=1$ and $T=0$ for the opening area) the q_o for the opening disk is zero. Hence, the governing equation for the enclosure is equation (3-43a) written for the cylindrical side wall and including in the summation only the radiation from the cylindrical wall to itself. As in example 3-8, the configuration factor is that for one ring of differential length on the cylindrical enclosure exchanging radiation with a second ring at a different axial location, as given by equation (3-46b). Equation (3-43a) then yields

$$q_o(\xi) - (1 - \epsilon) \int_{\eta=0}^{\infty} q_o(\eta) dF_{d\xi-d\eta}(|\eta - \xi|) = \epsilon \sigma T^4 \quad (3-47)$$

where $\xi = x/D$, $\eta = y/D$, and $dF_{d\xi-d\eta}(|\eta - \xi|)$ is given by equation (3-46b). After dividing by σT^4 which is constant, the apparent emissivity is found to be governed by the following integral equation:

$$\epsilon_a(\xi) - (1 - \epsilon) \int_{\eta=0}^{\infty} \epsilon_a(\eta) dF_{d\xi-d\eta}(|\eta - \xi|) = \epsilon \quad (3-48)$$

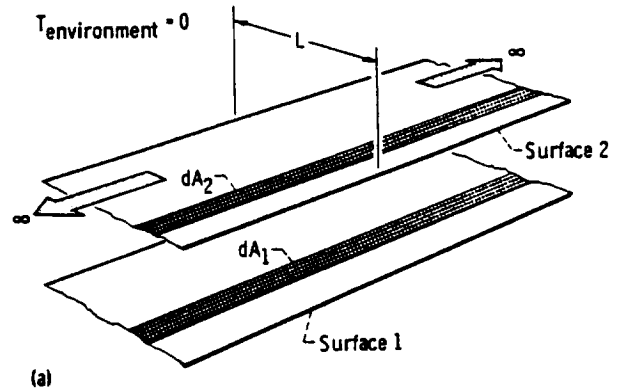
The solution of equation (3-48) was carried out for various surface emissivities ϵ , and the results for ϵ_a as a function of location along the hole are shown in figure 3-9(b). The radiation leaving the surface approaches that of a blackbody as the wall position is increased to greater depths into the hole. At the mouth of the hole, $\epsilon_a = \sqrt{\epsilon}$ as shown by Buckley (refs. 8 and 9).

EXAMPLE 3-10: What are the integral equations governing the radiation exchange between two parallel opposed plates finite in one dimension and infinite in the other as shown in figure 3-10? Each plate has a specified temperature variation which depends only on the x - or y -coordinate shown, and the environment is at zero temperature.

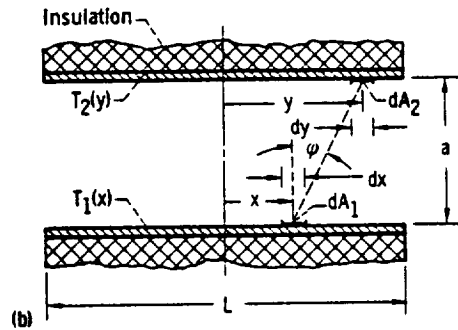
From the discussion in example 2-4, the configuration factors between the infinitely long parallel strips dA_1 and dA_2 are

$$dF_{d1-d2} = \frac{1}{2} d(\sin \varphi) = \frac{1}{2} \frac{a^2}{[(y-x)^2 + a^2]^{3/2}} dy$$

$$dF_{d2-d1} = \frac{1}{2} \frac{a^2}{[(y-x)^2 + a^2]^{3/2}} dx$$



(a)



(b)

(a) Parallel plates of width L and infinite length.

(b) Coordinates in cross section of gap between parallel plates.

FIGURE 3-10. —Geometry for radiation between two parallel plates infinitely long in one direction and of finite width.

The distribution of heat flux added to each plate can be found by applying equation (3-39) to each of the plates. As in examples 3-8 and 3-9, the environment at $T=0$ does not contribute anything since it provides an effective emissivity of unity and a temperature of zero at the edge opening between the plates. The governing equations are then

$$\frac{q_1(x)}{\epsilon_1} - \frac{1 - \epsilon_2}{\epsilon_2} \int_{-L/2}^{L/2} q_2(y) \frac{1}{2} \frac{a^2}{[(y-x)^2 + a^2]^{3/2}} dy = \sigma T_1^4(x) - \int_{-L/2}^{L/2} \sigma T_2^4(y) \frac{1}{2} \frac{a^2}{[(y-x)^2 + a^2]^{3/2}} dy \quad (3-49a)$$

$$\frac{q_2(y)}{\epsilon_2} - \frac{1 - \epsilon_1}{\epsilon_1} \int_{-L/2}^{L/2} q_1(x) \frac{1}{2} \frac{a^2}{[(y-x)^2 + a^2]^{3/2}} dx = \sigma T_2^4(y) - \int_{-L/2}^{L/2} \sigma T_1^4(x) \frac{1}{2} \frac{a^2}{[(y-x)^2 + a^2]^{3/2}} dx \quad (3-49b)$$

An alternate formulation can be obtained by applying equation (3-43a). This yields the following two equations for $q_{o,1}(x)$ and $q_{o,2}(y)$:

$$q_{o,1}(x) - (1 - \epsilon_1) \int_{-L/2}^{L/2} q_{o,2}(y) \frac{1}{2} \frac{a^2}{[(y-x)^2 + a^2]^{3/2}} dy = \epsilon_1 \sigma T_1^4(x) \quad (3-50a)$$

$$q_{o,2}(y) - (1 - \epsilon_2) \int_{-L/2}^{L/2} q_{o,1}(x) \frac{1}{2} \frac{a^2}{[(y-x)^2 + a^2]^{3/2}} dx = \epsilon_2 \sigma T_2^4(y) \quad (3-50b)$$

After the q_o 's are found, the desired $q_1(x)$ and $q_2(y)$ are obtained from equation (3-44a); they are

$$q_1(x) = \frac{\epsilon_1}{1 - \epsilon_1} [\sigma T_1^4(x) - q_{o,1}(x)] \quad (3-51a)$$

$$q_2(y) = \frac{\epsilon_2}{1 - \epsilon_2} [\sigma T_2^4(y) - q_{o,2}(y)] \quad (3-51b)$$

3.4.2 Methods for Solving Integral Equations

The previous examples have revealed that the unknown wall heat fluxes or temperatures along the surfaces of an enclosure are found from the solutions of single or simultaneous integral equations. The integral equations are linear; that is, the unknown q , q_o , or T^4 variables always appear to the first power (note that T^4 is considered as the variable rather than T). For linear integral equations there are a number of analytical and numerical solution methods that can be utilized. These are discussed in standard mathematics texts (e.g., chapter 4 of ref. 6). The use of some of these methods will now be discussed as applied to radiation problems, and some examples will be given.

3.4.2.1 Numerical integration yielding simultaneous equations.—In most instances the functions inside the integrals of the integral equations are complicated algebraic quantities. This is because these functions involve a configuration factor which, for most geometries, is not of a simple form. There is generally little chance that an exact analytical solution can be found. A numerical solution must then be attempted in most cases. The integrals are expressed in finite difference form by dividing each surface into a grid of small finite increments. The result is a set of simultaneous equations for the unknown quantities at each incremental position. This procedure is best illustrated by a specific example.

EXAMPLE 3-11: Referring to the integral equation in equations (3-46), derive a set of simultaneous algebraic equations to determine the $q_{o,2}$ distribution for a length $l=4$.

For simplicity, divide the length into four equal increments ($\Delta\eta=1$), and use the trapezoidal rule for integration. When equation (3-46a) is applied at the end of the tube where $x=0$, there is obtained

$$q_{o,2}(0) - [\frac{1}{2}q_{o,2}(0)K(|0-0|) + q_{o,2}(1)K(|1-0|) + q_{o,2}(2)K(|2-0|) + q_{o,2}(3)K(|3-0|) + \frac{1}{2}q_{o,2}(4)K(|4-0|)](1) = q_2 \quad (3-52)$$

The quantity included in brackets is the trapezoidal rule approximation for the integral. The quantity $K(|\eta-x|) = dF(|\eta-x|)/d\eta$ is the algebraic expression within the braces of equation (3-46b). The $q_{o,2}(0)$ terms in equation (3-52) may be grouped together to provide the first of equations (3-53). The other four equations of the set are obtained by writing the finite difference equation at the other incremental positions along the cylindrical enclosure

$$\left. \begin{aligned} q_{o,2}(0) [1 - \frac{1}{2}K(0)] - q_{o,2}(1)K(1) - q_{o,2}(2)K(2) - q_{o,2}(3)K(3) \\ \quad - \frac{1}{2}q_{o,2}(4)K(4) = q_2 \\ -\frac{1}{2}q_{o,2}(0)K(1) + q_{o,2}(1) [1 - K(0)] - q_{o,2}(2)K(1) \\ \quad - q_{o,2}(3)K(2) - \frac{1}{2}q_{o,2}(4)K(3) = q_2 \\ -\frac{1}{2}q_{o,2}(0)K(2) - q_{o,2}(1)K(1) + q_{o,2}(2) [1 - K(0)] \\ \quad - q_{o,2}(3)K(1) - \frac{1}{2}q_{o,2}(4)K(2) = q_2 \\ -\frac{1}{2}q_{o,2}(0)K(3) - q_{o,2}(1)K(2) - q_{o,2}(2)K(1) \\ \quad + q_{o,2}(3) [1 - K(0)] - \frac{1}{2}q_{o,2}(4)K(1) = q_2 \\ -\frac{1}{2}q_{o,2}(0)K(4) - q_{o,2}(1)K(3) - q_{o,2}(2)K(2) - q_{o,2}(3)K(1) \\ \quad + q_{o,2}(4) [1 - \frac{1}{2}K(0)] = q_2 \end{aligned} \right\} (3-53)$$

These equations are solved simultaneously for the unknown q_o values at the five surface locations. From the symmetry of the configuration and the fact that q_2 is uniform along the enclosure, it is possible in this instance to simplify the solution by using the equalities $q_{o,2}(0) = q_{o,2}(4)$ and $q_{o,2}(1) = q_{o,2}(3)$.

In practice a set of equations such as equations (3-53) is first solved for a moderate number of increments along the enclosure. Then the

increment size is reduced, and the set of equations is solved again. This process is continued until sufficiently accurate q_0 values are obtained. This procedure would generally be programmed on an electronic computer in terms of an arbitrary increment size.

Equations (3-53) were derived using the trapezoidal rule as a simple numerical approximation to the integrals. Other more accurate numerical integration schemes can be used which may reduce the number of increments required to provide sufficient accuracy in a given problem.

One precaution should be noted. The quantity $q_{0,j} dF_{dk-dj}$ may, in certain instances, go through rapid changes in magnitude because of the geometry involved in the configuration factor; for example, dF_{dk-dj} may decrease very rapidly as the distance between dA_k and dA_j is increased. This may mean that an integration approximation such as Simpson's rule will not be very accurate since the shape of $q_{0,j} dF_{dk-dj}$ may not be approximated well by passing a parabola locally through the function. Care should be taken in selecting an integration scheme that can approximate well the general behavior of the functions involved.

Example 3-11 contained only one integral equation. The situation described by equations (3-49) involves two integral equations. Surfaces 1 and 2 can both be divided into increments, and the equations can be written in finite difference form at each incremental location. This will yield a set of simultaneous equations equal to the total number of chosen positions on both plates, and the equations can then be solved simultaneously for the $q_1(x)$ and $q_2(y)$ distributions.

Another way of solving the two integral equations numerically is by iteration. With $T_1(x)$ and $T_2(y)$ specified, the right sides of the equations are known as functions of x and y . Starting with equation (3-49a), a distribution for $q_2(y)$ is assumed as a first trial. Then the integration can be carried out numerically for various x values to yield $q_1(x)$ at these x locations. This $q_1(x)$ distribution is then inserted into equation (3-49b) and a $q_2(y)$ distribution is determined. This $q_2(y)$ is then used to compute a new $q_1(x)$, and the process is continued until $q_1(x)$ and $q_2(y)$ are no longer changing as the iterations proceed.

3.4.2.2 *Use of approximate separable kernel.*—In an integral equation such as equation (3-46a), the solution can sometimes be simplified if the kernel is of a separable form, that is, equal to a product (or sum of products) of a function of \vec{r}_j alone and a function of \vec{r}_k alone. It is recalled from equation (3-36) that the kernel is

$$K(\vec{r}_j, \vec{r}_k) = dF_{dk-dj}(\vec{r}_j, \vec{r}_k)/dA_j$$

For a separable kernel, the function of \vec{r}_k can be taken out of the integral, thereby simplifying the integration. The general theory of integral

equations with separable kernels is given in the mathematics text (ref. 6). Generally, for radiation problems K will not be in a separable form. However, it may be possible to find a separable function that closely approximates K and can thus be substituted into the integral equation to provide a simplification.

Buckley (refs. 8 and 9) demonstrated that an especially useful form for a separable kernel is an exponential function or series of exponential functions. With this type of kernel, it is possible to change the integral equation into a differential equation, and sometimes an analytical solution can be obtained. This will be demonstrated in example 3-12. There is a mathematical point that should be mentioned here. The process of changing the integral equation into a differential equation requires taking derivatives of the approximate separable kernel. Even though the separable function may approximate the exact kernel fairly well, the approximation of the derivatives may become poor especially when higher derivatives are taken. The use of the separable kernel will now be demonstrated with an example.

EXAMPLE 3-12: Determine $q_{0,2}/q_2$ from equation (3-46a) by use of an exponential approximate separable kernel (ref. 7).

The governing equation is

$$\frac{q_{0,2}(\xi)}{q_2} - \int_{\eta=0}^l \frac{q_{0,2}(\eta)}{q_2} K(|\eta - \xi|) d\eta = 1 \quad (3-54a)$$

where

$$K(|\eta - \xi|) = 1 - \frac{|\eta - \xi|^3 + \frac{3}{2}|\eta - \xi|}{[(\eta - \xi)^2 + 1]^{3/2}} \quad (3-54b)$$

The $K(|\eta - \xi|)$ is plotted in figure 3-11, and it is reasonably well approximated by the function $e^{-2|\eta - \xi|}$. When the approximate kernel is substituted into equation (3-54a), the part of the function depending on ξ can be taken out of the integral to give the result

$$\frac{q_{0,2}(\xi)}{q_2} - e^{-2\xi} \int_0^\xi \frac{q_{0,2}(\eta)}{q_2} e^{2\eta} d\eta - e^{2\xi} \int_\xi^l \frac{q_{0,2}(\eta)}{q_2} e^{-2\eta} d\eta = 1 \quad (3-55)$$

By differentiating equation (3-55) twice, the integrals can be removed and the following differential equation obtained

$$\frac{d^2 \left[\frac{q_{0,2}(\xi)}{q_2} \right]}{d\xi^2} = -4$$

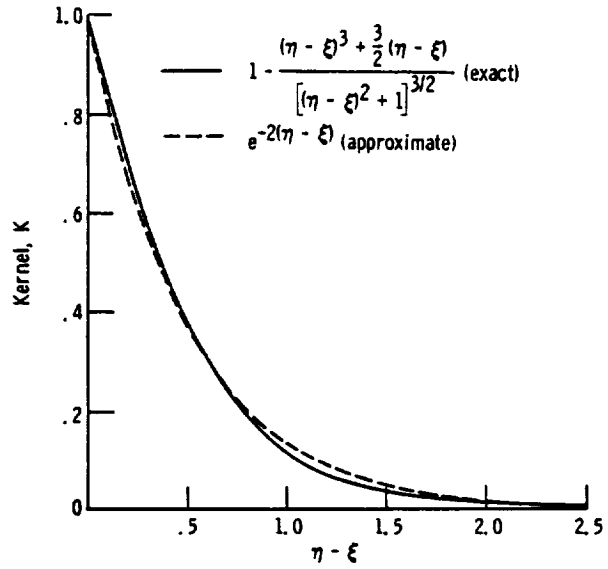


FIGURE 3-11.—Exponential approximation to configuration factor kernel for cylindrical enclosure.

This has the general solution, obtained by integrating twice,

$$\frac{q_{o,2}(\xi)}{q_2} = -2\xi^2 + C_1\xi + C_2 \tag{3-56a}$$

To obtain C_1 and C_2 , two boundary conditions are needed. From symmetry one boundary condition is

$$\frac{d\left(\frac{q_{o,2}}{q_2}\right)}{d\xi} = 0 \quad \text{at } \xi = \frac{l}{2}$$

which yields $C_1 = 2l$. To determine C_2 , a boundary condition can be obtained from equation (3-55) by evaluating it at $\xi = 0$ and $\xi = l$ and then utilizing the fact that $q_{o,2}(0) = q_{o,2}(l)$ to obtain the condition

$$\int_0^l \frac{q_{o,2}(\eta)}{q_2} e^{-2\eta} d\eta = e^{-2l} \int_0^l \frac{q_{o,2}(\eta)}{q_2} e^{2\eta} d\eta$$

Inserting $q_{o,2}/q_2 = -2\xi^2 + 2l\xi + C_2$ and integrating yield $C_2 = l + 1$. With C_1 and C_2 thus evaluated, the final result for $q_{o,2}/q_2$ by the separable kernel method is the parabola

$$\frac{q_{0,2}(\xi)}{q_2} = l + 1 + 2(\xi l - \xi^2) \quad (3-56b)$$

More generally, the boundary conditions to evaluate C_1 and C_2 could have been obtained even in an asymmetric case by evaluating the integral equation at both boundaries $x=0$ and $x=l$. This yields from equation (3-55)

$$\frac{q_{0,2}(0)}{q_2} - \int_0^l \frac{q_{0,2}(\eta)}{q_2} e^{-2\eta} d\eta = 1$$

$$\frac{q_{0,2}(l)}{q_2} - e^{-2l} \int_0^l \frac{q_{0,2}(\eta)}{q_2} e^{2\eta} d\eta = 1$$

Then $q_{0,2}/q_2$ from equation (3-56a) is substituted into these two boundary conditions. After integrating, two simultaneous equations result for C_1 and C_2 , leading to the same solution as before. The advantage of previously using the symmetry condition was only algebraic simplicity.

3.4.2.3 *Approximate solution by variational method.*—As mentioned in reference 6 (p. 495), an integral equation of the form

$$\varphi(\xi) = \int_a^b K(\xi, \eta) \varphi(\eta) d\eta + G(\xi) \quad (3-57)$$

can be solved by variational methods. A restriction is that $K(\xi, \eta)$ be symmetric, that is, K is not changed when the values of ξ and η are interchanged. The kernel of equation (3-54b) is an example of a symmetric kernel since, because of the absolute value signs, it is evident that $K(|\eta - \xi|) = K(|\xi - \eta|)$.

The variational method depends on the use of an auxiliary function that is related in a particular way to the integral equation given by equation (3-57). This auxiliary function is given by

$$J = \int_a^b \int_a^b K(\xi, \eta) \varphi(\xi) \varphi(\eta) d\xi d\eta - \int_a^b [\varphi(\xi)]^2 d\xi + 2 \int_a^b \varphi(\xi) G(\xi) d\xi \quad (3-58)$$

The significance of the J function is that, when the correct solution for $\varphi(\xi)$ is found, J will have a minimum value.

The procedure for obtaining an approximate solution is to let $\varphi(\xi)$ be represented by a polynomial with unknown coefficients,

$$\varphi(\xi) = \gamma_0 + \gamma_1 \xi + \gamma_2 \xi^2 + \dots + \gamma_n \xi^n \quad (3-59)$$

This polynomial is substituted into equation (3-58), and the integration is carried out. If K is so complicated algebraically that the integration cannot be performed analytically, the method is not practical. After the integration is carried out, the result is an analytical expression for J as a function of $\gamma_0, \gamma_1, \gamma_2, \dots, \gamma_n$. These unknown coefficients are then determined by differentiating J with respect to each of the individual coefficients and setting each result equal to zero, that is, $\partial J / \partial \gamma_0 = 0, \partial J / \partial \gamma_1 = 0, \dots, \partial J / \partial \gamma_n = 0$. This yields a set of $n+1$ simultaneous equations for the $n+1$ unknown coefficients. By differentiating J in this manner and setting the differentials equal to zero, the coefficients are found that make J a minimum value; thus the most accurate solution to the integral equation of the assumed form $\varphi(x) = \sum_{j=0}^n \gamma_j x^j$ is found.

This method has been applied for radiation in a cylindrical tube in reference 7 and radiation between parallel plates of finite width and infinite length in reference 12.

3.4.2.4 Approximate solution by Taylor series expansion.—The use of a Taylor series expansion method for solving a radiation integral equation was demonstrated in references 13 and 14. The physical idea that motivates this method of solution is that the geometric configuration factor can often decrease quite rapidly as the distance between the two elements exchanging radiation is increased. This means that the radiative heat balance at a given location may be significantly influenced only by the radiative fluxes leaving other surface elements in the immediate vicinity of that location.

As an example, consider the type of integral equation in equation (3-54). The function of $K(|\eta - \xi|)$ decreases rapidly as $\eta - \xi$ is increased as shown in figure 3-11. Then, if it is assumed that the important values of η are when η is close to the location ξ , the function $q_{0,2}(\eta)/q_2$ is expanded in a Taylor series about ξ

$$\frac{q_{0,2}(\eta)}{q_2} = \frac{q_{0,2}(\xi)}{q_2} + (\eta - \xi) \left[\frac{d \left(\frac{q_{0,2}}{q_2} \right)}{d\xi} \right]_{\xi} + \frac{(\eta - \xi)^2}{2!} \left[\frac{d^2 \left(\frac{q_{0,2}}{q_2} \right)}{d\xi^2} \right]_{\xi} + \dots \quad (3-60)$$

The derivatives in the Taylor expansion are evaluated at ξ and hence do not contain the variable η . This means that, when equation (3-60) is substituted into equation (3-54a), the derivatives can be taken out of the integrals to yield

$$\begin{aligned} \frac{q_{o,2}(\xi)}{q_2} - \frac{q_{o,2}(\xi)}{q_2} \int_{\eta=0}^1 K(|\eta - \xi|) d\eta \\ - \frac{d}{d\xi} \left[\frac{q_{o,2}(\xi)}{q_2} \right] \int_{\eta=0}^1 (\eta - \xi) K(|\eta - \xi|) d\eta \\ - \frac{1}{2!} \frac{d^2}{d\xi^2} \left[\frac{q_{o,2}(\xi)}{q_2} \right] \int_{\eta=0}^1 (\eta - \xi)^2 K(|\eta - \xi|) d\eta - \dots = 1 \quad (3-61) \end{aligned}$$

The integrations are then carried out; if this cannot be done analytically, the method is not of practical utility because it is as easy to carry out a numerical solution of the exact integral equation as of equation (3-61). If the integrals can be carried out analytically, equation (3-61) becomes a differential equation for $q_{o,2}(\xi)/q_2$, which can be solved analytically or numerically if the boundary conditions can be specified. The boundary conditions can be derived as illustrated in reference 14 from the physical constraints in the system; for example, symmetry or an overall heat balance. This method is probably of little value for enclosures involving more than one or two surfaces.

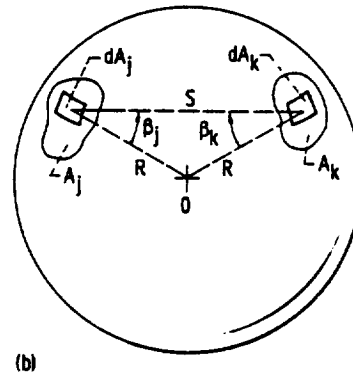
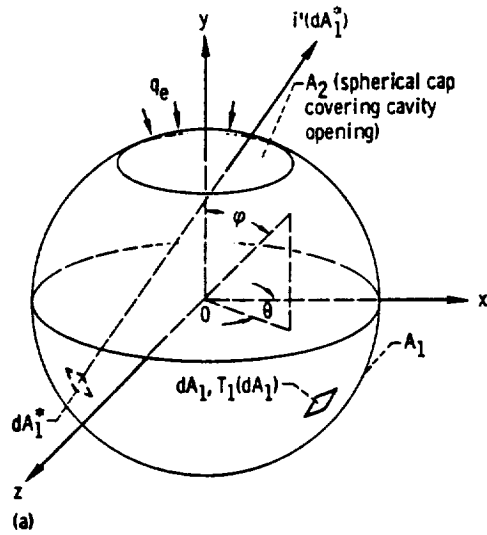
In the past four sections, methods have been discussed for solving single or sets of integral equations by numerical methods and by some approximate analytical methods. The analytical methods are probably of value only when the integral equations are relatively simple. In almost all practical cases the numerical method would be resorted to. There are a few instances where approximate or numerical solutions are not required since the radiation exchange integral equation has an exact analytical solution. One of these cases will now be discussed.

3.4.2.5 Exact solution of integral equation for radiation from a spherical cavity.—The radiation from a spherical cavity, as shown in figure 3-12(a), was analyzed by Jensen (ref. 15), discussed by Jakob (ref. 3), and further treated by Sparrow and Jonsson (ref. 16).

The spherical shape leads to a relatively simple integral equation solution because there is an especially simple geometrical configuration factor between elements on the inside of the spherical cavity. The configuration factor between two differential elements dA_j and dA_k shown in figure 3-12(b) is

$$dF_{d_j-d_k} = \frac{\cos \beta_j \cos \beta_k}{\pi S^2} dA_k \quad (3-62)$$

Since the sphere radius is normal to both elements dA_j and dA_k , the distance between these elements is given by



(a) Spherical cavity with diffuse entering radiation q_e and with surface at uniform temperature T_1 .
 (b) Area elements on spherical surface.

FIGURE 3-12. — Geometry involved in radiation within spherical cavity.

$$S = 2R \cos \beta_j = 2R \cos \beta_k$$

Then equation (3-62) becomes

$$dF_{d_j-d_k} = \frac{dA_k}{4\pi R^2} \tag{3-63}$$

If, instead of an infinitesimal area dA_k , the element dA_j exchanges with the finite area A_k , then equation (3-63) becomes

$$F_{dj-k} = \frac{1}{4\pi R^2} \int_{A_k} dA_k = \frac{A_k}{4\pi R^2} \quad (3-64)$$

Equation (3-64) is independent of the area element dA_j ; hence, dA_j could be replaced by a finite area A_j so that

$$F_{j-k} = \frac{A_k}{4\pi R^2} = \frac{A_k}{A_s} \quad (3-65)$$

where A_s is the surface area of the entire sphere.

Consider the spherical cavity shown in figure 3-12(a). The cavity surface has a temperature distribution $T_1(dA_1)$ and has a total surface area A_1 . The spherical cap that would cover the cavity opening has an area A_2 . Assume there is diffuse radiative flux q_e (per unit area of A_2) entering from the environment through the cavity opening. The q_e can be variable over A_2 . It is desired to compute the radiation intensity $i'(dA_1^*)$ leaving the cavity opening at a specified location and in a specified direction, as shown by the arrow in figure 3-12(a). The figure shows that the desired intensity will result from the flux leaving the element dA_1^* and will equal $q_{o,1}(dA_1^*)/\pi$ where the factor π arises from the relation between hemispherical flux q_o and intensity i' . The flux $q_{o,1}(dA_1^*)$ can be found by applying equation (3-43a)

$$q_{o,1}(dA_1^*) - (1 - \epsilon_1) \int_{A_1} q_{o,1}(dA_1) dF_{d1^*-d1} - (1 - \epsilon_1) \int_{A_2} q_e(dA_2) dF_{d1^*-d2} = \epsilon_1 \sigma T_1^4(dA_1^*) \quad (3-66)$$

The F factors from equation (3-63) are then substituted to give

$$q_{o,1}(dA_1^*) - \frac{1 - \epsilon_1}{4\pi R^2} \int_{A_1} q_{o,1}(dA_1) dA_1 = \frac{1 - \epsilon_1}{4\pi R^2} \int_{A_2} q_e(dA_2) dA_2 + \epsilon_1 \sigma T_1^4(dA_1^*) \quad (3-67)$$

where the known quantities are grouped on the right side of the equation. To solve equation (3-67), a trial solution of the form

$$q_{o,1}(dA_1^*) = f(dA_1^*) + C$$

is assumed, where f is an unknown function of the location of dA_1^* and C is a constant. Substituting into equation (3-67) gives

$$f(dA_1^*) + C - \frac{1 - \epsilon_1}{4\pi R^2} \int_{A_1} f(dA_1) dA_1 - \frac{1 - \epsilon_1}{4\pi R^2} CA_1$$

$$= \frac{1 - \epsilon_1}{4\pi R^2} \int_{A_2} q_e(dA_2) dA_2 + \epsilon_1 \sigma T_1^4(dA_1^*)$$

The only two terms that are functions of local position within the cavity are the first and last which gives $f(dA_1^*) = \epsilon_1 \sigma T_1^4(dA_1^*)$. The remaining terms are then equated to determine C . This gives the result for $q_{o,1}(dA_1^*)$

$$q_{o,1}(dA_1^*) = \epsilon_1 \sigma T_1^4(dA_1^*)$$

$$+ \frac{\frac{1 - \epsilon_1}{4\pi R^2} \left[\int_{A_1} \epsilon_1 \sigma T_1^4(dA_1) dA_1 + \int_{A_2} q_e(dA_2) dA_2 \right]}{1 - \frac{(1 - \epsilon_1)A_1}{4\pi R^2}} \quad (3-68)$$

The desired solution is $i'(dA_1^*) = q_{o,1}(dA_1^*)/\pi$.

3.5 CONCLUDING REMARKS

In this chapter, methods were developed for treatment of the energy exchange within enclosures having diffuse-gray surfaces; the surfaces can be of finite or infinitesimal size. The surfaces can have a specified net energy flux added to them by some external means, can have a specified surface temperature, or can be subjected to some combination of these conditions. A number of methods were presented for solution of the integral equations that resulted from the general formulation of these interchange problems. It was pointed out that most practical problems become so complex that only numerical techniques can successfully be used for the solution of the governing equations.

In succeeding chapters, extensions of the present procedures to nonidealized surfaces are made, and methods for incorporating coupled conduction and convection of energy will be introduced.

REFERENCES

1. HOTTEL, HOYT C.: Radiant-Heat Transmission. Heat Transmission. Third ed., William H. McAdams, McGraw-Hill Book Co., Inc., 1954, ch. 4.
2. POLJAK, G.: Analysis of Heat Interchange by Radiation Between Diffuse Surfaces. Tech. Phys. USSR, vol. 1, no. 5-6, 1935, pp. 555-590.
3. JAKOB, MAX: Heat Transfer. Vol. II. John Wiley & Sons, Inc., 1957.
4. GEBHART, B.: Unified Treatment for Thermal Radiation Transfer Processes—Gray, Diffuse Radiators and Absorbers. Paper No. 57-A-34, ASME, Dec. 1957.

5. SPARROW, E. M.: On the Calculation of Radiant Interchange Between Surfaces. Modern Developments in Heat Transfer. Warren Ibele, ed., Academic Press, 1963, pp. 181-212.
6. HILDEBRAND, FRANCIS B.: Methods of Applied Mathematics. Prentice-Hall, Inc., 1952.
7. USISKIN, C. M.; AND SIEGEL, R.: Thermal Radiation From a Cylindrical Enclosure with Specified Wall Heat Flux. J. Heat Transfer, vol. 82, no. 4, Nov. 1960, pp. 369-374.
8. BUCKLEY, H.: Radiation from the Interior of a Reflecting Cylinder. Phil. Mag., vol. 4, Oct. 1927, pp. 753-762.
9. BUCKLEY, H.: Radiation from Inside a Circular Cylinder. Phil. Mag., vol. 6, Sept. 1928, pp. 447-457.
10. ECKERT, E.: Das Strahlungsverhaeltnis von Flaechen mit Einbuchtungen und von zylindrischen Bohrungen. Archiv fur Waermewirtschaft, vol. 16, no. 5, May 1935, pp. 135-138.
11. SPARROW, E. M.; AND ALBERS, L. U.: Apparent Emissivity and Heat Transfer in a Long Cylindrical Hole. J. Heat Transfer, vol. 82, no. 3, Aug. 1960, pp. 253-255.
12. SPARROW, E. M.: Application of Variational Methods to Radiation Heat-Transfer Calculations. J. Heat Transfer, vol. 82, no. 4, Nov. 1960, pp. 375-380.
13. KRISHNAN, K. S.; AND SUNDARAM, R.: The Distribution of Temperature Along Electrically Heated Tubes and Coils. I. Theoretical. Roy. Soc. Proc., Ser. A, vol. 257, no. 1290, Sept. 20, 1960, pp. 302-315.
14. PERLMUTTER, M.; AND SIEGEL, R.: Effect of Specularly Reflecting Gray Surface on Thermal Radiation Through a Tube and From Its Heated Wall. J. Heat Transfer, vol. 85, no. 1, Feb. 1963, pp. 55-62.
15. JENSEN, H. H.: Some Notes on Heat Transfer by Radiation. K. Danske Vidensk. Selsk. Mat.-Fys. Medd., vol. 24, no. 8, 1948, pp. 1-26.
16. SPARROW, E. M.; AND JONSSON, V. K.: Absorption and Emission Characteristics of Diffuse Spherical Enclosures. NASA TN D-1289, 1962.

Chapter 4. Radiation in Enclosures Having Some Specularly Reflecting Surfaces

4.1 INTRODUCTION

In chapter 3 all the surfaces considered were assumed to be diffuse emitters *and* diffuse reflectors. In this chapter the surface characteristics of some of the surfaces will be changed. All of the surfaces are still assumed to *emit* in a diffuse fashion. Some of the surfaces in an enclosure will be assumed to reflect diffusely, as before. The remaining surfaces will be assumed to be specular; that is, they will reflect in a mirrorlike manner.

When reflection is diffuse, the directional history of the incident radiation is lost upon reflection: the reflected energy has the same directional distribution as if it had been absorbed and then diffusely reemitted. With a specular reflection, the reflection angle relative to the surface normal is equal in magnitude to the angle of incidence. Hence, in contrast to diffuse behavior the directional history of the incident radiation is not lost upon reflection. Consequently, when dealing with specular surfaces, it will be necessary to account for the directional paths that the reflected radiation follows between surfaces.

The specular reflectivities used in this chapter are assumed *independent of incident angle* of radiation; that is, the same fraction of the incident energy is reflected, regardless of the angle of incidence of the energy. In addition, all the surfaces are assumed to have *gray properties*; that is, the properties do not depend on wavelength.

4.2 SYMBOLS

A	area
c_p	specific heat
D	tube diameter
d	number of diffuse surfaces
F	configuration factor
L	length of enclosure side
N	total number of surfaces
Q	energy rate; energy per unit time
q	energy flux; energy per unit area and per unit time
T	absolute temperature
V	volume
X, x	position coordinates

α	absorptivity
ϵ	emissivity
ρ	reflectivity
ρ_M	density of material
σ	Stefan-Boltzmann constant
τ	time

Subscripts:

e	emitted
F	final
I	initial
i	incoming
j, k	j^{th} or k^{th} surface
o	outgoing
s	specular
1, 2	surface 1 or 2

Superscripts:

s	total specular exchange factor including all paths for specular interreflections plus direct exchange
"	bidirectional value
*	denotes a second portion of area on same surface

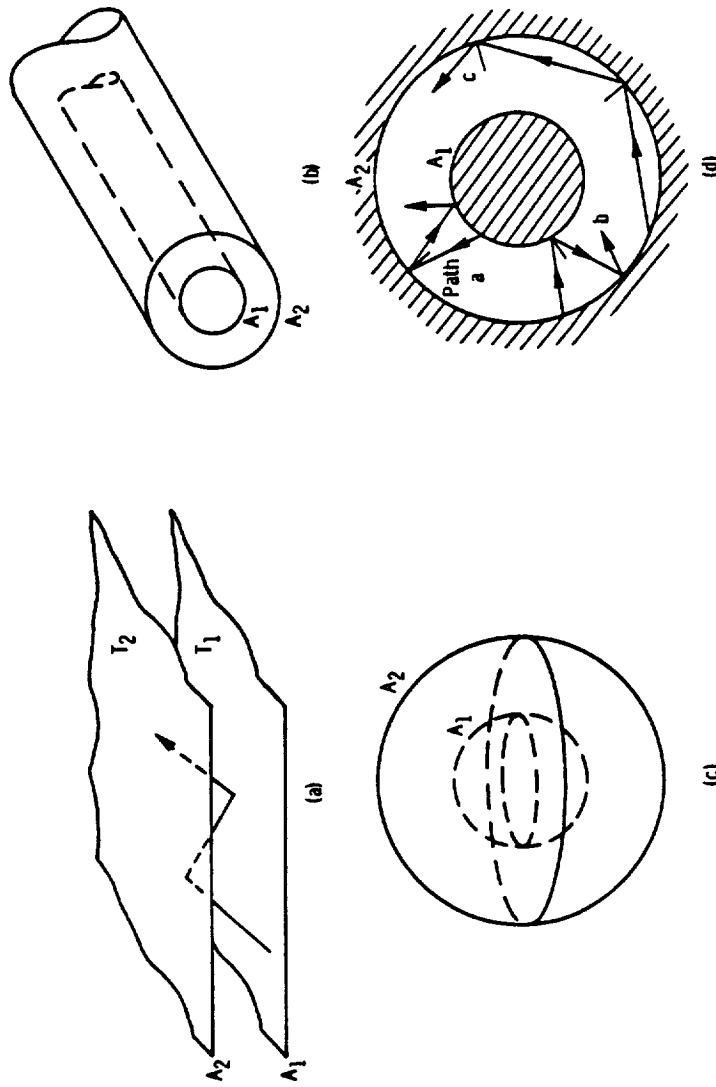
4.3 RADIATION BETWEEN PAIRS OF SURFACES WITH SPECULAR REFLECTIONS

4.3.1 Some Simple Cases

As an introduction, consider radiation exchange for some simple geometries: infinite parallel plates, concentric cylinders, and concentric spheres as shown in figure 4-1. Specular radiation exchange in these cases is well understood, having been discussed by Christiansen (ref. 1) and Saunders (ref. 2) some years ago. Because the radiative exchange process is easy to grasp for these cases, let us examine it at some length.

Consider radiation between two infinite gray parallel specular plates as shown in figure 4-1(a). All emitted and reflected radiation leaving surface 1 will reach surface 2 directly; similarly, all emitted and reflected radiation leaving surface 2 will reach surface 1 directly. This will be true whether the surfaces are specular or diffuse. Hence, for the specular case equation (3-10) also applies, and the net heat transfer from surface 1 and surface 2 is

$$Q_1 = -Q_2 = \frac{A_1 \sigma (T_1^4 - T_2^4)}{\frac{1}{\epsilon_1(T_1)} + \frac{1}{\epsilon_2(T_2)} - 1} \quad (4-1)$$



(b) Gap between infinitely long concentric cylinders.
(d) Paths for specular radiation in gap between concentric cylinders or spheres.

(a) Infinite parallel plates.
(c) Gap between concentric spheres.

FIGURE 4-1. — Radiation exchange for specular surfaces having simple geometries.

Now consider radiation between the concentric cylinders or spheres shown in figures 4-1(b) and (c). Typical radiation paths for specular exchange are shown in figure 4-1(d). As shown by path (a) all the radiation emitted by surface 1 will directly reach 2. A portion will be reflected from surface 2 back to 1, and a portion of this will be re-reflected from surface 1. This sequence of reflections between the surfaces continues until an insignificant amount of energy remains because the radiation has become partially absorbed on each contact with a surface. From the symmetry of the concentric geometry and the equal magnitudes of incidence and reflection angles for specular reflections, none of the radiation following path (a) can ever be reflected directly from a position on surface 2 to another element on surface 2. Thus the radiation exchange process for radiation emitted from surface 1 is the same as though the two concentric surfaces were infinite parallel plates. However, the radiation emitted from the outer surface 2 can travel along either of two types of paths (b) or (c) as shown in figure 4-1(d). The fraction F_{2-2} will follow paths of type (c). From the geometry of specular reflections these rays will always be reflected along surface 2 with none ever reaching 1. The fraction F_{2-1} will be reflected back and forth between the surfaces along path (b) in the same fashion as radiation emitted from surface 1. The amount of radiation following this type of path is

$$A_2 \epsilon_2 F_{2-1} \sigma T_2^4 = A_2 \epsilon_2 (A_1/A_2) \sigma T_2^4 = A_1 \epsilon_2 \sigma T_2^4$$

(the configuration factor $F_{2-1} = A_1/A_2$ has been employed). The fraction of the radiation leaving 2 that impinges on 1 thus depends on area A_1 and not on A_2 . Hence, for specular surfaces the exchange behaves as if both surfaces were equal portions of infinite parallel plates equal in size to the area of the inner body. The net heat transfer from surface 1 to surface 2 is then given by equation (4-1).

EXAMPLE 4-1: A spherical vacuum bottle consists of two silvered concentric glass spheres, the inner being 6 inches in diameter and the evacuated gap between the spheres being $\frac{1}{4}$ inch. The emissivity of the silver coating is 0.02. If hot coffee at 200° F is in the bottle and the outside temperature is 70° F, what is the radiative heat leakage out of the bottle?

Equation (4-1) will apply for concentric specular spheres. For the small rate of heat leakage expected, it is assumed that the surfaces will be close to 200° and 70° F. This gives

$$Q_1 = \frac{\pi \left(\frac{1}{2}\right)^2 0.173 \times 10^{-8} (660^4 - 530^4)}{\frac{1}{0.02} + \frac{1}{0.02} - 1} = 1.52 \text{ Btu/hr}$$

(If, instead of using the specular formulation, both surfaces had been assumed diffuse, then equation (3-14) would be applied. The denominator of the Q_1 equation becomes

$$\frac{1}{\epsilon_1} + \frac{A_1}{A_2} \left(\frac{1}{\epsilon_2} - 1\right) = \frac{1}{0.02} + \left(\frac{6}{6.5}\right)^2 \left(\frac{1}{0.02} - 1\right) = 91.8$$

instead of 99, as in the specular case. For diffuse surfaces the heat loss would be 1.64 Btu/hr.)

EXAMPLE 4-2: For the previous example, how long will it take for the coffee to cool from 200° to 120° F if the heat loss is only by radiation?

The heat capacity of the coffee is $\rho_M V c_p T_1$. Assuming the coffee is always well enough mixed so that it is at uniform temperature, the cooling rate will be equal to the *instantaneous* loss by radiation. The loss of energy by radiation at any time τ , given by equation (4-1), is related to the loss of internal energy of the coffee by

$$-\rho_M V c_p \frac{dT_1}{d\tau} = \frac{A_1 \sigma [T_1^4(\tau) - T_2^4]}{\frac{1}{\epsilon_1} + \frac{1}{\epsilon_2} - 1}$$

The approximations have been made that surface 1 is at the coffee temperature and surface 2 is at the outside environment temperature. Then

$$-\int_{T_1=T_i}^{T_1=T_f} \frac{dT_1}{T_1^4 - T_2^4} = \frac{A_1 \sigma}{\rho_M V c_p \left(\frac{1}{\epsilon_1} + \frac{1}{\epsilon_2} - 1\right)} \int_0^\tau d\tau$$

where T_i and T_f are the initial and final temperatures of the coffee and ϵ_1 and ϵ_2 are assumed independent of temperature. Carrying out the integration gives

$$\left(\frac{1}{4T_2^3} \ln \left| \frac{T_1 + T_2}{T_1 - T_2} \right| + \frac{1}{2T_2^3} \tan^{-1} \frac{T_1}{T_2} \right) \Big|_{T_i}^{T_f} = \frac{A_1 \sigma \tau}{\rho_M V c_p \left(\frac{1}{\epsilon_1} + \frac{1}{\epsilon_2} - 1\right)}$$

Then the cooling time from T_i to T_f is

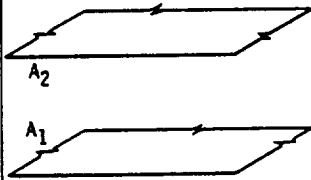
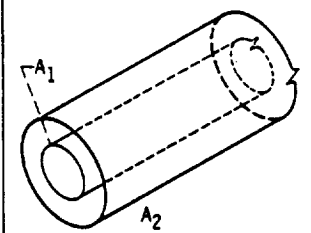
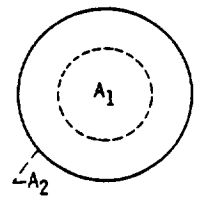
$$\tau = \frac{\rho_M V c_p \left(\frac{1}{\epsilon_1} + \frac{1}{\epsilon_2} - 1 \right)}{A_1 \sigma} \left[\frac{1}{4T_2^3} \ln \left| \frac{T_F + T_2}{T_F - T_2} \frac{T_1 + T_2}{T_1 - T_2} \right| + \frac{1}{2T_2^3} \left(\tan^{-1} \frac{T_F}{T_2} - \tan^{-1} \frac{T_1}{T_2} \right) \right]$$

Substituting the values $\rho_M = 62.4 \text{ lb/ft}^3$, $V = \frac{1}{6} \pi \left(\frac{1}{2} \right)^3 \text{ ft}^3$, $c_p = 1 \text{ Btu/(lb)(}^\circ\text{F)}$, $\epsilon_1 = \epsilon_2 = 0.02$, $A_1 = \pi \left(\frac{1}{2} \right)^2 \text{ ft}^2$, $\sigma = 0.173 \times 10^{-8} \text{ Btu/(hr)(ft}^2\text{)(}^\circ\text{R}^4)$, $T_2 = 530^\circ \text{ R}$, $T_1 = 660^\circ \text{ R}$, and $T_F = 580^\circ \text{ R}$ gives the cooling time as $\tau = 380 \text{ hr}$.

The coffee will stay hot for about 16 days if heat losses occur only by radiation. Conduction losses through the bottle neck usually cause the cooling rate to be much higher.

Equation (4-1) applies for infinite parallel plates, infinitely long

TABLE 4-1.—RADIANT INTERCHANGE BETWEEN SOME SIMPLY ARRANGED SURFACES

Geometry	Configuration	Surface type	Energy rate, Q_1
Infinite parallel plates		A_1 or A_2 , either specular or diffuse	$\frac{A_1 \sigma (T_1^4 - T_2^4)}{\frac{1}{\epsilon_1} + \frac{1}{\epsilon_2} - 1}$
Infinitely long concentric cylinders		A_1 , specular or diffuse A_2 , diffuse	$\frac{A_1 \sigma (T_1^4 - T_2^4)}{\frac{1}{\epsilon_1} + \frac{A_1}{A_2} \left(\frac{1}{\epsilon_2} - 1 \right)}$
		A_1 , specular or diffuse A_2 , specular	$\frac{A_1 \sigma (T_1^4 - T_2^4)}{\frac{1}{\epsilon_1} + \frac{1}{\epsilon_2} - 1}$
Concentric spheres		A_1 , specular or diffuse A_2 , diffuse	$\frac{A_1 \sigma (T_1^4 - T_2^4)}{\frac{1}{\epsilon_1} + \frac{A_1}{A_2} \left(\frac{1}{\epsilon_2} - 1 \right)}$
		A_1 , specular or diffuse A_2 , specular	$\frac{A_1 \sigma (T_1^4 - T_2^4)}{\frac{1}{\epsilon_1} + \frac{1}{\epsilon_2} - 1}$

concentric cylinders, and concentric spheres when both surfaces are specular. For infinite parallel plates, it also applies when both surfaces are diffuse or when one surface is diffuse and the other specular. For cylinders and spheres, equation (4-1) still applies if the surface of the inner body (surface 1) is diffuse as long as the outer body (surface 2) remains specular. This is because all radiation leaving surface 1 will go directly to 2 regardless of whether 1 is specular or diffuse. When surface 2 is diffuse, equation (3-14) applies and may be used when surface 1 is either specular or diffuse. The relations are summarized in table 4-I.

4.3.2 Energy Exchange Between Specular Surfaces

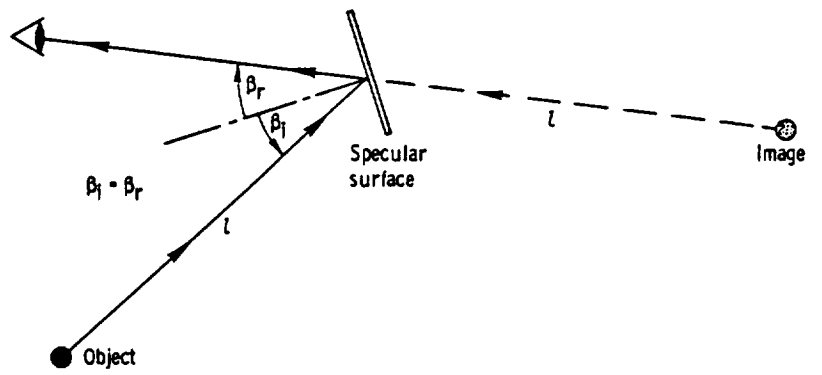
4.3.2.1 *Ray tracing and the construction of images.*—When mirrorlike reflections occur in enclosures, the well-developed procedures of geometric optics can be applied to simplify both the concepts and the mathematics of the radiative exchange process. The basic ideas are outlined in this section. More advanced ideas may be found in references 3 and 4.

An incident ray striking a specular surface is reflected in a symmetric fashion about the surface normal so that the angle of reflection is equal in magnitude to the angle of incidence. This fact is used to formulate the concept of *images*. An image is simply an apparent point of origin for an observed ray. For example, in figure 4-2(a), an observer views an object in a mirror. To the observer, the object appears to be *behind* the mirror in the position shown by the dotted object. This apparent object is called the image.

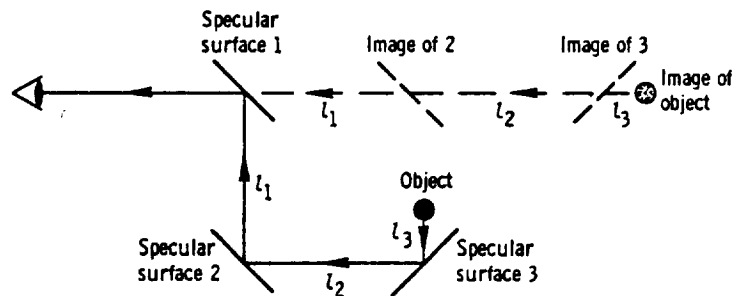
This procedure is readily extended to cases where a series of reflections occurs, as shown in figure 4-2(b).

To this point, it has been assumed that the mirrors in the system do nothing except change the direction of the rays originating at the source. In the formulation of thermal radiation problems, the specular surfaces will, in general, have a nonzero reflectivity. They will thus attenuate the energy of the rays from an object.

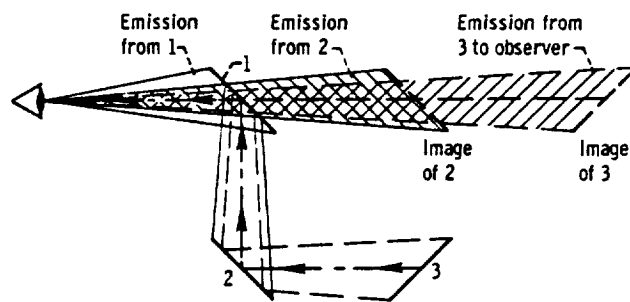
In addition to reflecting energy, the mirrors can emit energy. This emission can be conveniently analyzed with an image system rather than with the real mirror system. In the image system, all radiation acts along straight lines without the complexity of considering directional changes at each reflecting surface. The attenuation at each surface is accounted for by multiplying the intensity of the ray by the specular reflectivity at each reflection. The emission from three surfaces is illustrated in figure 4-2(c). For example, emitted energy reaching the viewer from surface 3 is considered to be coming directly from the image of 3, with attenuation due to reflections at 2 and 1 because of passage through these surfaces or their images.



(a)



(b)



(c)

- (a) Image formed by single reflection.
- (b) Image formed by multiple reflections.
- (c) Contributions due to emission from specular surfaces.

FIGURE 4-2. — Ray tracing and images formed by specular reflections.

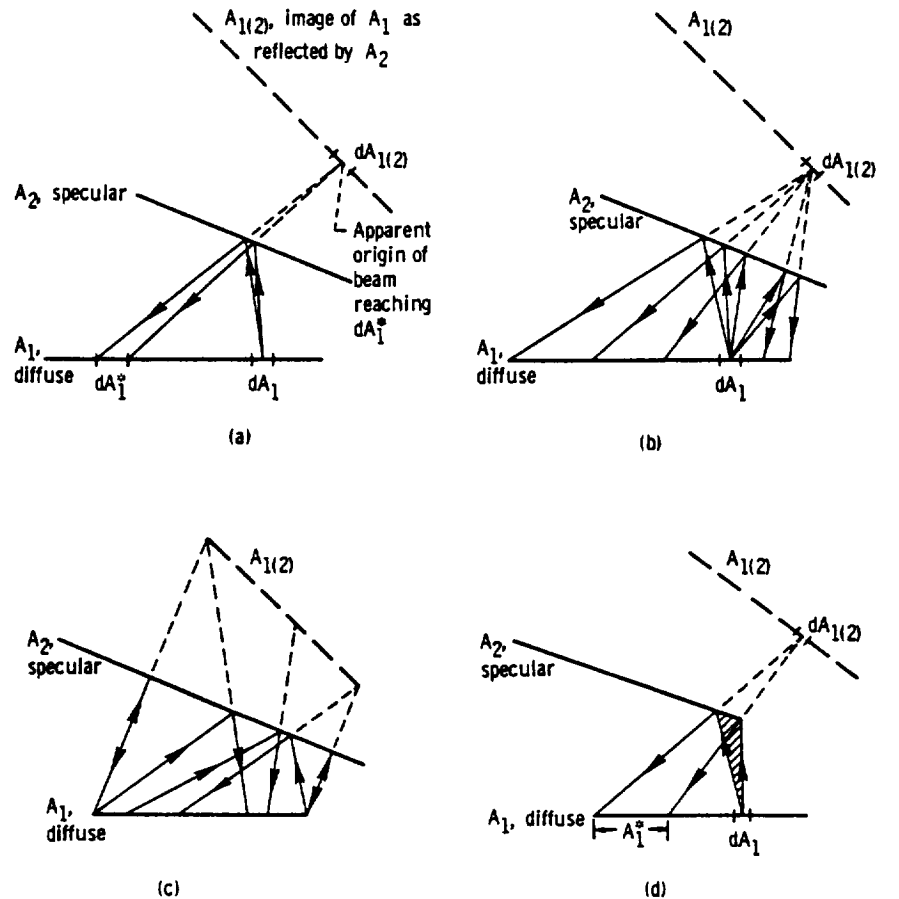
In some geometries, a ray may undergo multiple reflections from various surfaces before reaching the observer. An example of this is the "barber-chair" geometry, where mirrors are present on opposite walls of the barber shop. In this case, if the mirrors are parallel, an infinite number of reflections of a ray can occur, and a person receiving a haircut can view an infinite number of images of himself (if the mirrors are perfect, i.e., if $\rho_s = 1$).

4.3.2.2 *Energy exchange between simple specular surfaces.*—As an introduction to the radiation exchange in an enclosure having some surfaces that are specularly reflecting, a few examples will be considered for plane surfaces. The examples will further demonstrate the new features that enter when mirrorlike surfaces are present.

The emission from all surfaces is assumed diffuse. This is a fairly good assumption in most cases, as can be shown by the electromagnetic theory predictions of the emissivity of specular surfaces (fig. 4-5, Vol. I).

Figure 4-3(a) shows a diffusely reflecting plane surface A_1 facing a specularly reflecting plane surface A_2 . Surface 1 cannot view itself; the configuration factor from any part of A_1 to any other part of A_1 is thus zero. However, if A_2 is specular, then A_1 can view its image, and a path exists by means of a reflection from the specular surface A_2 for radiation to travel from the differential area dA_1 to dA_1^* . By looking at the diagram in figure 4-3(a), it is evident by the ray tracing techniques that the radiation arriving at dA_1^* from dA_1 appears to come from the image $dA_{1(2)}$. Thus, the geometric configuration factor between dA_1 and dA_1^* resulting from one reflection can be obtained as $dF_{d_{1(2)}-d_1}$. The subscript notation refers to a factor from the image of dA_1 (as seen in A_2) to dA_1^* .

There are points of similarity that should be noted when comparing the specular and diffuse cases. When A_1 and A_2 in figure 4-3(a) are both diffuse reflectors, radiation from dA_1 is received at dA_1^* by means of diffuse reflection from A_2 . Since the reflected energy is diffuse, it can be considered together with the emitted energy from A_2 , which is also diffuse, the sum being the outgoing flux $q_{o,2}$ as discussed in chapter 3. If, however, the exchange between dA_1 and dA_1^* by means of diffuse reflection at A_2 is examined separately from the emitted energy, it is governed by F_{d_1-2} and then dF_{2-d_1} (keeping in mind the uniform flux restrictions that are necessary in using configuration factors). The portion of the emitted energy $d^2Q_{e, d_1-d_1^*(2)}$ from dA_1 that reaches dA_1^* after one reflection from A_2 is the following, for the two cases of diffuse and specular A_2 , respectively:



(a) Radiation between two differential areas with one intermediate specular reflection.

(c) Radiation from finite area that is reflected back to that area by means of one specular reflection.

(b) Radiation from differential area to finite area by means of one intermediate specular reflection.

(d) Radiation from dA_1 can reach only portion of A_1 by means of specular reflection from A_2 .

FIGURE 4-3. — Radiation between a diffuse surface and itself by means of a specular surface.

$$d^2Q_{e, d_1-d_1^{*(2)}} = (dA_1 \epsilon_1 \sigma T_1^4) F_{d_1-2} \rho_2 dF_{2-d_1}$$

$$d^2Q_{e, d_1-d_1^{*(2)}} = (dA_1 \epsilon_1 \sigma T_1^4) \rho_{s,2} dF_{d_{1(2)}-d_1}$$

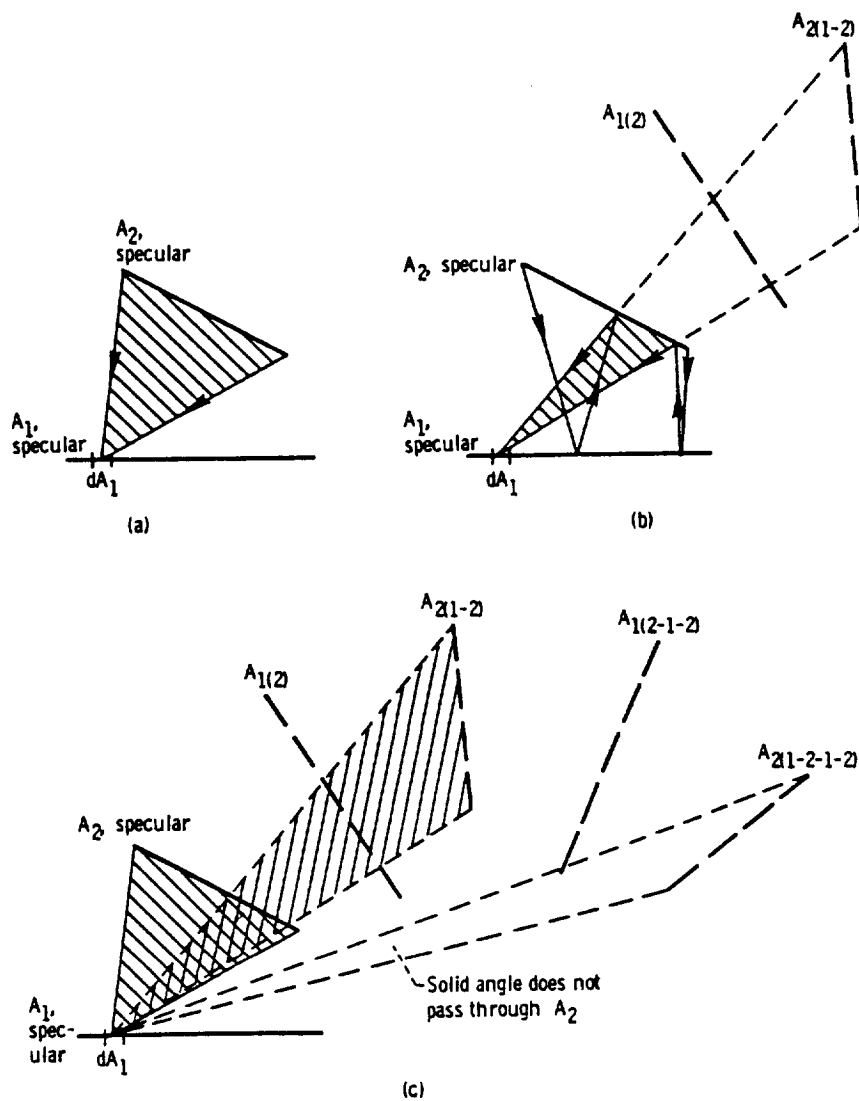
This reveals that, for $\rho_2 = \rho_{s,2}$, the difference in the two exchanges is incorporated in the configuration factors for reflected radiation. The difference in the factors results from the nature of the reflection being considered, which is a purely geometric effect.

Figure 4-3(b) describes the emitted radiation from dA_1 that reaches the entire area A_1 by means of one specular reflection. The reflected radiation appears to originate by diffuse emission from the image $dA_{1(2)}$. Thus the geometric configuration factor involved from dA_1 to A_1 is $F_{dA_1(2)-1}$.

Figure 4-3(c) shows several typical rays leaving A_1 that are reflected back to A_1 . These rays appear to originate from the image $A_{1(2)}$. The configuration factor from A_1 back to itself by means of one specular reflection is then $F_{1(2)-1}$. In this instance, all of the image $A_{1(2)}$ is visible in A_2 from any position on A_1 . In some instances, this will not be true. An example is shown in figure 4-3(d). The radiation from dA_1 has to be within the limited range of solid angle shown shaded in order that the radiation be reflected back to A_1 . The geometric configuration factor between dA_1 and A_1 is still $F_{dA_1(2)-1}$, but this factor is evaluated only over the portion of A_1 that receives reflected rays. $F_{dA_1(2)-1}$ is the factor by which $dA_{1(2)}$ views A_1 , and it must be kept in mind that *the view may be a partial one*. This factor will have a different value as the location of dA_1 along A_1 is changed. The fact that the view between dA_1 and A_1 varies with the position of dA_1 along A_1 means that the energy from A_1 that is reflected back to A_1 will have a nonuniform distribution along A_1 . The reflection of some of this energy from A_1 will provide a nonuniform q_o from A_1 , which violates the assumption in the enclosure theory of uniform q_o from each surface. When partial images are present, caution should be exercised in subdividing the enclosure area into sufficiently small portions so that the accuracy of the solution is adequate.

Now consider the geometry involved when there are two or more specular surfaces involved in the radiation exchange. This will lead to multiple reflections and many different paths by which radiation can travel between surfaces. At each reflection, the radiation is modified by the ρ_s of the reflecting surface. At present in this discussion, only the geometry is being considered; the ρ_s factors will be included later when heat balances are formulated.

In figure 4-4 are shown two specular surfaces. Energy is being emitted from A_2 and is traveling to surface A_1 . The fraction arriving at dA_1 is given by the geometric configuration factor dF_{2-d1} . This direct path is illustrated in figure 4-4(a). A portion of the energy intercepted by A_1 will be reflected back to A_2 and then reflected back again to A_1 . Hence, A_2 not only views dA_1 directly but also by means of an image formed by two reflections. This image is constructed in figure 4-4(b). First the reflected image $A_{1(2)}$ of A_1 reflected in A_2 is drawn. Then A_2 is reflected into this image to form $A_{2(1-2)}$. The notation $A_{2(1-2)}$ is read as the image of area 2 formed by reflections in area 1 and area 2 (in that order). The radiation paths and the shaded area shown in figure 4-4(b)



(a) Energy emitted from A_2 that directly reaches dA_1 .

(b) Energy emitted from A_2 that reaches dA_1 after two reflections.

(c) None of energy emitted by A_2 reaches dA_1 by means of four reflections.

FIGURE 4-4.—Radiant interchange between two specular reflecting surfaces.

reveal that the solid angle within which radiation leaving A_2 will reach dA_1 by means of two reflections is the same as the solid angle by which dA_1 views the image $A_{2(1-2)}$. Thus, the configuration factor involved for two reflections is $dF_{2(1-2)-d1}$. This is read as the factor from the image of surface 2 formed by reflections in surfaces 1 and 2 (in that order) to area element $d1$.

Consider the possibility of additional images. The geometric factor involved is always found by viewing dA_1 from the appropriate reflected image of A_2 as seen through the surface A_2 and all intermediate images. In the case of figure 4-4(c), the image of A_2 after four reflections $A_{2(1-2-1-2)}$ cannot view dA_1 by looking through A_2 . Hence, there is no radiation leaving A_2 that reaches dA_1 by means of four reflections, and no additional images need be considered.

EXAMPLE 4-3: An infinitely long groove as shown in figure 4-5 has specularly reflecting sides that emit diffusely. What fraction of the emitted energy from A_2 reaches the black receiver surface element dA_3 ? Express the result in terms of diffuse geometric configuration factors.

Consider first the energy that reaches dA_3 directly from A_2 and by means of an even number of reflections. The fraction of emitted radiation that reaches dA_3 directly from A_2 is dF_{2-d_3} , as illustrated in figure 4-5(a). A second portion will be emitted from A_2 to A_1 , reflected back to A_2 , and then reflected to dA_3 . From the diagram of images in figure 4-5(b), only part of the reflected image $A_{2(1-2)}$ can be viewed by dA_3 through A_2 . The fraction of emitted energy reaching dA_3 by this path is the configuration factor *evaluated only over the part of $A_{2(1-2)}$ visible to dA_3* multiplied by the two specular reflectivities, $\rho_{s,1}\rho_{s,2} dF_{2(1-2)-d_3}$. This is not an ordinary view factor, but it *takes into account the view through the image system*. In a similar fashion, there will be a contribution after two reflections from each of A_1 and A_2 . This is illustrated by the shaded solid angle in figure 4-5(c). The third image of A_2 , $A_{2(1-2-1-2)}$ cannot be viewed by dA_3 through A_2 ; hence, it will not make a contribution. Also, the third image of A_2 cannot view A_1 through A_2 ; consequently, there will be no additional images of A_2 . The fraction of energy emitted by A_2 that reaches dA_3 both directly and by means of the images of A_2 is then

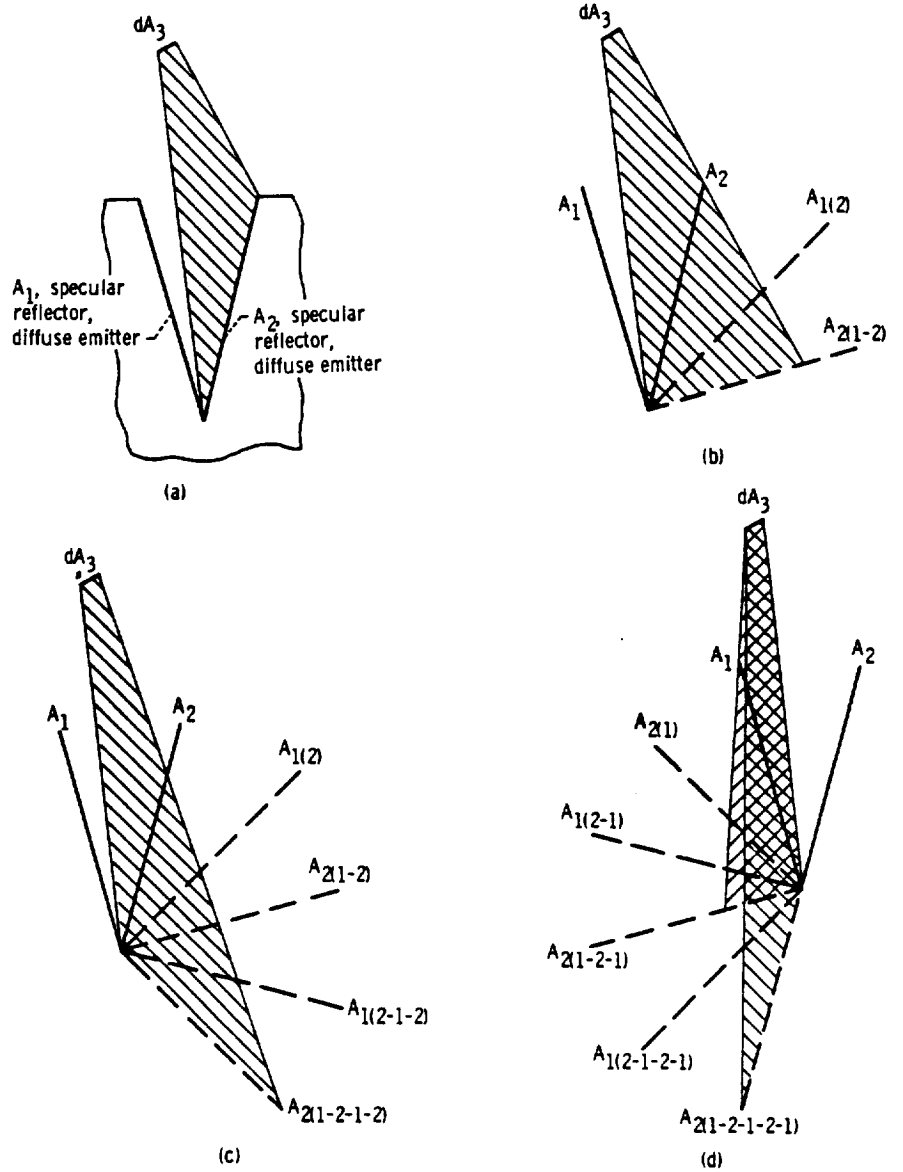
$$dF_{2-d_3} + \rho_{s,1}\rho_{s,2} dF_{2(1-2)-d_3} + \rho_{s,1}^2\rho_{s,2}^2 dF_{2(1-2-1-2)-d_3}$$

Now consider the energy fraction that will reach dA_3 from A_2 by means of an odd number of reflections. Using figure 4-5(d) and arguments similar to those for an even number of reflections results in

$$\rho_{s,1} dF_{2(1)-d_3} + \rho_{s,1}^2\rho_{s,2} dF_{2(1-2-1)-d_3} + \rho_{s,1}^3\rho_{s,2}^2 dF_{2(1-2-1-2-1)-d_3}$$

The first two of the F factors are only evaluated over the portions of the images that can be viewed by dA_3 .

The fraction of energy emitted by surface A_2 that reaches dA_3 directly and after all interreflections from both A_1 and A_2 is then



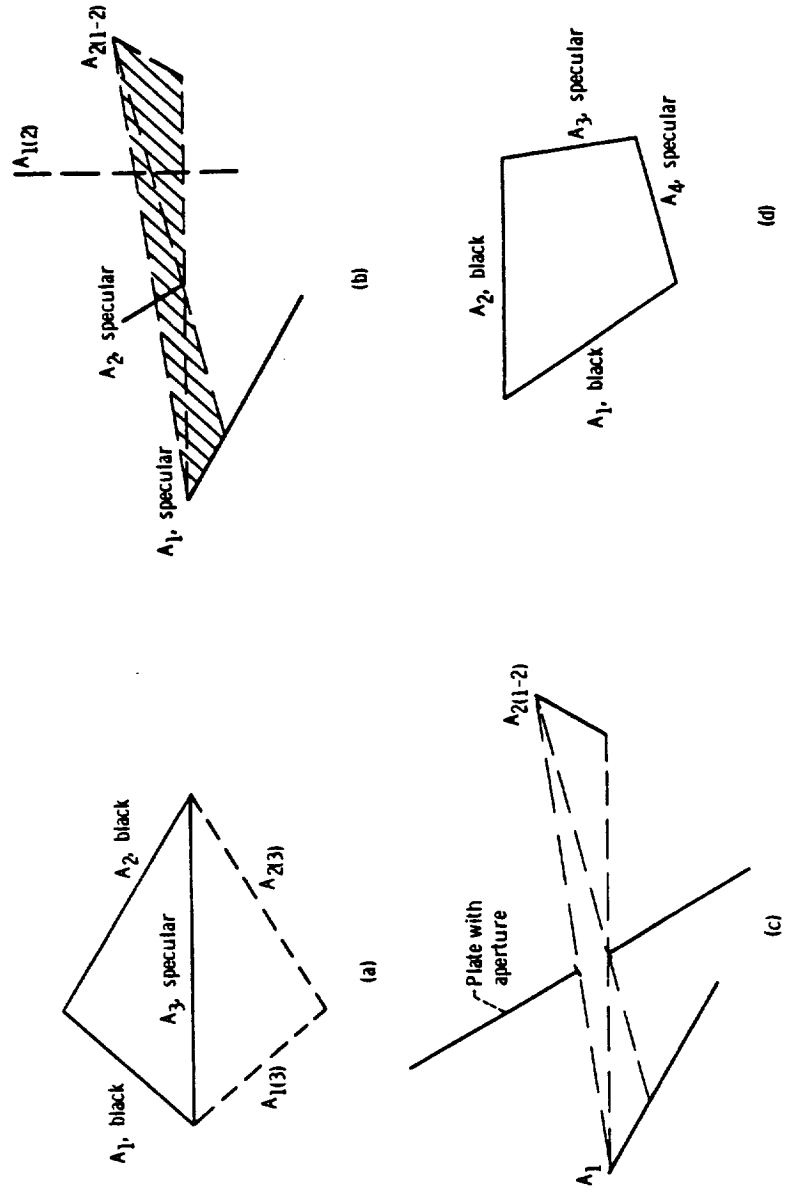
(a) Geometry of direct exchange from A_2 to dA_3 .

(c) Geometry of exchange for radiation from A_2 that reaches dA_3 by means of two intermediate reflections from each of A_1 and A_2 .

(b) Geometry of exchange for radiation from A_2 that reaches dA_3 by means of one intermediate reflection from each of A_1 and A_2 .

(d) Geometry of exchange for radiation from A_2 to A_3 by means of odd number of reflections.

FIGURE 4-5. — Radiation from one side of specularly reflecting groove to differential strip receiving area outside groove opening.



(a) Three-sided enclosure with one specular reflecting surface. (b) System of images of surfaces 1 and 2. (c) Energy exchange analog of image system in (b). (d) Enclosure with two specular and two black surfaces.

FIGURE 4-6. — Reciprocity of specular configuration factors.

figure 4-6(a), and the reciprocity relations for diffuse configuration factors.

A second type of reciprocity relation exists for specular surface configuration factors. To derive this relation, examine the energy exchange between two surfaces A_1 and A_2 contained within an isothermal enclosure. If both surfaces are specular, then the image system shown in figure 4-6(b) can be constructed for the case of radiation from 2 to 1 by means of a reflection at 1 and at 2. For any such system, an analogous system can be constructed in which a plate with an aperture is substituted for the restraints on the ray paths that are present, as is done in figure 4-6(c). The aperture is placed to allow passage of only those rays that pass through the image system by which A_1 can view at least a portion of $A_{2(1-2)}$ through A_2 and $A_{1(2)}$.

The emitted energy leaving specular surface A_2 in the analog system and absorbed by A_1 is

$$\begin{aligned} Q_{2(1-2) \rightarrow 1} &= Q_{e, 2} \rho_{s, 1} \rho_{s, 2} F_{2(1-2) \rightarrow 1} \alpha_1 \\ &= A_{2(1-2)} \epsilon_2 \sigma T^4 \rho_{s, 1} \rho_{s, 2} F_{2(1-2) \rightarrow 1} \epsilon_1 \end{aligned} \quad (4-5)$$

The reflectivities account for the reduction in energy by the two intermediate specular reflections. $F_{2(1-2) \rightarrow 1}$ is the diffuse surface configuration factor computed for the constrained paths passing through the aperture (see example 4-4). Since these paths are exactly those through the image system, this is also the specular configuration factor. Similarly, the energy along the reverse path is

$$Q_{1 \rightarrow 2(1-2)} = A_1 \epsilon_1 \sigma T^4 \rho_{s, 2} \rho_{s, 1} F_{1 \rightarrow 2(1-2)} \epsilon_2 \quad (4-6)$$

Equating the energy exchanges in either direction between A_1 and $A_{2(1-2)}$ for the isothermal enclosure results in the following reciprocity relation:

$$A_1 F_{1 \rightarrow 2(1-2)} = A_{2(1-2)} F_{2(1-2) \rightarrow 1} = A_2 F_{2(1-2) \rightarrow 1} \quad (4-7)$$

By generalizing for many intermediate reflections from surfaces A , B , C , D , and so forth, equation (4-7) can be written as

$$A_1 F_{1 \rightarrow 2(A-B-C-D \dots)} = A_2 F_{2(A-B-C-D \dots) \rightarrow 1} \quad (4-8)$$

EXAMPLE 4-4: A black surface A_1 faces a smaller parallel mirror A_2 as in figure 4-7. Compute the configuration factor $F_{1 \rightarrow 1(2)}$ between A_1 and the image of A_1 formed by means of one specular reflection in

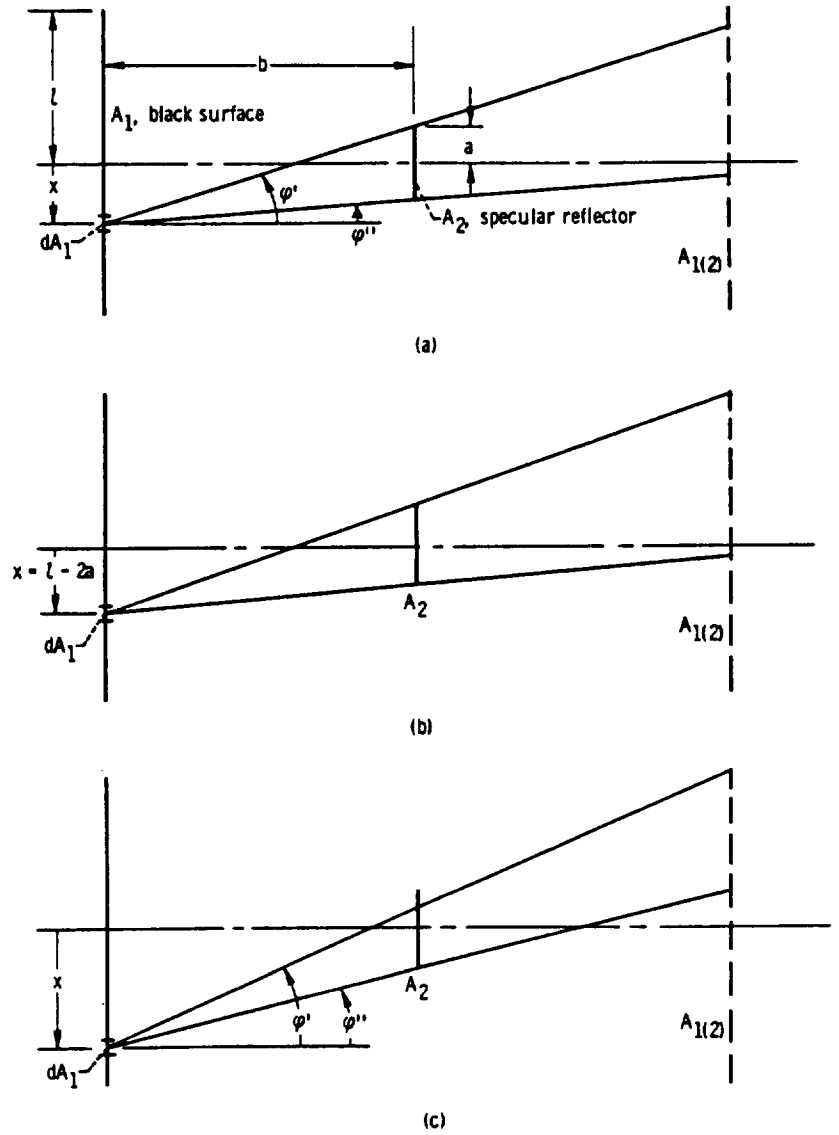


FIGURE 4-7.—Configuration factor computation involving partial views of surface and image (example 4-4).

A_2 . The surfaces are infinitely long in the direction normal to the plane of the drawing.

The factor is computed from the integral $F_{1-1(2)} = (1/A_1) \int_{A_1} F_{d1-1(2)} dA_1$.

Consider the element dA_1 at location x on A_1 . The configuration factor for radiation from dA_1 to the portion of $A_{1(2)}$ in view through A_2 is (see example 2-4)

$$F_{d1-1(2)} = \frac{1}{2} (\sin \varphi' - \sin \varphi'') = \frac{1}{2} \left[\frac{x+a}{\sqrt{(x+a)^2 + b^2}} - \frac{x-a}{\sqrt{(x-a)^2 + b^2}} \right]$$

This is valid until position $x = l - 2a$ is reached (fig. 4-7). For larger x values the geometry is as shown in figure 4-7(c). Then

$$F_{d1-1(2)} = \frac{1}{2} (\sin \varphi' - \sin \varphi'') = \frac{1}{2} \left[\frac{x+l}{\sqrt{(x+l)^2 + 4b^2}} - \frac{x-a}{\sqrt{(x-a)^2 + b^2}} \right]$$

The desired configuration factor is then

$$\begin{aligned} F_{1-1(2)} &= \frac{1}{2l} 2 \int_0^l F_{d1-1(2)} dx \\ &= \frac{1}{l} \left\{ \frac{1}{2} \int_0^{l-2a} \left[\frac{x+a}{\sqrt{(x+a)^2 + b^2}} - \frac{x-a}{\sqrt{(x-a)^2 + b^2}} \right] dx \right. \\ &\quad \left. + \frac{1}{2} \int_{l-2a}^l \left[\frac{x+l}{\sqrt{(x+l)^2 + 4b^2}} - \frac{x-a}{\sqrt{(x-a)^2 + b^2}} \right] dx \right\} \end{aligned}$$

The integrations are carried out, and the results simplify to

$$F_{1-1(2)} = \sqrt{1 + \left(\frac{b}{l}\right)^2} - \sqrt{\left(1 - \frac{a}{l}\right)^2 + \left(\frac{b}{l}\right)^2}$$

Consider a case where there are two or more specular surfaces in an isothermal enclosure at temperature T . For simplicity, an enclosure, such as figure 4-6(d), shall be discussed where there are two specular and two black surfaces. If the heat exchange between the two black surfaces is considered by direct exchange and all specular reflection paths, the following relation results:

$$\begin{aligned} \frac{Q_{1-2}}{\sigma T^4} &= A_1 [F_{1-2} + \rho_{s,3} F_{1(3)-2} + \rho_{s,4} F_{1(4)-2} \\ &\quad + \rho_{s,3} \rho_{s,4} F_{1(3-4)-2} + \dots + \rho_{s,3}^m \rho_{s,4}^m F_{1(3^m-4^m)-2} + \dots] \quad (4-9a) \end{aligned}$$

$$\frac{Q_{2-1}}{\sigma T^4} = A_2 [F_{2-1} + \rho_{s,3} F_{2(3)-1} + \rho_{s,4} F_{2(4)-1} + \rho_{s,3}\rho_{s,4} F_{2(4-3)-1} + \dots + \rho_{s,3}^m \rho_{s,4}^n F_{2(4^m-3^n)-1} + \dots] \quad (4-9b)$$

The shorthand notation $(3^m - 4^n)$ means m reflections in 3 and n in 4. Equation (4-9) can also be written as

$$\frac{Q_{1-2}}{\sigma T^4} = \frac{Q_{2-1}}{\sigma T^4} = A_1 F_{1-2}^s = A_2 F_{2-1}^s \quad (4-10)$$

where F^s is an exchange factor equal to the quantity in parentheses in equation (4-9).

Now look at equation (4-9) in more detail. Since $A_1 F_{1-2} = A_2 F_{2-1}$ and from equation (4-4) for one reflection

$$A_1 F_{1(3)-2} = A_2 F_{2(3)-1} \quad \text{and} \quad A_1 F_{1(4)-2} = A_2 F_{2(4)-1}$$

the equality in equation (4-9) reduces to

$$A_1 [\rho_{s,3}\rho_{s,4} F_{1(3-4)-2} + \dots + \rho_{s,3}^m \rho_{s,4}^n F_{1(3^m-4^n)-2} + \dots] = A_2 [\rho_{s,3}\rho_{s,4} F_{2(4-3)-1} + \dots + \rho_{s,3}^m \rho_{s,4}^n F_{2(4^m-3^n)-1} + \dots] \quad (4-11)$$

Dividing by $\rho_{s,3}\rho_{s,4}$ results in

$$A_1 [F_{1(3-4)-2} + \dots + \rho_{s,3}^{m-1} \rho_{s,4}^{n-1} F_{1(3^m-4^n)-2} + \dots] = A_2 [F_{2(4-3)-1} + \dots + \rho_{s,3}^{m-1} \rho_{s,4}^{n-1} F_{2(4^m-3^n)-1} + \dots] \quad (4-12)$$

This equality must hold in the limit as $\rho_{s,3}$ and $\rho_{s,4}$ approach zero so that

$$A_1 F_{1(3-4)-2} = A_2 F_{2(4-3)-1} \quad (4-13)$$

which is a geometric property of the system. A continuation of this reasoning leads to the general reciprocity relation

$$A_1 F_{1(A-B-C-D \dots)-2} = A_2 F_{2(\dots D-C-B-A)-1} \quad (4-14)$$

Note that combining equations (4-8) and (4-14) results in the identity

$$A_1 F_{1(A-B-C-D \dots)-2} = A_2 F_{2(\dots D-C-B-A)-1} = A_1 F_{1-2(A-B-C-D \dots)} \quad (4-15)$$

or

$$F_{1(A-B-C-D \dots)-2} = F_{1-2(A-B-C-D \dots)} \quad (4-16)$$

This latter relation can also be deduced directly from the fact that an image system can be constructed either starting with the real surface 1 and working toward image 2 ($A-B-C-D \dots$), or starting with image 1 ($A-B-C-D \dots$) and working toward real surface 2; in either system, the geometry of the construction will be identical. Thus, the configuration factors between the initial surface and the final surface must be the same.

4.4 NET RADIATION METHOD IN ENCLOSURES HAVING SPECULAR AND DIFFUSE SURFACES

4.4.1 Enclosures With Plane Surfaces

In this section, the radiation exchange in an enclosure composed of specularly and diffusely reflecting surfaces will be considered. As an introduction to enclosure theory when specular surfaces are present, consider an enclosure composed of three plane surfaces at different uniform specified temperatures as shown in figure 4-8(a). Later, the boundary condition of specified heat flux will be considered. All the surfaces are diffuse emitters, but two are diffuse reflectors while the third reflects specularly. For simplicity, it is assumed that the enclosure is sufficiently long that the effect of the ends can be neglected.

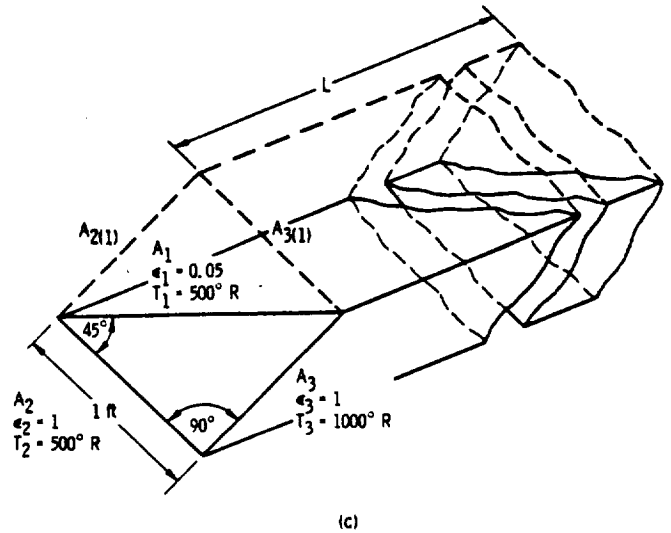
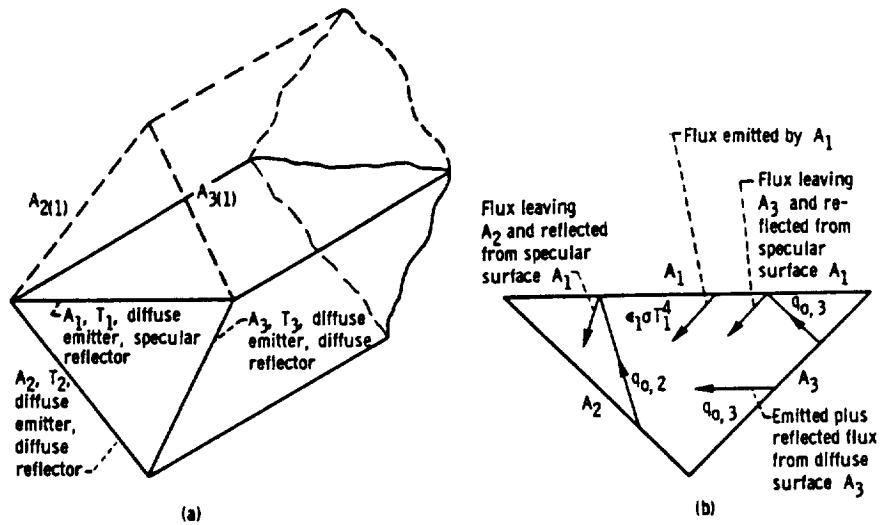
In applying the net radiation method, the heat balance equations (eqs. (3-1) and (3-2)) do not depend on the type of reflection occurring and, hence, will apply for both diffuse and specular surfaces. Then for all three surfaces of the enclosure

$$Q_k = q_k A_k = (q_{o,k} - q_{i,k}) A_k \quad k = 1, 2, 3 \quad (4-17)$$

$$q_{o,k} = \epsilon_k \sigma T_k^4 + (1 - \epsilon_k) q_{i,k} \quad k = 1, 2, 3 \quad (4-18)$$

There is a difference in interpretation of q_o when the surface is specular. For a diffuse reflector, both emitted and reflected intensities are uniform over all directions; hence, $\epsilon \sigma T^4$ and $(1 - \epsilon) q_i$ have the same directional character and the diffuse configuration factors can be applied for both of these quantities. For a specular reflector, however, the $(1 - \epsilon) q_i$ term will have a directional distribution different from that of the diffuse emission $\epsilon \sigma T^4$. Thus, when surface k is specular, the specular portion of $q_{o,k}$ will have to be treated differently than the diffuse portion.

Now the equations for $q_{i,k}$ for specular surfaces in the enclosure will be derived that are comparable to equation (3-3) or (3-5). Refer to figure 4-8(a); the energy arriving at surface 1 comes directly from the



(a) General geometry.

(b) Energy fluxes that contribute to flux incident upon A_2 .

(c) Enclosure for example 4-5.

FIGURE 4-8. — Enclosure having one specular reflecting surface and two surfaces that are diffuse reflectors.

diffuse surfaces 2 and 3 without any intermediate specular reflections. Hence, equation (3-5) applies

$$q_{i,1} = F_{1-2}q_{o,2} + F_{1-3}q_{o,3} \tag{4-19}$$

For surface 2, the incoming radiation is composed of four parts which originate as shown in figure 4-8(b). The first is the diffuse term for energy originating from A_3 , and going directly to A_2 which is $q_{0,3}A_3F_{3-2}$. The remaining three parts arrive by means of A_1 and consist of a diffuse emitted portion $\epsilon_1\sigma T_1^4A_1F_{1-2}$ plus two reflected specular portions. The specular portions arise from the energy leaving A_2 and A_3 that is specularly reflected to A_2 and will appear to come from the images $A_{2(1)}$ and $A_{3(1)}$ in figure 4-8(a). The specular portions are equal to

$$q_{0,2}\rho_{s,1}A_2F_{2(1)-2} + q_{0,3}\rho_{s,1}A_3F_{3(1)-2}$$

Note that multiple reflections cannot occur when only one planar specular surface is present. The sum of the terms for the incoming radiation to surface 2 is then

$$A_2q_{i,2} = \epsilon_1\sigma T_1^4A_1F_{1-2} + q_{0,2}\rho_{s,1}A_2F_{2(1)-2} + q_{0,3}A_3F_{3-2} + q_{0,3}\rho_{s,1}A_3F_{3(1)-2}$$

After applying configuration factor reciprocity (eqs. (2-25) and (4-8)), this can be regrouped into the form

$$q_{i,2} = \epsilon_1\sigma T_1^4F_{2-1} + q_{0,2}\rho_{s,1}F_{2-2(1)} + q_{0,3}[F_{2-3} + \rho_{s,1}F_{2-3(1)}] \quad (4-20)$$

Similarly, for surface 3

$$q_{i,3} = \epsilon_1\sigma T_1^4F_{3-1} + q_{0,2}[F_{3-2} + \rho_{s,1}F_{3-2(1)}] + q_{0,3}\rho_{s,1}F_{3-3(1)} \quad (4-21)$$

Equations (4-20) and (4-21) are two simultaneous equations involving the unknowns $q_{0,2}$ and $q_{0,3}$. If $q_{i,2}$ and $q_{i,3}$ are eliminated by use of equation (4-18), there is obtained

$$\frac{q_{0,2} - \epsilon_2\sigma T_2^4}{1 - \epsilon_2} = \epsilon_1\sigma T_1^4F_{2-1} + q_{0,2}\rho_{s,1}F_{2-2(1)} + q_{0,3}[F_{2-3} + \rho_{s,1}F_{2-3(1)}]$$

$$\frac{q_{0,3} - \epsilon_3\sigma T_3^4}{1 - \epsilon_3} = \epsilon_1\sigma T_1^4F_{3-1} + q_{0,2}[F_{3-2} + \rho_{s,1}F_{3-2(1)}] + q_{0,3}\rho_{s,1}F_{3-3(1)}$$

After rearrangement, this yields

$$\begin{aligned} q_{0,2}[1 - \rho_{s,1}(1 - \epsilon_2)F_{2-2(1)}] - q_{0,3}(1 - \epsilon_2)[F_{2-3} + \rho_{s,1}F_{2-3(1)}] \\ = \epsilon_1(1 - \epsilon_2)F_{2-1}\sigma T_1^4 + \epsilon_2\sigma T_2^4 \end{aligned} \quad (4-22)$$

$$\begin{aligned}
 -q_{o,2}(1-\epsilon_3)[F_{3-2} + \rho_{s,1}F_{3-2(1)}] + q_{o,3}[1 - \rho_{s,1}(1-\epsilon_3)F_{3-3(1)}] \\
 = \epsilon_1(1-\epsilon_3)F_{3-1}\sigma T_1^4 + \epsilon_3\sigma T_3^4 \quad (4-23)
 \end{aligned}$$

Equations (4-22) and (4-23) can be solved for $q_{o,2}$ and $q_{o,3}$ in terms of known quantities. After $q_{o,2}$ and $q_{o,3}$ are found, they are used in equations (4-19), (4-20), and (4-21) to find the q_i for each surface and then equation (4-18) is used to find $q_{o,1}$. Equation (4-17) is then employed to determine the Q for each surface, which is the heat addition required to maintain the surfaces at their specified temperatures, or in other words, is the net radiative heat lost from each surface. Equations (4-22) and (4-23) are analogous to the system of equations for diffuse surfaces given by equation (3-21).

EXAMPLE 4-5: An enclosure is made up of three sides as shown in figure 4-8(c). The length L is sufficiently long so that the triangular ends can be neglected in the radiative heat balances. Two of the surfaces are black, and the third is a gray diffuse emitter of emissivity $\epsilon_1 = 0.05$. What is the heat added per foot of length to each surface for each of the two cases: (1) area 1 is a diffuse reflector and (2) area 1 is a specular reflector?

The configuration factors are computed first. From symmetry $F_{1-2} = F_{1-3}$. Also $F_{1-2} + F_{1-3} = 1$, so that $F_{1-2} = F_{1-3} = 1/2$. From reciprocity $F_{2-1} = A_1 F_{1-2} / A_2 = \sqrt{2}/2 = F_{3-1}$. Now $F_{2-1} + F_{2-3} = 1$. Hence $F_{2-3} = 1 - \sqrt{2}/2 = F_{3-2} = F_{2-2(1)} = F_{3-3(1)}$. Finally, $F_{3-2(1)} = F_{2-3(1)} = 1 - F_{3-2} - F_{3-3(1)} = \sqrt{2} - 1$.

For case (1), apply equation (3-18) to obtain

$$\begin{aligned}
 \frac{Q_1}{\sigma\sqrt{2}} \frac{1}{0.05} &= (500)^4 - \frac{1}{2} (500)^4 - \frac{1}{2} (1000)^4 \\
 -\frac{Q_1}{\sigma\sqrt{2}} \frac{\sqrt{2}}{2} \frac{(1-0.05)}{0.05} + \frac{Q_2}{\sigma(1)} &= \frac{-\sqrt{2}}{2} (500)^4 + (500)^4 - \left(1 - \frac{\sqrt{2}}{2}\right) (1000)^4 \\
 -\frac{Q_1}{\sigma\sqrt{2}} \frac{\sqrt{2}}{2} \frac{(1-0.05)}{0.05} + \frac{Q_3}{\sigma(1)} &= \frac{-\sqrt{2}}{2} (500)^4 - \left(1 - \frac{\sqrt{2}}{2}\right) (500)^4 + (1000)^4
 \end{aligned}$$

The solution of these three equations yields the Q 's per foot of enclosure length as $Q_1 = -57$ Btu/hr, $Q_2 = -1018$ Btu/hr, and $Q_3 = 1075$ Btu/hr. The heat supplied to A_3 is removed from A_1 and A_2 . The amount removed from A_1 is small because A_1 is a poor absorber.

For case (2) apply equations (4-22) and (4-23) to compute $q_{o,2}$ and $q_{o,3}$. Since $\epsilon_2 = \epsilon_3 = 1$, these equations yield simply $q_{o,2} = \sigma T_2^4$ and

$q_{o,3} = \sigma T_3^4$ which would be expected for the outgoing fluxes from black surfaces. Then equations (4-19), (4-20), and (4-21) yield the q_i for each surface as

$$\frac{q_{i,1}}{\sigma} = \frac{1}{2} (500)^4 + \frac{1}{2} (1000)^4$$

$$\begin{aligned} \frac{q_{i,2}}{\sigma} = 0.05(500)^4 \frac{\sqrt{2}}{2} + (500)^4(1-0.05) \left(1 - \frac{\sqrt{2}}{2}\right) \\ + (1000)^4 \left[1 - \frac{\sqrt{2}}{2} + (1-0.05)(\sqrt{2}-1)\right] \end{aligned}$$

$$\begin{aligned} \frac{q_{i,3}}{\sigma} = 0.05(500)^4 \frac{\sqrt{2}}{2} + (500)^4 \left[1 - \frac{\sqrt{2}}{2} + (1-0.05)(\sqrt{2}-1)\right] \\ + (1000)^4(1-0.05) \left(1 - \frac{\sqrt{2}}{2}\right) \end{aligned}$$

Equation (4-18) gives $q_{o,1}$ as

$$\frac{q_{o,1}}{\sigma} = 0.05(500)^4 + (1-0.05) \left[\frac{1}{2} (500)^4 + \frac{1}{2} (1000)^4\right]$$

With q_i and q_o known for each of the surfaces, equation (4-17) is applied to find Q . This yields per foot of enclosure length $Q_1 = -57$ Btu/hr, $Q_2 = -1113$ Btu/hr, and $Q_3 = 1170$ Btu/hr.

Comparing cases (1) and (2) reveals that, by making A_1 specular, the heat transferred from A_3 to A_2 is increased from 1018 to 1113 Btu/hr or an increase of 10 percent.

There are some general ideas that should be emphasized with regard to example 4-5. Look first at equations (4-20) and (4-21). The $q_{i,2}$ and $q_{i,3}$ for the two diffuse surfaces are expressed in terms of the diffuse quantities, $\epsilon_1 \sigma T_1^4$, $q_{o,2}$, and $q_{o,3}$ where $\epsilon_1 \sigma T_1^4$ is the diffuse portion of the outgoing energy from the specular surface A_1 . The energy reflected from the specular surface enters equations (4-20) and (4-21) only through the geometric configuration factors. As a result, equations (4-22) and (4-23) have only the two unknown fluxes $q_{o,2}$ and $q_{o,3}$ for the diffuse surfaces, and these quantities can be determined without considering the $q_{o,1}$ for the specular surface. The value of $q_{o,1}$, if desired, is found by using equation (4-18). The number of equations that must be solved simultaneously is thus equal to the number of *diffuse* reflecting surfaces; these equations express the outgoing radiation from each diffuse surface

in terms of the diffuse portions of the outgoing radiation from all the surfaces.

To demonstrate further and begin to generalize the radiative heat balances in an enclosure having some specular reflecting surfaces, consider the rectangular geometry shown in figure 4-9. All of the surfaces

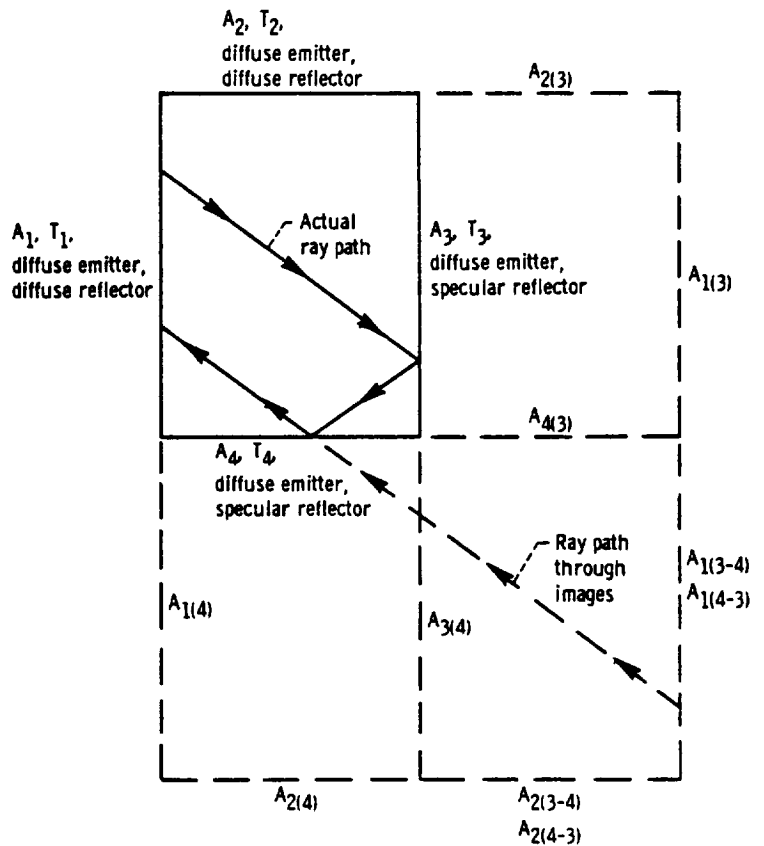


FIGURE 4-9.—Rectangular enclosure and reflected images when two adjacent surfaces are specular reflectors and other two are diffuse reflectors.

are diffuse emitters; two of the surfaces are diffuse reflectors while the remaining two are specular. Shown dashed are the reflected images. The reflection process continues until all of the outer perimeter enclosing the composite of original enclosure plus reflected images is made up of either diffuse (or nonreflecting, such as an opening) surfaces or images of diffuse surfaces.

For the enclosure in figure 4-9, the first step is to obtain $q_{0,1}$ and $q_{0,2}$ for the two diffuse areas. From equation (4-18) these can be written as

$$q_{0,1} = \epsilon_1 \sigma T_1^4 + (1 - \epsilon_1) q_{i,1} \quad (4-24)$$

$$q_{0,2} = \epsilon_2 \sigma T_2^4 + (1 - \epsilon_2) q_{i,2} \quad (4-25)$$

The $q_{i,1}$ and $q_{i,2}$ are determined from the diffuse portions of the outgoing energies from all the enclosure surfaces as follows: Consider, for example, the quantities that form $q_{i,1}$. Part of $q_{0,1}$ returns to A_1 by three paths: (1) direct reflection from A_3 , (2) reflection from A_3 to A_4 and then to A_1 , and (3) reflection from A_4 to A_3 and then to A_1 . Thus, the portion of the energy leaving A_1 that returns to A_1 is

$$q_{0,1} A_1 [\rho_{s,3} F_{1(3)-1} + \rho_{s,3} \rho_{s,4} F_{1(3-4)-1} + \rho_{s,4} \rho_{s,3} F_{1(4-3)-1}]$$

The factor $F_{1(3-4)-1}$ is the view factor by which $A_{1(3-4)}$ is viewed from A_1 through A_4 and then $A_{3(4)}$, which are the reflection areas by means of which the $A_{1(3-4)}$ image was formed. Similarly, $F_{1(4-3)-1}$ is the view factor by which the same area $A_{1(3-4)}$ is viewed from A_1 through A_3 and then $A_{4(3)}$. The $q_{0,2}$ leaving A_2 contributes to $q_{i,1}$ by reaching A_1 along four paths: (1) direct exchange, (2) reflection from A_3 , (3) reflection from A_4 , and (4) reflection from A_3 to A_4 . There will be no energy from A_2 that reaches A_1 by means of reflections from A_4 and then A_3 . This is because A_1 cannot view the image $A_{2(4-3)}$ through area A_3 .

The diffuse energy leaving the specular surface A_3 (and similarly for A_4) consists only of the emitted energy $\epsilon_3 A_3 \sigma T_3^4$. There are two paths by which some of this will reach A_1 : (1) by direct exchange, and (2) by means of specular reflection from A_4 .

Combining all of these terms yields $q_{i,1}$, the incoming energy to A_1 , in terms of the diffuse quantities leaving all the surfaces,

$$\begin{aligned} A_1 q_{i,1} = & A_1 q_{0,1} \{ \rho_{s,3} F_{1(3)-1} + \rho_{s,3} \rho_{s,4} [F_{1(3-4)-1} + F_{1(4-3)-1}] \} \\ & + A_2 q_{0,2} [F_{2-1} + \rho_{s,3} F_{2(3)-1} + \rho_{s,4} F_{2(4)-1} + \rho_{s,3} \rho_{s,4} F_{2(3-4)-1}] \\ & + A_3 \epsilon_3 \sigma T_3^4 [F_{3-1} + \rho_{s,4} F_{3(4)-1}] + A_4 \epsilon_4 \sigma T_4^4 [F_{4-1} + \rho_{s,3} F_{4(3)-1}] \end{aligned} \quad (4-26)$$

The angle factor reciprocity relation (eq. (4-15)) can then be applied to replace all areas in equation (4-26) with A_1 , which can then be eliminated. The resulting equation is equated to $q_{i,1}$ from equation (4-24) to give

$$\begin{aligned} \frac{q_{o,1} - \epsilon_1 \sigma T_1^4}{1 - \epsilon_1} &= q_{o,1} \{ \rho_{s,3} F_{1-1(3)} + \rho_{s,3} \rho_{s,4} [F_{1-1(3-4)} + F_{1-1(4-3)}] \} \\ &+ q_{o,2} [F_{1-2} + \rho_{s,3} F_{1-2(3)} + \rho_{s,4} F_{1-2(4)} + \rho_{s,3} \rho_{s,4} F_{1-2(3-4)}] \\ &+ \epsilon_3 \sigma T_3^4 [F_{1-3} + \rho_{s,4} F_{1-3(4)}] + \epsilon_4 \sigma T_4^4 [F_{1-4} + \rho_{s,3} F_{1-4(3)}] \end{aligned} \quad (4-27)$$

In a similar fashion, considering $q_{i,2}$ for surface 2 yields

$$\begin{aligned} \frac{q_{o,2} - \epsilon_2 \sigma T_2^4}{1 - \epsilon_2} &= q_{o,1} [F_{2-1} + \rho_{s,3} F_{2-1(3)} + \rho_{s,4} F_{2-1(4)} + \rho_{s,3} \rho_{s,4} F_{2-1(4-3)}] \\ &+ q_{o,2} \{ \rho_{s,4} F_{2-2(4)} + \rho_{s,3} \rho_{s,4} [F_{2-2(4-3)} + F_{2-2(3-4)}] \} \\ &+ \epsilon_3 \sigma T_3^4 [F_{2-3} + \rho_{s,4} F_{2-3(4)}] + \epsilon_4 \sigma T_4^4 [F_{2-4} + \rho_{s,3} F_{2-4(3)}] \end{aligned} \quad (4-28)$$

Equations (4-27) and (4-28) are solved simultaneously for $q_{o,1}$ and $q_{o,2}$.

For the two specular surfaces, the $q_{i,3}$ and $q_{i,4}$ can be found as soon as the q_o 's for the diffuse surfaces are known. For specular surface A_3 , the incoming radiation is

$$\begin{aligned} A_3 q_{i,3} &= A_1 q_{o,1} [F_{1-3} + \rho_{s,4} F_{1(4-3)}] \\ &+ A_2 q_{o,2} [F_{2-3} + \rho_{s,4} F_{2(4-3)}] + A_4 \epsilon_4 \sigma T_4^4 F_{4-3} \end{aligned} \quad (4-29)$$

By using reciprocity, the A_3 can be eliminated; thus

$$q_{i,3} = q_{o,1} [F_{3-1} + \rho_{s,4} F_{3-1(4)}] + q_{o,2} [F_{3-2} + \rho_{s,4} F_{3-2(4)}] + \epsilon_4 \sigma T_4^4 F_{3-4} \quad (4-30)$$

Similarly, for $q_{i,4}$,

$$q_{i,4} = q_{o,1} [F_{4-1} + \rho_{s,3} F_{4-1(3)}] + q_{o,2} [F_{4-2} + \rho_{s,3} F_{4-2(3)}] + \epsilon_3 \sigma T_3^4 F_{4-3} \quad (4-31)$$

For the diffuse surfaces, the net flux added to maintain thermal equilibrium is, from equation (3-6),

$$\frac{Q_1}{A_1} = \frac{\epsilon_1}{1 - \epsilon_1} (\sigma T_1^4 - q_{o,1}) \quad (4-32)$$

$$\frac{Q_2}{A_2} = \frac{\epsilon_2}{1 - \epsilon_2} (\sigma T_2^4 - q_{o,2}) \quad (4-33)$$

while for the specular surfaces, by eliminating q_o from equations (4-17) and (4-18), the result is

$$\frac{Q_3}{A_3} = \epsilon_3(\sigma T_3^4 - q_{i,3}) \quad (4-34)$$

$$\frac{Q_4}{A_4} = \epsilon_4(\sigma T_4^4 - q_{i,4}) \quad (4-35)$$

All factors needed for solution of the problem are now known. When surface 1 (or 2) is black, equation (4-32) (or eq. (4-33)) cannot be used because $q_{o,1} = \sigma T_1^4$ and $1 - \epsilon_1 = 0$ so that an indeterminate expression results for Q_1 . In this case, as in example 4-5, $q_{i,1}$ is found from equation (4-26) and then $Q_1/A_1 = q_{o,1} - q_{i,1} = \sigma T_1^4 - q_{i,1}$.

Generalization to the case of an N surface enclosure is possible. For the enclosure surfaces at specified uniform temperatures, examine the equations for q_o from the diffusely reflecting surfaces, as given by equations (4-27) and (4-28) for the enclosure in figure 4-8. These can be rewritten in the form

$$\begin{aligned} q_{o,1} &= \epsilon_1 \sigma T_1^4 + (1 - \epsilon_1)(q_{o,1}[\rho_{s,3} F_{1-1(3)} + \rho_{s,3} \rho_{s,4} [F_{1-1(3-4)} + F_{1-1(4-3)}]] \\ &\quad + q_{o,2} [F_{1-2} + \rho_{s,3} F_{1-2(3)} + \rho_{s,4} F_{1-2(4)} + \rho_{s,3} \rho_{s,4} F_{1-2(3-4)}] \\ &\quad + \epsilon_3 \sigma T_3^4 [F_{1-3} + \rho_{s,4} F_{1-3(4)}] + \epsilon_4 \sigma T_4^4 [F_{1-4} + \rho_{s,3} F_{1-4(3)}]) \\ &= \epsilon_1 \sigma T_1^4 + (1 - \epsilon_1)(q_{o,1} F_{1-1}^s + q_{o,2} F_{1-2}^s + \epsilon_3 \sigma T_3^4 F_{1-3}^s + \epsilon_4 \sigma T_4^4 F_{1-4}^s) \end{aligned} \quad (4-36)$$

and

$$\begin{aligned} q_{o,2} &= \epsilon_2 \sigma T_2^4 + (1 - \epsilon_2)(q_{o,1} [F_{2-1} + \rho_{s,3} F_{2-1(3)} + \rho_{s,4} F_{2-1(4)}] \\ &\quad + \rho_{s,3} \rho_{s,4} F_{2-1(4-3)}] + q_{o,2} [\rho_{s,4} F_{2-2(4)} \\ &\quad + \rho_{s,3} \rho_{s,4} [F_{2-2(4-3)} + F_{2-2(3-4)}]] + \epsilon_3 \sigma T_3^4 [F_{2-3} + \rho_{s,4} F_{2-3(4)}] \\ &\quad + \epsilon_4 \sigma T_4^4 [F_{2-4} + \rho_{s,3} F_{2-4(3)}]) \\ &= \epsilon_2 \sigma T_2^4 + (1 - \epsilon_2)(q_{o,1} F_{2-1}^s + q_{o,2} F_{2-2}^s + \epsilon_3 \sigma T_3^4 F_{2-3}^s + \epsilon_4 \sigma T_4^4 F_{2-4}^s) \end{aligned} \quad (4-37)$$

where the factors F_{A-B}^s give the fraction of the diffuse energy leaving

surface A and reaching surface B by direct exchange and by all possible paths of specular reflection.

For an N surface enclosure made up of d diffuse and $N-d$ specular reflecting surfaces at specified temperatures, a general set of equations of energy exchange can be written by generalizing equations (4-36) and (4-37). Let the diffuse surfaces be numbered from 1 to d and the specular surfaces from $d+1$ to N . Then the general equation is written for each diffuse surface as

$$q_{o,k} - (1 - \epsilon_k) \sum_{j=1}^d q_{o,j} F_{k-j} = \epsilon_k \sigma T_k^4 + (1 - \epsilon_k) \sigma \sum_{j=d+1}^N \epsilon_j T_j^4 F_{k-j} \quad 1 \leq k \leq d \quad (4-38)$$

This set of equations is solved for the q_o for the diffuse surfaces. For each specular surface, the q_o 's for the diffuse surfaces are used to obtain $q_{i,k}$ in the form (a generalization of eqs. (4-30) and (4-31))

$$q_{i,k} = \sum_{j=1}^d q_{o,j} F_{k-j} + \sigma \sum_{j=d+1}^N \epsilon_j T_j^4 F_{k-j} \quad d+1 \leq k \leq N \quad (4-39)$$

The net external energy added to each diffuse surface is

$$Q_k = A_k \frac{\epsilon_k}{1 - \epsilon_k} (\sigma T_k^4 - q_{o,k}) \quad 1 \leq k \leq d \quad (4-40)$$

and, to each specular surface

$$Q_k = A_k \epsilon_k (\sigma T_k^4 - q_{i,k}) \quad d+1 \leq k \leq N \quad (4-41)$$

Equations (4-38) to (4-41) are the general energy interchange relations for enclosures made up of diffuse surfaces and specular surfaces.

If the k th diffuse surface is black, then $q_{o,k} = \sigma T_k^4$ and $1 - \epsilon_k = 0$, so that equation (4-40) is indeterminate. In this case, the following equation can be used:

$$Q_k = A_k (\sigma T_k^4 - q_{i,k})$$

where $q_{i,k}$ is found from equation (4-39) with $1 \leq k \leq d$.

If the heat input Q_k rather than T_k is specified for a diffuse surface $1 \leq k \leq d$, then T_k is unknown in equations (4-38). Equation (4-40) can be used to eliminate this unknown in terms of $q_{o,k}$ and the known Q_k .

If the heat input Q_k is specified for a specular surface, $d+1 \leq k \leq N$,

then one of the T_j^i in the last term of equation (4-38) will be unknown. Equation (4-41) is combined with equation (4-39) to eliminate $q_{i,k}$ which gives

$$\sigma T_k^i - \frac{Q_k}{A_k \epsilon_k} = \sum_{j=1}^d q_{o,j} F_{k-j}^i + \sigma \sum_{j=d+1}^N \epsilon_j T_j^i F_{k-j}^i \quad d+1 \leq k \leq N \quad (4-42)$$

Since Q_k is known, equation (4-42) can be combined with equation (4-38) to yield a simultaneous set of equations to determine the q_o of the diffusely reflecting surfaces and the T for the specularly reflecting surfaces having specified Q .

An alternate form of the final equations can be found by using equations (4-40) and (4-41) to eliminate q_i and q_o from equations (4-38) and (4-39). This gives a set of equations all of the same form that directly relate the Q 's and T 's,

$$\frac{1}{\epsilon_k} \frac{Q_k}{A_k} - \sum_{j=1}^d \frac{Q_j}{A_j} \frac{1-\epsilon_j}{\epsilon_j} F_{k-j}^i = \sigma T_k^i - \sum_{j=1}^d \sigma T_j^i F_{k-j}^i - \sum_{j=d+1}^N \sigma \epsilon_j T_j^i F_{k-j}^i \quad 1 \leq k \leq N \quad (4-43)$$

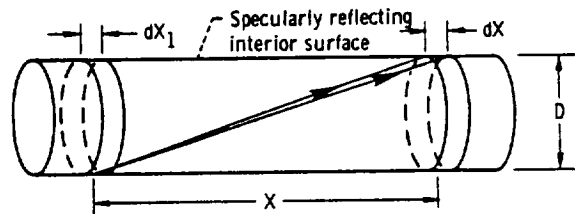
4.4.2 Curved Specular Reflecting Surfaces

In the previous discussion, all of the specular surfaces have been planar. Here, curved specular reflecting surfaces will be considered, and in this instance, the geometry of the reflected images can become quite complex. To demonstrate some of the basic ideas, a relatively simple case will be examined; this is the radiation exchange within a specular tube (ref. 6), as shown in figure 4-10.

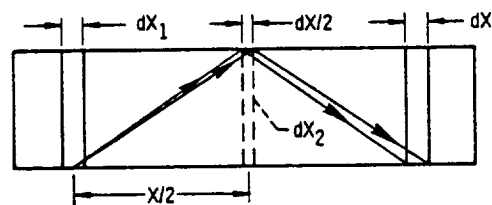
It is assumed that the imposed temperature or heating conditions depend only on axial position and are independent of the location around the tube circumference. To compute the radiative exchange within the tube for axisymmetric heating conditions, it is necessary to have the configuration factor between two ring elements on the tube wall. The direct exchange (fig. 4-10(a)) is governed by the factor (see example 3-8, and note that $|\eta - \xi|$ in that example is equal to X/D here)

$$dF_{dx_1-dx} = \left\{ 1 - \frac{\left(\frac{X}{D}\right)^3 + \frac{3X}{2D}}{\left[\left(\frac{X}{D}\right)^2 + 1\right]^{3/2}} \right\} dX$$

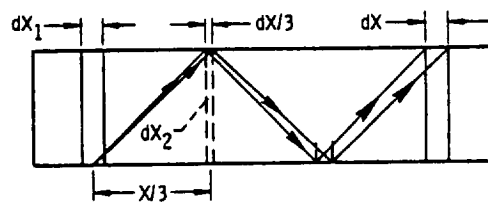
Figure 4-10(b) illustrates the configuration factor for one reflection.



(a)



(b)



(c)

(a) Direct exchange between two ring elements.

(b) Exchange by one reflection.

(c) Exchange by two reflections.

FIGURE 4-10. — Radiation exchange within specularly reflecting cylindrical tube.

Because of the symmetry of the tube, all of the radiation from dX_1 that reaches dX by one reflection will be reflected from a ring element halfway between dX_1 and dX . The ring at $X/2$ is only $dX/2$ wide so that the beam subtending it will spread to a width dX at the location X . The configuration factor for one reflection is then the factor between dX_1 and the dashed element $dX/2$

$$dF_{dX_1, -(dX/2)} = \left\{ 1 - \frac{\left(\frac{X}{2D}\right)^3 + \frac{3X}{4D}}{\left[\left(\frac{X}{2D}\right)^2 + 1\right]^{3/2}} \right\} \frac{dX}{2}$$

In a similar fashion, the geometric factor for exchange between dX_1 and dX by two reflections is given by

$$dF_{dX_1-(dX/3)} = \left\{ 1 - \frac{\left(\frac{X}{3D}\right)^3 + \frac{3X}{6D}}{\left[\left(\frac{X}{3D}\right)^2 + 1\right]^{3/2}} \right\} \frac{dX}{3}$$

and for n reflections

$$dF_{dX_1-(dX/(n+1))} = \left(1 - \frac{\left[\frac{X}{(n+1)D}\right]^3 + \frac{3X}{2(n+1)D}}{\left\{\left[\frac{X}{(n+1)D}\right]^2 + 1\right\}^{3/2}} \right) \frac{dX}{n+1}$$

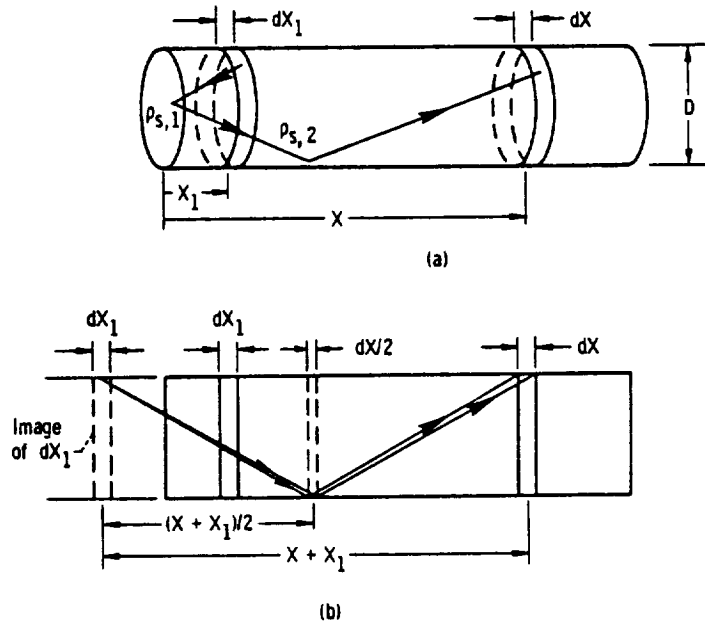
In general, the geometric factor for *any* number of reflections can be found by considering the exchange between the originating element (dX_1 in this case) and the element (call it dX_2) from which the *first* reflection is made (the dashed element in figs. 4-10(b) and (c)). This is because the fraction of energy leaving dX_1 in the solid angle subtended by dX_2 remains the same through the succeeding reflections along the path to dX .

At each reflection, the energy must be multiplied by the specular reflectivity ρ_s . If all the contributions are summed, the fraction of energy leaving dX_1 that reaches dX by direct exchange and all reflection paths provides the specular exchange factor

$$dF_{dX_1-dX}^s = \sum_{n=0}^{\infty} \rho_s^n \left(1 - \frac{\left[\frac{X}{(n+1)D}\right]^3 + \frac{3X}{2(n+1)D}}{\left\{\left[\frac{X}{(n+1)D}\right]^2 + 1\right\}^{3/2}} \right) \frac{dX}{n+1} \quad (4-44)$$

When the geometry is even slightly more involved than the cylindrical geometry, the reflection patterns can become quite complex. Some further specific examples of radiation within a specular conical cavity and a specular cylindrical cavity with a specular end plane are given in reference 7. A more generalized treatment of nonplanar reflections is given in reference 8.

EXAMPLE 4-6: A cylindrical cavity has a specularly reflecting cylindrical wall and base (fig. 4-11(a)). Determine the fraction of radiation from ring element dX_1 that reaches dX by means of one reflection from the base with reflectivity ρ_1 and one reflection from the cylindrical wall with reflectivity ρ_2 .



(a) Cavity geometry.

(b) Image of dX_1 formed by reflection in cavity base.

FIGURE 4-11.—Reflection in cylindrical cavity with specular curved wall and base.

As shown in figure 4-11(b), for this geometry, the reflected radiation from the base can be regarded as originating from an image of dX_1 . The second reflection will occur from an element of width $dX/2$ located midway between the image dX_1 and dX . The desired radiation fraction is given by the view factor from the image dX_1 to the dashed ring area $dX/2$, that is,

$$dF_{dX_1-dX} = \rho_{s,1}\rho_{s,2} \left\{ 1 - \frac{\left(\frac{X+X_1}{2D}\right)^3 + \frac{3(X+X_1)}{4D}}{\left[\left(\frac{X+X_1}{2D}\right)^2 + 1\right]^{3/2}} \right\} \frac{dX}{2}$$

4.5 CONCLUDING REMARKS

In this chapter, the treatment has been presented of radiative interchange between specularly reflecting surfaces and in enclosures containing both specularly and diffusely reflecting surfaces. In many instances, as in example 4-5, the interchange of energy in enclosures is modified only a small amount by the consideration of specular surfaces in place of diffuse surfaces; however, in certain configurations, for

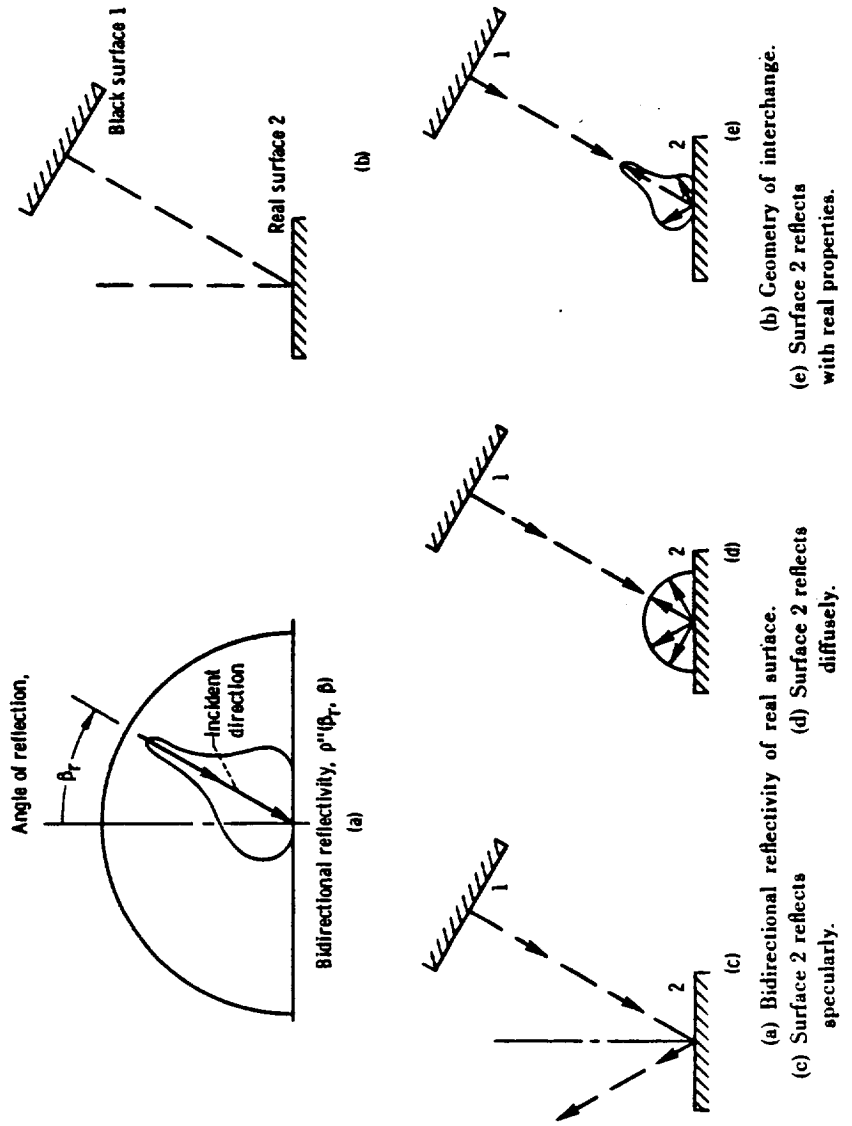


FIGURE 4-12. — Radiant interchange with various idealizations of surface properties.

example, those found in the design of solar furnaces, large effects of specular reflection are present.

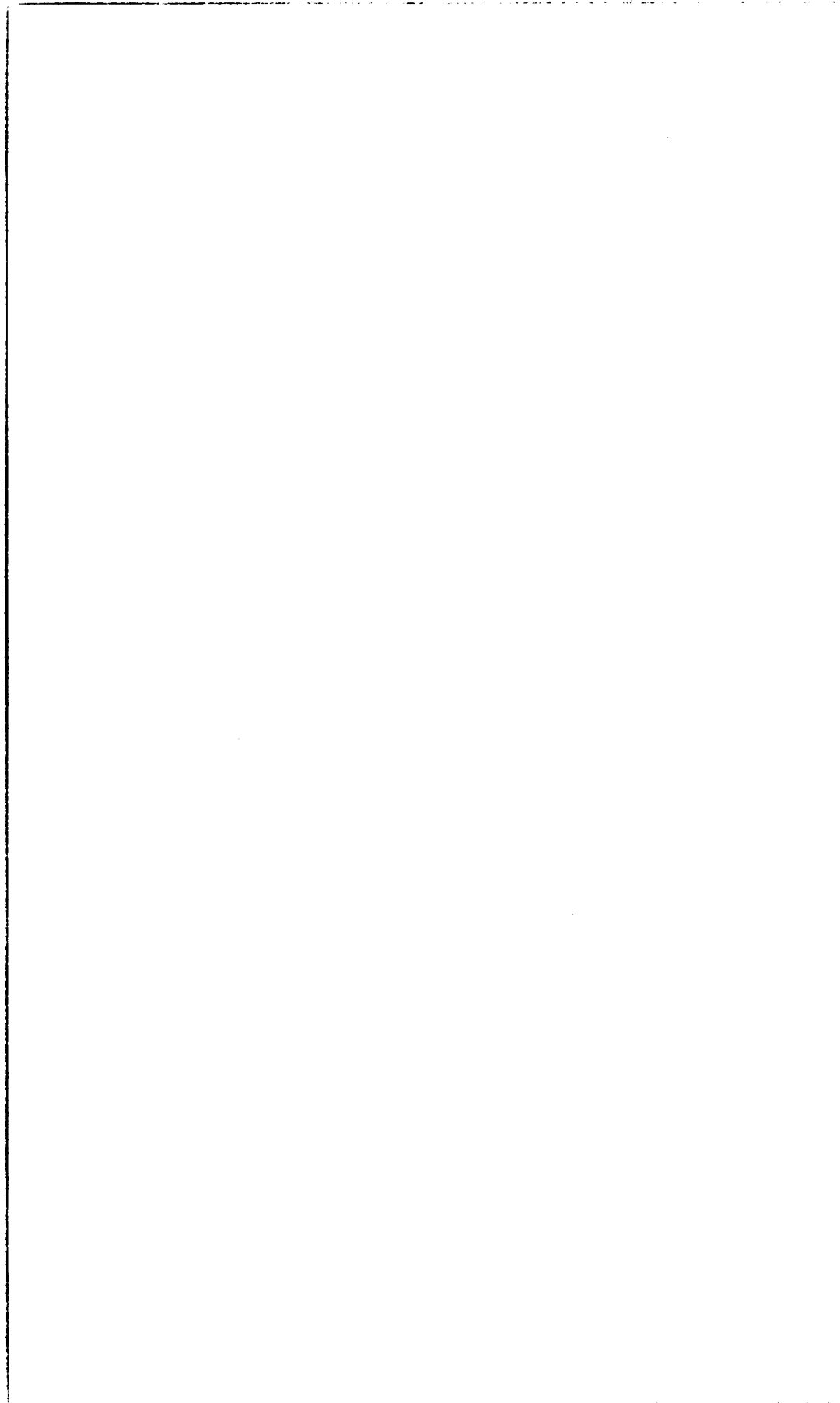
Bobco (ref. 9), Sparrow and Lin (ref. 10), and Sarofim and Hottel (ref. 11) have examined radiative exchange in enclosures involving surfaces with a reflectivity having both a diffuse *and* a specular component.

Another remark may be apropos at this point. It has sometimes been implied that the actual energy transfer between two real surfaces can be bracketed by calculation of two limiting magnitudes: (1) interchange between diffuse surfaces of the same total hemispherical emissivities as the real surfaces, and (2) interchange between specularly reflecting surfaces of the same total hemispherical emissivities as the real surfaces. This implication is not always true, however. Consider a surface which has a reflectivity as given by figure 4-12(a) (this is the type of reflectivity expected for the surface of the Moon). Now consider the radiant exchange between this real surface 2 and a black surface 1 as shown in figure 4-12(b). If surface 2 is given specular properties, it will return no energy to the black surface by reflection (fig. 4-12(c)). If given diffuse properties, it will return a portion of the incident energy by reflection (fig. 4-12(d)). If allowed to take on its real directional properties, however, it will reflect more energy to the black surface than *either* of the so-called limiting ideal surfaces (fig. 4-12(e)). Thus, the ideal directional surfaces do not constitute limiting cases for energy transfer in general. Figure 5-11 demonstrates another case where diffuse and specular properties do not provide limiting solutions. At best, calculations based on specular and diffuse assumptions for the surface characteristics give some indication of the possible magnitude of directional effects. Within enclosures, these directional effects may be small because of the many reflections taking place between the surfaces.

REFERENCES

1. CHRISTIANSEN, C.: Absolute Determination of the Heat Emission and Absorption Capacity. *Ann. d. Physik von Wied.*, vol. 19, 1883, pp. 267-283.
2. SAUNDERS, O. A.: Notes on Some Radiation Heat Transfer Formulae. *Proc. Phys. Soc. (London)*, vol. 41, Aug. 15, 1929, pp. 569-575.
3. BORN, MAX; AND WOLF, EMIL: *Principles of Optics*. Second ed., Macmillan Co., 1964.
4. STONE, JOHN M.: *Radiation and Optics*. McGraw-Hill Book Co., Inc., 1963.
5. HOWELL, JOHN R.; AND PERLMUTTER, MORRIS: Directional Behavior of Emitted and Reflected Radiant Energy From a Specular, Gray, Asymmetric Groove. NASA TN D-1874, 1963.
6. PERLMUTTER, M.; AND SIEGEL, R.: Effect of Specularly Reflecting Gray Surface on Thermal Radiation Through a Tube and From Its Heated Wall. *J. Heat Transfer*, vol. 85, no. 1, Feb. 1963, pp. 55-62.
7. LIN, S. H.; AND SPARROW, E. M.: Radiant Interchange Among Curved Specularly Reflecting Surfaces—Application to Cylindrical and Conical Cavities. *J. Heat Transfer*, vol. 87, no. 2, May 1965, pp. 299-307.

8. PLAMONDON, J. A.; AND HORTON, T. E.: On the Determination of the View Function to the Images of a Surface in a Nonplanar Specular Reflector. *Int. J. Heat Mass Transfer*, vol. 10, no. 5, May 1967, pp. 665-679.
9. BOBCO, R. P.: Radiation Heat Transfer in Semigray Enclosures with Specularly and Diffusely Reflecting Surfaces. *J. Heat Transfer*, vol. 86, no. 1, Feb. 1964, pp. 123-130.
10. SPARROW, E. M.; AND LIN, S. L.: Radiation Heat Transfer at a Surface Having Both Specular and Diffuse Reflectance Components. *Int. J. Heat Mass Transfer*, vol. 8, no. 5, May 1965, pp. 769-779.
11. SAROFIM, A. F.; AND HOTTEL, H. C.: Radiative Exchange Among Non-Lambert Surfaces. *J. Heat Transfer*, vol. 88, no. 1, Feb. 1966, pp. 37-44.



PRECEDING PAGE BLANK NOT FILMED.

Chapter 5. The Exchange of Thermal Radiation Between Nondiffuse Nongray Surfaces

5.1 INTRODUCTION

The analysis of radiation exchange within enclosures, as discussed in chapters 3 and 4, was restricted to cases where the enclosure surfaces were either black or gray. If gray, the surfaces were assumed both to emit and to reflect diffusely, or to emit diffusely and to reflect specularly. The additional restriction was sometimes made that the radiative properties were independent of temperature. As shown by the graphs of real properties in chapter 5 of Vol. I, most engineering materials deviate (in some instances radically) from the idealizations of being black, gray, diffuse, specular, or having temperature-independent radiative properties. In most practical engineering situations, the assumption of idealized surfaces is made to simplify the computations. This is often the most reasonable approach for two reasons:

(1) The radiative properties are not known to high accuracy especially with regard to their detailed dependence on wavelength and direction; hence, performing a refined computation would be fruitless when only crude property data are available.

(2) In an enclosure, the many reflections and rereflections tend to average out radiative nonuniformities; for example, the radiation leaving (emitted plus reflected) a directionally emitting surface may be fairly diffuse if it consists mostly of reflected energy arising from radiation incident from all directions.

In order to gain some insight as to where simplifying assumptions are at all reasonable, it is necessary to carry out some exchange computations using as exact a solution procedure as possible. Then results of those computations can be compared with those obtained from simplified methods such as those in chapters 3 and 4. To provide the tools for making refined computations, some methods of treating the radiative interchange between nonideal surfaces will be examined in this chapter. Analysis of such problems is inherently more difficult than for ideal surfaces, and a complete treatment of real surfaces including all variations, while possible in principle when all radiative properties are known, is seldom attempted or justified. As stated earlier, the directional-spectral properties are often not available. Property variations with wavelength for the normal direction are available for a number of materials; the data are usually sparse at the short- and long-wave-

length ranges of the spectrum.¹ Directional variations for some materials with optically smooth surfaces can be computed using electromagnetic theory (chapter 4 of Vol. I).

Certain problems demand inclusion of the effects of spectral and directional property variations and the methods presented here must be utilized. One example would be the use of spectrally selective coatings for temperature control in systems involving solar radiation.

5.2 SYMBOLS

A	area
a_0	autocorrelation distance of surface roughness
C_1, C_2	first and second constants, respectively, in Planck's spectral energy distribution
D	perpendicular distance between parallel areas
e	emissive power
F	configuration factor
$F_{0-\lambda}$	fraction of blackbody intensity in spectral range 0 to λ
G	function of emissivities in example 5-5
i	intensity
L	width of infinitely long parallel plates
l	L/D , parameter in example 5-6
Q	energy rate; energy per unit time
q	energy flux; energy per unit area and per unit time
R	radius of disk in example 5-7
r	R/D , parameter in example 5-7
S	distance between area elements
T	absolute temperature
x, y, z	Cartesian coordinates
α	absorptivity
β	cone angle
ϵ	emissivity
η	angle in plane perpendicular to surface
θ	circumferential angle
λ	wavelength
Ξ	absorption efficiency defined in example 5-6
ξ	distance along width of plane surface having finite width and infinite length
ρ	reflectivity

¹The range for which data are available depends on the equipment used in taking the data, and, of course, whether data have been gathered at all for the material desired. Typically, data are not available for most materials at wavelengths of less than 0.3 μm or greater than 15 μm . If the common lead sulfide detector is used to obtain data, the sensitivity limits measurements to less than about 3 μm .

σ	Stefan-Boltzmann constant
σ_0	root-mean-square amplitude of surface roughness
ω	solid angle
\int_{Ω}	integration over solid angle of entire enclosing hemisphere

Superscripts:

'	directional quantity
"	bidirectional quantity

Subscripts:

a	absorbed
b	blackbody
e	emitted
i	incident, incoming
k	quantity for k^{th} surface
max	maximum
min	minimum
o	outgoing
r	reflected
s	specular
λ	spectrally dependent
$\Delta\lambda$	average over wavelength region $\Delta\lambda$
1, 2, 3	property of surface 1, 2, or 3

5.3 ENCLOSURE THEORY FOR DIFFUSE SURFACES WITH SPECTRALLY DEPENDENT PROPERTIES

By considering diffusely emitting and reflecting surfaces there are no directional effects, and it is possible to see more clearly how the spectral variations of properties can be accounted for. The surface emissivity, absorptivity, and reflectivity are independent of direction, but may depend on both wavelength λ and surface temperature T . These properties must be available as a function of T and λ in order to evaluate the radiative interchange between surfaces.

For diffusely emitting and reflecting spectral surfaces, the concept of configuration factor is still valid since these factors involve only geometric effects and were computed for diffuse radiation leaving a surface. In general, then, the energy balance equations and methods developed in chapters 2 to 4 remain valid so long as they are written for the energy in each *wavelength interval* $d\lambda$. Often, however, the boundary conditions that are specified apply to the *total* (including all wavelengths) energy, and care must be taken to apply the boundary conditions correctly. These total boundary conditions cannot generally be applied to

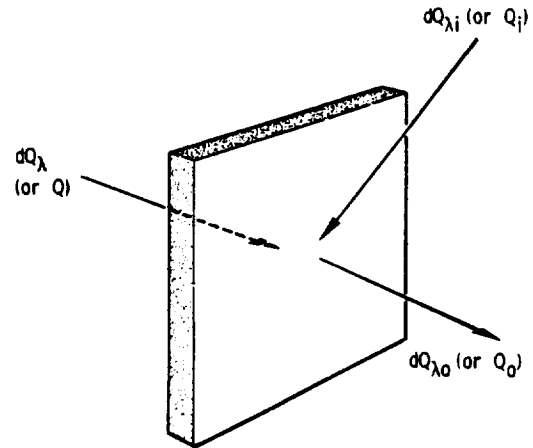


FIGURE 5-1.—Spectral (or total) energy quantities at a surface.

the spectral energies. As an example, consider the surface of figure 5-1 having an incident total radiation Q_i and a radiation leaving by combined emission and reflection Q_o . If the surface is otherwise perfectly insulated (an *adiabatic* surface), then there is no heat Q being added externally and Q_i and Q_o will be equal to each other,

$$Q_o - Q_i = Q = 0 \quad (5-1)$$

However, at a given wavelength, the incident and outgoing dQ_λ are *not* necessarily equal, so that in general

$$dQ_{\lambda o} - dQ_{\lambda i} = dQ_\lambda \neq 0 \quad (5-2)$$

Rather, an *adiabatic* surface only has a *total* radiation gain or loss of zero, or restating equation (5-1) in terms of the quantities in (5-2),

$$Q = \int_{\lambda=0}^{\infty} dQ_\lambda = \int_{\lambda=0}^{\infty} (dQ_{\lambda o} - dQ_{\lambda i}) = 0 \quad (5-3)$$

The dQ_λ is net energy supplied at λ as a result of incident energy at other wavelengths. At a given wavelength, the dQ_λ can vary widely from zero for an *adiabatic* surface, depending on the property variations with wavelength and the spectral distribution of incident energy.

More generally, consider now a *diabatic*² surface. The total energy

²To quote Breene (ref. 1), "In certain circles 'nonadiabatic' is considered as an 'atrocious, pleonastic synonym,' and the author quit using the term as soon as he discovered how bad it was."

added by external means to the surface is given by

$$Q = \int_{\lambda=0}^{\infty} dQ_{\lambda} = \int_{\lambda=0}^{\infty} (dQ_{\lambda o} - dQ_{\lambda i}) \quad (5-4)$$

The Q may either be specified as an imposed condition, or may be a quantity that is to be determined in order that a surface can be maintained at a specified temperature. In any small wavelength interval, the net energy $dQ_{\lambda o} - dQ_{\lambda i}$ may be positive or negative. The boundary condition states only that the integral of all such spectral energy values must be equal to Q . To become familiar with the use of these concepts, they are now applied to some example situations.

EXAMPLE 5-1: Two infinite parallel plates of tungsten at specified temperatures T_1 and T_2 ($T_1 > T_2$) are exchanging radiant energy. Branstetter (ref. 2) has determined the hemispherical spectral, temperature-dependent emissivity of tungsten by using the relations of electromagnetic theory to extrapolate limited experimental data, and a portion of his results is shown in figure 5-2. Using these data, compare the net energy exchange between the tungsten plates to that for the case of gray parallel plates.

The solution for gray plates has been given in example 3-1. The present case follows in the same fashion except that the equations are written spectrally. From equations (3-1) and (3-2) the energy quantities

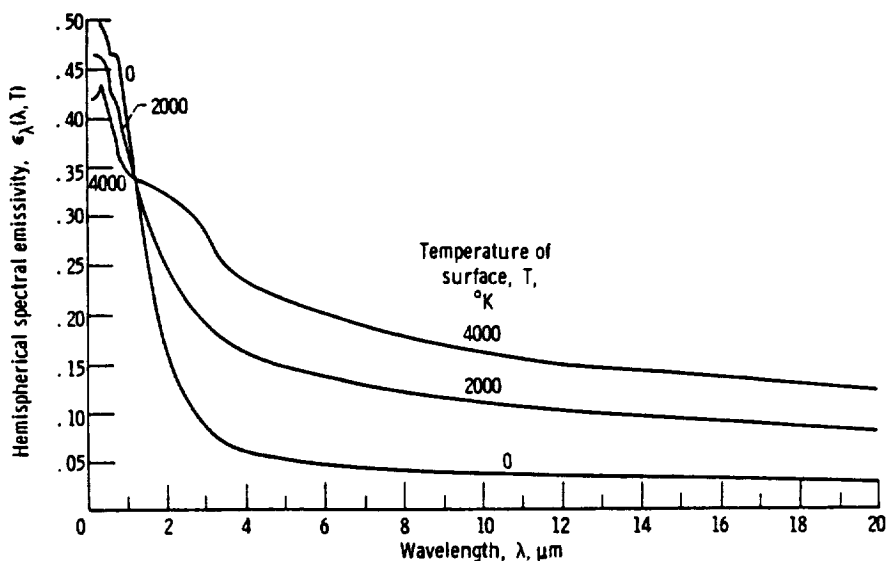


FIGURE 5-2. — Hemispherical spectral emissivity of tungsten.

at surface 1 per unit area and time in a wavelength interval $d\lambda$ are related by

$$dq_{\lambda, 1} = dq_{\lambda o, 1} - dq_{\lambda i, 1} \quad (5-5)$$

$$dq_{\lambda o, 1} = \epsilon_{\lambda, 1}(\lambda, T_1) e_{\lambda b, 1}(\lambda, T_1) d\lambda + \rho_{\lambda, 1}(\lambda, T_1) dq_{\lambda i, 1} \quad (5-6)$$

For diffuse opaque surfaces, the hemispherical properties are related by $\rho_{\lambda} = 1 - \alpha_{\lambda} = 1 - \epsilon_{\lambda}$, and equation (5-6) becomes

$$dq_{\lambda o, 1} = \epsilon_{\lambda, 1}(\lambda, T_1) e_{\lambda b, 1}(\lambda, T_1) d\lambda + [1 - \epsilon_{\lambda}(\lambda, T_1)] dq_{\lambda i, 1} \quad (5-7)$$

Eliminating $dq_{\lambda i, 1}$ from equations (5-5) and (5-7) gives

$$dq_{\lambda, 1} = \frac{\epsilon_{\lambda, 1}(\lambda, T_1)}{1 - \epsilon_{\lambda, 1}(\lambda, T_1)} [e_{\lambda b, 1}(\lambda, T_1) d\lambda - dq_{\lambda o, 1}] \quad (5-8)$$

Since for infinite parallel plates, the configuration factor $F_{2-1} = 1$, then $q_{\lambda i, 1} = q_{\lambda o, 2}$ (see eq. (3-5b)) and equation (5-5) becomes

$$dq_{\lambda, 1} = dq_{\lambda o, 1} - dq_{\lambda o, 2} \quad (5-9)$$

Equations (5-8) and (5-9) are analogous to equations (3-8a) and (3-8b) for the gray case. The equations for surface 2 are written in a similar fashion. Then the $dq_{\lambda o}$'s are eliminated, and the solution for one wavelength interval $d\lambda$ follows as in equation (3-10),

$$dq_{\lambda, 1} = -dq_{\lambda, 2} = \left[\frac{e_{\lambda b, 1}(\lambda, T_1) - e_{\lambda b, 2}(\lambda, T_2)}{\frac{1}{\epsilon_{\lambda, 1}(\lambda, T_1)} + \frac{1}{\epsilon_{\lambda, 2}(\lambda, T_2)} - 1} \right] d\lambda \quad (5-10)$$

The total heat flux exchanged (supplied to 1 and removed from 2) is found by substituting the property data of figure 5-2 into equation (5-10) and then integrating over all wavelengths,

$$q_1 = -q_2 = \int_0^{\infty} dq_{\lambda, 1} = \int_0^{\infty} \left[\frac{e_{\lambda b, 1}(\lambda, T_1) - e_{\lambda b, 2}(\lambda, T_2)}{\frac{1}{\epsilon_{\lambda, 1}(\lambda, T_1)} + \frac{1}{\epsilon_{\lambda, 2}(\lambda, T_2)} - 1} \right] d\lambda \quad (5-11)$$

The integration is performed numerically for each set of specified plate temperatures T_1 and T_2 .

The results of such integrations, as carried out by Branstetter (ref. 2), are shown in figure 5-3 where the ratio of gray-diffuse to nongray-diffuse

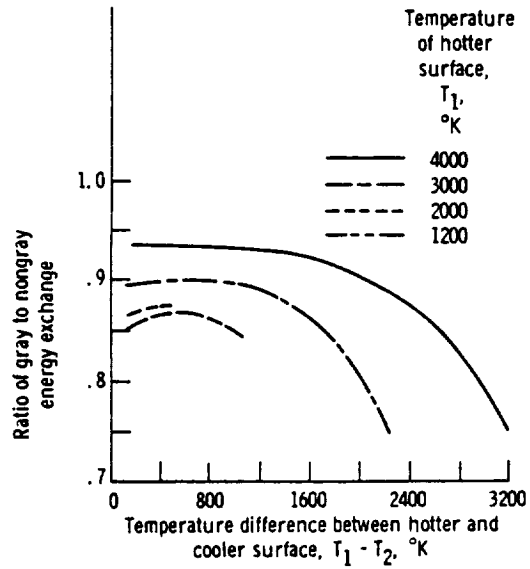


FIGURE 5-3.—Comparison of effect of gray and nongray surfaces on computed energy exchange between infinite tungsten plates (from ref. 2).

exchange is given. The gray-diffuse results were obtained using equation (3-10) with hemispherical total emissivities computed from the hemispherical spectral emissivities of figure 5-2. (In the gray computation by Branstetter, the emissivity of the colder surface 2 was inserted at the mean temperature $\sqrt{T_1 T_2}$ rather than at T_2 , which is a modification based on electromagnetic theory that is sometimes recommended for metals (ref. 3)). Over the range of surface temperatures shown, deviations of 25 percent below the nongray energy exchange are noted in the gray results.

EXAMPLE 5-2: Two infinite parallel plates and their spectral emissivities at their respective temperatures are shown in figure 5-4. What is the total heat flux q passing across the gap?

From equation (5-11)

$$q = \int_0^3 \frac{e_{\lambda b, 1}(\lambda, T_1) - e_{\lambda b, 2}(\lambda, T_2)}{\frac{1}{0.4} + \frac{1}{0.7} - 1} d\lambda + \int_3^5 \frac{e_{\lambda b, 1}(\lambda, T_1) - e_{\lambda b, 2}(\lambda, T_2)}{\frac{1}{0.8} + \frac{1}{0.7} - 1} d\lambda + \int_5^{\infty} \frac{e_{\lambda b, 1}(\lambda, T_1) - e_{\lambda b, 2}(\lambda, T_2)}{\frac{1}{0.8} + \frac{1}{0.3} - 1} d\lambda$$

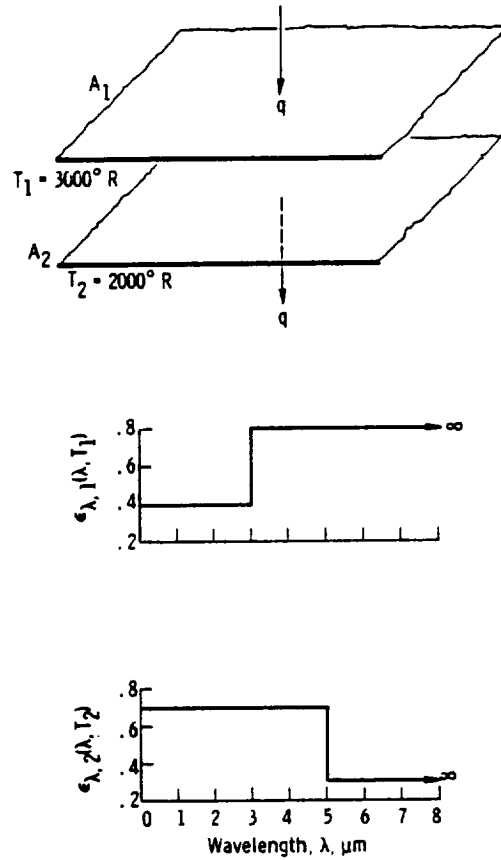


FIGURE 5-4.—Example of heat transfer across space between infinite parallel plates having spectrally dependent emissivities.

which can be written as

$$\begin{aligned}
 q = \sigma T_1^4 & \left[\frac{0.341}{\sigma T_1^4} \int_0^3 e_{\lambda b, 1}(\lambda, T_1) d\lambda + \frac{0.596}{\sigma T_1^4} \int_3^5 e_{\lambda b, 1}(\lambda, T_1) d\lambda \right. \\
 & \left. + \frac{0.279}{\sigma T_1^4} \int_5^\infty e_{\lambda b, 1}(\lambda, T_1) d\lambda \right] - \sigma T_2^4 \left[\frac{0.341}{\sigma T_2^4} \int_0^3 e_{\lambda b, 2}(\lambda, T_2) d\lambda \right. \\
 & \left. + \frac{0.596}{\sigma T_2^4} \int_3^5 e_{\lambda b, 2}(\lambda, T_2) d\lambda + \frac{0.279}{\sigma T_2^4} \int_5^\infty e_{\lambda b, 2}(\lambda, T_2) d\lambda \right]
 \end{aligned}$$

An integral such as $\frac{1}{\sigma T_1^4} \int_3^5 e_{\lambda b, 1}(\lambda, T_1) d\lambda$ is the fraction of blackbody

radiation at T_1 between $\lambda = 3$ and $5 \mu\text{m}$, which is $F_{3T_1-5T_1} = F_{9000-15000}$ and can be computed from the table of blackbody radiation functions (table V in the appendix of Vol. I). The $F_{\lambda T}$ should not be confused with the geometric configuration factor. Then

$$q = \sigma T_1^4 (0.341 F_{0-3T_1} + 0.596 F_{3T_1-5T_1} + 0.279 F_{5T_1-\infty})$$

$$- \sigma T_2^4 (0.341 F_{0-3T_2} + 0.596 F_{3T_2-5T_2} + 0.279 F_{5T_2-\infty}) = 43600 \text{ Btu/(hr)(ft}^2\text{)}$$

EXAMPLE 5-3: An enclosure is made up of three plates of finite width and infinite length, as shown (in cross section) in figure 5-5. The

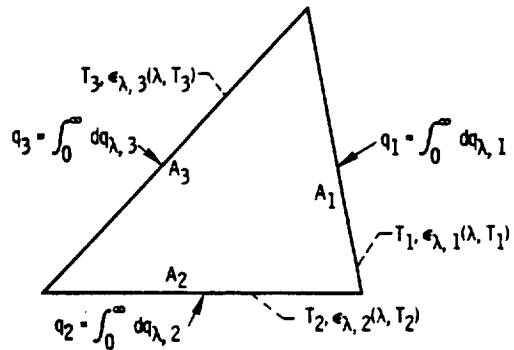


FIGURE 5-5. — Radiant interchange in enclosure with surfaces having spectrally varying radiation properties.

radiative properties of each surface are dependent upon wavelength and temperature, and the temperatures of the plates are T_1 , T_2 , and T_3 . Derive a set of equations governing the radiative energy exchange among the surfaces.

The configuration factors for such a geometry are derived in example problem 2-15. The net spectral energy flux supplied to surface 1 can be written as

$$dq_{\lambda,1} = \frac{dQ_{\lambda,1}}{A_1} = \frac{\epsilon_{\lambda,1}(\lambda, T_1)}{1 - \epsilon_{\lambda,1}(\lambda, T_1)} [e_{\lambda b,1}(\lambda, T_1) d\lambda - dq_{\lambda b,1}] \quad (5-12)$$

and

$$dq_{\lambda,1} = \frac{dQ_{\lambda,1}}{A_1} = dq_{\lambda b,1} - F_{1-2} dq_{\lambda b,2} - F_{1-3} dq_{\lambda b,3} \quad (5-13)$$

These equations are derived in direct analogy with those for a gray surface, equations (3-6) and (3-7), and by noting that $F_{1-1} = 0$. It should be emphasized that dq_λ is the energy supplied to the surface in wavelength interval $d\lambda$ as a result of external heat addition to the surface and energy transferred in from other wavelength regions.

Similar equations are written for surfaces 2 and 3. The result is a set of six simultaneous equations for the six unknowns $dq_{\lambda 0, 1}$, $dq_{\lambda 0, 2}$, $dq_{\lambda 0, 3}$, $dq_{\lambda, 1}$, $dq_{\lambda, 2}$, and $dq_{\lambda, 3}$. The solution is carried out for the dq_λ in each wavelength interval $d\lambda$.

If the properties of the surfaces are invariant over some fairly large spectral interval $\Delta\lambda$, then the equations may be solved over this entire interval. In this instance, the emissive power $e_{\lambda b, 1}(\lambda, T_1)\Delta\lambda$ would be replaced by $\sigma T_1^4 F_{\lambda T_1 - (\lambda + \Delta\lambda) T_1}$, the amount of blackbody radiation at T_1 in the interval from λ to $\lambda + \Delta\lambda$. Finally, q at each surface is found by integrating dq_λ for that surface over all wavelengths

$$q = \int_0^\infty dq_\lambda \quad (5-14)$$

This is the heat flux that must be supplied to the surface externally in order to maintain its specified surface temperature.

EXAMPLE 5-4: Consider the geometry of figure 5-5. Total energy flux is supplied to the three infinitely long plates at the rates q_1 , q_2 , and q_3 . Determine the temperatures of the plates.

The equations are exactly the same as in example 5-3. Now, however, the prescribed boundary conditions have made the problem much more difficult to solve. Because the surface temperatures are unknown, the emissivities are also unknown because of their temperature dependence. The solution is carried out as follows: A temperature is assumed for each surface, and $dq_\lambda(\lambda, T)$ for each surface is computed. The $dq_\lambda(\lambda, T)$ values are then integrated to find q_1 , q_2 , and q_3 , which are compared to the specified boundary values. New temperatures are chosen and the process is repeated until the computed q values agree with the specified values. The new temperatures for successive iterations must be guessed on the basis of the property variations and experience about the manner in which changes in T are reflected in changes in q throughout the system.

5.4 THE BAND ENERGY APPROXIMATION

The solution method presented and demonstrated in section 5.3 for spectrally dependent surfaces has required integrations over all wavelengths in order to compute the net total energy transfer. These integra-

tions are the complication that makes surfaces with spectrally dependent properties so much more difficult to deal with than gray surfaces. Shortcut methods are desirable for circumventing the tedious numerical integrations that are required for rigorous solution of these problems. Some loss of accuracy in the integration may be acceptable in a practical application because of the uncertainty already present in many of the spectral property values that are used.

5.4.1 Multiple Bands

- One method of approximation of the integrals is the *band energy approximation*. This is the conceptually simple approximation of replacing the single integral extending over all wavelengths by a summation of smaller integrals, where each of the smaller integrals extends over a portion of the spectrum. An example will serve to illustrate the application of this method.

EXAMPLE 5-5: Two infinite parallel plates of tungsten are at temperatures of 4000° and 2000° K. Using the data of figure 5-2, compute the net energy exchange between the surfaces by using the band energy approximation.

In example 5-1, the net exchange between the plates is given by the exact expression (eq. (5-11))

$$q_1 = -q_2 = \int_0^{\infty} \left[\frac{e_{\lambda b, 1}(\lambda, T_1) - e_{\lambda b, 2}(\lambda, T_2)}{\frac{1}{\epsilon_{\lambda, 1}(\lambda, T_1)} + \frac{1}{\epsilon_{\lambda, 2}(\lambda, T_2)} - 1} \right] d\lambda$$

By using the substitution

$$G_{\lambda} = \frac{1}{\frac{1}{\epsilon_{\lambda, 1}} + \frac{1}{\epsilon_{\lambda, 2}} - 1}$$

to shorten the notation, this can be written as

$$q_1 = \int_0^{\infty} G_{\lambda} e_{\lambda b, 1} d\lambda - \int_0^{\infty} G_{\lambda} e_{\lambda b, 2} d\lambda$$

The integrals are now written as approximate sums

$$q_1 \approx \sum_l (G_{\Delta\lambda} e_{\Delta\lambda, b, 1} \Delta\lambda)_l - \sum_m (G_{\Delta\lambda} e_{\Delta\lambda, b, 2} \Delta\lambda)_m \quad (5-15)$$

where $G_{\Delta\lambda}$ and $e_{\Delta\lambda, b}$ are average values applicable to the wavelength interval $\Delta\lambda$. Depending upon the way in which $G_{\Delta\lambda}$ and $e_{\Delta\lambda, b}$ are evaluated, equation (5-15) can have various degrees of accuracy. As a simple approximation the terms $e_{\Delta\lambda, b}$ can be taken as an arithmetic mean of the blackbody emissive power over $\Delta\lambda$. To obtain a better degree of approximation for large $\Delta\lambda$ intervals, $e_{\Delta\lambda, b}$ can be evaluated using the blackbody functions as

$$e_{\Delta\lambda, b} \Delta\lambda = \int_{\lambda}^{\lambda+\Delta\lambda} e_{\lambda b} d\lambda = [F_{0-(\lambda+\Delta\lambda)} - F_{0-\lambda}] \sigma T^4 \quad (5-16)$$

where λ and $\lambda + \Delta\lambda$ are the upper and lower limits of wavelength for the interval $\Delta\lambda$. Equation (5-16) will be used for the computations given here. It was previously used to evaluate the exact integrals for a simple problem in example 5-2. The $G_{\Delta\lambda}$ terms in equation (5-15) are approximated most simply by

$$G_{\Delta\lambda} = \frac{1}{\frac{1}{\epsilon_{\Delta\lambda, 1}} + \frac{1}{\epsilon_{\Delta\lambda, 2}} - 1} \quad (5-17)$$

where the $\epsilon_{\Delta\lambda}$ are appropriate mean emissivities over the wavelength interval $\Delta\lambda$.

In figure 5-6, the required emissivities of tungsten are plotted, and

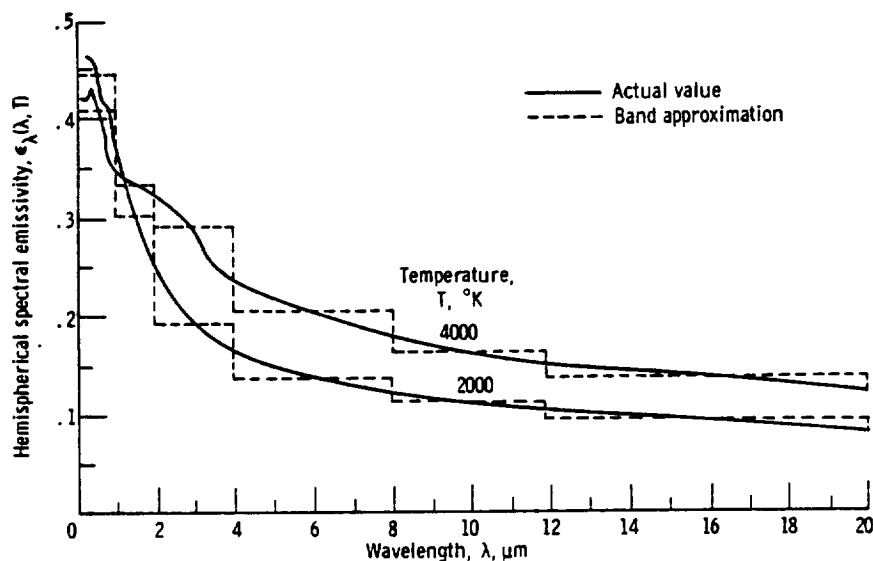


FIGURE 5-6. — Band approximations to hemispherical spectral emissivity of tungsten.

arithmetic mean values are shown for seven $\Delta\lambda$ intervals (the seventh interval being for $\lambda > 20\mu\text{m}$). For temperatures of 2000° and 4000°K , the peak in the $e_{\lambda b}$ function occurs at about 1.5 and $0.75\mu\text{m}$, respectively. For large values of λ , such as $\lambda > 4\mu\text{m}$ in this example, the $e_{\lambda b}$ is small and $G_{\lambda}e_{\lambda b}$ will contribute little to the integrals in this wavelength region. Thus, the accuracy of the averages at large values of λ is not important in this example. The computations for q_1 are carried out using these seven intervals in the following tabulation:

$\Delta\lambda$, μm	$\epsilon_{\Delta\lambda, 1}$	$\epsilon_{\Delta\lambda, 2}$	$G_{\Delta\lambda}$	$\epsilon_{\Delta\lambda, b, 1}\Delta\lambda$, W/cm^2	$\epsilon_{\Delta\lambda, b, 2}\Delta\lambda$, W/cm^2	$G_{\Delta\lambda}\epsilon_{\Delta\lambda, b, 1}\Delta\lambda$, W/cm^2	$G_{\Delta\lambda}\epsilon_{\Delta\lambda, b, 2}\Delta\lambda$, W/cm^2
0 to 1	0.410	0.445	0.271	0.698×10^2	0.0061×10^2	1.89×10^2	0.017×10^2
1 to 2	.335	.300	.188	.545	.0374	1.03	.071
2 to 4	.290	.195	.132	.171	.034	.23	.045
4 to 8	.205	.140	.0907	.032	.011	.03	.010
8 to 12	.160	.115	.0717	.004	.002	~ 0	.002
12 to 20	.140	.095	.0600	.001	~ 0	~ 0	~ 0
> 20	~ 0	~ 0	~ 0	~ 0	~ 0	~ 0	~ 0
Totals						3.18×10^2	0.145×10^2

Substituting the sums from the tabulation into the approximate band energy exchange equation gives $q_1 = (3.18 - 0.15) \times 10^2 = 303 \text{ W/cm}^2$.

Branstetter (ref. 2), using numerical integration, found the exact result of $q_1 = 300 \text{ W/cm}^2$ for this case. The approximate band solution using seven intervals is thus in error by a very small amount. Examination of figure 5-3 shows that the gray body assumption, which can be considered as a one-band approximation, yields answers that are in error by almost 10 percent (note that the gray results in fig. 5-3 were modified from the usual gray analysis by inserting ϵ_2 at $\sqrt{T_1 T_2}$ rather than at T_2).

A close examination of the tabulation shows that most of the significant energy transfer for this example occurs in the wavelength range of 0 to $2\mu\text{m}$. If necessary, the accuracy of the band energy approximation could be improved by dividing this range of most significant energy transfer into a larger number of increments and repeating the calculation. The errors in the band energy approximation will arise in the regions where both $e_{\lambda b}$ and ϵ_{λ} are large; thus the wavelength range should be divided such that most of the bands lie within these regions.

The band energy approximation is nothing more than a simple form

of numerical integration carried out by using a relatively small number of wavelength intervals. If the number of intervals is increased, the exact results for energy transfer are approached. Dunkle and Bevans (ref. 4) give a calculation similar to example 5-5 and show errors from an exact numerical result of less than 2 percent for the band energy solution as compared to about 30 percent error for the gray surface approximation. They give other examples of applications in enclosures with specified temperatures or net energy fluxes.

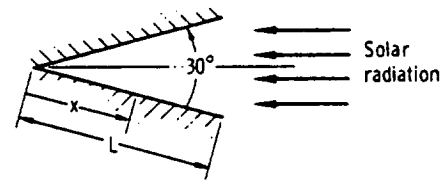
Some additional references providing analyses of energy exchange between spectrally dependent surfaces are those of Love and Gilbert (ref. 5), Goodman (ref. 6), and Rolling and Tien (ref. 7). In reference 5, the analytical results compare well with experimental results for a geometry closely approximating infinite parallel plates.

5.4.2 The Semigray Approximations

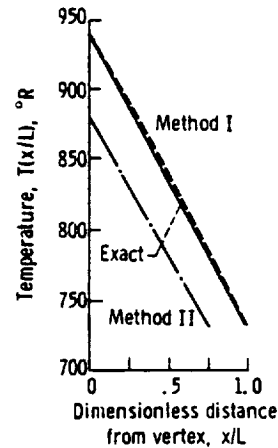
In some practical situations, there is a natural division of the energy within an enclosure into two well-defined spectral regions. This is the case for an enclosure with an opening through which solar energy is entering. The solar energy will have a spectral distribution concentrated in a short wavelength region, while the energy originating by emission from the lower temperature surfaces within the enclosure will be in a longer wavelength region. A practical way of treating this situation is to define a hemispherical total absorptivity for incident solar radiation and a second hemispherical total absorptivity for incident energy originating by emission within the enclosure. This approach can be carried to the point of defining j different absorptivities for surface k , one absorptivity for incident energy from each enclosure surface j .

The assumption entering these analyses is that each absorptivity $\alpha_k(T_k, T_j)$ is based on an incident *blackbody* spectral distribution at the temperature of the originating surface T_j . Of course, the incident spectrum may actually be quite far removed from the Planckian form, and this is the weakness of the method. Often, the dependence of α_k on T_k is small, so that the principal dependence is on T_j or, in other words, on the distribution of the incident spectrum. Because the absorptivity $\alpha_k(T_k, T_j)$ and emissivity $\epsilon_k(T_k)$ of surface k are not in general equal, this approach is often called the *semigray enclosure theory*. Reference 8 contains the formulation of a semigray analysis for a general enclosure.

Plamondon and Landram (ref. 9) have compared the semigray and exact solutions of the temperature profiles along the surface of a nongray wedge cavity exposed to incident solar radiation, as shown in figure 5-7. The wedge cavity is assumed to be nonconducting, to be in a vacuum with an environment at zero degrees except for the solar radiation, to have properties independent of surface temperature, and to have



(a)



(b)

(a) Geometry of wedge cavity.

(b) Temperature distribution along wedge. $\alpha_{solar} = 0.220$; $\alpha_{infrared} = 0.099$.

FIGURE 5-7.—Effect of semigray approximations on computed temperature distribution in wedge cavity.

diffuse surfaces. Three solution techniques are given in reference 9. The first is an exact solution of the complete integral equations and is called the "exact" solution. The first approximation to the exact solution, called "Method I," is the semigray analysis which assigns an absorptivity α_{solar} for radiation (direct and reflected) that originated from the incident solar energy, and a second absorptivity $\alpha_{infrared}$ (equal to the surface emissivity) for radiation originating by emission from the wedge surfaces. Finally, "Method II" is a poorer approximation that retains the same two absorptivities but applies α_{solar} only for the incident solar energy, and then uses $\alpha_{infrared}$ for all energy after reflection, regardless of its source. The results of these methods are shown in figure 5-7(b) for a polished aluminum surface in a 30° wedge. Method I, the full semigray analysis, is seen to give excellent agreement with the exact solution while Method II underestimates the exact temperatures by about 10 percent.

5.5 DIRECTIONAL-GRAY SURFACES

Some attention has been paid to the development of treatments of radiation interchange between surfaces or in enclosures where directionally dependent properties must be considered. The bulk of radiation analyses invoke the assumption of diffuse emitting and reflecting surfaces although some treatments do include the effect of specular reflections as outlined in chapter 4. The diffuse or specular surface conditions are convenient to treat analytically and in most instances the detailed considerations of directional emission and reflection effects are unwarranted. There are, nevertheless, certain materials and certain geometric situations that require the consideration of directional effects. In this section, some methods of considering radiant interchange between surfaces with directional properties will be presented.

The difficulty in treating the general case of directionally dependent properties is perhaps best illustrated by performing an energy balance in a simple geometry. Let such a balance for the radiative interchange between two infinitely long parallel gray nondiffuse surfaces of finite width L (fig. 5-8) be examined. The intensity of radiation leaving element

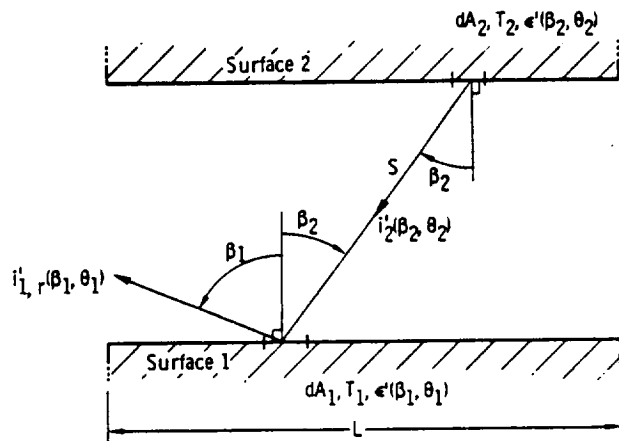


FIGURE 5-8.—Radiant interchange between infinitely long parallel directional surfaces of finite width L .

dA_1 in direction (β_1, θ_1) is composed of an emitted intensity $i'_{1,e}(\beta_1, \theta_1)$ and a reflected intensity $i'_{1,r}(\beta_1, \theta_1)$, or

$$i'_{1}(\beta_1, \theta_1) = i'_{1,e}(\beta_1, \theta_1) + i'_{1,r}(\beta_1, \theta_1) \quad (5-18)$$

These two components are given by modifications of equations (3-3a) and (3-25) of Vol. I as

$$i'_{1,e}(\beta_1, \theta_1) = \epsilon'_1(\beta_1, \theta_1) i'_{b,1}(T_1) \quad (5-19)$$

and

$$i'_{1,r}(\beta_1, \theta_1) = \int_{A_2} \rho''_1(\beta_1, \theta_1, \beta_2, \theta_2) i'_2(\beta_2, \theta_2) \frac{\cos \beta_2 \cos \beta_2}{S^2} dA_2 \quad (5-20)$$

In equation (5-20) the energy incident upon dA_1 from each element dA_2 is multiplied by the bidirectional total reflectivity ρ''_1 to give the contribution to the reflected intensity from dA_1 into direction (β_1, θ_1) . This is then integrated over all energy incident on dA_1 from A_2 . The definition of ρ'' is that given in Vol. I, which is

$$\rho''(\beta_r, \theta_r, \beta, \theta) = \frac{i''_r(\beta_r, \theta_r, \beta, \theta)}{i'_i(\beta, \theta) \cos \beta d\omega} \quad (5-21)$$

The $\rho''(\beta_r, \theta_r, \beta, \theta)$ is the ratio of reflected *intensity* in the (β_r, θ_r) direction to the *energy flux* incident from the (β, θ) direction.

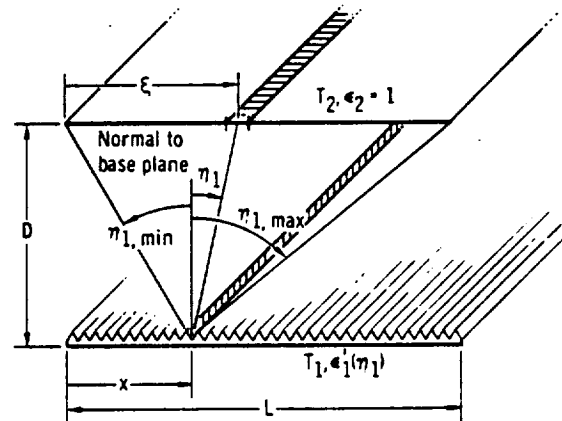
Equation (5-18) for the intensity leaving the element dA_1 then becomes

$$i'_1(\beta_1, \theta_1) = \epsilon'_1(\beta_1, \theta_1) i'_{b,1}(T_1) + \int_{A_2} \rho''_1(\beta_1, \theta_1, \beta_2, \theta_2) i'_2(\beta_2, \theta_2) \frac{\cos^2 \beta_2}{S^2} dA_2 \quad (5-22)$$

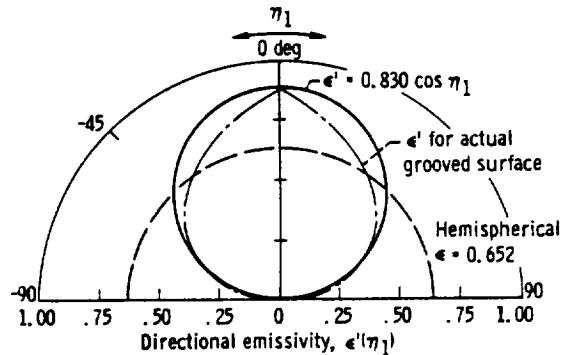
A similar equation may be written for an arbitrary element dA_2 on surface 2. This results in a very complicated coupled pair of integral equations that must be solved for $i'(\beta, \theta)$ at each point and for each direction on the two surfaces. This set of integral equations is analogous to equations (3-50) that were derived for gray-diffuse surfaces. Tabulated property data of $\epsilon'(\beta, \theta)$ and $\rho''(\beta_r, \theta_r, \beta, \theta)$ for such a situation are seldom available. For the case when T_1 and T_2 are not known and the temperature dependence of the properties is considerable, the solution of the entire energy exchange determination becomes prohibitively tedious. To avoid the extreme amount of computation, a number of approximations can be invoked in the situations where they are justified. Some of these methods are outlined in references 10 to 14. Rather than try to present all the possible approximations, an example will be given, and the reader is left to his ingenuity in approximating the conditions of more realistic problems. Usually, such approximations involve analytically simulating the real properties by simple functions, omitting certain portions of energy that are deemed negligible, or ignoring all directional

effects except those expected to provide significant changes from diffuse or specular analyses.

EXAMPLE 5-6: Two parallel isothermal plates of infinite length and finite width L are arranged as shown in figure 5-9(a). The upper plate 2



(a)



(b)

(a) Geometry of problem. (Environment at zero temperature.)

(b) Emissivity of directional surface.

FIGURE 5-9.—Interchange between grooved directional surface and black surface.

is black while the lower is composed of a highly reflective material with parallel deep grooves of open angle 1° cut into the surface and running in the infinite direction. Such a surface might be made by stacking polished razor blades. Compute the net energy gain by the directional surface if $T_2 > T_1$ and compare the result to the net energy gain by a diffuse surface with emissivity equivalent to the hemispherical emissivity of the directional surface. The surroundings are at zero temperature.

The directional emissivity for the grooved surface is obtained from reference 15, where the directional emissivity at the opening of an infinitely long groove with specularly reflecting walls of surface emissivity 0.01 was calculated. The directional emissivity for the grooved surface is given by the dot-dashed line in figure 5-9(b). The angle η is measured from the normal of the base plane of the grooved surface and is in a plane perpendicular to the length of the groove as shown in figure 5-9(a). The $\epsilon'_i(\eta_1)$, as given in reference 15, has already been averaged over all circumferential angles for a fixed η_1 . Thus, it is an effective emissivity from a strip on the grooved surface to a parallel infinitely long strip element on an imaginary semicylinder over the groove and with its axis parallel to the grooves. The angle η_1 is different from the usual cone angle β_1 . The angle β_1 would vary along the strip element of the semicylinder while η_1 remains constant since it is the projected angle on a plane normal to the groove. The actual emissivity $\epsilon'_i(\eta_1)$ of figure 5-9(b) is approximated for convenience by the analytical expression

$$\epsilon'_i(\eta_1) \approx 0.830 \cos \eta_1$$

By using cylindrical coordinates to perform the integration over all η_1 , the corresponding hemispherical emissivity of this surface is

$$\epsilon_1 = \frac{Q_1}{Q_b} = \frac{\int_{-\pi/2}^{\pi/2} \epsilon'_i(\eta_1) \cos \eta_1 d\eta_1}{\int_{-\pi/2}^{\pi/2} \cos \eta_1 d\eta_1} = 0.830 \int_0^{\pi/2} \cos^2 \eta_1 d\eta_1 = 0.652$$

and this result is shown in figure 5-9(b) as a dashed line.

The energy gained by surface 1 when 2 is a black surface and 1 is a diffuse surface with $\epsilon = 0.652$ will first be determined. The energy emitted by the diffuse surface per unit of the infinite length and per unit time is

$$Q_{e,1} = 0.652 \sigma T_1^4 L$$

Since surface 2 is black, none of this energy will be reflected back to 1. The energy per unit length and time emitted by surface 2 that is absorbed by surface 1 is

$$Q_{a,1} = 0.652 \sigma T_2^4 \int_{A_2} \int_{A_1} dF_{a2-d1} dA_2 = 0.652 \sigma T_2^4 \int_{A_1} \int_{A_2} dF_{d1-a2} dA_1$$

The desired energy gained by 1 is $Q_{a,1} - Q_{e,1}$. To evaluate $Q_{a,1}$, the configuration factor between infinite parallel strips was found in example 2-4 as

$$dF_{d1-\alpha} = \frac{d(\sin \eta_1)}{2}$$

By integrating over A_2 , the double integral becomes

$$\int_{A_1} \left(\int_{A_2} dF_{d1-\alpha} \right) dA_1 = \frac{1}{2} \int_{x=0}^L (\sin \eta_{1, \max} - \sin \eta_{1, \min}) dx$$

The value of $\sin \eta_1$ is found from figure 5-9(a) to be

$$\sin \eta_1 = \frac{\xi - x}{[(\xi - x)^2 + D^2]^{1/2}}$$

and, solving now for $Q_{a,1}$, gives

$$\begin{aligned} Q_{a,1} &= 0.652 \sigma T_2^4 \frac{1}{2} \int_{x=0}^L \left[\frac{L-x}{(x^2 - 2xL + L^2 + D^2)^{1/2}} + \frac{x}{(x^2 + D^2)^{1/2}} \right] dx \\ &= 0.652 \sigma T_2^4 [(L^2 + D^2)^{1/2} - D] \end{aligned}$$

The net energy gained by surface 1, $Q_{a,1} - Q_{e,1}$, divided by the energy emitted by surface 2 is a measure of the efficiency of a surface as a directional absorber. For surface 1 being diffuse, this ratio is

$$\bar{\epsilon}_{diffuse} = \frac{Q_{a,1} - Q_{e,1}}{\sigma T_2^4 L} = \frac{0.652}{l} \left[(1 + l^2)^{1/2} - 1 - \frac{T_1^4}{T_2^4} l \right]$$

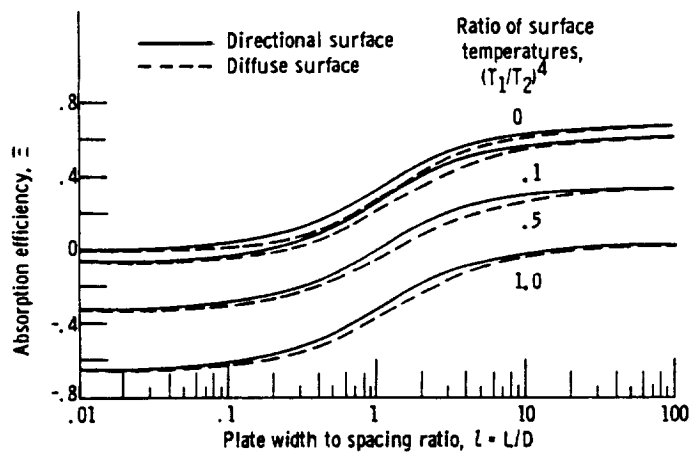


FIGURE 5-10. — Effect of directional emissivity on absorption efficiency of surface.

where $l = L/D$.

The analysis for surface 1, being a directional (grooved) surface, will now be carried out. The emitted energy from 1 is the same as that for the diffuse surface since both have the same hemispherical emissivity. The energy absorbed by the grooved surface is

$$\begin{aligned}
 Q_{a,1} &= \sigma T_2^4 \int_{A_2} \int_{A_1} \alpha'_1(\eta_1) dF_{a2-d1} dA_2 \\
 &= \frac{0.830 \sigma T_2^4}{2} \int_{x=0}^L \int_{\eta_{1,\min}}^{\eta_{1,\max}} \cos^2 \eta_1 d\eta_1 dx \\
 &= \frac{0.830 \sigma T_2^4}{2} \int_{x=0}^L \frac{1}{2} (\sin \eta_1 \cos \eta_1 + \eta_1) \Big|_{\eta_{1,\min}}^{\eta_{1,\max}} dx \\
 &= \frac{0.830 \sigma T_2^4}{4} \int_{x=0}^L \left[\frac{D(L-x)}{(x^2 - 2xL + L^2 + D^2)} + \tan^{-1} \left(\frac{L-x}{D} \right) \right. \\
 &\quad \left. + \frac{xD}{x^2 + D^2} + \tan^{-1} \frac{x}{D} \right] dx
 \end{aligned}$$

$$Q_{a,1} = \frac{0.830 \sigma T_2^4 L}{2} \tan^{-1} \frac{L}{D}$$

The absorption efficiency Ξ of the directional surface is then

$$\Xi_{\text{directional}} = \frac{0.830}{2} \tan^{-1} l - 0.652 \left(\frac{T_1}{T_2} \right)^4$$

The absorption efficiencies Ξ of the grooved and diffuse surfaces are plotted in figure 5-10 as a function of l with $(T_1/T_2)^4$ as a parameter. It is seen that Ξ for the directional surface is higher than that for the diffuse surface for all values of l , indicating that the directional surface will always be a more efficient absorber in this configuration. As l approaches zero, the configuration approaches that of infinite elemental strips, and emission from surface 1 becomes much larger than the absorption from surface 2. Thus, Ξ_{diffuse} and $\Xi_{\text{directional}}$ are nearly equal since the surfaces always emit the same amount. As l approaches infinity, the configuration approaches infinite parallel plates for which directional effects are lost. Again, the Ξ becomes equal for the two different surface conditions. At intermediate values of l , a 10-percent difference in absorption efficiency appears attainable.

The effects of directional properties on the local heat loss can be a considerable factor in many geometries. In figure 5-11, a number of

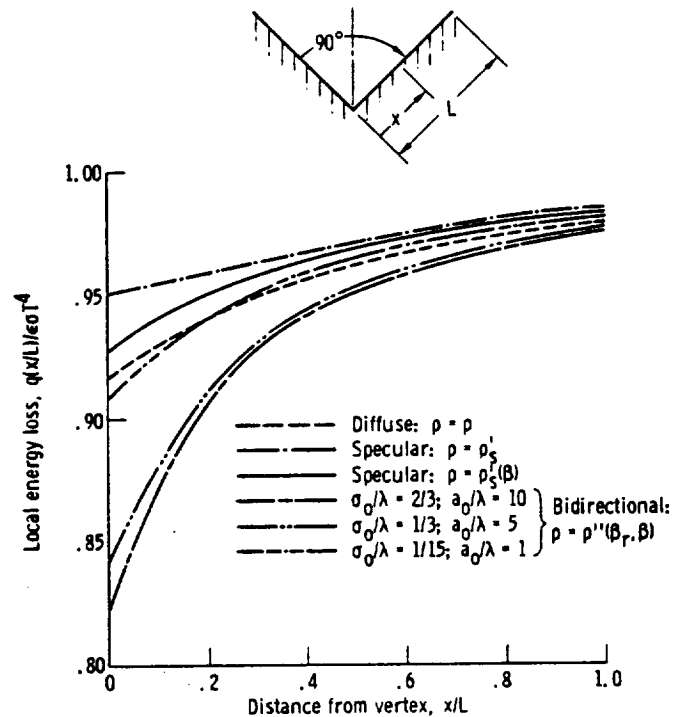


FIGURE 5-11. — Local radiative energy loss from surface of isothermal groove cavity. (Hemispherical emissivity of surface, 0.1.)

assumed directional distributions of reflectivity are examined for their influence on the local heat loss from the walls of an infinitely long groove cavity. The results are taken from reference 12 where, for comparison, the curves were gathered from original work and from diverse sources (refs. 13, 14, 16, and 17). The walls of the groove are at 90° to each other, and the surface emissivity distributions are all normalized to give a hemispherical emissivity of 0.1. Curves are presented for diffuse reflectivity ρ , specular reflectivity assumed independent of incident angle ρ'_s , specular reflectivity dependent upon incident angle $\rho'_s(\beta)$ based upon electromagnetic theory, and three distributions of bidirectional reflectivity $\rho''(\beta_r, \beta)$. The bidirectional distributions are based on the work of Beckmann and Spizzichino (ref. 18) for rough surfaces having various combinations of root-mean-square optical surface roughness amplitude to radiation wavelength ratio σ_o/λ and roughness auto-correlation distance to radiation wavelength ratio α_o/λ .

Note that the results shown in figure 5-11 for the simple specular and diffuse models do *not* provide upper and lower limits to all the solutions as is sometimes claimed.

5.6 SURFACES WITH DIRECTIONALLY AND SPECTRALLY DEPENDENT PROPERTIES

The general case of radiative transfer in enclosures with surfaces having temperature-dependent radiative properties that depend on both wavelength and direction is a most complex and difficult one to treat fully. Closed-form solution of such problems is not possible unless many restrictive assumptions are introduced. When such problems must be treated, numerical techniques are necessary. The Monte Carlo method is a likely candidate, and example applications of the method to simple directional spectral surfaces is made in chapter 6. Toor (ref. 13) has studied radiation interchange by the Monte Carlo method for a variety of simply arranged surfaces with directional properties.

In this section, the general integral equations for radiation in such systems are formulated, and one considerably simplified example problem is carried out. The procedure is a combination of the previously considered diffuse-spectral and directional-gray analyses. The equations will be formulated at one wavelength as in section 5.3 and will also be formulated in terms of intensities as in section 5.5. In this manner, both spectral and directional effects can be accounted for. For simplicity, the interaction between only two plane surfaces will be treated. This treatment can then be generalized to a multisurface enclosure as has been done for gray surfaces in chapter 3.

Consider an element dA_1 of surface A_1 in the x - y plane as shown in figure 5-12. The surface is isothermal and has directional spectral properties. Consider the spectral radiation intensity outgoing from dA_1 in direction $(\beta_{r,1}, \theta_{r,1})$ by means of both emission and reflection. The spectral intensity emitted by dA_1 in direction $(\beta_{r,1}, \theta_{r,1})$ is

$$i'_{\lambda e,1}(\lambda, \beta_{r,1}, \theta_{r,1}) = \epsilon'_{\lambda,1}(\lambda, \beta_{r,1}, \theta_{r,1}) i'_{\lambda b,1}(\lambda) \quad (5-23)$$

These quantities are also functions of T_1 , but this designation is omitted to simplify the notation somewhat. The intensity reflected from dA_1 into direction $(\beta_{r,1}, \theta_{r,1})$ results from the intensity incident from A_2 . It would be desirable to have an expression for the intensity incident within solid angle $d\omega_1$; then by integrating over all such $d\omega_1$, the incident radiation from all of A_2 would be accounted for. If the incident intensity

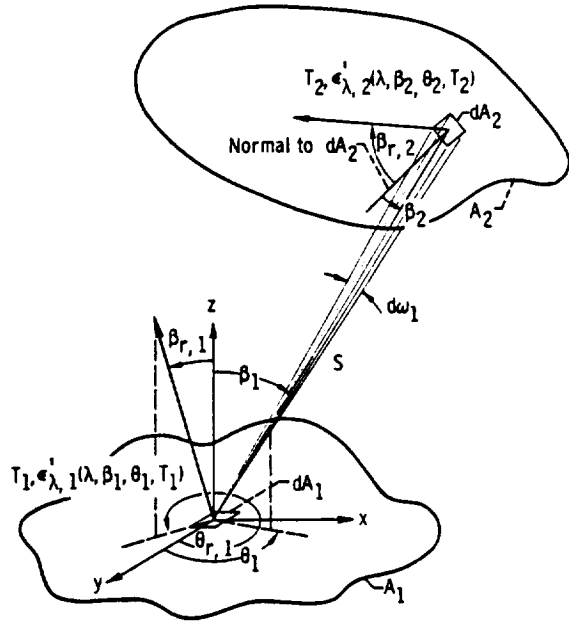


FIGURE 5-12. — Interchange between surfaces having directional-specular properties. (Environment at zero temperature.)

within $d\omega_1$ is called $i'_{\lambda i, 1}(\lambda, \beta_1, \theta_1)$, then the energy reflected from dA_1 into direction $(\beta_{r, 1}, \theta_{r, 1})$ is

$$i'_{\lambda r, 1}(\lambda, \beta_{r, 1}, \theta_{r, 1}) = \int_{A_2} \rho''_{\lambda, 1}(\lambda, \beta_{r, 1}, \theta_{r, 1}, \beta_1, \theta_1) i'_{\lambda i, 1}(\lambda, \beta_1, \theta_1) \cos \beta_1 d\omega_1 \quad (5-24)$$

The surroundings are taken to be at zero temperature so that the only incident intensity is that from A_2 . The spectral intensity outgoing from dA_1 in direction $(\beta_{r, 1}, \theta_{r, 1})$ is then the sum of emitted and reflected quantities

$$\begin{aligned} i'_{\lambda o, 1}(\lambda, \beta_{r, 1}, \theta_{r, 1}) &= i'_{\lambda e, 1}(\lambda, \beta_{r, 1}, \theta_{r, 1}) + i'_{\lambda r, 1}(\lambda, \beta_{r, 1}, \theta_{r, 1}) \\ &= \epsilon'_{\lambda, 1}(\lambda, \beta_{r, 1}, \theta_{r, 1}) i'_{\lambda b, 1}(\lambda) \\ &\quad + \int_{A_2} \rho''_{\lambda, 1}(\lambda, \beta_{r, 1}, \theta_{r, 1}, \beta_1, \theta_1) i'_{\lambda i, 1}(\lambda, \beta_1, \theta_1) \cos \beta_1 d\omega_1 \end{aligned} \quad (5-25)$$

In equation (5-25) the $i'_{\lambda_i, 1}(\lambda, \beta_1, \theta_1)$ results from the outgoing intensity $i'_{\lambda_o, 2}(\lambda, \beta_2, \theta_2)$ from surface 2. This outgoing intensity is composed of both emitted energy and energy incident from 1 that is reflected. The energy leaving dA_2 that reaches dA_1 is

$$i'_{\lambda_o, 2}(\lambda, \beta_2, \theta_2) dA_2 \cos \beta_2 dA_1 \cos \beta_1 / S^2$$

In terms of the incident intensity $i'_{\lambda_i, 1}(\lambda, \beta_1, \theta_1)$, the incident energy in $d\omega_1$ is

$$i'_{\lambda_i, 1}(\lambda, \beta_1, \theta_1) dA_1 \cos \beta_1 d\omega_1 \quad \text{or} \quad i'_{\lambda_i, 1}(\lambda, \beta_1, \theta_1) dA_1 \cos \beta_1 dA_2 \cos \beta_2 / S^2$$

Thus,

$$i'_{\lambda_i, 1}(\lambda, \beta_1, \theta_1) = i'_{\lambda_o, 2}(\lambda, \beta_2, \theta_2) \quad (5-26)$$

Substituting equation (5-26) into equation (5-25) gives

$$i'_{\lambda_o, 1}(\lambda, \beta_{r, 1}, \theta_{r, 1}) = \epsilon'_{\lambda, 1}(\lambda, \beta_{r, 1}, \theta_{r, 1}) i'_{\lambda_o, 1}(\lambda) + \int_{A_2} \rho''_{\lambda, 1}(\lambda, \beta_{r, 1}, \theta_{r, 1}, \beta_1, \theta_1) i'_{\lambda_o, 2}(\lambda, \beta_2, \theta_2) \cos \beta_1 d\omega_1 \quad (5-27a)$$

Similarly for surface 2

$$i'_{\lambda_o, 2}(\lambda, \beta_{r, 2}, \theta_{r, 2}) = \epsilon'_{\lambda, 2}(\lambda, \beta_{r, 2}, \theta_{r, 2}) i'_{\lambda_o, 2}(\lambda) + \int_{A_1} \rho''_{\lambda, 2}(\lambda, \beta_{r, 2}, \theta_{r, 2}, \beta_2, \theta_2) i'_{\lambda_o, 1}(\lambda, \beta_1, \theta_1) \cos \beta_2 d\omega_2 \quad (5-27b)$$

Equations (5-27) are both in terms of outgoing intensities. Thus, they form a set of simultaneous integral equations for $i'_{\lambda_o, 1}$ and $i'_{\lambda_o, 2}$. An iterative numerical solution technique would generally be required. The radiative properties and temperature can, in general, vary across each surface.

When the $i'_{\lambda_o, 1}$ and $i'_{\lambda_o, 2}$ have been obtained, the total energy can be determined that must be supplied to each surface element to maintain the specified surface temperature. The total energy supplied is the difference between the total emitted energy Q_e and the total absorbed energy Q_a . For element dA_1 ,

$$\begin{aligned}
 dQ_1 &= dQ_{e,1} - dQ_{a,1} = dA_1 \int_{\lambda=0}^{\infty} \int_{\Omega} \epsilon'_{\lambda,1}(\lambda, \beta_1, \theta_1) i'_{\lambda b,1}(\lambda) \cos \beta_1 d\omega_1 d\lambda \\
 &\quad - dA_1 \int_{\lambda=0}^{\infty} \int_{A_2} \alpha'_{\lambda,1}(\lambda, \beta_1, \theta_1) i'_{\lambda i,1}(\lambda, \beta_1, \theta_1) \cos \beta_1 d\omega_1 d\lambda \\
 dQ_1 &= \epsilon_1 \sigma T_1^4 dA_1 - dA_1 \int_{\lambda=0}^{\infty} \int_{A_2} \alpha'_{\lambda,1}(\lambda, \beta_1, \theta_1) i'_{\lambda o,2}(\lambda, \beta_2, \theta_2) \\
 &\quad \frac{\cos \beta_1 \cos \beta_2}{S^2} dA_2 d\lambda \quad (5-28)
 \end{aligned}$$

where ϵ_1 is the hemispherical total emissivity of surface 1.

If $dQ_1(x, y)$ rather than $T_1(x, y)$ is specified, then $T_1(x, y)$ must be determined, and the solutions can be quite tedious. A temperature distribution must be assumed for each surface, and the set of equations of the form of equations (5-27) solved to find $i'_{\lambda o}$ at each point. These outgoing intensities are substituted into equation (5-28), and the computed dQ_1 from equation (5-28) is compared to the given values. Adjustments are then made in the assumed distribution of temperatures, and this procedure is repeated until agreement between given and computed $dQ_1(x, y)$ is attained.

EXAMPLE 5-7: A small area element dA_1 is placed on the axis of and parallel to a black circular disk as shown in figure 5-13. The element is at temperature T_1 and the disk is at T_2 . The environment is at $T=0$. The element has a directional spectral emissivity that is independent of θ and can be approximated by the expression

$$\epsilon'_{\lambda,1}(\lambda, \beta_1, T_1) = 0.8 \cos \beta_1 (1 - e^{-C_2/\lambda T_1})$$

where C_2 is one of the constants in Planck's spectral energy distribution. (As will be evident, this distribution was chosen to simplify this example.) Find the energy dQ_1 added to dA_1 in order to maintain it at T_1 . Assume that T_1 is close to T_2 .

Equation (5-28) can be employed immediately because $i'_{\lambda o,2}$ is known from the specification of A_2 being a black surface. The emitted energy from dA_1 is given by

$$dQ_{e,1} = \epsilon_1 \sigma T_1^4 dA_1 = dA_1 \int_{\lambda=0}^{\infty} \int_{\Omega} \epsilon'_{\lambda,1}(\lambda, \beta_1) i'_{\lambda b,1}(\lambda) \cos \beta_1 d\omega_1 d\lambda$$

Now insert the expressions for $\epsilon'_{\lambda,1}$, $i'_{\lambda b,1}$ ((eq. 2-11a) of Vol. I), and

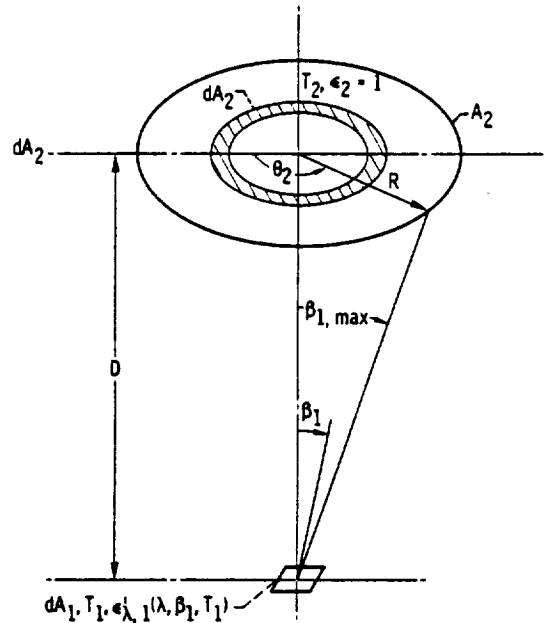


FIGURE 5-13. — Energy exchange involving directional-spectral surface element. (Environment at zero temperature.)

$d\omega_1 = \sin \beta_1 d\beta_1 d\theta_1$ to obtain

$$dQ_{e,1} = 0.8 dA_1 \int_{\lambda=0}^{\infty} \int_{\Omega} \cos \beta_1 (1 - e^{-C_2/\lambda T_1}) \frac{2C_1}{\lambda^5 (e^{C_2/\lambda T_1} - 1)} \\ \times \cos \beta_1 \sin \beta_1 d\beta_1 d\theta_1 d\lambda \\ = 0.8 dA_1 \int_{\lambda=0}^{\infty} \left(\int_{\Omega} \cos^2 \beta_1 \sin \beta_1 d\beta_1 d\theta_1 \right) \frac{2C_1}{\lambda^5 e^{C_2/\lambda T_1}} d\lambda$$

Carrying out the integral over the hemisphere gives

$$dQ_{e,1} = 0.8 dA_1 \left(\frac{2\pi}{3} \right) \int_0^{\infty} \frac{2C_1}{\lambda^5 e^{C_2/\lambda T_1}} d\lambda$$

Use the transformation $\zeta = C_2/\lambda T_1$

$$dQ_{e,1} = 0.8 dA_1 \left(\frac{4C_1\pi}{3} \right) \int_0^{\infty} \frac{T_1^4 \zeta^3}{C_2^4 e^{\zeta}} d\zeta$$

Then using the relation $\int_0^{\infty} \zeta^3 e^{-\zeta} d\zeta = 3!$ (ref. 19) gives

$$dQ_{e,1} = 6.4 dA_1 C_1 \pi \frac{T_1^4}{C_2}$$

But the Stefan-Boltzmann constant $\sigma = 2C_1\pi^5/15C_2^4$ so that

$$dQ_{e,1} = \frac{48}{\pi^4} \sigma T_1^4 dA_1$$

The energy absorbed by dA_1 is

$$dQ_{a,1} = dA_1 \int_{\lambda=0}^{\infty} \int_{A_2} \alpha'_\lambda(\lambda, \beta_1, \theta_1) i'_{\lambda_0,2}(\lambda, \beta_2, \theta_2) \frac{\cos \beta_1 \cos \beta_2 dA_2}{S^2} d\lambda$$

By using Kirchhoff's law, the directional spectral absorptivity and emissivity can be equated without restriction. Then, for dA_2 taken as a ring element, the solid angle $\cos \beta_2 dA_2/S^2$ can be written as $2\pi \sin \beta_1 d\beta_1$. This is used to write the absorbed energy as

$$\begin{aligned} dQ_{a,1} &= 2\pi(0.8)dA_1 \int_{\lambda=0}^{\infty} \int_{\beta_1=0}^{\beta_{1,max}} (\cos^2 \beta_1 \sin \beta_1 d\beta_1) i'_{\lambda_0,2}(\lambda) (1 - e^{-C_2/\lambda T_2}) d\lambda \\ &= -1.6\pi dA_1 \frac{\cos^3 \beta_1}{3} \Big|_0^{\beta_{1,max}} \int_0^{\infty} \frac{2C_1(1 - e^{-C_2/\lambda T_1})}{\lambda^5(e^{C_2/\lambda T_2} - 1)} d\lambda \\ &= \frac{3.2\pi C_1 dA_1}{3} \left[1 - \frac{D^3}{(D^2 + R^2)^{3/2}} \right] \int_0^{\infty} \frac{1 - e^{-C_2/\lambda T_1}}{\lambda^5(e^{C_2/\lambda T_2} - 1)} d\lambda \end{aligned}$$

If the approximation is invoked that T_1 is close in value to T_2 , the integration over λ can be carried out with the following result:

$$Q_{a,d1} = \frac{48}{\pi^4} \left[1 - \frac{1}{(1+r^2)^{3/2}} \right] \sigma T_2^4 dA_1$$

where $r = R/D$. Finally, the heat added to dA_1 to maintain it at T_1 is given by

$$dQ_1 = dQ_{e,1} - dQ_{a,1} = \frac{48\sigma}{\pi^4} \left\{ T_1^4 - T_2^4 \left[1 - \frac{1}{(1+r^2)^{3/2}} \right] \right\} dA_1$$

Even for this illustrative example, it was difficult to construct a realistic analytical function for ϵ'_λ that could be integrated in closed form over both angle and wavelength. Almost invariably, it is necessary to use numerical methods to obtain solutions to problems of this type.

5.7 CONCLUDING REMARKS

Although the formulation of radiation exchange problems involving directional and/or spectral property effects is not conceptually difficult, it is often very tedious to obtain solutions to the resulting integral equations. To simplify the equations, it is necessary to invoke many assumptions and approximations. The approximations that can be invoked with validity vary from case to case and are so numerous that they have not been discussed in any depth. Numerical techniques of many types can be used for directional spectral problems since closed-form analytical solutions rarely can be obtained. The number and range of conditions and parameters in these problems preclude the specification of any one numerical technique as being the best. As more and more interchange problems of this type are investigated, perhaps the most valuable techniques will emerge from the present unresolved jungle of individual solutions. One technique is the Monte Carlo method, which is the subject of the next chapter.

REFERENCES

1. BREENE, ROBERT G., JR.: *The Shift and Shape of Spectral Lines*. Pergamon Press, 1961, p. 52.
2. BRANSTETTER, J. ROBERT: *Radiant Heat Transfer Between Nongray Parallel Plates of Tungsten*. NASA TN D-1088, 1961.
3. ECKERT, E. R. G.; AND DRAKE, ROBERT M. JR.: *Heat and Mass Transfer*. Second ed., McGraw-Hill Book Co., Inc., 1959, p. 375.
4. DUNKLE, R. V.; AND BEVANS, J. T.: Part 3. A Method for Solving Multinode Networks and a Comparison of the Band Energy and Gray Radiation Approximations. *J. Heat Transfer*, vol. 82, no. 1, Feb. 1960, pp. 14-19.
5. LOVE, TOM J.; AND GILBERT, JOEL S.: *Experimental Study of Radiative Heat Transfer Between Parallel Plates*. Oklahoma Univ. (ARL-66-0103, DDC No. AD-643307), June 1966.
6. GOODMAN, STANLEY: *Radiant-Heat Transfer Between Nongray Parallel Plates*. *J. Res. Nat'l Bur. Standards*, vol. 58, no. 1, Jan. 1957, pp. 37-40.
7. ROLLING, R. E.; AND TIEN, C. L.: *Radiant Heat Transfer for Nongray Metallic Surfaces at Low Temperatures*. Paper No. 67-335, AIAA, Apr. 1967.
8. BOBCO, R. P.; ALLEN, G. E.; AND OTHMER, P. W.: *Local Radiation Equilibrium Temperatures in Semigray Enclosures*. *J. Spacecraft Rockets*, vol. 4, no. 8, Aug. 1967, pp. 1076-1082.
9. PLAMONDON, J. A.; AND LANDRAM, C. S.: *Radiant Heat Transfer from Nongray Surfaces with External Radiation*. *Thermophysics and Temperature Control of Spacecraft and Entry Vehicles*. Vol. 18 of *Progress in Astronautics and Aeronautics*. G. B. Heller, ed., Academic Press, 1966, pp. 173-197.
10. BEVANS, J. T.; AND EDWARDS, D. K.: *Radiation Exchange in an Enclosure with Directional Wall Properties*. *J. Heat Transfer*, vol. 87, no. 3, Aug. 1965, pp. 388-396.
11. HERING, R. G.: *Theoretical Study of Radiant Heat Exchange for Non-Gray Non-Diffuse Surfaces in a Space Environment*. Rep. No. ME-TN-036-1 (NASA CR-81653), Illinois Univ., Sept. 1966.

12. VISKANTA, RAYMOND; SCHORNHORST, JAMES R.; AND TOOR, JASWANT S.: Analysis and Experiment of Radiant Heat Exchange Between Simply Arranged Surfaces. Purdue Univ. (AFFDL-TR-67-94, DDC no. AD-655335), June 1967.
13. TOOR, J. S.: Radiant Heat Transfer Analysis Among Surfaces Having Direction Dependent Properties by the Monte Carlo Method. M.S. thesis, Purdue University, 1967.
14. HERING, R. G.: Radiative Heat Exchange Between Specularly Reflecting Surfaces With Direction-Dependent Properties. Proceedings of the Third International Heat Transfer Conference, Chicago, Ill., Aug. 7-12, 1966. Vol. 5. AIChE, 1966, pp. 200-206.
15. HOWELL, JOHN R.; AND PERLMUTTER, MORRIS: Directional Behavior of Emitted and Reflected Radiant Energy From a Specular, Gray, Asymmetric Groove. NASA TN D-1874, 1963.
16. SPARROW, E. M.; GREGG, J. L.; SZEL, J. V.; AND MANOS, P.: Analysis, Results, and Interpretation for Radiation Between Some Simply-Arranged Gray Surfaces. J. Heat Transfer, vol. 83, no. 2, May 1961, pp. 207-214.
17. ECKERT, E. R. G.; AND SPARROW, E. M.: Radiative Heat Exchange Between Surfaces With Specular Reflection. Int. J. Heat Mass Transfer, Vol. 3, No. 1, 1961, pp. 42-54.
18. BECKMANN, PETER; AND SPIZZICHINO, ANDRÉ: The Scattering of Electromagnetic Waves From Rough Surfaces. Macmillan Co., 1963.
19. DWIGHT, HERBERT B.: Tables of Integrals and Other Mathematical Data. Fourth ed., Macmillan Co., 1961, p. 230.

Chapter 6. The Monte Carlo Approach to Radiant Interchange Problems

6.1 INTRODUCTION

In chapter 5 it was found that the enclosure theory analysis became very complex when directional and spectral surface property variations were accounted for. An alternate approach that can deal with these complexities of radiation interchange is presented in this chapter; this approach is the Monte Carlo method.

Since Monte Carlo is a statistical numerical method, it is first necessary to discuss some of the concepts of statistical theory. Then the basic procedure is outlined with regard to radiative exchange; to demonstrate the method, two example problems are formulated. Because the use of Monte Carlo requires a digital computer, complete example problem solutions are not given. Only the straightforward Monte Carlo approach will be presented. The many refinements that can shorten computation time by increasing accuracy will only be mentioned in passing.

A general view of the radiation heat transfer problems solved in the literature by Monte Carlo will be given. This will further show how the method can be utilized and will provide a source for available techniques that have been developed. Much of the material presented here is taken from reference 1.

6.1.1 Definition of Monte Carlo

Herman Kahn (ref. 2) has given the following definition of the Monte Carlo method which seems to incorporate the salient ideas: "The expected score of a player in any reasonable game of chance, however complicated, can in principle be estimated by averaging the results of a large number of plays of the game. Such estimation can be rendered more efficient by various devices which replace the game with another known to have the same expected score. The new game may lead to a more efficient estimate by being less erratic, that is, having a score of lower variance or by being cheaper to play with the equipment on hand. There are obviously many problems about probability that can be viewed as problems of calculating the expected score of a game. Still more, there are problems that do not concern probability but are none the less equivalent for some purposes to the calculation of an expected score. The Monte Carlo method refers simply to the exploitation of these remarks."

This definition also provides a good outline for use of the method. Indeed, what must be done for a specific problem is to set up a game or model that obeys the same behavior and hence is expected to produce the same outcome as the physical problem which the model simulates; make the game as simple and fast to play as possible; then play the game many times and find the average outcome. After some remarks on the history of the method and on the approach being taken here to summarize and outline it, this formalism will be applied to problems in radiative heat transfer.

6.1.2 History

The history of "experimental mathematics" can be traced quite far into the past. Hammersley and Handscomb (ref. 3) give references to over 300 works dealing with Monte Carlo and closely related material published over the last six decades. They mention a determination of the value of π by a mathematical experiment performed some thousands of years ago (ref. 4). However, the great bulk of the literature has appeared since 1950.

Many early workers actually carried out numerical experiments by such means as throwing dice or playing card games many times over to determine the probability of a given outcome, but useful results from such methods awaited the unique abilities of high-speed digital computers. These machines could play simulations of the game at a high rate and thus compile accurate averages in a reasonable time.

Credit for development of Monte Carlo techniques, as they are presently used in engineering and science, goes to the extremely competent group of physicists and mathematicians who gathered at Los Alamos during the early work on nuclear weapons, including especially John von Neumann and Stanley Ulam.

6.1.3 General References

Referring to "the" Monte Carlo method is probably meaningless although such terminology will be applied. Any specific problem more likely entails "a" Monte Carlo method, as the label has been placed on a large class of loosely related techniques. A number of general books and monographs are available that detail methods and/or review the literature. A valuable early outline is given in reference 5, which is the first work to use the term "Monte Carlo" for the approach being considered here. For clarity and usefulness, both references 2 and 3 are valuable, as are the general texts by Cashwell and Everett (ref. 6); Schreider (ref. 7) (who gives 282 references, many to the foreign liter-

ature); Brown (ref. 8); and the many excellent papers gathered in the symposium volume edited by Meyer (ref. 9).

The references cited give mathematical justification for some of the methods employed in Monte Carlo. Those who cannot sleep without such reassurance are urged to read these works carefully. Here, however, it is intended to give arguments based on physical foundations, with emphasis on why the mathematical forms evolve. No attempts to provide proofs of statistical laws will be made; the standard texts in statistics carry out these proofs in detail.

Some mention should be made about the machine running time of Monte Carlo programs. No definitive method of predicting running time exists for most problems. The time used will depend, of course, on the machine used, and, perhaps, more strongly on the ability of the programmer to pick methods and shortcuts that will reduce the burden on the machine. An example of such a shortcut is the use of special subroutines for computation of such functions as sine and cosine. These routines sacrifice some accuracy to a gain in speed. If problem answers accurate to a few percent are desired, then the use of eight-place functions from a relatively slow subroutine is a needless luxury, especially if the subroutine is to be used tens of thousands of times.

Finally, only this paragraph will be devoted to the fruitless argument as to whether Monte Carlo or some other method is a "better" way of attacking a given radiation problem. Suppose that a set of integral equations must be solved simultaneously in order to obtain an analytical solution to a given physical problem. A Monte Carlo solution of a physical analog may lead to a lengthy computer run. The question facing the programmer is then: Is it better to program the solution of the integral equations by finite difference iterative techniques, with the possibility that convergence to correct solutions will not be attained because of round-off errors or instabilities, or by Monte Carlo, which, though long running, will give the answer sooner or later? In general, there can be no reply to this question. Only the background and intuition of the individual researcher can give some clue as to the most likely direction of attack. It is hoped that the following material will provide a basis for such decisions.

6.2 SYMBOLS

A	surface area
$A, B, C, D \dots$	constants
E	exchange factor including direct exchange and all reflection paths
$F_{0-\lambda}$	fraction of total energy emitted by a blackbody in wavelength range of 0 to λ

$f(\xi)$	frequency distribution of events occurring at ξ
I	total number of subsets used to compute mean
i	radiant intensity
l, m	lattice indices in square mesh corresponding to x, y positions, respectively
N	total number of sample bundles per unit time
n	individual sample index
P	probability density function
\bar{P}	mean of calculated values of P
Q	energy per unit time
R	number chosen at random from evenly distributed set of numbers in range 0 to 1, random number
S	number of events occurring at some position
T	temperature
w	energy carried by sample Monte Carlo bundle
x, y	positions in Cartesian coordinate system
α	radiative surface absorptivity
β	cone angle
γ	standard deviation defined by eq. (6-15)
$\delta, \delta', \delta''$	indices in computer program, fig. 6-7
ϵ	radiative surface emissivity
η	function defined by eq. (6-14)
θ	circumferential angle
λ	wavelength
μ	probable error
ξ	variable
σ	Stefan-Boltzmann constant

Subscripts:

b	blackbody
e	emitted
λ	spectrally dependent
1, 2	at surface 1 or 2

Superscripts:

'	quantity in one direction
"	bidirectional quantity
*	denotes dummy variable

6.3 DETAILS OF THE METHOD

6.3.1 The Random Walk

Any reader looking into the background of the material to be presented here will soon encounter the term *Markov chain*. A Markov chain is sim-

ply a chain of events occurring in sequence with the condition that the probability of each succeeding event in the chain is uninfluenced by prior events. The usual example of this is a totally inebriated gentleman who begins a walk through a strange city. At each street corner that he reaches, he becomes confused. In continuing his walk, he chooses completely at random one of the streets leading from the intersection. In fact, he may walk up and down the same block several times before he chances to move off down a new street. The history of his walk is then a Markov chain, as his decision at any point is not influenced by where he has been.

Because of the randomness of his choice at each intersection, it might be possible to simulate a sample walk by constructing a "four-holer"; that is, a roulette wheel with only four positions, each corresponding to a possible direction. The probability of the gentleman starting at his hotel bar and reaching any point in the city limits could then be found by simulating a large number of histories, using the four-holer to determine the direction of the walk at each decision point in each history.

It might be noted that the probability of the man reaching intersection (l, m) on a square grid representing the city street map is simply

$$P(l, m) = \frac{1}{4} [P(l+1, m) + P(l-1, m) + P(l, m+1) + P(l, m-1)] \quad (6-1)$$

where the factors in the square bracket are the probabilities of his being at each of the adjacent four intersections. This is because the probability of reaching $P(l, m)$ from a given adjacent intersection is one-fourth. This type of random walk is a convenient model for processes that are described by Laplace's equation; equation (6-1) is recognized as the finite difference analog of the Laplace equation.

The probability of a certain occurrence for other processes is usually not as immediately obvious as is the case for equation (6-1). More often, the probability of an event must be determined from physical constraints, and then the decision as to what event will occur is made on the basis of this probability. Some of the basic methods of choosing an event from a known probability distribution of events will now be examined. Also, means of constructing these distributions will be discussed.

6.3.2 Choosing From Probability Distributions

Consider a very poor archer firing arrows at a target with an outer radius of 10 feet. After firing many arrows, the number of arrows $F(\xi)$ that are found to have struck the target within a small radius increment $\Delta\xi$ about some radius ξ can be represented by a histogram of the frequency function $f(\xi) = F(\xi)/\Delta\xi$. A smooth curve can then be passed

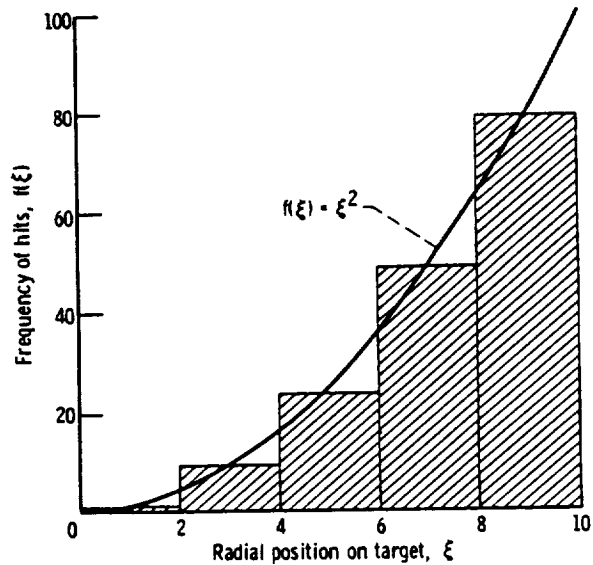


FIGURE 6-1.—Frequency distribution of arrows at various target radii.

through the histogram to give a continuous frequency distribution, perhaps similar to that of figure 6-1. What is now needed is a method for simulating further shots. This method should assign an expected radius ξ on the target to each of a group of succeeding arrows. In addition, the distribution of ξ values should correspond to the frequency distribution that the archer has previously fired as shown in figure 6-1. (It is assumed that all his arrows have hit somewhere on the target.)

This situation is analogous to that encountered in many Monte Carlo processes. The distribution of values that occurs in a given physical process is known, and a method of assigning values to individual samples is desired so that the distribution of values for all the samples will agree with the required distribution. In radiant heat transfer, for example, it is known that the distribution with wavelength of the spectral energy emitted by a blackbody must follow the Planck spectral emission curve. How are individual energy "bundles" of radiation each assigned a wavelength so that, after a large number of bundles are emitted from a blackbody, the distribution of emitted energy is indeed Planckian?

In addition, for a Markov process, the values at each step must be assigned in a random manner so that each decision in the chain is independent.

Following the archer's progress will show how this is done. The frequency curve given in figure 6-1 can, in this case, be approximated by the analytical expression

$$f(\xi) = \xi^2 \quad (6-2)$$

in the interval $0 \leq \xi \leq 10$, and $f(\xi) = 0$ elsewhere because all the arrows struck the target. Equation (6-2) is normalized by dividing by the area under the frequency curve (i.e., the total number of arrows) to obtain

$$P(\xi) = \frac{f(\xi)}{\int_0^{10} f(\xi) d\xi} = \frac{3\xi^2}{1000} \quad (6-3)$$

If the frequency with which arrows have struck the target radii is taken as the basis for estimating the locations the next set will strike, then the *probability density function* defined by equation (6-3) is the average distribution that must be satisfied by the ξ values determined by the simulation scheme. The probability density function is plotted in figure 6-2 and is interpreted physically as the proportion of values (arrows) that lie in the region $\Delta\xi$ around ξ .

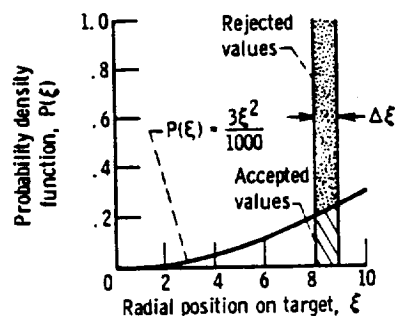


FIGURE 6-2. — Probability density function of arrows on target.

To determine ξ values, the simulation scheme can proceed as follows: Choose two *random numbers*, R_A and R_B , from a large set of numbers evenly distributed in the range 0 to 1. (How these numbers are chosen in a practical calculation is discussed in section 6.3.3.) The two random numbers are then used to select a point $(P(\xi), \xi)$ in figure 6-2 by setting $P(\xi) = R_A$ and $\xi = (\xi_{max} - \xi_{min})R_B = 10R_B$. This value of $P(\xi)$ is then compared to the value of $P(\xi)$ computed at ξ from equation (6-3). If the randomly selected value lies above the computed value of $P(\xi)$, then the randomly selected value of ξ is rejected, and two new random numbers are selected. Otherwise, the value of ξ that has been found is listed as the location that the arrow will strike. Referring again to figure 6-2, it is seen that such a procedure assures that the correct fraction of ξ values selected for use will lie in each increment $\Delta\xi$ after a

large number of completely random selections of $(P(\xi), \xi)$ is made.

The difficulty with such an event-choosing procedure is that in some cases a large portion of the ξ values may be rejected because they lie above the $P(\xi)$ curve. A more efficient method for choosing ξ is therefore desirable.

One such method is to integrate the probability density function $P(\xi)$ using the general relation

$$R(\xi) = \int_{-\infty}^{\xi} P(\xi^*) d\xi^* \quad (6-4)$$

where $R(\xi)$ can take on values only in the range 0 to 1 because the integral under the entire $P(\xi)$ curve is unity according to equation (6-3). Equation (6-4) is the general definition of the *cumulative distribution function*. A plot of R against ξ from equation (6-4) shows the probability of an event occurring in the range $-\infty$ to ξ . For the method given here, the function R is taken to be a random number; each value of ξ is then obtained by choosing an R value at random and using the functional relation $R(\xi)$ to determine the corresponding value of ξ . To show that the probability density of ξ formed in this way corresponds to the required $P(\xi)$, the probability density function of figure 6-2 can be used as an illustrative example. Inserting the example $P(\xi)$ of equation (6-3) into equation (6-4) and noting that $P(\xi) = 0$ for $-\infty < \xi < 0$ give

$$R = \int_0^{\xi} P(\xi^*) d\xi^* = \frac{\xi^3}{1000} \quad 0 \leq R \leq 1 \quad (6-5)$$

Equation (6-5) is shown plotted in figure 6-3.

Now it will be shown that choosing R at random and determining a corresponding value of ξ from equation (6-5) is equivalent to taking the derivative of the cumulative distribution function and that this derivative is, by examination of equations (6-5) and (6-3), simply $P(\xi)$. Divide the range of ξ into a number of equal increments $\Delta\xi$. Suppose that M values of R are now chosen in the range 0 to 1 and that these M values are chosen at equal intervals along R . There will be M values of ξ which correspond to these M values of R . The fraction of the M values of ξ which occurs per given increment $\Delta\xi$ is then $M_{\Delta\xi}/M = \Delta R$ which gives

$$\frac{\left(\frac{M_{\Delta\xi}}{M}\right)}{\Delta\xi} = \frac{\Delta R}{\Delta\xi} \quad (6-6)$$

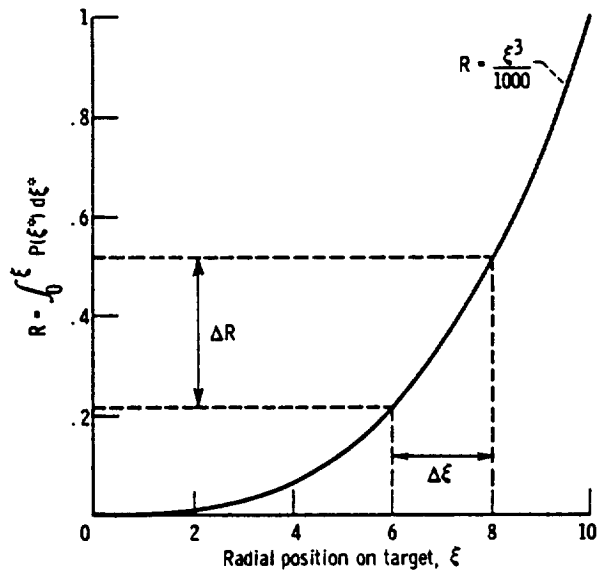


FIGURE 6-3. — Cumulative distribution of arrows on target.

The quantity $\Delta R/\Delta \xi$ approaches $dR/d\xi$ if a large enough value is used for M and small increments $\Delta \xi$ are examined. But $dR/d\xi$ can be seen from equations (6-5) and (6-3) to be simply $P(\xi)$; therefore, by obtaining values of ξ as described preceding equation (6-5), the required probability distribution is indeed generated.

Often physical problems arise in which the frequency distribution depends on more than one variable. For example, if the archer discussed previously suffered from astigmatism, then a dependence on circumferential angle θ might appear in the distribution of arrows on the target in addition to the dependence on radius. If the interdependence of the variables is such that the frequency distribution can be factored into a product form, then the following can be written:

$$f(\xi, \theta) = g(\xi)h(\theta) \tag{6-7}$$

and values of $P(\xi)$ and $P(\theta)$ can be found by integrating out each variable in turn to give

$$\begin{aligned}
 P(\xi) &= \frac{\int_{\theta_{\min}}^{\theta_{\max}} f(\xi, \theta) d\theta}{\int_{\xi_{\min}}^{\xi_{\max}} \int_{\theta_{\min}}^{\theta_{\max}} f(\xi, \theta) d\theta d\xi} = \frac{f(\xi) \int_{\theta_{\min}}^{\theta_{\max}} f(\theta) d\theta}{\int_{\xi_{\min}}^{\xi_{\max}} f(\xi) d\xi \int_{\theta_{\min}}^{\theta_{\max}} f(\theta) d\theta} \\
 &= \frac{f(\xi)}{\int_{\xi_{\min}}^{\xi_{\max}} f(\xi) d\xi} \quad (6-8)
 \end{aligned}$$

and similarly,

$$P(\theta) = \frac{\int_{\xi_{\min}}^{\xi_{\max}} f(\xi, \theta) d\xi}{\int_{\theta_{\min}}^{\theta_{\max}} \int_{\xi_{\min}}^{\xi_{\max}} f(\xi, \theta) d\xi d\theta} = \frac{f(\theta)}{\int_{\theta_{\min}}^{\theta_{\max}} f(\theta) d\theta} \quad (6-9)$$

The methods given previously in this section are used to evaluate ξ and θ independently of one another after choosing two random numbers.

If $f(\xi, \theta)$ cannot be placed in the form of equation (6-7) (i.e., if there are no independent $g(\xi)$ and $h(\theta)$), then it can be shown (refs. 2 and 7) that ξ and θ values can be determined by choosing two random numbers R_ξ and R_θ . Note that

$$P(\xi, \theta) = \frac{f(\xi, \theta)}{\int_{\xi_{\min}}^{\xi_{\max}} \int_{\theta_{\min}}^{\theta_{\max}} f(\xi, \theta) d\theta d\xi}$$

Then ξ and θ are found from the equations

$$R_\xi = \int_{-\infty}^{\xi} \int_{\theta_{\min}}^{\theta_{\max}} P(\xi^*, \theta) d\theta d\xi^* \quad (6-10)$$

and

$$R_\theta = \int_{-\infty}^{\theta} P(\theta^*, \xi = \text{fixed}) d\theta^* \quad (6-11)$$

where ξ in equation (6-11) is that value obtained from equation (6-10). This procedure may be extended to any number of variables. Equations (6-10) and (6-11) define the *marginal* and *conditional* distributions of $P(\xi, \theta)$, respectively.

6.3.3 Random Numbers

6.3.3.1 *Definition of random numbers.*—Formally, a random number can be taken here as a number chosen without sequence from a large set of numbers spaced at equivalued intervals in the range 0 to 1. If the numbers 0, 0.01, 0.02, 0.03, . . . 0.99, 1.00 are placed on slips of paper and then the jumbled slips are placed in a hat, there would be fair assurance that, if a few numbers are picked, they will be random numbers. If many choices are to be made, then perhaps smaller intervals (more slips) should be used; after it is drawn, each slip should be replaced and randomly mixed in the hat.

For a typical computer problem, random numbers might be needed for 10^5 or more decisions. It is desirable that the numbers be obtained in a rapid way and that the numbers chosen be truly random.

6.3.3.2 *How random numbers are generated.*—On the modern digital computer, it is impractical to fit a mechanical arm and an optical scanner to choose and interpret slips pulled from a hat. To give truly random numbers, one possibility would be to sample a truly random process. Such phenomena as noise in an electronic circuit or radioactive decay particle counts per unit time have been tried, but in the main they are found to be too slow for direct computer linkage.

A second means is to obtain or generate tables of random numbers (refs. 10 and 11) perhaps by one of the processes mentioned previously, and then enter these tables in the computer memory. This allows rapid access to random numbers, but for complex problems requiring a large quantity of random numbers, the required storage space becomes prohibitive. This method has been widely used, however, when a modest problem is to be solved.

The most widely practiced method at present for obtaining random numbers for a digital computer is a pseudorandom number generator. This is simply a subroutine that exploits the apparent randomness of groups of digits in large numbers. One simple example of such a routine is to take an 8-digit number, square it, and then choose the middle 8 digits of the resulting 16-digit number as the required random number. When a new random number is needed, the previous random number is squared, and the new random numbers is taken as the middle 8 digits of the result. This process is said by Schreider (ref. 7) to degenerate after a few thousand cycles by propagating to an all-zero number.

A more satisfactory routine used at the Lewis Research Center of NASA is based on suggestions in reference 12. Here a random number is generated by taking the low order 36 bits of the product $R_{n-1}K$, where $K=5^{15}$ and R_{n-1} is the previously computed random number. The subroutine is started by taking $R_0=1$, or the programmer may

give R_0 an arbitrary value. By always starting a given program with the same R_0 , it is possible to check solutions through step-by-step tracing of a few histories.

6.3.3.3 *How the numbers are made sufficiently random.*—The fact that such subroutines generate pseudorandom numbers immediately raises a danger flag. How can it be established that such pseudorandomness is sufficiently random for the problem being treated? Does the sequence repeat; if so, after how many numbers? Certain standard tests exist that give partial answers to these questions, and a full discussion of them is given in references 3, 12, and 13. None of these tests is sufficient to establish randomness, although passage of them is necessary. Kendall and Smith (ref. 13) describe four such tests. The names they ascribe give the flavor of the methods: the frequency test, the serial test, the poker test, and the gap test. These tests are described as “. . . useful and searching. They are, however, not sufficient. . . .”

Perhaps the safest course to follow is to obtain a standard subroutine whose properties have been established by such tests and use it only within its proven limits. The applicability of a given pseudorandom number generator can be checked to some extent by generating the mean of some known distributions appearing in the problem at hand, and comparing the results with analytically determined means.

6.3.4 Evaluation of Error

Because the solutions obtained by Monte Carlo are averages over the results of a number of individual samples, they will, in general, contain fluctuations about a mean value. As in any process of this type, the mean can be more accurately determined by increasing the number of values used in determining the mean. Although it is not possible to ascribe a 100-percent confidence in the value obtained, such confidence can be approached as closely as desired if the budget for computer time can stand the strain. More generally, some ad hoc rules of economy and an estimate of desired accuracy to a given problem can be applied, and solutions can be obtained by trading off within these limits.

To establish the accuracy of the solutions, one of the following tests can be applied. For example, suppose it is desired to know the probability of the randomly staggering attendee of an engineering convention (who was discussed in section 6.3.1) reaching a certain bar at the city limits. To determine his success exactly, an infinite number of hypothetical engineers would have to be followed and the probability $P(l, m)$ of reaching the boundary point (l, m) would be determined as

$$P(l, m) = \left[\frac{S(l, m)}{N} \right]_{N \rightarrow \infty} \quad (6-12)$$

where $S(l, m)/N$ is the number of samples $S(l, m)$ reaching the boundary point divided by the total number of samples N . Obviously, following an infinite number of samples would not be economical, and a probability would be computed based on some finite number of samples N , of order perhaps 10^2 to 10^6 . Then an estimate is needed of the error μ involved in approximating infinity by these relatively small sample sizes.

For a sample size greater than about $N=20$, it is found (refs. 3 and 7), from application of the "central limit theorem" and the relations governing normal probability distributions, that the following relation holds whenever the samples S in question can be considered to leave a source and either reach a scoring position with probability P or not reach it with probability $1-P$. The probability that the average $S(l, m)/N$ for finite N differs by less than some value μ from $[S(l, m)/N]_{N \rightarrow \infty}$ is given by

$$P \left[\left| \frac{S}{N} - \left(\frac{S}{N} \right)_{N \rightarrow \infty} \right| \leq \mu \right] = \frac{2}{\sqrt{\pi}} \int_0^{\eta/\sqrt{2}} \exp(-\eta^{*2}) d\eta^* \\ = \text{erf}(\eta/\sqrt{2}) \quad (6-13)$$

where

$$\eta \approx \mu \left\{ \frac{N}{\left[\left(\frac{S}{N} \right) \left(1 - \frac{S}{N} \right) \right]} \right\}^{1/2} \quad (6-14)$$

Compilations of the error function (erf) are given in many standard reference tables (refs. 14 and 15).

In many problems, such an error estimation procedure cannot be applied because the samples do not originate from a single source. For example, the radiative energy flux at a point on the boundary of an enclosure may depend on the energy arriving from many sources. For such situations, the most straightforward way of estimating the error in a result (such as the error in radiative heat flux at a point) is to subdivide the calculation of the desired statistical mean result into a group of I submeans. The "central limit theorem" then applies. This theorem states that the statistical fluctuations in the submeans are distributed in a normal or Gaussian distribution about the overall mean. For such a distribution, a measure of the fluctuations in the means can be calculated. This measure is called the variance. For example, if 200 samples are examined, a mean result \bar{P} is calculated on the basis of 200 samples, and 20 submeans P_1, P_2, \dots, P_I of 10 samples each are calculated. Then the variance γ^2 of the mean solution \bar{P} is given by

$$\gamma^2 = \frac{1}{I-1} \left[\sum_{i=1}^I (P_i - \bar{P})^2 \right] = \frac{1}{I-1} \left[\sum_{i=1}^I P_i^2 - \frac{\left(\sum_{i=1}^I P_i \right)^2}{I} \right] \quad (6-15)$$

This variance is an estimate of the mean square deviation of the sample mean \bar{P} from the true mean, where the true mean would be obtained by using an infinite number of samples. From the properties of the normal frequency distribution, which the fluctuations in the results computed by Monte Carlo will in general follow, it is shown in most texts on statistics that the probability of the sample mean \bar{P} lying within $\pm \gamma$ of the true mean is about 68 percent, of lying within $\pm 2\gamma$ is about 95 percent, and of lying within $\pm 3\gamma$ is 99.7 percent.

Another measure of the statistical fluctuations in the mean is γ , the *standard deviation*. Because γ is given by the square root of equation (6-15), it is evident that in order to reduce γ by half, the number of samples which are used in computing the results must be quadrupled (thereby quadrupling I for constant submean size). This probably means quadrupling the computer time involved unless the term in brackets can somehow be reduced by decreasing the variance (scatter) of the individual submeans. Much time and ingenuity have been expended in attempts at the latter, under such labels as "stratified sampling," "splitting," and "importance sampling." These and other variance-reducing techniques are discussed in references 3 and 7. The savings in computer time available from application of these techniques is abundant reward for their study, and the reader who intends to use Monte Carlo for any problem of significant complexity is urged to apply them.

6.4 APPLICATION TO THERMAL RADIATIVE TRANSFER

6.4.1 Introduction

As discussed in chapters 4 and 5, the formulation of radiation exchange heat balances in enclosures leads to integral equations for the unknown surface temperature or heat flux distributions. Integral equations also result when considering radiation exchange within a radiating medium such as a gas. These equations can be quite difficult to solve and are a consequence of using a "macroscopic" viewpoint when deriving the heat flow quantities. By invoking a probabilistic model of the radiative exchange process and applying Monte Carlo sampling techniques, it is possible to utilize a "semimacroscopic"³ approach and avoid many of the difficulties inherent in the averaging processes of the usual integral equation formulations. In this way, actions of small parts of the total energy can be examined on an individual basis, rather than attempting to solve simultaneously for the entire behavior of all the energy involved. A microscopic type of model for the radiative exchange process will be examined; then the solution of two examples will be outlined.

³ Or, perhaps, "semimicroscopic."

6.4.2 Model of the Radiative Exchange Process

In engineering radiation calculations, the usual quantities of interest are the local temperatures and energy fluxes. It seems reasonable to model the radiative exchange process by following the progress of discrete amounts ("bundles") of energy since local energy flux is then easily computed as the number of these energy "bundles" arriving per unit area and time at some position. The obvious bundle to visualize is the photon, but the photon has a disadvantage as a basis for a model; its energy depends on its wavelength, which would introduce a needless complication. Therefore, a model particle is devised that is more convenient. This is the "photon bundle," which is a bundle carrying a given amount of energy w ; it can be thought of as a group of photons bound together. For spectral problems where the wavelength of the bundle is specified, enough photons of that wavelength are grouped together to make the energy of the bundle equal to w .

By assigning equal energies to all photon bundles, local energy flux is computed by counting the number of bundles arriving at a position of interest per unit time and per unit area and multiplying by the energy of the bundle. The bundle paths and histories are computed by the Monte Carlo method as will now be demonstrated by an example problem.

6.4.3 Sample Problem

For an example, look at a simple problem outlined in reference 16 and examine the energy radiated from element dA_1 at temperature T_1 that is absorbed by an infinite plane A_2 at temperature $T_2 = 0$ (see fig. 6-4). Let element dA_1 have emissivity

$$\epsilon'_{\lambda, 1} = \epsilon'_{\lambda, 1}(\lambda, \beta_1, T_1) \quad (6-16)$$

let area 2 have emissivity

$$\epsilon'_{\lambda, 2} = \epsilon'_{\lambda, 2}(\lambda, \beta_2, T_2) \quad (6-17)$$

and assume only that the emissivity of both surfaces is independent of circumferential angle θ .

For surface element dA_1 , the total emitted energy per unit time is

$$dQ_{e, 1} = \epsilon_1(T_1) \sigma T_1^4 dA_1 \quad (6-18)$$

where $\epsilon_1(T_1)$ is the hemispherical total emissivity given in this case by (eq. (3-6a) of Vol. I)

$$\epsilon_1(T_1) = \frac{\int_0^\infty \int_{\Omega} \epsilon'_{\lambda,1}(\lambda, \beta_1, T_1) i'_{\lambda b,1}(\lambda, T_1) \cos \beta d\omega d\lambda}{\sigma T_1^4} \quad (6-19)$$

where $i'_{\lambda b,1}(\lambda, T_1)$ is the Planck spectral distribution of blackbody radiant intensity at T_1 .

If it is assumed that $dQ_{e,1}$, the total energy emitted per unit time by dA_1 , is composed of N energy bundles emitted per unit time, then the energy assigned to each bundle is

$$w = \frac{dQ_{e,1}}{N} \quad (6-20)$$

To determine the energy radiated from element dA_1 that is absorbed by surface A_2 , follow N bundles of energy after their emission from dA_1 and determine the number S_2 absorbed at A_2 . If the energy reflected from A_2 back to dA_1 and then rereflected to A_2 is neglected, the energy transferred per unit time from dA_1 to A_2 will be

$$dQ_{1-\text{absorbed by } 2} = wS_2 = \frac{\epsilon_1(T_1)\sigma T_1^4 dA_1}{N} S_2 \quad (6-21)$$

The next question is how to determine the path direction and wavelength that is assigned to each bundle. This must be done in such a way that the directions and wavelengths of the N bundles conform to the constraints given by the emissivity of the surface and the laws governing radiative processes. For example, if wavelengths are assigned to N bundles, the spectral distribution of emitted energy generated by the Monte Carlo process (comprised of the energy $wN_\lambda \Delta\lambda$ for discrete intervals $\Delta\lambda$) must closely approximate the spectrum of the actual emitted energy (plotted as $\pi\epsilon_{\lambda,1} i'_{\lambda b,1} d\lambda$ against λ). To assure this, the methods of section 6.3.2 are applied.

The energy emitted by element dA_1 per unit time in the wavelength interval $d\lambda$ about a wavelength λ and in the angular interval $d\beta_1$ about β_1 is

$$d^3Q'_{\lambda e,1}(\lambda, \beta_1) = 2\pi\epsilon'_{\lambda,1}(\lambda, \beta_1, T_1) i'_{\lambda b,1}(\lambda, T_1) \cos \beta_1 dA_1 \sin \beta_1 d\beta_1 d\lambda \quad (6-22)$$

The total energy emitted by dA_1 per unit time is given by equation (6-18). The probability $P(\lambda, \beta_1) d\beta_1 d\lambda$ of emission in a wavelength interval about λ and in an angular interval around β_1 is then the energy in $d\beta_1 d\lambda$

(eq. (6-22)) divided by the total emitted energy (eq. (6-18))

$$\begin{aligned}
 P(\lambda, \beta_1) d\beta_1 d\lambda &= \frac{d^2 Q'_{\lambda e, 1}(\lambda, \beta_1)}{dQ_{e, 1}} \\
 &= \frac{2\pi \epsilon'_{\lambda, 1}(\lambda, \beta_1) i'_{\lambda b, 1}(\lambda) \cos \beta_1 \sin \beta_1 d\beta_1 d\lambda}{\epsilon_1 \sigma T_1^4} \quad (6-23)
 \end{aligned}$$

(The T_1 in the functional notation has been dropped for simplicity.)

It is assumed here for simplicity that the directional-spectral emissivity is a product function of the variables, angle and wavelength, that is,

$$\epsilon'_\lambda(\lambda, \beta_1) = \Phi_1(\lambda) \Phi_2(\beta_1) \quad (6-24)$$

This assumption is probably not valid for many real surfaces since, in general, the angular distribution of emissivity depends on wavelength as shown, for example, by figure 5-1 of Vol. I. For the assumed form in equation (6-24), it follows that the emissivity dependence on either variable may be found by integrating out the other variable (see eq. (6-9)). Then the normalized probability of emission occurring in the interval $d\lambda$ is

$$\begin{aligned}
 P(\lambda) d\lambda &= d\lambda \int_0^{\pi/2} P(\lambda, \beta_1) d\beta_1 \\
 &= \frac{2\pi d\lambda \int_0^{\pi/2} \epsilon'_{\lambda, 1}(\lambda, \beta_1) i'_{\lambda b, 1}(\lambda) \sin \beta_1 \cos \beta_1 d\beta_1}{\epsilon_1 \sigma T_1^4} \quad (6-25a)
 \end{aligned}$$

Substituting into equation (6-4) and noting that $P(\lambda) d\lambda$ is zero in the range $-\infty < \lambda < 0$ give

$$R_\lambda = \frac{2\pi \int_0^\lambda \int_0^{\pi/2} \epsilon'_{\lambda, 1}(\lambda^*, \beta_1) i'_{\lambda b, 1}(\lambda^*) \sin \beta_1 \cos \beta_1 d\beta_1 d\lambda^*}{\epsilon_1 \sigma T_1^4} \quad (6-25b)$$

where the asterisk denotes a dummy variable of integration. If the number of bundles N is very large and this equation is solved for λ each time a random R_λ value is chosen, the computing time becomes too large for practical calculations. To circumvent this difficulty, equations like equation (6-25b) can be numerically integrated once over the range of λ values and a curve can be fitted to the result. A polynomial approximation

$$\lambda = A + BR_\lambda + CR_\lambda^2 + \dots \quad (6-26)$$

is often adequate. Equation (6-26) rather than equation (6-25b) is used in the problem-solving program.

Following a similar procedure for the variable cone angle of emission β_1 gives the relation

$$R_{\beta_1} = \int_0^{\beta_1} \int_0^\infty P(\beta_1^*, \lambda) d\lambda d\beta_1^* \\ = \frac{2\pi \int_0^{\beta_1} \int_0^\infty \epsilon'_{\lambda,1}(\lambda, \beta_1^*) i'_{\lambda b,1}(\lambda) \sin \beta_1^* \cos \beta_1^* d\lambda d\beta_1^*}{\epsilon_1 \sigma T_1^4} \quad (6-27)$$

which is curve fit to give

$$\beta_1 = D + ER_{\beta_1} + FR_{\beta_1}^2 + \dots \quad (6-28)$$

If dA_1 is a diffuse-gray surface, equation (6-25b) reduces to

$$R_{\lambda, \text{diffuse-gray}} = \frac{\pi \int_0^\lambda i'_{\lambda b,1}(\lambda^*) d\lambda^*}{\sigma T_1^4} = F_{0-\lambda} \quad (6-29)$$

where $F_{0-\lambda}$ is the fraction of blackbody emission in the wavelength interval 0 to λ . Equation (6-27) for this case reduces to

$$R_{\beta_1, \text{diffuse-gray}} = 2 \int_0^{\beta_1} \sin \beta_1^* \cos \beta_1^* d\beta_1^* = \sin^2 \beta_1 \quad (6-30a)$$

or

$$\sin \beta_1 = \sqrt{R_{\beta_1, \text{diffuse-gray}}} \quad (6-30b)$$

The point to be made here is that computational difficulty is not greatly different in obtaining λ from either equation (6-26) or (6-29), nor is it much different for obtaining β_1 from either equation (6-28) or (6-30b). The difference between the nondiffuse-nongray case and the diffuse-gray case is mainly in the auxiliary numerical integrations of equations (6-25b) and (6-27). These integrations are performed once to obtain the curve fits; then as far as the main problem-solving program is concerned, the more difficult case might just as well be handled. Thus, increasing problem complexity leads to only gradual increases in the complexity of the Monte Carlo program and similar gradual increases in computer time.

For emission of an individual energy bundle from surface dA_1 , a wave-

length λ can be obtained from equation (6-26), and a cone angle of emission β_1 can be obtained from equation (6-28) by choosing two random numbers R_λ and R_{β_1} . To define the bundle path, there remains only specification of the circumferential angle θ_1 . Because of the assumption made earlier that emission does not depend on θ_1 , it is shown by the formalism outlined and is also fairly obvious from intuition that θ_1 can be determined by

$$\theta_1 = 2\pi R_{\theta_1} \quad (6-31)$$

where R_{θ_1} is again a random number chosen from the range between 0 and 1.

Because the position of plane A_2 with respect to dA_1 is known, it is a simple matter to determine whether a given energy bundle will strike A_2 after leaving dA_1 in direction (β_1, θ_1) . (It will hit A_2 whenever $\cos \theta_1 \geq 0$ as shown in fig. 6-4.) If it misses A_2 , another bundle must be emitted

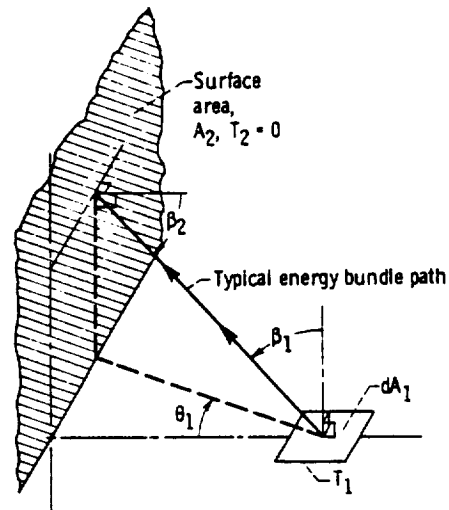


FIGURE 6-4. — Radiant interchange between two surfaces.

from dA_1 . If the bundle strikes A_2 , it must be determined whether it is absorbed or reflected. To do this, the geometry is used to find the angle of incidence β_2 of the bundle on A_2 , that is,

$$\cos \beta_2 = \sin \beta_1 \cos \theta_1 \quad (6-32)$$

Knowing the absorptivity of A_2 from Kirchhoff's law

$$\alpha'_{\lambda, 2}(\lambda, \beta_2) = \epsilon'_{\lambda, 2}(\lambda, \beta_2) \quad (6-33)$$

and having determined the wavelength λ of the incident bundle from equation (6-26) and the incident angle β_2 from equation (6-32), the probability of absorption of the bundle at A_2 can be determined. The probability of absorption is simply the absorptivity of A_2 evaluated at β_2 and λ . This follows from the definition of directional-spectral absorptivity $\alpha'_{\lambda, 2}(\lambda, \beta_2)$ as the fraction of energy incident on A_2 in a given wavelength interval and within a given solid angle that is absorbed by the surface. This is also a precise definition of the probability of absorption of an individual bundle. The absorptivity is therefore the probability density function for the absorption of incident energy. It is now easy to determine whether a given incident energy bundle is absorbed by comparing the surface absorptivity $\alpha'_{\lambda, 2}(\lambda, \beta_2)$ with a random number R_o . If

$$R_o \leq \alpha'_{\lambda, 2}(\lambda, \beta_2) \quad (6-34)$$

the bundle of energy is absorbed and a counter S_2 in the computer memory is increased by one to keep account of the absorbed bundles. Otherwise, the bundle is assumed to be reflected and is not further accounted for. If the bundle path were followed further, rereflections from dA_1 would have to be considered. The neglect of rereflections is reasonable if the absorptivity of A_2 is large, or if the directional reflectivity is such that few bundles are reflected back along the direction of incidence. If such reflections cannot be neglected, angles of reflection must be chosen from known directional reflectivities, and the bundle is followed further along its path until it is absorbed by A_2 or lost from the system. For the purposes of this example, little is to be gained by following the bundle after reflection from surface A_2 because the derivation of the necessary relations is similar to that already presented.

A new bundle is now chosen at dA_1 , and its history is followed. This procedure is continued until N bundles have been emitted from dA_1 . The energy absorbed at A_2 is then calculated from equation (6-21).

The derivation of the equations needed for solution of the example is now complete. In putting together a flow chart to aid in formulating a computer program (fig. 6-5), some methods for shortening machine computing time can be invoked. For example, the angle θ_1 is computed first. If the bundle is not going to strike A_2 on the basis of the calculated θ_1 , there is no point in computing λ and β_1 for that bundle. Alternately, because θ_1 values are isotropically distributed, it can be noted that exactly half the bundles must strike A_2 . Therefore, the calculated θ_1 values can be constrained to the range $-\pi/2 < \theta_1 < \pi/2$.

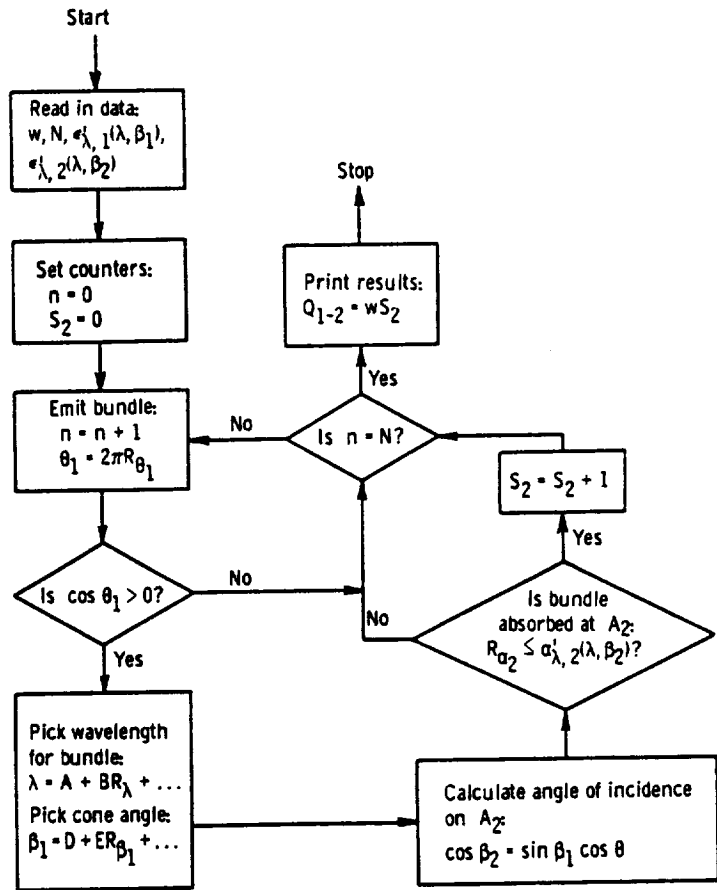


FIGURE 6-5. —Computer flow diagram for example radiant interchange problem.

The formulation of this problem for a Monte Carlo solution is now complete. An astute observer will note that this example could be solved without much trouble by standard integral methods. A more astute observer might note further that extension to only slightly more difficult problems would cause serious consequences for the standard treatments. For example, consider introducing a third surface with directional properties into the problem and accounting for all interactions.

6.4.4 Useful Functions

A number of useful relations for choosing angles of emission and assigning a wavelength to bundles are given in the previous section. These and other functions from the literature dealing with radiative transfer are summarized in table 6-I.

TABLE 6-1.—CONVENIENT FUNCTIONS RELATING RANDOM NUMBERS TO VARIABLES FOR EMISSION (ASSUMING NO DEPENDENCE ON CIRCUMFERENTIAL ANGLE θ)

Variable	Type of emission	Relation
Cone angle β	Diffuse	$\sin \beta = R_{\beta}^{1/2}$
	Directional gray	$R_{\beta} = \frac{2 \int_0^{\beta} \epsilon'(\beta^*) \sin \beta^* \cos \beta^* d\beta^*}{\epsilon}$
	Directional nongray	$R_{\beta} = \frac{2\pi \int_0^{\beta} \int_0^{2\pi} \epsilon_{\lambda}'(\beta^*, \lambda) i_{\lambda,b}(\lambda) \sin \beta^* \cos \beta^* d\lambda d\beta^*}{\epsilon \sigma T^4}$
Circumferential angle θ	Diffuse	$\theta = 2\pi R_{\theta}$
Wavelength λ	Black or gray	$F_{0-\lambda} = R_{\lambda}$
	Nongray diffuse	$R_{\lambda} = \frac{\pi \int_0^{\lambda} \epsilon_{\lambda}(\lambda^*) i_{\lambda,b}(\lambda^*) d\lambda^*}{\epsilon \sigma T^4}$
	Nongray directional	$R_{\lambda} = \frac{2\pi \int_0^{\lambda} \int_0^{\pi/2} \epsilon_{\lambda}'(\beta, \lambda^*) i_{\lambda,b}(\lambda^*) \sin \beta \cos \beta d\beta d\lambda^*}{\epsilon \sigma T^4}$

EXAMPLE 6-1: A wedge is made up of two very long parallel sides of equal width joined at an angle of 90° , as shown in figure 6-6. The surface temperatures are $T_1 = 1000^\circ \text{K}$ and $T_2 = 2000^\circ \text{K}$. The effects of the ends may be neglected. Surface 1 is diffuse-gray with an emissivity of 0.5, while the properties of surface 2 are directional-gray with directional-total emissivity and absorptivity given by

$$\epsilon_2'(\beta_2) = \alpha_2'(\beta_2) = 0.5 \cos \beta_2 \quad (6-35)$$

Assume for simplicity that surface 2 reflects diffusely. Set up a Monte Carlo flow sheet for determining the energy to be added to each surface

in order to maintain its temperature. Assume that the environment is at $T=0^\circ$ K.

The energy flux emitted by surface 1 is

$$q_{e,1} = \epsilon_1 \sigma T_1^4$$

If N_1 -emitted sample energy bundles are to be followed per unit time and area from surface 1, then the amount of energy per bundle will be

$$w = \frac{q_{e,1}}{N_1} = \frac{\epsilon_1 \sigma T_1^4}{N_1} \quad (6-36)$$

The energy flux emitted from surface 2 is

$$\begin{aligned} q_{e,2} &= 2\sigma T_2^4 \int_0^{\pi/2} \epsilon'_2(\beta) \cos \beta \sin \beta \, d\beta \\ &= \sigma T_2^4 \int_0^{\pi/2} \cos^2 \beta \sin \beta \, d\beta = \frac{\sigma T_2^4}{3} \end{aligned}$$

If the same amount of energy w is assigned to each bundle emitted by wall 2 as was used for wall 1, then

$$wN_2 = \frac{\sigma T_2^4}{3}$$

Substituting equation (6-36), the value of ϵ_1 , and the known surface temperatures gives

$$N_2 = \frac{\sigma T_2^4}{3} \frac{N_1}{\epsilon_1 \sigma T_1^4} = \frac{32}{3} N_1 \quad (6-37)$$

Because each bundle has equal energy and $32/3$ as many bundles are emitted from surface 2 as from surface 1, it is obvious that surface 2 will make the major contribution to the energy transfer.

Now the distributions of directions for emitted bundles from the two surfaces will be derived. Surface 1 emits diffusely, so that equation (6-30b) applies. For surface 2, however, equation (6-27) must be used. Substituting equation (6-35) into equation (6-27) gives, for the directional-gray case,

$$R_{\beta_2} = \frac{2\pi i'_{b,2} \int_0^{\beta_2} (0.5 \cos \beta_2^*) \sin \beta_2^* \cos \beta_2^* \, d\beta_2^*}{\epsilon_2 \sigma T_2^4}$$

The hemispherical total emissivity is substituted from equation (6-19) to give

$$R_{\beta_2} = \frac{\int_0^{\beta_2} \cos^2 \beta_2^* \sin \beta_2^* d\beta_2^*}{\int_0^{\pi/2} \cos^2 \beta_2 \sin \beta_2 d\beta_2} = 1 - \cos^3 \beta_2$$

The fact that R and $1 - R$ are both uniform random distributions in the range $0 \leq R \leq 1$ can be used to write this as

$$\cos \beta_2 = R_{\beta_2}^{1/3}$$

Note that, by similar reasoning, equation (6-30b) can be written

$$\cos \beta_1 = R_{\beta_1}^{1/2}$$

Since there is no dependence on angle θ for either surface, equation (6-31) applies for both surfaces.

The distributions of directions at which bundle emission will occur has now been determined. Next, the position on each surface from which

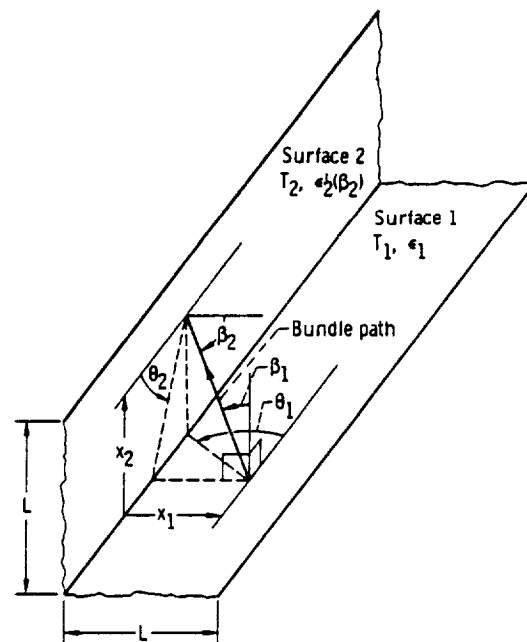


FIGURE 6-6. — Geometry of example 6-1.

each bundle will be emitted must be determined. Because the wedge sides are isothermal, the emission from a given side will be uniform. In such a case, random positions x (fig. 6-6) on a given side could be picked as points of emission. Such a procedure requires generation of a random number. The computer time required to generate a random number can be saved by noting that the bundle emission is the initial process in each Monte Carlo history; hence, there is no prior history to be eliminated by using a random number. In this case, x positions along L can be sequentially chosen as

$$x = \frac{n}{N} L$$

where n is the sample history index for the history being begun, $1 \leq n \leq N$.

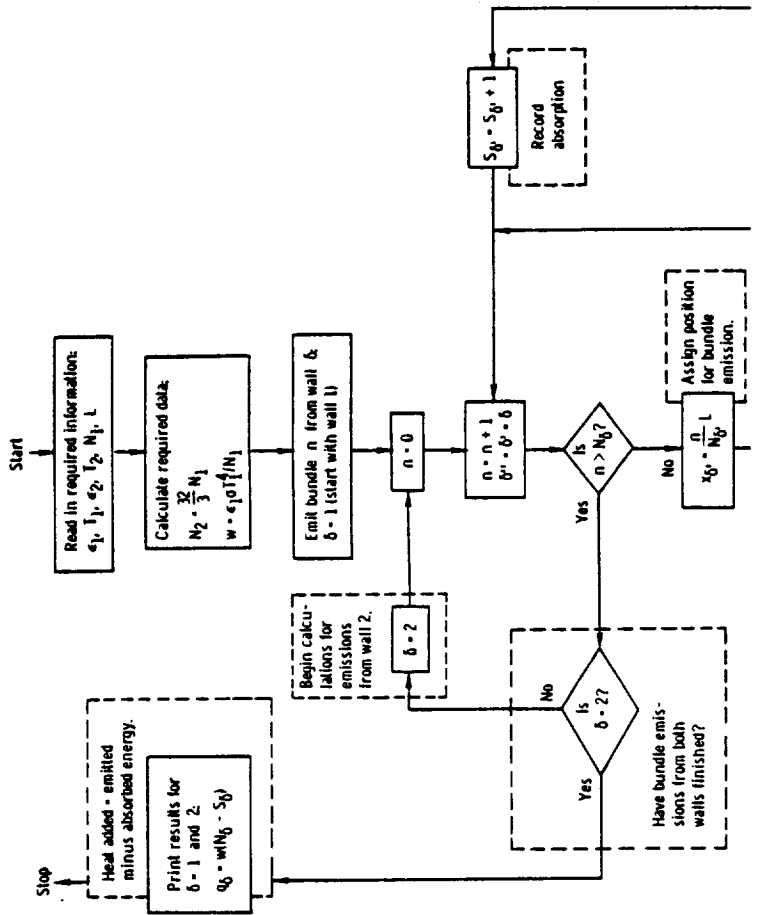
The point of emission and direction of emission for each bundle leaving either surface can now be determined. The remaining calculations involve determination of whether the emitted bundles will strike the adjacent wall or will leave the cavity. Examination of figure 6-6 shows that, for either surface, when $\pi \leq \theta \leq 2\pi$, the bundles will leave the cavity for any β , and when $0 < \theta < \pi$, they will leave if

$$\sin \beta < \frac{\frac{x}{\sin \theta}}{\left[\left(\frac{x}{\sin \theta}\right)^2 + L^2\right]^{1/2}} = \frac{1}{\left[1 + \left(\frac{L \sin \theta}{x}\right)^2\right]^{1/2}}$$

The angle of incidence β_i on a surface is given in terms of the angles β_s and θ_s at which the bundle leaves the other surface by

$$\cos \beta_i = \sin \beta_s \sin \theta_s$$

All the necessary relations are now at hand. Now a flow diagram is constructed to combine these relations in the correct sequence. Diffuse reflection is assumed from both surfaces. The resulting flow diagram is shown in figure 6-7. Study of this figure will show one way of constructing the flow of events for the problem at hand. The use of the indices δ , δ' , and δ'' is an artifice to reduce the size of the chart. The index δ always refers to the wall from which the original emission of the bundle occurred, and δ' refers to the wall from which emission or reflection is presently occurring. The index δ'' is used to make the emitted distribution of β angles correspond to either $R_{\beta_1}^{1/2}$ or $R_{\beta_2}^{1/2}$ and have all the reflected bundles correspond to a diffuse distribution.



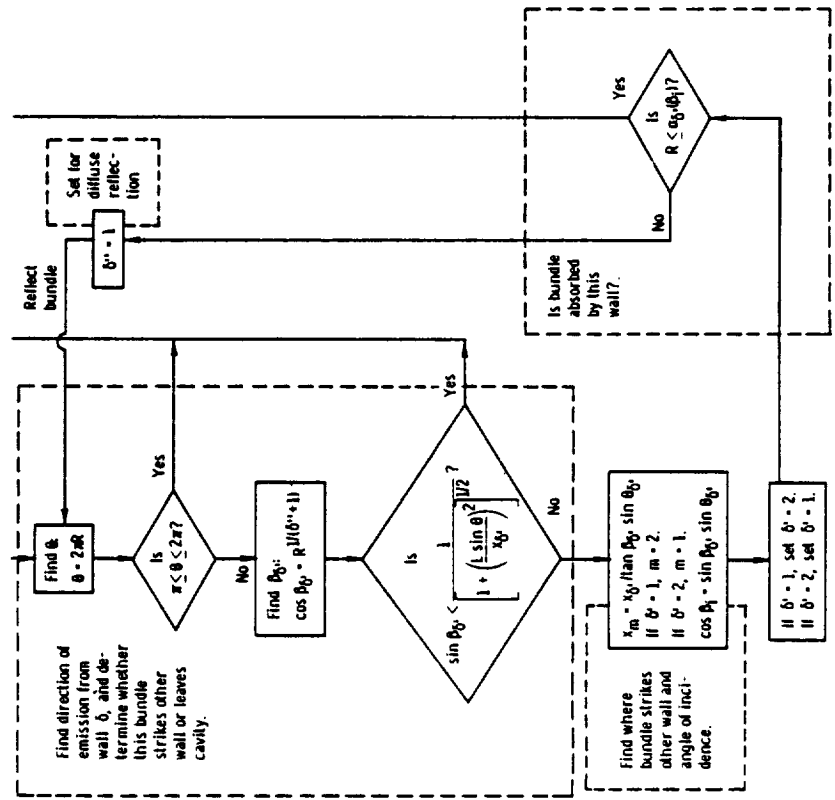


FIGURE 6-7. — Monte Carlo flow chart for example 6-1.

6.4.5. Literature on Application to Radiation Exchange Between Surfaces

The standard or conventional methods for solving problems of radiative transport between surfaces in the absence of absorbing media were formulated in chapters 2 to 5. The standard methods have advantages for certain types of problems and will outshine the Monte Carlo approach in speed and accuracy over some range of radiation calculations. This range is outlined roughly by the complexity of the problem, and the areas of usefulness of the Monte Carlo approach will now be discussed.

The chief usefulness of Monte Carlo to the thermal radiation analyst lies in this fact: Monte Carlo program complexity increases roughly in proportion to problem complexity for radiative interchange problems while the difficulty of carrying out conventional solutions increases roughly with the square of the complexity of the problem because of the matrix form into which the conventional formulations fall. However, because Monte Carlo is somewhat more difficult to apply to the simplest problems, it is most effective in problems where complex geometries and variable properties must be considered. In complex geometries, Monte Carlo has the additional advantage that simple relations will specify the path of a given energy bundle, whereas most other methods require explicit or implicit integrations over surface areas. Such integrations become difficult when a variety of curved or skewed surfaces are present.

6.4.5.1 Configuration factor computation.—The calculation of radiative configuration factors by standard means usually involves certain assumptions that place restrictions on the application of these factors in exchange computations. The assumptions required when using the ordinary configuration factors as derived in chapter 2 are that the surfaces involved are diffuse-gray emitters and reflectors, that each surface is isothermal, and that the total flux arriving at and leaving each surface is evenly distributed across the surface. Any of these assumptions may be very poor; most surfaces are neither diffuse nor gray, and the distribution of reflected flux usually deviates from uniformity to some extent. Where deviations from the assumptions must be considered, calculation of the configuration factors becomes difficult, and if geometries with nonplanar surfaces are involved, Monte Carlo techniques may become invaluable. It should be noted, however, that unless a parametric study of the interchange of radiant energy within an enclosure with specified characteristics is being carried out, it may be easier to compute directly the entire radiative flux distribution by Monte Carlo. This would be simpler than computing configuration factors by Monte Carlo and then using an auxiliary program to calculate energy exchange by means of these factors.

As computed by Monte Carlo, configuration factors are identically

equal to the fraction of the total energy bundles emitted from a surface that is incident upon a second surface. No restrictions are made to diffuse-gray surfaces with evenly distributed, emitted, and reflected flux.

Corlett (ref. 17) has computed exchange factors (as distinguished from configuration factors) for a variety of geometries, including louvers, and circular and square ducts with various combinations of diffusely and specularly reflecting interior surfaces and ends. These factors give the fraction of energy emitted by a given surface that reaches another surface by all paths, including intermediate reflections. One set of results, the exchange factors between the black ends of a cylinder with a diffusely reflecting internal surface, is shown in figure 6-8.

Weiner et al. (ref. 18) carried out the Monte Carlo evaluation of some simple configuration factors for comparison with analytical solutions. They then considered energy exchange within an enclosure with five specularly reflecting sides, each side being assumed to have a directional emissivity dependent upon cone angle of emission.

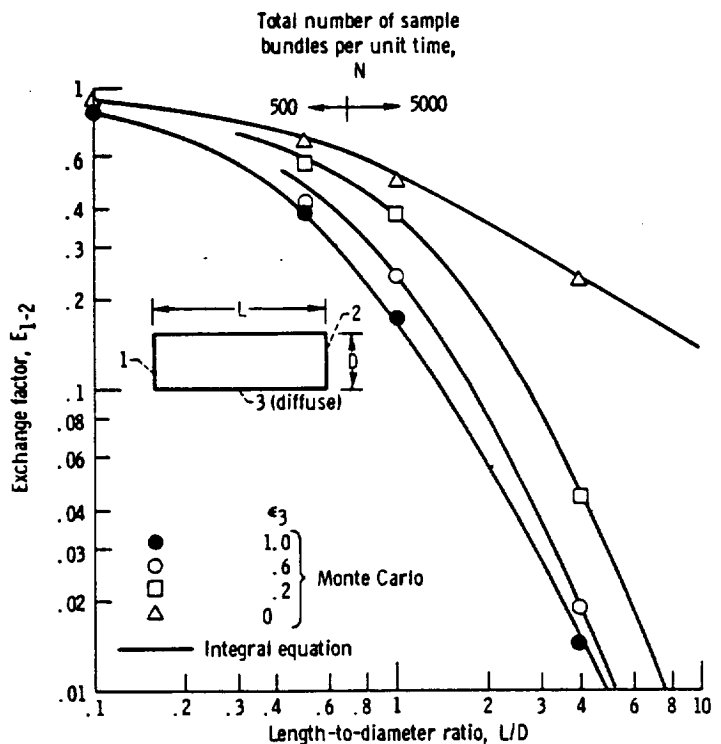


FIGURE 6-8.—Radiation exchange factors between black ends of diffuse walled cylinder (from ref. 17). $\epsilon_1 = \epsilon_2 = 1$.

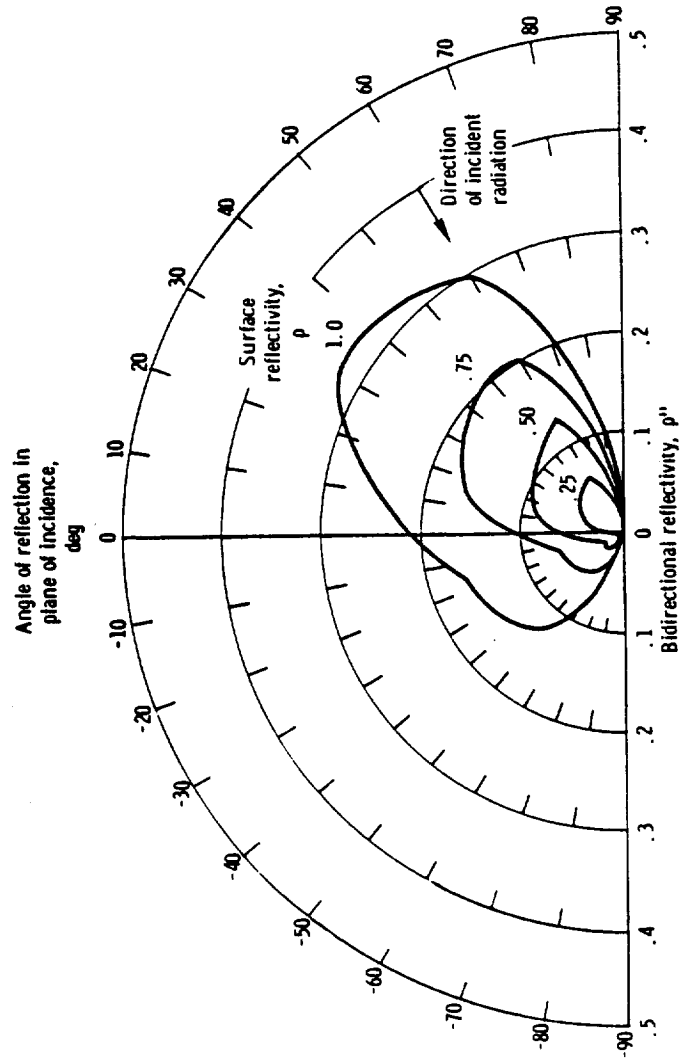


FIGURE 6-9.—Bidirectional reflectivity of diffusely reflecting conical cavity. Cone angle of cavity, 30°; angle of incidence of radiation, 60° (from ref. 19).

They also worked out the case of interchange within a simulated optical system. This system is constructed of a combination of spherical and conical surfaces that enclose a cylindrical specular reflector with two surfaces. This is obviously an interchange problem to cause many unhappy hours of analyzing integral limits in the usual formulations.

6.4.5.2 *Cavity properties.*—At least one Monte Carlo solution exists in the literature for a surface interaction with a distant source. This is the case of a conical cavity with diffusely reflecting inner surface. Polgar and Howell (ref. 19) analyzed the bidirectional reflectivity of the cavity when exposed to a beam of parallel incident radiation and also determined the directional emissivity of the cavity. Parameters varied were the angle of incidence, cone angle, and emissivity of the inner surface of the cone. One set of representative results is shown in figure 6-9. No results were found in the literature for direct comparison of the computed directional properties; however, the hemispherical absorptivity results were obtained by integrating the directional values and were compared in reference 20 to analytical results from reference 21. The comparison is shown in figure 6-10.

The bidirectional reflectivity results computed by Monte Carlo in reference 19 illustrate the scatter of the computed points that depends on the number of energy bundles reflected from the cone interior through any given area element on a unit hemisphere imagined over the conical

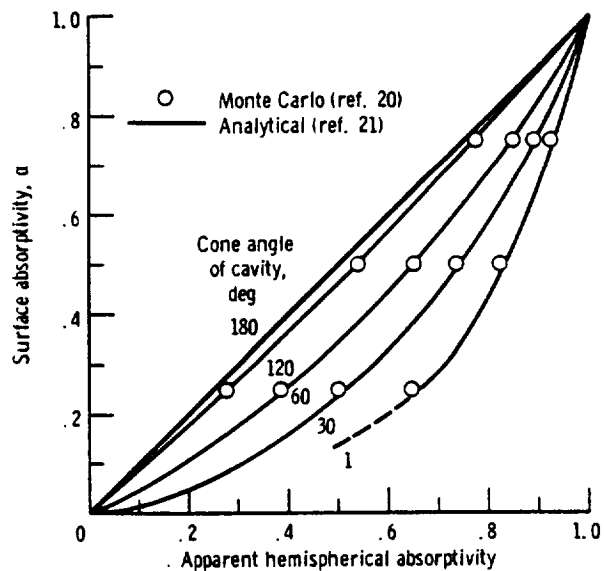


FIGURE 6-10.—Comparison of Monte Carlo results for absorptivity of conical cavities (ref. 20) with analytical results (ref. 21).

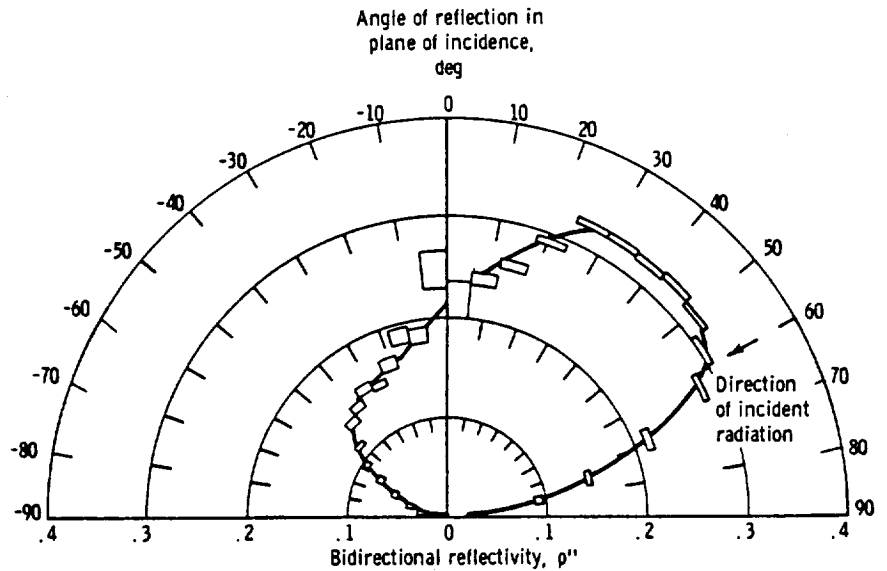


FIGURE 6-11.—Expected standard deviation of results for bidirectional reflectivity of diffuse conical cavity. Cone angle of cavity, 30° ; angle of incidence of radiation, 60° (from ref. 19).

cavity. The scatter is shown in figure 6-11, which gives the standard deviation of the computed reflectivity at various angles of reflection. The solid angle subtended to the base by area elements of equal angular increment $\Delta\beta\Delta\theta$ on the hemisphere varies with the sine of the angle of reflection, so the number of sample energy bundles per unit solid angle $d\omega = \sin\beta d\beta d\theta$ near the cone axis becomes very small. This leads to larger scatter at angles near the cone axis, where $\sin\beta \rightarrow 0$.

6.4.5.3 *Extension to directional and spectral surfaces.*—Few references exist that treat problems involving both directionally and spectrally dependent properties. The reasons for this omission seem twofold. First, accurate and complete directional-spectral properties, especially the former, are not often found in the literature. An analyst desiring to include such effects might thus be unable to find the requisite data for his system. Second, when solutions are attained to such problems, they are often so specialized that little interest exists to warrant their wide dissemination in the open literature. As pointed out by Dunn et al. (ref. 22), when the radiative properties become available, the methods for handling such surface radiative energy exchange problems now exist, and Monte Carlo appears to be one of the better-suited techniques.

Toor, Viskanta, and Schornhorst (refs. 23 to 26) have successfully applied Monte Carlo techniques to some interchange problems involving

surfaces with directional and spectral property variations. Some of these results were discussed in chapter 5.

6.4.6 Statistical Difficulties of Monte Carlo Technique

Monte Carlo calculations give results that fluctuate around the "real" answer because the method is a repetitive experiment using a mathematical model in place of the actual physical situation. The uncertainty can be found by applying standard statistical tests; the uncertainty can be reduced in the same manner as experimental error, that is, by averaging over more tests (bundle histories), and/or by reducing the variance of individual tests.

No rigorous criteria exist to guarantee the convergence of Monte Carlo results to valid solutions; however, convergence has not as yet been a difficulty in thermal radiation problems. It would often be immediately evident that convergence to invalid solutions was occurring because of the limiting solutions and physical constraints that are known for most radiative problems.

Most of the difficulties that do arise in Monte Carlo sampling techniques are concerned with obtaining an optimum sample size. Such difficulties have been sufficiently common in transport processes that are mathematically related to radiative transport so that special methods of "weighting" the free paths of bundles have been developed to obtain adequate samples. Using these methods saves computer time and increases accuracy; these gains, however, are at the expense of added complexity.

6.4.7 Closing Remarks

In this chapter, Monte Carlo has been discussed as a method suitable for the solution of complex radiative exchange problems. Two sample problems were outlined to demonstrate its application, and some of the advantages and disadvantages of the technique were discussed along with pertinent literature references.

From this, certain conclusions emerge. First, Monte Carlo appears to have a definite advantage over other radiative exchange calculation techniques when the difficulty of the problem being treated lies above some undefined level. This level usually cannot be defined since it depends not only on the specific problem but is probably a function of the experience, competence, and prejudice of the individual working the problem. However, problems with complexity above this nebulous benchmark can be treated by Monte Carlo with great flexibility, simplicity, and speed. The Monte Carlo approach does lack a kind of generality common to other approaches in that each problem may require

an individual technique, and a dash of ingenuity often helps. This places a greater burden on the programmer's backlog of experience and intuition whereas standard methods may allow programing through "cookbook" application of their formalism if they can be applied at all.

Second, for the thermal-radiation problems carried out to date, the parameters and mathematical relations involved usually lie in ranges which allow straightforward Monte Carlo programing without the need of the more exotic schemes occasionally necessary in other Monte Carlo transport studies.

Third, with all its advantages, the method suffers from certain difficulties. The worst of these are the statistical nature of the results and the lack of guaranteed statistical convergence to the true mean value. It should be noted that the latter fault is common to many methods when complex problems are being treated because rigorous mathematical criteria to guarantee convergence to a solution are available only in certain cases.

Finally, it must be commented that the person using Monte Carlo techniques often develops a physical grasp of the problems encountered because the model being utilized is simple, and the mathematics describing it are therefore on a less sophisticated basis. This is in contrast to the rather poor physical interpretations and predictions which can be made when working with, say, a matrix of integral equations.

REFERENCES

1. HOWELL, J. R.: Application of Monte Carlo to Heat Transfer Problems. *Advances in Heat Transfer*. Vol. 5. J. P. Hartnett and T. F. Irvine, eds., Academic Press, 1968.
2. KAHN, HERMAN: Applications of Monte Carlo. Rep. No. RM-1237-AEC (AEC No. AECU-3259), Rand Corp., Apr. 27, 1956.
3. HAMMERSLEY, J. M.; AND HANDSCOMB, D. C.: *Monte Carlo Methods*. John Wiley & Sons, Inc., 1964.
4. THE HOLY BIBLE: 1 Kings, 7:23; and 2 Chronicles, 4:2.
5. METROPOLIS, NICHOLAS; AND ULAM, S.: The Monte Carlo Method. *J. Am. Statist. Assoc.*, vol. 44, no. 247, Sept. 1949, pp. 335-341.
6. CASHWELL, E. D.; AND EVERETT, C. J.: *A Practical Manual on the Monte Carlo Method for Random Walk Problems*. Pergamon Press, 1959.
7. SCHREIDER, YU. A., ED.: *Method of Statistical Testing—Monte Carlo Method*. American Elsevier, 1964.
8. BROWN, G. W.: *Monte Carlo Methods*. *Modern Mathematics for the Engineer*. E. F. Bechenbach, ed., McGraw-Hill Book Co., Inc., 1956, pp. 279-307.
9. MEYER, HERBERT A., ED.: *Symposium on Monte Carlo Methods*. John Wiley & Sons, Inc., 1956.
10. RAND CORP.: *A Million Random Digits with 100,000 Normal Deviates*. Free Press, Glencoe, Ill., 1955.
11. KENDALL, M. G.; AND SMITH, B. BABINGTON: *Tables of Random Sampling Numbers*. Second series, Cambridge Univ. Press, 1954.

12. TAUSSKY, O.; AND TODD, J.: Generating and Testing of Pseudo-Random Numbers. Symposium on Monte Carlo Methods. Herbert A. Meyer, ed., John Wiley & Sons, Inc., 1956, pp. 15-28.
13. KENDALL, M. G.; AND SMITH, B. B.: Randomness and Random Sampling Numbers. Roy. Stat. Soc. J., pt. 1, 1938, pp. 147-166.
14. DWIGHT, H. B.: Mathematical Tables of Elementary and Some Higher Mathematical Functions. Second ed., Dover Publications, 1958.
15. JAHNKE, EUGENE; AND EMDE, FRITZ: Tables of Functions with Formulae and Curves. Fourth ed., Dover Publications, 1945.
16. HOWELL, JOHN R.: Calculation of Radiant Heat Exchange by the Monte Carlo Method. Paper No. 65-WA/HT-54, ASME, Nov. 1965.
17. CORLETT, R. C.: Direct Monte Carlo Calculation of Radiative Heat Transfer in Vacuum. J. Heat Transfer, vol. 88, no. 4, Nov. 1966, pp. 376-382.
18. WEINER, M. M.; TINDALL, J. W.; AND CANDELL, L. M.: Radiative Interchange Factors by Monte Carlo. Paper No. 65-WA/HT-51, ASME, Nov. 1965.
19. POLGAR, LESLIE G.; AND HOWELL, JOHN R.: Directional Thermal-Radiative Properties of Conical Cavities. NASA TN D-2904, 1965.
20. POLGAR, LESLIE G.; AND HOWELL, JOHN R.: Directional Radiative Characteristics of Conical Cavities and Their Relation to Lunar Phenomena. Thermophysics and Temperature Control of Spacecraft and Entry Vehicles. G. B. Heller, ed., Academic Press, 1966, pp. 311-323.
21. SPARROW, E. M.; AND JONSSON, V. K.: Radiant Emission Characteristics of Diffuse Conical Cavities. J. Opt. Soc. Am., vol. 53, no. 7, July 1963, pp. 816-821.
22. DUNN, S. THOMAS; RICHMOND, JOSEPH C.; AND PARMER, JEROME F.: Survey of Infrared Measurement Techniques and Computational Methods in Radiant Heat Transfer. J. Spacecraft Rockets, vol. 3, no. 7, July 1966, pp. 961-975.
23. TOOR, JASWANT S.: Radiant Heat Transfer Analysis Among Surfaces Having Direction Dependent Properties by the Monte Carlo Method. M.S. thesis, Purdue University, 1967.
24. VISKANTA, RAYMOND; SCHORNHORST, JAMES R.; AND TOOR, JASWANT S.: Analysis and Experiment of Radiant Heat Exchange Between Simply Arranged Surfaces. Purdue University (AFFDL-TR-67-94, DDC No. AD-655335), June 1967.
25. TOOR, J. S.; AND VISKANTA, R.: A Numerical Experiment of Radiant Heat Exchange by the Monte Carlo Method. Int. J. Heat Mass Transfer, vol. 11, no. 5, May 1968, pp. 883-897.
26. TOOR, J. S.; AND VISKANTA, R.: Effect of Direction Dependent Properties on Radiant Interchange. J. Spacecraft Rockets, vol. 5, no. 6, June 1968, pp. 742-743.



PRECEDING PAGE BLANK NOT FILMED.

Chapter 7. Radiation in the Presence of Other Modes of Energy Transfer

7.1 INTRODUCTION

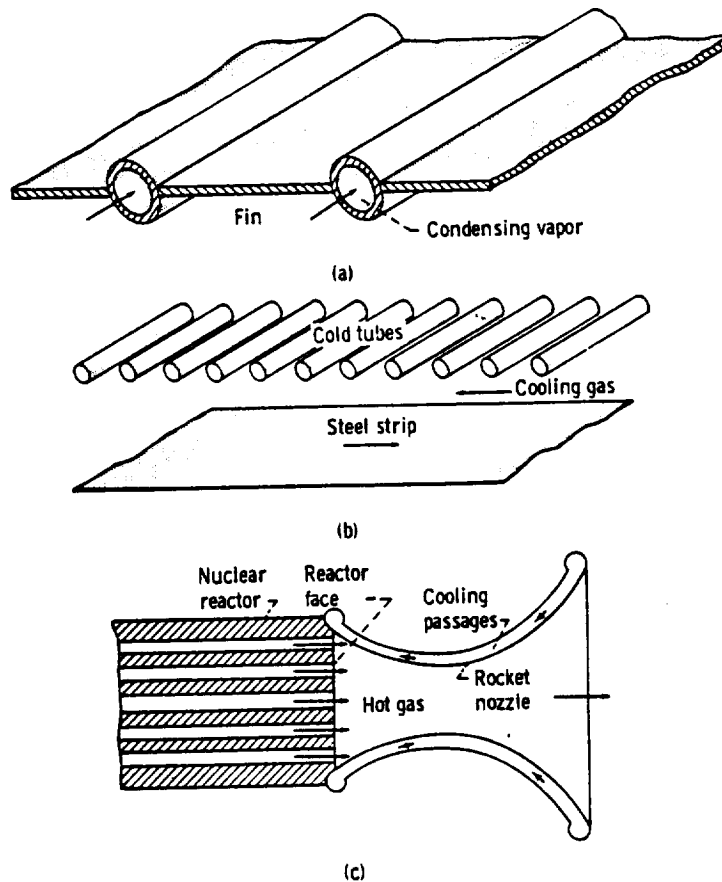
In the preceding chapters, radiation exchange was the only mode of heat transfer considered to be present. In many practical systems, however, a significant amount of heat conduction and/or convection may be occurring simultaneously, and the combined effect of all the heat transfer modes must be accounted for. The interaction of heat transfer modes may be simple in some cases; for example, the heat dissipation by radiation and convection may be essentially independent and hence can be computed separately and then added. In other instances, the interaction can be quite complex.

The following are some examples of situations having combined heat transfer effects. For a vapor cycle powerplant operating in outer space, the waste heat is rejected by radiation. In the space radiator, as shown in figure 7-1(a), the vapor used as the working fluid in a thermodynamic cycle is condensed, thereby releasing its latent heat. The heat is then conducted through the condenser wall and into fins that radiate the energy into space. The temperature distribution in the fins and the fin efficiency depends on the combined radiation and conduction processes.

In one type of steel strip cooler in a steel mill, figure 7-1(b), a sheet of hot metal moves past a bank of cold tubes and loses heat to them by radiation. At the same time, cooling gas is blown over the sheet. A combined radiation and convection analysis must be performed to determine the temperature distribution along the steel strip moving through the cooler.

In a nuclear rocket engine such as illustrated by figure 7-1(c), hydrogen gas is heated by flowing through a high-temperature nuclear reactor core. The hot gas then passes out through the rocket nozzle. The interior surface of the rocket nozzle receives heat by radiation from the exit face of the reactor core and by convection from the flowing propellant stream. Both these energy quantities are conducted through the nozzle wall and removed by a flowing stream of coolant.

The examples cited all involve the transfer of heat by two or more heat transfer modes. Heat may flow first by one mode and then by a second, as is the case of conduction through a plate followed by radiation from the surface, and the modes are considered to be in series. Heat flow may also occur by parallel modes, such as by simultaneous conduc-



(a) Space radiator.
 (b) Steel strip cooler.
 (c) Nuclear rocket.

FIGURE 7-1.—Heat transfer devices involving combined radiation, conduction, and convection.

tion and radiation through a transparent medium. The modes can thus be acting in series, parallel, or both.

In this chapter, combined radiation, conduction, and convection problems will be examined subject to an important restriction: The medium through which the radiation is passing does not absorb or emit radiation; that is, it is completely transparent. This restriction will be removed in the third volume of this series which deals with media that absorb, emit, and scatter radiation.

The various heat transfer modes depend on temperature to different powers. When radiation exchange between black surfaces is considered,

the energy fluxes depend upon surface temperatures to the fourth power. For nonblack surfaces, the exponent on the temperature may be somewhat different from 4 because of the variation of emissivity with temperature. If conduction is present, the Fourier conduction law prescribes a dependence of heat flow upon local temperature gradient, thus introducing derivatives of the first power of the temperature (when the thermal conductivity does not depend on temperature). If convection enters the problem, it provides a heat flow that depends approximately on a difference of the first powers of the temperatures, the exact power depending on the type of flow; for example, free convection depends on temperature difference between the 1.25 and 1.4 power. Physical properties that vary with temperature will introduce additional temperature dependencies. The fact that such a wide variation in powers of temperature are involved in the energy transfer process means that the governing equations are highly nonlinear.

Because the radiation terms are usually in the form of integrals that give the amount of radiative energy from the surroundings, and the conduction terms involve derivatives, the energy balance equations are in the form of nonlinear integrodifferential equations. Such equations are not easily solved using presently available mathematical techniques. Except in the simplest cases, it is usually necessary to resort to numerical evaluation of the solutions. Each problem requires its own most efficient method of attack, and for this reason, no general discussion of numerical or other mathematical solution techniques will be given here. For such techniques, the reader is referred to the extensive mathematical literature on numerical methods and the representative radiation papers referenced throughout this chapter. This chapter will concentrate on the methods of setting up the energy balance equations and gaining insight into the physical problems, leaving the actual solution methods to the mathematical texts except where specialized approaches are of value.

7.2 SYMBOLS

<i>A</i>	area
<i>a</i>	spacing between fins; coefficients in matrix
<i>B</i>	parameter in example 7-4
<i>b</i>	thickness of conducting medium; fin thickness; tube wall thickness
<i>c</i>	correction factors
<i>c_p</i>	specific heat
<i>D</i>	tube diameter
<i>F</i>	configuration factor
<i>f</i>	coefficients in eq. (7-12)
<i>G</i>	parameter in eq. (7-30)

H	parameter defined in example 7-5
h	heat transfer coefficient
k	thermal conductivity
L	length of tube
l	dimensionless tube length, L/D
M	parameter in eq. (7-30)
N	parameter defined in connection with eq. (7-25)
Nu	Nusselt number, hD/k
n	normal direction
P	perimeter
Pr	Prandtl number, $c_p\mu_f/k$
Q	energy rate; energy per unit time
q	energy flux; energy per unit area per unit time
R	dimensionless radius of example 7-3
Re	Reynolds number, $Du_m\rho_f/\mu_f$
r	radius
S	parameter defined in example 7-5
T	absolute temperature
t	dimensionless temperature
u_m	mean fluid velocity
W	width of fin in example 7-4
X	distance from tube entrance to ring element
x, z	Cartesian coordinate positions
γ, δ	dimensionless parameters of example 7-3
ϵ	emissivity
η	fin efficiency, defined in example 7-3
Θ	dimensionless temperatures in examples 7-3 and 7-4
μ	dimensionless parameter defined in example 7-4
μ_f	fluid viscosity
Ξ	distance from tube entrance
ξ	distance from fin base
ρ_f	density of fluid
ρ_m	density of solid material
σ	Stefan-Boltzmann constant
τ	time

Subscripts:

a	base surface between fins
b	evaluated at base of fin
c	conduction
e	environment
f	fin or fluid
g	gas

i	in or inner
o	out or outer
R	radiation
r	reservoir
w	wall
x	at position x
ξ	at position ξ
1, 2	evaluated at surfaces 1, 2 or at inlet and exit ends of tube

7.3 PROBLEMS INVOLVING COMBINED RADIATION AND CONDUCTION

Physical situations that involve only conduction and radiation are fairly common. Some examples are heat losses through the walls of a vacuum Dewar, heat transfer through "superinsulation" made up of separated layers of highly reflective material, and heat losses and temperature distributions in satellite and spacecraft structures.

The sophistication of the radiative portion of the analysis can range from assuming finite black surfaces and using diffuse configuration factors to a complete treatment of local directional-spectral effects via a Monte Carlo or integral equation approach. The choice of radiative formulation depends on the accuracy required, and the relative importance on the quantities desired of the radiative mode in relation to the heat conduction. If conduction dominates, then fairly rough approximations can be invoked in the radiative portion of the analysis, and vice versa. Some simple examples of situations involving radiation and conduction are now examined, and progress is then made to more sophisticated treatments.

7.3.1 Uncoupled Problems

The simplest situation exists when the radiation and conduction contributions to an unknown quantity, say heat flux, are independent; the contributions are then computed separately and the individual results added. The heat transfer modes are said to be *uncoupled* with regard to the desired quantity.

EXAMPLE 7-1: As an example of an uncoupled situation, consider two black infinite parallel plates separated by a medium of thickness b that has thermal conductivity k and is transparent to thermal radiation. If one plate is at temperature T_1 and the other is at temperature T_2 , what is the net energy exchange between the plates?

The net energy transferred is composed of Q_R , the net radiative exchange, and Q_c , the transfer by conduction. The net energy transferred is also equal to the energy Q_1 that must be added to plate 1 to maintain

it at its specified temperature,

$$Q_1 = Q_R + Q_c$$

The energy transfer per unit time and area by radiation between two infinite parallel black plates is simply

$$\frac{Q_R}{A} = \sigma(T_1^4 - T_2^4)$$

and that by conduction is

$$\frac{Q_c}{A} = \frac{k}{b}(T_1 - T_2)$$

The total energy transfer per unit time and area is then the sum of the separate contributions or

$$\frac{Q_1}{A} = \sigma(T_1^4 - T_2^4) + \frac{k}{b}(T_1 - T_2)$$

Example 7-1 demonstrates a situation where the conductive and radiative components are *uncoupled* from one another; that is, the presence of one parallel heat transfer mode does not affect the other with regard to the computations of Q/A . The Q/A for each mode is computed independently and they are then added. The radiative transfer would have been the same in the presence of conduction and vice versa. In such problems, all the methods of radiative computation developed heretofore can be applied without modification, since the radiation is computed independently.

7.3.2 Coupled Nonlinear Problems

Unhappily, the uncoupled problems described in the previous section are not as common as *coupled* problems. In coupled problems the *desired unknown quantity cannot be found by adding separate radiation and conduction solutions*; the governing energy equation must be solved with the two modes simultaneously included. In some situations, it is possible to assume that the modes are uncoupled because of the weak coupling that occurs. This assumption, when valid, allows escape from some of the difficulties that will become manifest in succeeding sections of this chapter.

EXAMPLE 7-2: As a simple example of a coupled problem, consider from another viewpoint the situation in the previous example; that is, two black infinite parallel plates that are separated by a transparent medium of thickness b having thermal conductivity k . Plate 2 is at temperature T_2 , and a known amount of energy Q_1/A is added per unit area to plate 1 and removed at plate 2. What is the temperature T_1 of plate 1?

This is the same situation as example 7-1, except that Q_1 is now known and T_1 is to be found. The same energy equation applies as in example 7-1 and is rewritten to place the unknown on the left

$$\sigma T_1^4 + \frac{k}{b} T_1 = \sigma T_2^4 + \frac{k}{b} T_2 + \frac{Q_1}{A_1}$$

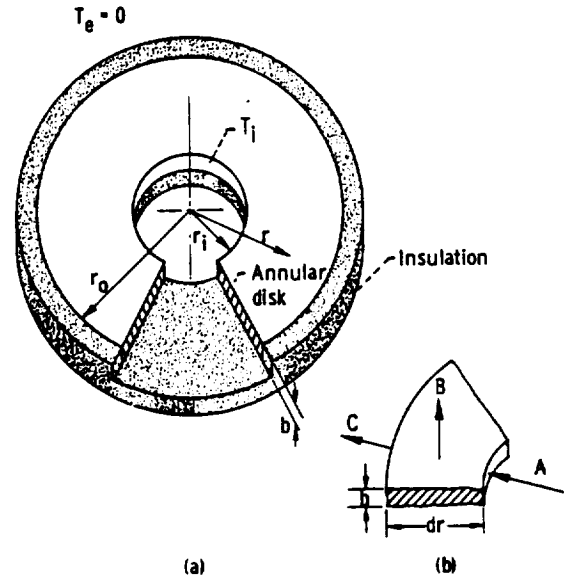
The problem is *coupled* with regard to the desired unknown T_1 in that T_1 must be found from an equation that simultaneously incorporates *both* heat transfer processes. The equation for T_1 is nonlinear and can be solved iteratively.

These first two examples demonstrate that the types of boundary conditions that are specified govern the possibility of uncoupling the radiative and conductive calculations. When all temperatures are specified, the determination of the heat fluxes can usually be uncoupled. If energy fluxes are specified, however, the entire problem must be treated simultaneously because of nonlinear coupling governing the unknown temperatures. The treatment can become more difficult if variations of physical properties as functions of temperature must be included.

In devices that operate in outer space, a means for dissipating energy is to employ radiating fins. The energy is conducted into the fin and radiated away from the fin surface. The determination of the unknown temperature distribution within the fin requires a coupled solution. The next example will deal with an analysis of the performance of a single circular fin.

EXAMPLE 7-3: A thin annular fin in a vacuum is embedded in insulation so that it is insulated on one face and around its outside edge as shown in figure 7-2(a). The disk is of thickness b , inner radius r_i , outer radius r_o , and thermal conductivity k . Energy is being supplied to the inner edge, for instance, from a solid rod of radius r_i that fits the central hole, and this maintains the inner edge at T_i . The exposed annular surface, which is diffuse-gray with emissivity ϵ , radiates to the environment, which is at temperature $T_e = 0$. Find the temperature distribution as a function of radial position along the annular disk.

Assume that the disk is thin enough so that the local temperature can



(a) Disk geometry.

(b) Portion of ring element on annular disk.

FIGURE 7-2. — Geometry for finding temperature distribution in thin radiating annular plate insulated on one side and around outside edge.

be taken as constant across the thickness b ; then for any ring element of width dr as shown in figure 7-2(b), an energy balance can be made of the form

$$A = B + C$$

In this equation, A and C are the conduction entering and leaving the element, and B is the radiation from the element; thus,

$$A = -k2\pi rb \frac{dT}{dr}$$

$$B = \epsilon\sigma T^4 2\pi r dr$$

$$C = -k2\pi rb \frac{dT}{dr} + \frac{d}{dr} \left(-k2\pi rb \frac{dT}{dr} \right) dr$$

If ϵ and k are constant, then the energy balance becomes

$$kb \frac{d}{dr} \left(r \frac{dT}{dr} \right) - \epsilon \sigma T^4 = 0 \quad (7-1)$$

This equation is to be solved for the temperature distribution $T(r)$ subject to the two boundary conditions: at the inner edge,

$$T = T_i \quad \text{at } r = r_i$$

and, at the insulated outer edge where there is no heat flow,

$$\frac{dT}{dr} = 0 \quad \text{at } r = r_o$$

By using the dimensionless variable $\Theta = T/T_i$ and $R = (r - r_i)/(r_o - r_i)$, the energy equation becomes

$$\frac{d^2\Theta}{dR^2} + \frac{1}{R + \frac{r_i}{r_o - r_i}} \frac{d\Theta}{dR} - \frac{(r_o - r_i)^2 \epsilon \sigma T_i^3}{kb} \Theta^4 = 0$$

Using the two parameters $\delta = r_o/r_i$ and $\gamma = (r_o - r_i)^2 \epsilon \sigma T_i^3 / kb$ results in the energy equation taking the form

$$\frac{d^2\Theta}{dR^2} + \frac{1}{R + \frac{1}{\delta - 1}} \frac{d\Theta}{dR} - \gamma \Theta^4 = 0 \quad (7-2)$$

with the following boundary conditions:

$$\Theta = 1 \quad \text{at } R = 0$$

and

$$\frac{\partial \Theta}{\partial R} = 0 \quad \text{at } R = 1$$

Equation (7-2) is a second-order differential equation which is non-linear because it contains Θ raised to two different powers. The temperature distribution depends only on the two parameters δ and γ . A solution can be obtained by numerical methods.

A quantity of interest in the utilization of cooling fins is the *fin efficiency* η . This is defined as the energy actually radiated away by the fin divided by the energy that would be radiated if the entire fin were at

the temperature T_i . The fin efficiency for the circular fin being studied here is then

$$\eta = \frac{2\pi\epsilon\sigma \int_{r_i}^{r_o} r T^4 dr}{\pi(r_o^2 - r_i^2)\epsilon\sigma T_i^4} = \frac{2 \int_0^1 [R(\delta - 1) + 1] \Theta^4 dR}{\delta + 1}$$

This integral may be carried out after Θ has been determined from the differential equation. The fin efficiency for this type of annular fin has been obtained by Chambers and Somers (ref. 1) and is shown in figure 7-3.

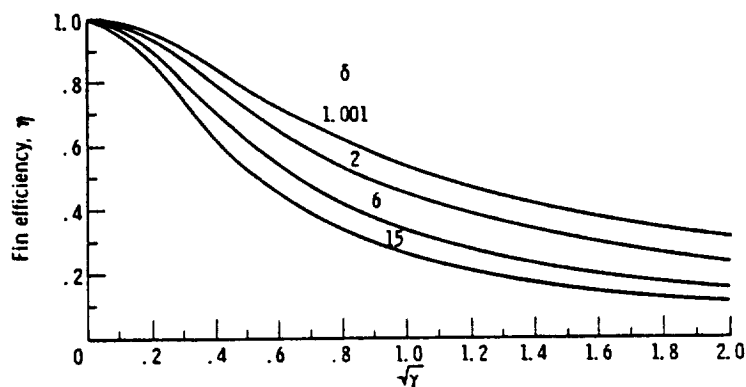


FIGURE 7-3. — Radiation fin efficiency for fin of example 7-3.

Because of the interest in radiator design for application in space power systems, many conducting-radiating systems have been analyzed. Typical are references 1 to 8 listed at the end of this chapter; many other references are to be found in the literature.

For a transient situation where the temperature of the radiating fin is changing with time, a heat storage term must be included in the energy balance. For the ring element in example 7-3 this term is

$$\rho_m c_p b 2\pi r dr \frac{\partial T}{\partial \tau}$$

With this term included, the energy balance equation (eq. (7-1)) becomes a partial differential equation in which temperature is a function of radius and time

$$kb \frac{\partial}{\partial r} \left(r \frac{\partial T}{\partial r} \right) - \epsilon r \sigma T^4 = \rho_m c_p \frac{\partial T}{\partial \tau} \quad (7-3)$$

Results for the transient behavior of a radiating fin are given in reference 4.

For a thin radiating fin, the temperature within the fin was assumed uniform across the fin thickness, and hence the temperature variation was only in a direction parallel to the radiating surface. If the solid is thick, however, the temperature will vary also with distance normal to the radiating surface. The radiation acts as a boundary condition for the solid conduction problem; thus, locally at the surface of a solid that is emitting but not receiving radiation, the boundary condition is

$$-k \frac{\partial T}{\partial n} = \epsilon \sigma T^4 \quad (7-4a)$$

where n is the outward normal from the surface. More generally, when the surface is both receiving and losing radiant energy,

$$-k \frac{\partial T}{\partial n} = q_o - q_i \quad (7-4b)$$

Time-dependent temperature distributions within solids having surface radiation were investigated in reference 8. The transient heat conduction equation was solved with the boundary conditions of equations (7-4).

Example 7-3 considered only a single radiating fin. One additional complication that must usually be considered is the mutual interaction of radiation among the fins on a multifinned surface. This will introduce integral terms into the equations as will be evident from the next example.

EXAMPLE 7-4: An infinite array of thin fins of thickness b , width W , and infinite length are attached to a black base that is held at a constant temperature T_b as pictured in figure 7-4. The fin surface radiates in a diffuse-gray manner, and the fins are in vacuum. Set up the equation necessary for describing the local fin temperature, assuming the environment to be at $T_e = 0$.

Because the fins are thin, it will be assumed that the local temperature of the fin is constant across the thickness b . An energy balance will now be derived for the circled differential element of one fin shown in the inset of figure 7-4. Since there is an infinite row of fins, the surrounding environment is identical for each fin and is the same on both sides of each fin. Hence, from symmetry, only half the fin thickness need be considered. Also, the problem is simplified because the temperature distribution $T(\xi)$ of the adjacent fin is the same as $T(x)$. Thus, the energy balance need be considered for only one fin. The conduction terms for the energy into and out of the element dx per unit time and *per unit length of fin* in the z -direction are

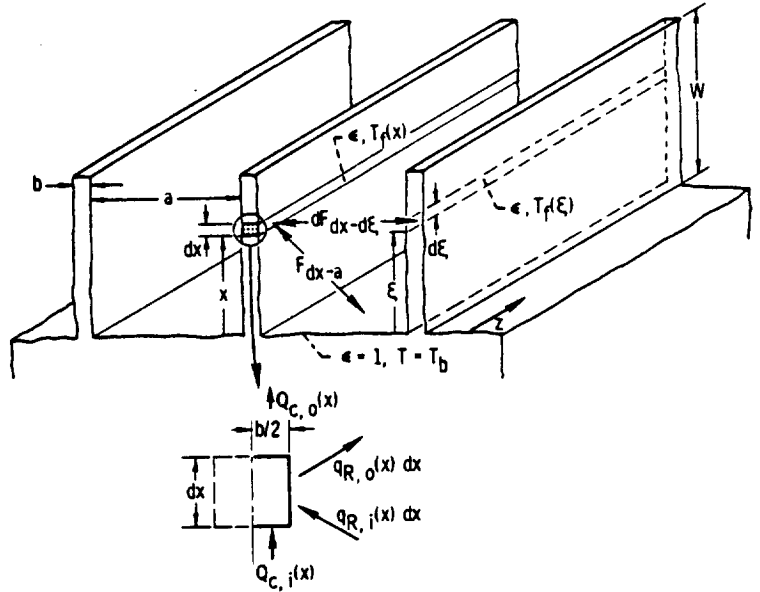


FIGURE 7-4. — Geometry for determination of local temperatures on parallel fins.

$$Q_{c,i}(x) = -k \frac{b}{2} \frac{dT_f}{dx}$$

$$Q_{c,o}(x) = Q_{c,i} + dQ_{c,i} = -k \frac{b}{2} \frac{dT_f}{dx} + \frac{d}{dx} \left(-k \frac{b}{2} \frac{dT_f}{dx} \right) dx$$

The radiation terms are formulated by using Poljak's net radiation method from section 3.4.1. The incoming radiation to the element originates from the adjacent fin and from the base surface,

$$\begin{aligned} q_{R,i}(x) dx &= \int_{\xi=0}^w q_{R,o}(\xi) dF_{d\xi-dx} d\xi + \alpha \sigma T_b^4 dF_{a-dx} \\ &= dx \int_{\xi=0}^w q_{R,o}(\xi) dF_{dx-d\xi} + dx \sigma T_b^4 F_{dx-a} \end{aligned} \quad (7-5)$$

The outgoing radiation is composed of emission plus reflected incident radiation

$$q_{R,o}(x) dx = \epsilon \sigma T_f^4(x) dx + (1 - \epsilon) q_{R,i}(x) dx \quad (7-6)$$

The energy balance on the element is composed of the conduction and radiation quantities

$$q_{R,o} dx + Q_{c,o}(x) = q_{R,i} dx + Q_{c,i}(x)$$

By substituting the conduction terms and assuming constant thermal conductivity, the energy balance becomes

$$q_{R,i}(x) dx = q_{R,o}(x) dx - k \frac{b}{2} \frac{d^2 T_f(x)}{dx^2} dx \quad (7-7)$$

Equation (7-7) along with equations (7-5) and (7-6) for $q_{R,i}(x)$ and $q_{R,o}(x)$ give three equations in the unknowns $q_{R,i}(x)$, $q_{R,o}(x)$, and $T_f(x)$. (Note that $q_{R,o}(\xi) = q_{R,o}(x)$.) Eliminating the two energy rates $q_{R,i}$ and $q_{R,o}$ from the three equations results in

$$-\mu \frac{d^2 \Theta(X)}{dX^2} + \Theta^4(X) = F_{dX-B} + \int_{Z=0}^1 \left[-\mu(1-\epsilon) \frac{d^2 \Theta(Z)}{dZ^2} + \Theta^4(Z) \right] dF_{dX-dZ} \quad (7-8)$$

where $\Theta(X) = T_f(x)/T_b$, $B = a/W$, $\mu = kb/2\epsilon\sigma T_b^3 W^2$, $X = x/W$, and $Z = \xi/W$.

Equation (7-8) is a nonlinear integrodifferential equation and can be solved numerically. Since it is a second-order equation, two boundary conditions are needed. At the base of the fin $T_f(x=0) = T_b$ so that

$$\Theta = 1 \quad \text{at } X = 0 \quad (7-9a)$$

A second condition is obtained at the outer edge of the fin $x = W$. The conduction to this boundary must equal the heat radiated

$$-k \frac{\partial T}{\partial x} \Big|_{x=W} = \epsilon\sigma T^4(W)$$

or in terms of Θ

$$-\frac{d\Theta}{dX} = \frac{\epsilon\sigma T_b^3}{k} \Theta^4 = \frac{1}{2\mu} \frac{b}{W} \Theta^4 \quad \text{at } X = 1 \quad (7-9b)$$

and it is evident that the fin thickness to width ratio b/W now enters the problem as a new parameter. If $(b/W)/2\mu$ is very small, then $d\Theta/dX$ can be taken as zero.

The configuration factors in equation (7-8) are found by the methods of examples 2-4 and 2-6 (for $\alpha = 90^\circ$ in those equations), which give

$$F_{ax-B} = \frac{1}{2} \left[1 - \frac{x}{\sqrt{a^2 + x^2}} \right] = \frac{1}{2} \left[1 - \frac{X}{\sqrt{B^2 + X^2}} \right]$$

$$dF_{ax-az} = \frac{1}{2} \frac{a^2}{[a^2 + (\xi - x)^2]^{3/2}} d\xi = \frac{1}{2} \frac{B^2}{[B^2 + (Z - X)^2]^{3/2}} dZ$$

Solutions to other fin problems involving mutual interactions are found in references 9 to 18.

The examples given in this section are simplified in that no property variations have been included. When properties are variable, the basic concepts are the same as demonstrated by the examples, although the inclusion of property variations does add some complexity to the functional form of the equations. The usual warnings concerning the inadequacy, in some cases, of the diffuse-gray assumptions carry over to multimode problems.

When finite difference techniques are used in the solution of combined conduction-radiation problems, the energy equation is replaced by a set of simultaneous nonlinear algebraic equations. When the physical properties are constant, the conduction terms will contain temperatures to the first power while the radiation terms will have temperatures to the fourth power. To solve a set of nonlinear equations of this type, Ness (ref. 19) has presented a rapid convergence iteration method for the digital computer based on the Newton-Raphson technique. Assume that the set of finite difference equations for the radiation conduction problem has the form

$$\begin{aligned} (a_{11}t_1 + a'_{11}t_1^4) + (a_{12}t_2 + a'_{12}t_2^4) + \dots + (a_{1n}t_n + a'_{1n}t_n^4) - b_1 &= 0 \\ \vdots & \\ (a_{i1}t_1 + a'_{i1}t_1^4) + \dots + (a_{ij}t_j + a'_{ij}t_j^4) + \dots + (a_{in}t_n + a'_{in}t_n^4) - b_i &= 0 \quad (7-10) \\ \vdots & \\ (a_{n1}t_1 + a'_{n1}t_1^4) + \dots + (a_{nj}t_j + a'_{nj}t_j^4) + \dots + (a_{nn}t_n + a'_{nn}t_n^4) - b_n &= 0 \end{aligned}$$

The j th temperature is t_j and the coefficients for the linear and nonlinear contributions of this temperature are a_{ij} and a'_{ij} , respectively.

In the Newton-Raphson procedure, an approximate value for each temperature is assumed. Let t_{j0} be this approximation for the j th temperature. Then a correction factor c_j will be computed so that $t_j = t_{j0} + c_j$. This corrected temperature is used to compute a new c_j , and the process is continued until the c_j becomes smaller than a specified value. The c_j are found from the following set of linear equations:

$$\begin{aligned}
 f_{11}c_1 + f_{12}c_2 + \cdots + f_{1n}c_n + f_1 &= 0 \\
 \vdots \\
 f_{i1}c_1 + \cdots + f_{ij}c_j + \cdots + f_{in}c_n + f_i &= 0 \\
 \vdots \\
 f_{n1}c_1 + f_{n2}c_2 + \cdots + f_{nn}c_n + f_n &= 0
 \end{aligned}
 \tag{7-11}$$

The coefficients f_i are given by

$$f_i = \sum_{j=1}^n (a_{ij}t_{j0} + a'_{ij}t_{j0}^4) - b_i \tag{7-12}$$

and the f_{ij} are

$$f_{ij} = a_{ij} + 4a'_{ij}t_{j0}^3 \tag{7-13}$$

7.4 RADIATION AND CONVECTION

The treatment of problems involving combined heat transfer by convection and radiation is quite similar to that for conduction-radiation problems. The temperature differences that govern convection will appear in place of the derivatives governing conduction; otherwise, the governing energy equations remain of the same nature (i.e., nonlinear and often almost intractable).

Radiation-convection interaction problems are found in consideration of convection cells and their effect on radiation from stars, furnace design where heat transfer from surfaces occurs by parallel radiation and convection, the effect of incident solar radiation interacting with the Earth's surface to produce complex free convection patterns and thus complicate the art of weather forecasting, and marine environment studies for predicting free convection patterns in oceans and lakes. Representative solutions are found in references 20 to 23. To illustrate the concepts involved in an engineering problem, an example will now be considered that involves gas flow through a heated tube.

EXAMPLE 7-5: A transparent gas enters a black circular tube of geometry shown in figure 7-5. The wall of the tube is thin, and the outer surface of the tube is perfectly insulated. The tube wall is heated electrically to provide a uniform input of energy per unit area per unit time. The variation of local wall temperature along the tube length is to be determined. The convective heat transfer coefficient h between the gas and the inside of the tube is assumed constant. The gas has a mean velocity u_m , heat capacity c_p , and density ρ_f .

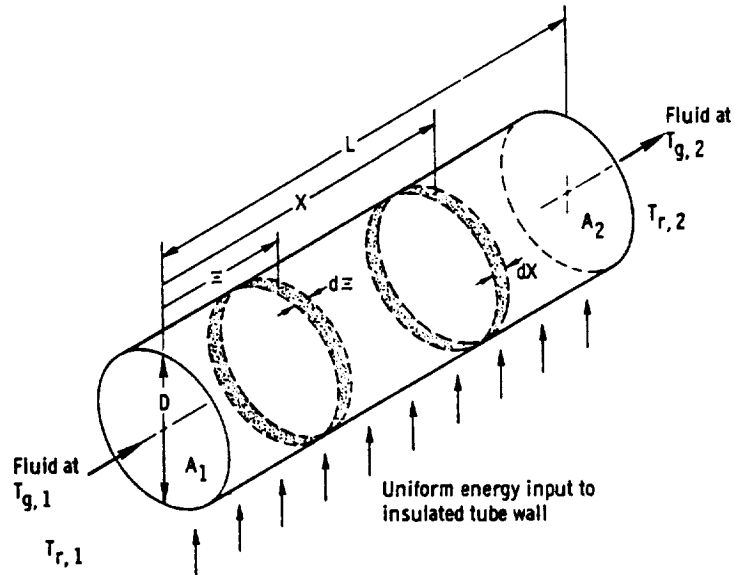


FIGURE 7-5.—Flow through tube with uniform internal energy input to wall and outer surface insulated.

If radiation were not considered, the local heat addition to the gas would be equal to the local electrical heating (since the outside of the tube is insulated) and hence would be invariant with axial position X along the tube. As a consequence, both the gas temperature and wall temperature would rise linearly with X . On the other hand, if convection were not considered, the only means for heat removal would be by radiation out the ends of the tube as discussed in example 3-8. In this instance, for equal environment temperatures at both ends of the tube, the wall temperature has a maximum at the center of the tube and decreases continuously toward both ends. The solution of the combined radiation-convection problem is expected to exhibit partially both of the trends of the limiting solutions.

Consider an energy balance on a ring area element of length dX on the interior of the tube wall at position X as in figure 7-5. The energy supplied to the ring per unit time is

$$q_w \pi D dX + \int_{\Xi=0}^L \sigma T_w^4(\Xi) dF_{d\Xi-dX}(|\Xi-X|) \pi D d\Xi \\ + \sigma T_{r,1}^4 \frac{\pi D^2}{4} dF_{1-dX}(X) + \sigma T_{r,2}^4 \frac{\pi D^2}{4} dF_{2-dX}(L-X)$$

The terms are, respectively, the energy supplied by electrical heating of the tube wall, the energy radiated to dA_X by other wall elements of

the tube interior (see section 3.4.1.3), and the energy radiated to dA_x from the inlet and the exit reservoirs. The reservoirs are assumed to act as black disks at the inlet and outlet reservoir temperatures which would have to be specified. Usually, the reservoirs are assumed to be at the inlet and outlet gas temperatures. The energy transferred away from the ring element at X by convection and radiation is

$$h\pi D dX [T_w(X) - T_g(X)] + \sigma T_w^4(X) \pi D dX$$

If axial heat conduction in the tube wall is neglected, the energy supplied to the ring element must equal that transferred away, and the energy quantities are equated to yield the following expression (reciprocity has been used on the F factors so that dX could be divided out of the equation):

$$h [T_w(X) - T_g(X)] + \sigma T_w^4(X) = q_w + \int_{\Xi=0}^L \sigma T_w^4(\Xi) dF_{dx-d\Xi}(|X-\Xi|) \\ + \sigma T_{r,1}^4 F_{dx-1}(X) + \sigma T_{r,2}^4 F_{dx-2}(L-X) \quad (7-14)$$

This equation has two unknowns $T_w(X)$ and $T_g(X)$; hence, a second equation must be found before a solution can be obtained. This is done by forming an energy balance on the volume within the tube occupying the length dX . The energy that enters this volume by being carried by the flowing gas is

$$Q_{i,g} = u_m \rho_f c_p T_g(X) \frac{\pi D^2}{4}$$

An additional amount of energy is added to the volume by convection from the wall, namely,

$$dQ_{i,g} = \pi D h [T_w(X) - T_g(X)] dX$$

Energy leaves by being carried out by the flowing gas

$$Q_{o,g} = u_m \rho_f c_p \frac{\pi D^2}{4} \left[T_g(X) + \frac{dT_g(X)}{dX} dX \right]$$

Equating the outgoing to the incoming energies gives the energy balance

$$u_m \rho_f c_p \frac{D}{4} \frac{dT_g(X)}{dX} = h [T_w(X) - T_g(X)] \quad (7-15)$$

By defining the dimensionless quantities

$$S = \frac{4h}{u_m \rho_f c_p} = \frac{4Nu}{Re Pr}$$

$$H = \frac{h}{q_w} \left(\frac{q_w}{\sigma} \right)^{1/4}$$

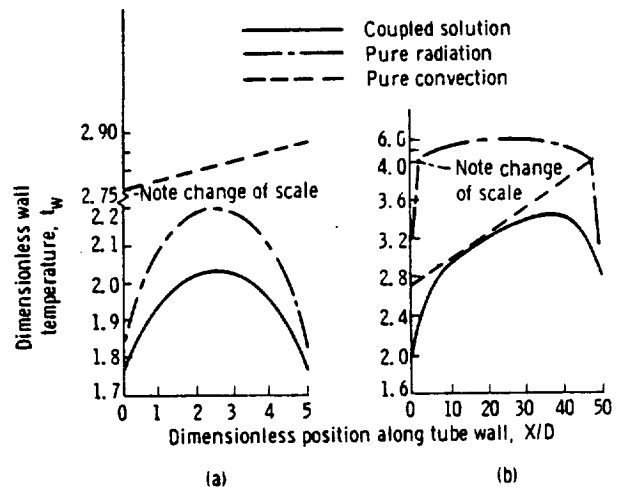
$$t = T \left(\frac{\sigma}{q_w} \right)^{1/4}$$

and $x = X/D$, $\xi = \Xi/D$, $l = L/D$, the energy balances on the wall and fluid elements can be written, respectively, as

$$t_w^4(x) + H[t_w(x) - t_g(x)] = 1 + \int_0^x t_w^4(\xi) dF_{dx-d\xi}(x-\xi) + \int_x^l t_w^4(\xi) dF_{dx-d\xi}(\xi-x) + t_{r,1}^4 F_{dx-1}(x) + t_{r,2}^4 F_{dx-2}(l-x) \quad (7-16)$$

$$\frac{dt_g(x)}{dx} = S[t_w(x) - t_g(x)] \quad (7-17)$$

giving two equations involving the unknowns $t_w(x)$ and $t_g(x)$, and having



(a) Tube length, $L/D = 5$. (b) Tube length, $L/D = 50$.

FIGURE 7-6. — Tube wall temperatures resulting from combined radiation and convection for transparent gas flowing in uniformly heated black tube for $S = 0.02$, $H = 0.8$, $t_{r,1} = t_{g,1} = 1.5$, and $t_{r,2} = t_{g,2}$.

six parameters: S , H , l , $t_{r,1}$, $t_{r,2}$, and $t_{g,1}$. The configuration factors can be obtained from known disk-to-disk factors by the technique of example 2-19 and equation (2-57), and they are given in example 3-8.

To solve equations (7-16) and (7-17), it is noted that equation (7-17) is a first-order linear differential equation, which can be solved in general form by the use of an integrating factor. The boundary condition is that at $x=0$, the gas temperature has a specified value $t_{g,1}$. The general solution is then

$$t_g(x) = S e^{-sx} \int_0^x e^{s\xi} t_w(\xi) d\xi + t_{g,1} e^{-sx} \quad (7-18)$$

This can be substituted into equation (7-16) to eliminate $t_g(x)$ and yield the following integral equation for the desired variation in tube wall temperature:

$$\begin{aligned} t_w^4 + H t_w - H S e^{-sx} \int_{\xi=0}^x e^{s\xi} t_w(\xi) d\xi - H t_{g,1} e^{-sx} \\ = 1 + \int_{\xi=0}^x t_w^4(\xi) dF_{dx-d\xi}(x-\xi) + \int_{\xi=x}^l t_w^4(\xi) dF_{dx-d\xi}(\xi-x) \\ + t_{r,1}^4 F_{dx-1}(x) + t_{r,2}^4 F_{dx-2}(l-x) \end{aligned} \quad (7-19)$$

Solutions to equation (7-19) have been obtained by Perlmutter and Siegel (ref. 20), and some representative results, as calculated by numerical integration, are shown in figure 7-6. Note that the predicted temperatures for combined radiation-convection fall below the temperatures predicted for either convection or radiation acting independently. For a short tube, the radiation effects are significant over the entire tube length, and for the parameters shown, the combined mode temperature distribution is similar to that for radiation alone. For a long tube, however, the combined mode distribution is very close to that for convection alone over the central portion of the tube. The heat transfer resulting from combined convection-radiation is more efficient than by either mode alone. This means that the wall temperature distribution predicted in the combined problem will always lie below both of the distributions predicted by using either mode alone.

EXAMPLE 7-6: If the tube in example 7-5 had a diffuse-gray interior surface, rather than being black, what would be the governing energy equations?

Using the net radiation method, a heat balance on an area element at X gives

$$q_w(X) + q_i(X) = q_o(X) + h[T_w(X) - T_g(X)] \quad (7-20)$$

where q_i and q_o are the incoming and outgoing radiation fluxes. For the outgoing radiation flux, there can be written

$$q_o(X) = \epsilon \sigma T_w^4(X) + (1 - \epsilon) q_i(X) \quad (7-21)$$

Equations (7-20) and (7-21) are combined to eliminate q_i with the following result:

$$q_o(X) = \frac{1 - \epsilon}{\epsilon} \{h[T_w(X) - T_g(X)] - q_w\} + \sigma T_w^4(X) \quad (7-22)$$

The analysis leading to equation (7-14) applies for the gray case if the radiation leaving the surface σT_w^4 is replaced by q_o . This gives

$$h[T_w(X) - T_g(X)] + q_o(X) = q_w + \int_{\Xi=0}^L q_o(\Xi) dF_{dx-d\Xi}(|X - \Xi|) \\ + \sigma T_{r,1}^4 F_{dx-1}(X) + \sigma T_{r,2}^4 F_{dx-2}(L - X) \quad (7-23)$$

Equation (7-15) is unchanged by having the wall gray. Thus equations (7-22), (7-23), and (7-15) comprise a set of three equations in the unknowns: $T_w(X)$, $q_o(X)$, and $T_g(X)$. Some numerical solutions for this system of equations are given in reference 21.

7.5 RADIATION COMBINED WITH BOTH CONDUCTION AND CONVECTION

The basic elements of the derivations in sections 7.3 and 7.4 can be combined when both conduction and convection are present in a radiating system. The energy equations become more complicated as they now contain both temperature differences arising from convection and temperature derivatives arising from conduction. There are also a greater number of independent parameters. These will arise from such things as the convective heat transfer coefficients, thermal conductivity of the body, and body dimensions: In other words, the quantities that govern both convection and conduction. As a result of these complexities, there are no "classical" solutions or solution methods, and results must usually be obtained using numerical techniques.

The basic ideas involved will now be given by discussing a few specific problems. Additional information and results are given in references 24 to 30.

EXAMPLE 7-7: Consider again the tube in example 7-5. The tube is uniformly heated, perfectly insulated on the outside, and has a black interior surface. Gas flows through the tube, and the convective heat transfer coefficient h is assumed constant. The axial heat conduction within the tube wall will now be included. The tube wall has thermal conductivity k_w , its thickness is b , the tube inside diameter is D_i , and the outside diameter is D_o . The desired result is the temperature distribution along the tube length. The tube wall is assumed sufficiently thin so that the temperature at each axial position is constant across the wall thickness.

The energy balance as given by equation (7-14) must be modified to include axial wall conduction. The heat conduction into an elemental length of the tube wall is

$$Q_{c,i} = -k_w \frac{\pi(D_o^2 - D_i^2)}{4} \frac{dT_w(X)}{dX}$$

while that conducted out of the element is

$$Q_{c,o} = -k_w \frac{\pi(D_o^2 - D_i^2)}{4} \left[\frac{dT_w(X)}{dX} + \frac{d^2T_w(X)}{dX^2} dX \right]$$

The net gain of the energy by the element from conduction is then

$$k_w \pi \frac{(D_o^2 - D_i^2)}{4} \frac{d^2T_w(X)}{dX^2} dX$$

This term is divided by the internal area of the ring $\pi D_i dX$ and is then added to the right side of equation (7-14) to obtain the energy balance

$$\begin{aligned} h[T_w(X) - T_g(X)] + \sigma T_w^4(X) &= q_w + k_w \frac{(D_o^2 - D_i^2)}{4D_i} \frac{d^2T_w(X)}{dX^2} \\ &+ \int_{\Xi=0}^L \sigma T_w^4(\Xi) dF_{dX-d\Xi}(|X-\Xi|) + \sigma T_{r,1}^4 F_{dX-1}(X) + \sigma T_{r,2}^4 F_{dX-2}(L-X) \end{aligned} \quad (7-24)$$

As in connection with equation (7-16), all lengths are nondimensionalized by dividing by the internal tube diameter, and dimensionless parameters are introduced. The conduction term yields a new parameter

$$N = \frac{k_w}{4q_w D_i} \left[\left(\frac{D_o}{D_i} \right)^2 - 1 \right] \left(\frac{q_w}{\sigma} \right)^{1/4}$$

For thin walls where $(D_o - D_i)/2 = b \ll 1$, this reduces to

$$N = \frac{k_w b}{2q_w D_i^2} \left(\frac{q_w}{\sigma} \right)^{1/4}$$

which is the parameter used in some of the references.

The dimensionless form of the energy equation is

$$t_w^*(x) + H[t_w(x) - t_g(x)] = 1 + N \frac{d^2 t_w(x)}{dx^2} + \int_{\xi=0}^x t_w^*(\xi) dF_{dx-d\xi}(x-\xi) \\ + \int_{\xi=x}^l t_w^*(\xi) dF_{dx-d\xi}(\xi-x) + t_{r,1}^* F_{dx-1}(x) + t_{r,2}^* F_{dx-2}(l-x) \quad (7-25)$$

The energy equation for the fluid within the tube element remains

$$\frac{dt_g(x)}{dx} = S[t_w(x) - t_g(x)] \quad (7-26)$$

as in equation (7-17). These equations may be further combined as in equation (7-19).

Hottel (ref. 24) has discussed this problem in terms of slightly different parameters. He obtained a numerical solution before the common

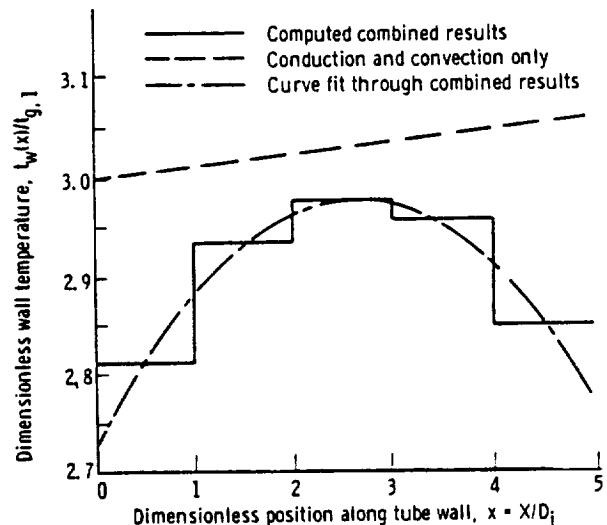


FIGURE 7-7. — Wall temperature distribution for flow of transparent fluid through black tube with combined radiation, convection, and conduction for $l=5$, $S=0.005$, $N=0.316$, $H=1.58$, $t_{r,1}=t_{g,1}=0.316$, and $t_{r,2}=t_{g,2}$.

utilization of high-speed computers. For one set of parameters and for five ring-area intervals on the tube wall, the solution required 10 hours of hand computation. This illustrates the complexities arising in such problems. The results are shown in figure 7-7 in terms of the parameters derived here.

Two additional factors that enter this problem are the conduction boundary conditions. The solution of equation (7-25) requires two boundary conditions because of the arbitrary constants introduced by integrating the d^2t_w/dx^2 term. These boundary conditions depend on the physical construction at the ends of the tube which determine the amount of conduction present. In reference 25, some detailed results were obtained. It was assumed, for simplicity, that the end edges of the tube were insulated, that is,

$$\left. \frac{dT_w}{dX} \right|_{X=0} = \left. \frac{dT_w}{dX} \right|_{X=L} = 0$$

The extension was also made in reference 25 to let the convective heat transfer coefficient vary with position along the tube. This would account for the variation of h in the thermal entrance region.

EXAMPLE 7-8: As a second type of problem including combined conduction, convection, and radiation, consider a fin as shown in figure 7-8. A gas at T_e is flowing over the fin and removing heat by convection.

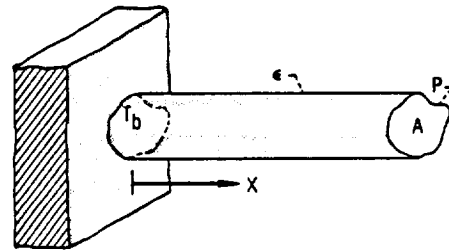


FIGURE 7-8.—Fin of constant cross-sectional area transferring energy by radiation and convection. (Flowing gas and environment at T_e .)

The environment to which the fin radiates is assumed to be at T_e also. The cross section of the fin has area A and perimeter P .

An energy balance on an element of length dX yields

$$kA \frac{d^2T}{dX^2} dX = \epsilon \sigma (T^4 - T_e^4) P dX + hP dX (T - T_e) \quad (7-27)$$

The term on the left is the net conduction into the element. The terms on the right are the radiative and convective losses. The radiative exchange between the fin and its base is being neglected. This equation is to be solved for T as a function of X . Multiply equation (7-27) by $[1/(kA \, dX)]dT/dX$ to obtain

$$\frac{d^2T}{dX^2} \frac{dT}{dX} = \frac{\epsilon\sigma P}{kA} (T^4 - T_e^4) \frac{dT}{dX} + \frac{hP}{kA} (T - T_e) \frac{dT}{dX}$$

This can be integrated once to obtain

$$\frac{1}{2} \left(\frac{dT}{dX} \right)^2 = \frac{\epsilon\sigma P}{kA} \left(\frac{T^5}{5} - TT_e^4 \right) + \frac{hP}{kA} \left(\frac{T^2}{2} - TT_e \right) + C \quad (7-28)$$

where C is a constant of integration.

As a simplified example, let $T_e \approx 0$ and let the fin be very long. Then for large X , $T(X) \rightarrow 0$ and $dT/dX \rightarrow 0$, and from equation (7-28), the constant $C = 0$. Then solving for dT/dX results in

$$\frac{dT}{dX} = - \left(\frac{2}{5} \frac{P\epsilon\sigma}{kA} T^5 + \frac{hP}{kA} T^2 \right)^{1/2} \quad (7-29)$$

The minus sign has been used when taking the square root since T decreases as X increases. The variables in equation (7-29) can be separated and the equation integrated with the condition that $T(X) = T_b$ at $X = 0$,

$$\int_0^X dX = - \int_{T_b}^T \frac{dT}{T \left(\frac{2}{5} \frac{P\epsilon\sigma}{kA} T^3 + \frac{hP}{kA} \right)^{1/2}}$$

Integration yields

$$X = \frac{1}{3} M^{-1/2} \left[\ln \frac{(GT_b^3 + M)^{1/2} - M^{1/2}}{(GT_b^3 + M)^{1/2} + M^{1/2}} - \ln \frac{(GT^3 + M)^{1/2} - M^{1/2}}{(GT^3 + M)^{1/2} + M^{1/2}} \right] \quad (7-30)$$

where $G = (2/5)(P\epsilon\sigma/kA)$ and $M = hP/kA$. Hence, for this simplified case, a closed-form analytical solution for the temperature distribution is obtained.

A detailed treatment of this type of fin problem with both convection and radiation from the surface is given in references 31 to 33.

7.6 COMPUTER PROGRAMS FOR MULTIMODE ENERGY TRANSFER

Except in simple geometries, the solution of problems involving radiation transfer plus energy transfer by other modes becomes exceedingly difficult. Examination of the examples will show that, for this reason, only fairly simple cases have been solved here. Because of the mathematical difficulties involved, a number of generalized finite-difference computer programs have been developed for multimode problems, and some of these are outlined in references 34 to 40. Such programs allow "cookbook" solution of problems that fall within their limitations. Each program referenced allows consideration of combined conduction, radiation, and convection, and most of the programs also allow inclusion of the effects of internal energy generation, flow, transients, variable properties, mass transfer, changes of state, heat capacity in the media considered, and three-dimensional geometries. The referenced programs are all written in one of the Fortran languages, and each uses an electrical network analog as a method of formulating the mathematics and determining values of the input parameters. Though impressive in their generality, these programs are limited by the common assumption of diffuse-gray surfaces, and each has its individual peculiarities and limitations. Whether the researcher cares to take the time to learn the unusual characteristics of a given general program and adapt his particular problem to its limitations, or instead write a specific program of his own, is a matter for each person to decide.

7.7 CONCLUDING REMARKS

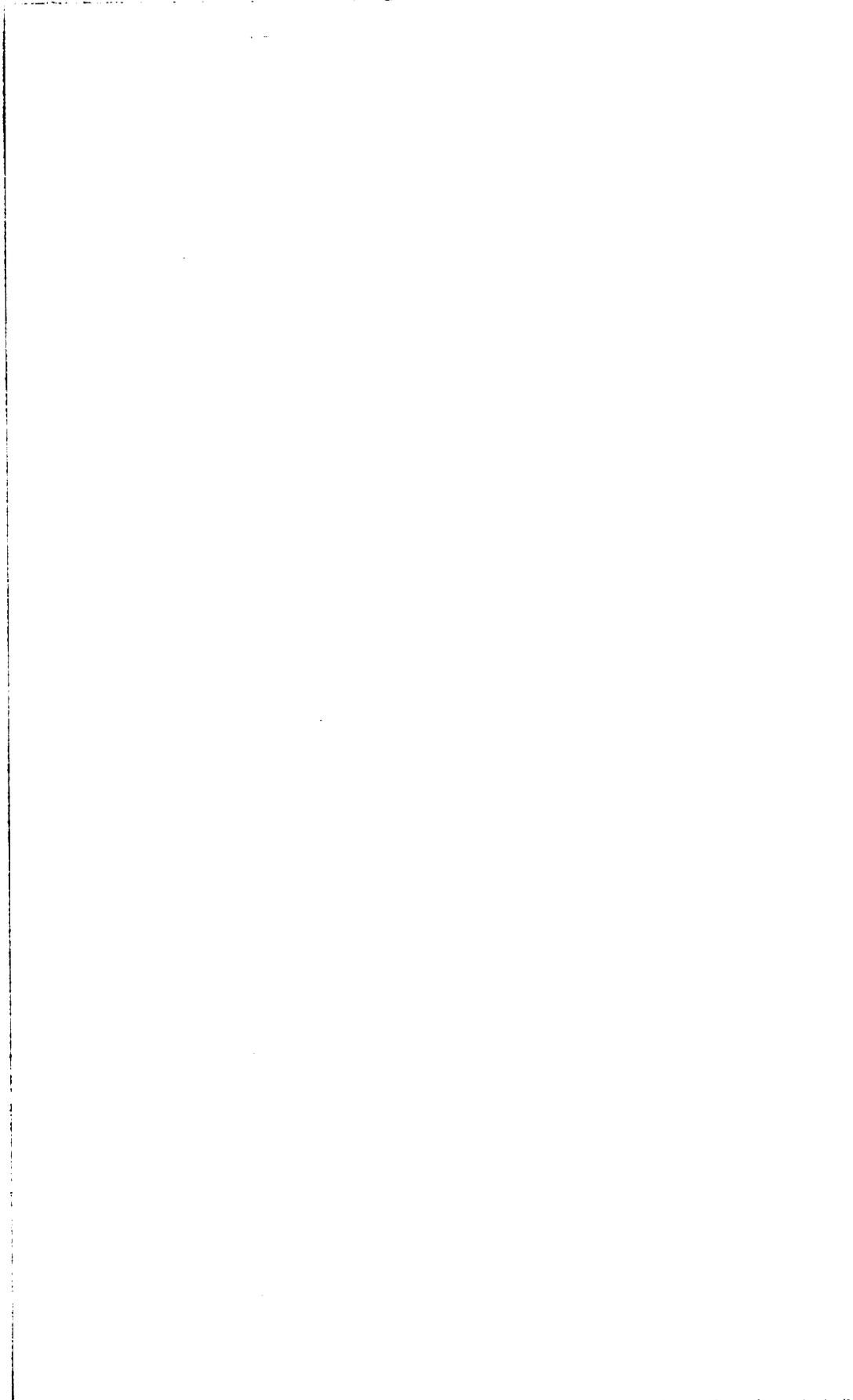
The treatment of multimode energy transfer problems involving radiant transfer through transparent media has been examined. Conceptually, the treatment of such problems involves only the careful construction of energy balance equations over finite areas or on discrete elements. The chief difficulty then becomes the mathematical treatment of these energy balance equations.

Many mathematical methods have been applied with some success to these multimode problems. When a problem of this type is encountered, the techniques that have been successful for similar problems in the literature should be examined. These range from brute force finite-difference formulations through quite sophisticated analytical treatments. The reference list at the end of this chapter gives representative problems and solution techniques along with some expositions of specific mathematical techniques.

REFERENCES

1. CHAMBERS, R. L.; AND SOMERS, E. V.: Radiation Fin Efficiency for One-Dimensional Heat Flow in a Circular Fin. *J. Heat Transfer*, vol. 81, no. 4, Nov. 1959, pp. 327-329.
2. UNGAR, ERIC E.; AND MEKLER, L. A.: Tube Metal Temperatures for Structural Design. *J. Eng. Industry*, vol. 82, no. 3, Aug. 1960, pp. 270-276.
3. MACKAY, DONALD B.; AND LEVENTHAL, E. LEE: Radiant Heat Transfer from a Flat Plate Uniformly Heated on One Edge. Paper No. 23, AIChE Fourth National Heat Transfer Conference, Buffalo, N.Y., Aug. 1960.
4. HICKMAN, R. S.: Transient Response and Steady-State Temperature Distribution in a Heated, Radiating, Circular Plate. Tech. Rep. 32-169, Jet Propulsion Lab., Calif. Inst. Tech., Nov. 22, 1961.
5. WILKINS, J. ERNEST, JR.: Minimum-Mass Thin Fins and Constant Temperature Gradients. *J. Soc. Ind. Appl. Math.*, vol. 10, no. 1, Mar. 1962, pp. 62-73.
6. JAEGER, J. C.: Conduction of Heat in a Solid with a Power Law of Heat Transfer at Its Surface. *Cambridge Philo. Soc. Proc.*, vol. 46, pt. 4, Oct. 1950, pp. 634-641.
7. CHAMBRÉ, PAUL L.: Nonlinear Heat Transfer Problem. *J. Appl. Phys.*, vol. 30, no. 11, Nov. 1959, pp. 1683-1688.
8. ABARBANEL, SAUL S.: Time Dependent Temperature Distribution in Radiating Solids. *J. Math. Phys.*, vol. 39, no. 4, Dec. 1960, pp. 246-257.
9. STOCKMAN, NORBERT O.; AND KRAMER, JOHN L.: Effect of Variable Thermal Properties on One-Dimensional Heat Transfer in Radiating Fins. NASA TN D-1878, 1963.
10. TATOM, JOHN W.: Shell Radiation. Paper No. 60-WA-234, ASME, Nov. 1960.
11. SPARROW, E. M.; AND ECKERT, E. R. G.: Radiant Interaction Between Fin and Base Surfaces. *J. Heat Transfer*, vol. 84, no. 1, Feb. 1962, pp. 12-18.
12. HERING, R. G.: Radiative Heat Exchange Between Conducting Plates With Specular Reflection. Paper No. 65-HT-28, ASME, Aug. 1965.
13. SPARROW, E. M.; MILLER, G. B.; AND JONSSON, V. K.: Radiating Effectiveness of Annular-Finned Space Radiators. Including Mutual Irradiation Between Radiator Elements. *J. Aero/Space Sci.*, vol. 29, no. 11, Nov. 1962, pp. 1291-1299.
14. SCHREIBER, L. H.; MITCHELL, R. P.; GILLESPIE, G. D.; AND OLCOTT, T. M.: Techniques for Optimization of a Finned-Tube Radiator. Paper No. 61-SA-44, ASME, June 1961.
15. HEASLET, MAX A.; AND LOMAX, HARVARD: Numerical Predictions of Radiative Interchange Between Conducting Fins With Mutual Irradiations. NASA TR R-116, 1961.
16. NICHOLS, LESTER D.: Surface-Temperature Distribution on Thin-Walled Bodies Subjected to Solar Radiation in Interplanetary Space. NASA TN D-584, 1961.
17. KOTAN, K.; AND ARNAS, O. A.: On the Optimization of the Design Parameters of Parabolic Radiating Fins. Paper No. 65-HT-42, ASME, Aug. 1965.
18. RUSSELL, LYNN D.; AND CHAPMAN, ALAN J.: Analytical Solution of the "Known-Heat-Load" Space Radiator Problem. *J. Spacecraft Rockets*, vol. 4, no. 3, Mar. 1967, pp. 311-315.
19. NESS, A. J.: Solution of Equations of a Thermal Network on a Digital Computer. *Solar Energy*, vol. 3, no. 2, 1959, p. 37.
20. PERLMUTTER, M.; AND SIEGEL, R.: Heat Transfer by Combined Forced Convection and Thermal Radiation in a Heated Tube. *J. Heat Transfer*, vol. 84, no. 4, Nov. 1962, pp. 301-311.
21. SIEGEL, R.; AND PERLMUTTER, M.: Convective and Radiant Heat Transfer for Flow of a Transparent Gas in a Tube With a Gray Wall. *Int. J. Heat Mass Transfer*, vol. 5, July 1962, pp. 639-660.
22. CESS, R. D.: The Effect of Radiation Upon Forced-Convection Heat Transfer. *Appl. Sci. Res.*, vol. 10, Sec. A, 1961, pp. 430-438.

23. KESHOCK, E. G.; AND SIEGEL, R.: Combined Radiation and Convection in an Asymmetrically Heated Parallel Plate Flow Channel. *J. Heat Transfer*, vol. 86, no. 3, Aug. 1964, pp. 341-350.
24. HOTTEL, H. C.: Geometrical Problems in Radiant Heat Transfer. *Heat Transfer Lectures*. Vol. II. Don Cowen, Comp. Rep. NEPA-979-IER-13, Fairchild Engine and Airplane Corp., June 1, 1949, pp. 76-95.
25. SIEGEL, ROBERT; AND KESHOCK, EDWARD G.: Wall Temperatures in a Tube with Forced Convection, Internal Radiation Exchange, and Axial Wall Heat Conduction. NASA TN D-2116, 1964.
26. ROBBINS, WILLIAM H.; AND TODD, CARROLL A.: Analysis, Feasibility, and Wall-Temperature Distribution of a Radiation-Cooled Nuclear-Rocket Nozzle. NASA TN D-878, 1962.
27. KREBS, RICHARD P.; HALLER, HENRY C.; AND AUER, BRUCE M.: Analysis and Design Procedures for a Flat, Direct-Condensing, Central Finned-Tube Radiator. NASA TN D-2474, 1964.
28. OKAMOTO, YOSHIZO: Thermal Performance of Radiative and Convective Plate-Fins with Mutual Irradiation. *Bull. JSME*, vol. 9, no. 33, 1966, pp. 150-165.
29. OKAMOTO, YOSHIZO: Temperature Distribution and Efficiency of a Single Sheet of Radiative and Convective Fin Accompanied by Internal Heat Source. *Bull. JSME*, vol. 7, no. 28, 1964, pp. 751-758.
30. OKAMOTO, YOSHIZO: Temperature Distribution and Efficiency of a Plate and Annular Fin with Constant Thickness. *Bull. JSME*, vol. 9, no. 33, 1966, pp. 143-150.
31. SHOUMAN, A. R.: An Exact Solution for the Temperature Distribution and Radiant Heat Transfer Along a Constant Cross Sectional Area Fin with Finite Equivalent Surrounding Sink Temperature. *Proceedings of the Ninth Midwestern Mechanics Conference, Madison, Wis., Aug. 16-18, 1965*, pp. 175-186.
32. SHOUMAN, A. R.: Nonlinear Heat Transfer and Temperature Distribution Through Fins and Electric Filaments of Arbitrary Geometry with Temperature-Dependent Properties and Heat Generation. NASA TN D-4257, 1968.
33. SHOUMAN, A. R.: An Exact General Solution for the Temperature Distribution and the Radiation Heat Transfer along a Constant Cross-Sectional-Area Fin. Paper No. 67-WA/HT-27, ASME, Nov. 1967.
34. STRONG, P. F.; AND EMSLIE, A. G.: The Method of Zones for the Calculation of Temperature Distribution. Report No. I. Rep. C-65670, Arthur D. Little Co. (NASA CR-56800), July 1963.
35. SEPETOSKI, W. K.; SOX, C. H.; AND STRONG, P. F.: Description of a Transient Thermal Analysis Program for Use with the Method of Zones. Report No. II. Rep. C-65670, Arthur D. Little Co. (NASA CR-56722), Aug. 1963.
36. BAGWELL, DAVID: TØSS-An IBM-7090 Code for Computing Transient or Steady State Temperature Distributions. Rep. K-1494, Oak Ridge Gaseous Diffusion Plant, Dec. 1, 1961.
37. MINTZ, MICHAEL D.: Finite Difference Representation and Solution of Practical Heat-Transfer Problems. Rep. UCRL-7960 (Rev. 1), Univ. California Lawrence Radiation Lab., 1965.
38. GASKI, J. D.; AND LEWIS, D. R.: Chrysler Improved Numerical Differencing Analyzer: CINDA 3G. Rep. TN-AP-67-287, Chrysler Corp., Space Division, Oct. 1967.
39. STEPHENS, G. L.; AND CAMPBELL, D. J.: Program THTB for Analysis of General Transient Heat Transfer Systems. Rep. R60 FPD 647, General Electric Co., Apr. 1961.
40. SCHULTZ, H. D.: Thermal Analyzer Computer Program for the Solution of General Heat Transfer Problems. Rep. LR-18902, Lockheed California Co. (NASA CR-65581), July 16, 1965.



PRECEDING PAGE BLANK NOT FILMED.

Appendix A

Diffuse Configuration Factors

This appendix contains tables of references to over 150 configuration factors that are available in the literature. The table is composed of three parts. Part (a) is for configuration factors between two elemental surfaces, part (b) gives references for factors between an elemental and a finite surface, and part (c) is for factors between two finite areas. More than one reference is given for some factors, and in certain cases, the reference in which a factor was originally derived is not given because of the difficulty in obtaining such earlier works.

The factors are arranged in the following manner: Factors involving only plane surfaces are given first, followed by those involving cylindrical bodies, conical bodies, spherical bodies, and more complex bodies. Within each such category, progression is made from simpler to more complex geometries.

REFERENCES

1. JAKOB, MAX: Heat Transfer. Vol. 2. John Wiley & Sons, Inc., 1957.
2. SOTOS, CAROL J.; AND STOCKMAN, NORBERT O.: Radiant-Interchange View Factors and Limits of Visibility for Differential Cylindrical Surfaces With Parallel Generating Lines. NASA TN D-2556, 1964.
3. SPARROW, E. M.; AND JONSSON, V. K.: Angle Factors for Radiant Interchange Between Parallel-Oriented Tubes. J. Heat Transfer, vol. 85, no. 4, Nov. 1963, pp. 382-384.
4. USISKIN, C. M.; AND SIEGEL, R.: Thermal Radiation From a Cylindrical Enclosure With Specified Wall Heat Flux. J. Heat Transfer, vol. 82, no. 4, Nov. 1960, pp. 369-374.
5. SPARROW, E. M.; AND CESS, R. C.: Radiation Heat Transfer. Brooks/Cole Publ. Co., 1966.
6. SPARROW, E. M.; ALBERS, L. U.; AND ECKERT, E. R. G.: Thermal Radiation Characteristics of Cylindrical Enclosures. J. Heat Transfer, vol. 84, no. 1, Feb. 1962, pp. 73-81.
7. SPARROW, E. M.; MILLER, G. B.; AND JONSSON, V. K.: Radiative Effectiveness of Annular-Finned Space Radiators, Including Mutual Irradiation Between Radiator Elements. J. Aerospace Sci., vol. 29, no. 11, Nov. 1962, pp. 1291-1299.
8. SPARROW, E. M.; AND JONSSON, V. K.: Radiant Emission Characteristics of Diffuse Conical Cavities. J. Opt. Soc. Am., vol. 53, no. 7, July 1963, pp. 816-821.
9. KEZIOS, STOTHE P.; AND WULFF, WOLFGANG: Radiative Heat Transfer Through Openings of Variable Cross Sections. Proceedings of the Third International Heat Transfer Conference. Vol. 5. AIChE, 1966, pp. 207-218.
10. SPARROW, E. M.; AND JONSSON, V. K.: Absorption and Emission Characteristics of Diffuse Spherical Enclosures. NASA TN D-1289, 1962.

11. NICHOLS, LESTER D.: Surface-Temperature Distribution on Thin-Walled Bodies Subjected to Solar Radiation in Interplanetary Space. NASA TN D-584, 1961.
12. CAMPBELL, JAMES P.; AND MCCONNELL, DUDLEY G.: Radiant-Interchange Configuration Factors for Spherical and Conical Surfaces to Spheres. NASA TN D-4457, 1968.
13. GRIER, NORMAN T.; AND SOMMERS, RALPH D.: View Factors for Toroids and Their Parts. NASA TN D-5006, 1969.
14. HAMILTON, D. C.; AND MORGAN, W. R.: Radiant-Interchange Configuration Factors. NACA TN 2836, 1952.
15. KREITH, FRANK: Radiation Heat Transfer. International Textbook Co., 1962.
16. WIEBELT, JOHN A.: Engineering Radiation Heat Transfer. Holt, Rinehart and Winston, 1966.
17. MOON, PARRY: The Scientific Basis of Illuminating Engineering. Dover Publications, Inc., 1961.
18. STEVENSON, J. A.; AND GRAFTON, J. C.: Radiation Heat Transfer Analysis for Space Vehicles. Rep. SID-61-91, North American Aviation (AFASD TR 61-119, pt. 1), Sept. 9, 1961.
19. HOTTEL, H. C.; AND SAROFIM, A. F.: Radiation Transfer. McGraw-Hill Book Co., Inc., 1967.
20. HOTTEL, H. C.: Radiant-Heat Transmission. Heat Transmission. Third ed., William H. McAdams, McGraw-Hill Book Co., Inc., 1954, pp. 55-125.
21. LEUENBERGER, H.; AND PERSON, R. A.: Compilation of Radiation Shape Factors for Cylindrical Assemblies. Paper No. 56-A-144, ASME, Nov. 1956.
22. SPARROW, E. M.; AND ECKERT, E. R. G.: Radiant Interaction between Fin and Base Surfaces. J. Heat Transfer, vol. 84, no. 1, Feb. 1962, pp. 12-18.
23. HOLCOMB, R. S.; AND LYNCH, F. E.: Thermal Radiation Performance of a Finned Tube with a Reflector. Rep. No. ORNL-TM-1613, Oak Ridge National Lab., Apr. 1967.
24. JOERG, PIERRE; AND MCFARLAND, B. L.: Radiation Effects in Rocket Nozzles. Rep. No. S62-245, Aerojet-General Corp., 1962.
25. CUNNINGHAM, F. G.: Power Input to a Small Flat Plate from a Diffusely Radiating Sphere, with Application to Earth Satellites. NASA TN D-710, 1961.
26. LIEBERT, CURT H.; AND HIBBARD, ROBERT R.: Theoretical Temperatures of Thin-Film Solar Cells in Earth Orbit. NASA TN D-4331, 1968.
27. GOETZE, DIETER; AND GROSCH, CHARLES B.: Earth-Emitted Infrared Radiation Incident Upon a Satellite. J. Aerospace Sci., vol. 29, no. 5, May 1962, pp. 521-524.
28. MORIZUMI, S. J.: Analytical Determination of Shape Factors from a Surface Element to an Axisymmetric Surface. AIAA J., vol. 2, no. 11, Nov. 1964, pp. 2028-2030.
29. ROBBINS, WILLIAM H.; AND TODD, CARROLL A.: Analysis, Feasibility, and Wall-Temperature Distribution of a Radiation-Cooled Nuclear-Rocket Nozzle. NASA TN D-878, 1962.
30. ROBBINS, WILLIAM H.: An Analysis of Thermal Radiation Heat Transfer in a Nuclear-Rocket Nozzle. NASA TN D-586, 1961.
31. FEINGOLD, A.: Radiant-Interchange Configuration Factors Between Various Selected Plane Surfaces. Proc. Roy. Soc., Ser. A, vol. 292, no. 1428, May 3, 1966, pp. 51-60.
32. HSU, CHIA-JUNG: Shape Factor Equations for Radiant Heat Transfer Between Two Arbitrary Sizes of Rectangular Planes. Can. J. Chem. Eng., vol. 45, no. 1, Feb. 1967, pp. 58-60.
33. DUMMER, R. S.; AND BRECKENRIDGE, W. T., JR.: Radiation Configuration Factors Program. Rep. ERR-AN-224, General Dynamics/Astronautics, Feb. 1963.
34. PLAMONDON, JOSEPH A.: Numerical Determination of Radiation Configuration Factors for Some Common Geometrical Situations. Tech. Rep. 32-127, Jet Propulsion Lab., California Inst. Tech., July 7, 1961.

35. TRIPP, W.; HWANG, C.; AND CRANK, R. E.: Radiation Shape Factors for Plane Surfaces and Spheres, Circles or Cylinders. Special Rep. No. 16, Kansas State Univ. Bull., vol. 46, no. 4, Apr. 1962.
36. BIEN, DARL D.: Configuration Factors for Thermal Radiation From Isothermal Inner Walls of Cones and Cylinders. J. Spacecraft Rockets, vol. 3, no. 1, Jan. 1966, pp. 155-156.
37. BUSCHMAN, ALBERT J., JR.; AND PITTMAN, CLAUD M.: Configuration Factors for Exchange of Radiant Energy Between Axisymmetrical Sections of Cylinders, Cones, and Hemispheres and Their Bases. NASA TN D-944, 1961.
38. STEPHENS, CHARLES W.; AND HAIRE, ALAN M.: Internal Design Considerations for Cavity-Type Solar Absorbers. ARS J., vol. 31, no. 7, July 1961, pp. 896-901.
39. WIEBELT, J. A.; AND RUO, S. Y.: Radiant-Interchange Configuration Factors for Finite Right Circular Cylinder to Rectangular Planes. Int. J. Heat Mass Transfer, vol. 6, no. 2, Feb. 1963, pp. 143-146.
40. ALEKSANDROV, V. T.: Determination of the Angular Radiation Coefficients for a System of Two Coaxial Cylindrical Bodies. Inz.-Fiz. Zh., vol. 8, no. 5, May 1965, pp. 609-612.
41. WATTS, R. G.: Radiant Heat Transfer to Earth Satellites. J. Heat Transfer, vol. 87, no. 3, Aug. 1965, pp. 369-373.
42. JONES, L. R.: Diffuse Radiation View Factors Between Two Spheres. J. Heat Transfer, vol. 87, no. 3, Aug. 1965, pp. 421-422.
43. STASENKO, A. L.: Self-Irradiation Coefficient of a Moebius Strip of Given Shape. Akad. Nauk SSSR, Izv. Energetika i Transport, July-Aug. 1967, pp. 104-107.
44. TOUPS, K. A.: A General Computer Program for the Determination of Radiant-Interchange Configuration and Form Factors: Confac-I. Rep. SID-65-1043-1, North American Aviation, Inc. (NASA CR-65256), Oct. 1965.

TABLE A-I.—TABLE OF REFERENCES FOR CONFIGURATION FACTORS
 (a) Factors for two differential elements

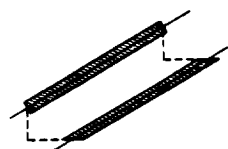
Configuration number	Geometry	Configuration	Source
A-1	Two elemental areas in arbitrary configuration		Eq. (2-8)
A-2	Two elemental areas lying on parallel generating lines		Example 2-3
A-3	Elemental area to infinitely long strip of differential width lying on parallel generating line		Example 2-4 and ref. 1
A-4	Infinitely long strip of differential width to similar strip on parallel generating line		Example 2-4 and ref. 1
A-5	Strip of finite length and differential width to strip of same length on parallel generating line		Ref. 2

TABLE A-I.—TABLE OF REFERENCES FOR CONFIGURATION FACTORS—Continued
 (a) Factors for two differential elements—Continued

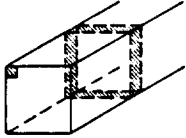
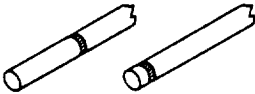
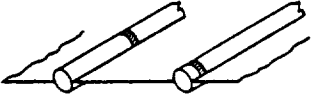
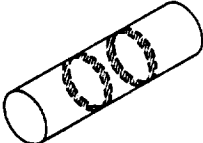
Configuration number	Geometry	Configuration	Source
A-6	Corner element of end of square channel to sectional wall element on channel		Example 2-19
A-7	Exterior element on tube surface to exterior element on adjacent parallel tube of same diameter		Ref. 3
A-8	Exterior element on partitioned tube to similar element on adjacent parallel tube of same diameter		Ref. 3
A-9	Two ring elements on interior of right circular cylinder		Refs. 4, 5

TABLE A-I.—TABLE OF REFERENCES FOR CONFIGURATION FACTORS—Continued
 (a) Factors for two differential elements—Continued

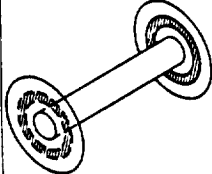
Configuration number	Geometry	Configuration	Source
A-10	Band of differential length on inside of cylinder to differential ring on cylinder base		Ref. 6
A-11	Ring element on f_1 to ring element on adjacent f_2		Ref. 7
A-12	Two elements on interior of right circular cone		Refs. 8, 9

TABLE A-I.—TABLE OF REFERENCES FOR CONFIGURATION FACTORS—Continued
 (a) Factors for two differential elements—Concluded

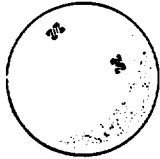
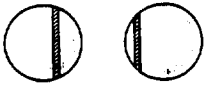
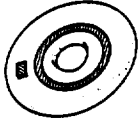
Configuration number	Geometry	Configuration	Source
A-13	Two differential elements on interior of spherical cavity		Refs. 1, 5, 9-11
A-14	Band on outside of sphere to band on another sphere of same radius		Ref. 12
A-15	Two differential elements on exterior of toroid		Ref. 13
A-16	Element on exterior of toroid to ring element on exterior of toroid		Ref. 13
A-17	Element on exterior of toroid to hoop element on exterior of toroid		Ref. 13

TABLE A-I.—TABLE OF REFERENCES FOR CONFIGURATION FACTORS—Continued
 (b) Factors for exchange between differential element and finite area

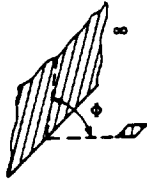
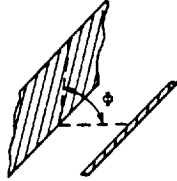
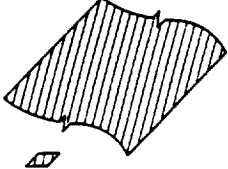
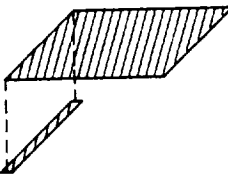
Configuration number	Geometry	Configuration	Source
B-1	Plane element to plane extending to infinity and intersecting plane of element at angle ϕ		Refs. 14-16
B-2	Plane strip element of any length to plane of finite width and infinite length		Example 2-7
B-3	Plane element to infinitely long surface of arbitrary shape generated by line moving parallel to itself and plane of element		Refs. 14-18
B-4	Strip element of finite length to rectangle in plane parallel to strip; strip is opposite to one edge of rectangle		Refs. 5, 14-16

TABLE A-I.—TABLE OF REFERENCES FOR CONFIGURATION FACTORS—Continued
 (b) Factors for exchange between differential element and finite area—Continued

Configuration number	Geometry	Configuration	Source
B-5	Strip element of finite length to plane rectangle that intercepts plane of strip at angle ϕ and with one edge parallel to strip		Refs. 5 (for $\phi = 90^\circ$ only), 14-16
B-6	Plane element to plane rectangle; normal to element passes through corner of rectangle; surfaces are on parallel planes		Refs. 1, 5, 14-17, 19, 20
B-7	Area element to any parallel rectangle		Ref. 1
B-8	Plane element to plane rectangle; planes containing two surfaces intersect at angle ϕ		Refs. 1, 5 (for $\phi = 90^\circ$ only), 14-16

TABLE A-I.—TABLE OF REFERENCES FOR CONFIGURATION FACTORS—Continued
 (b) Factors for exchange between differential element and finite area—Continued

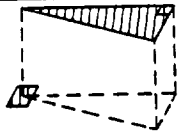
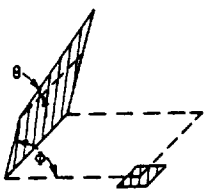
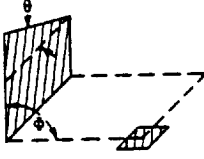
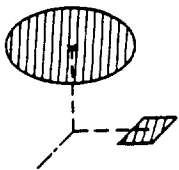
Configuration number	Geometry	Configuration	Source
8-9	Plane element to right triangle in plane parallel to plane of element; normal to element passes through vertex of triangle		Example 2-17
8-10	Plane element to plane area with added triangular area; element is on corner of rectangle with one side in common with plane area at angle ϕ		Refs. 14-16
8-11	Same geometry as preceding with triangle reversed relative to plane element		Refs. 14-16
8-12	Plane element to circular disk on plane parallel to that of element		Refs. 1, 5, 14-16

TABLE A-I.—TABLE OF REFERENCES FOR CONFIGURATION FACTORS—Continued
 (b) Factors for exchange between differential element and finite area—Continued

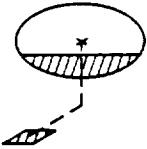
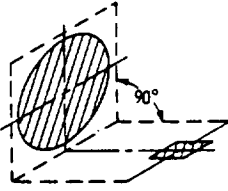
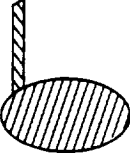
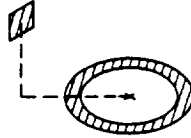
Configuration number	Geometry	Configuration	Source
B-13	Plane element to segment of disk in plane parallel to element		Ref. 5
B-14	Plane element to circular disk; planes containing element and disk intersect at 90°, and centers of element and disk lie in plane perpendicular to those containing areas		Refs. 5, 14-16, 18, 21 and example 2-6
B-15	Strip element of finite length to perpendicular circular disk located at one end of strip		Refs. 18, 21
B-16	Plane element to ring area in plane perpendicular to element		Example 2-9

TABLE A-I.—TABLE OF REFERENCES FOR CONFIGURATION FACTORS—Continued
 (b) Factors for exchange between differential element and finite area—Continued

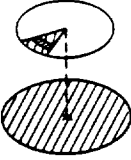
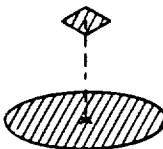
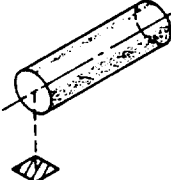
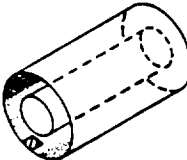
Configuration number	Geometry	Configuration	Source
B-17	Radial and wedge elements on circle to disk in parallel plane		Refs. 19, 21
B-18	Area element to parallel elliptical plate		Ref. 17
B-19	Plane element to right circular cylinder of finite length; normal to element passes through center of one end of cylinder and is perpendicular to cylinder axis		Refs. 5, 14-16
B-20	Element is at end of wall on inside of finite length cylinder enclosing concentric cylinder of same length; factor is from element to inside surface of outer cylinder		Refs. 14-16, 18, 21

TABLE A-I.—TABLE OF REFERENCES FOR CONFIGURATION FACTORS—Continued
 (b) Factors for exchange between differential element and finite area—Continued

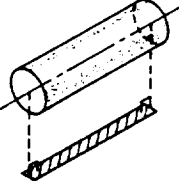
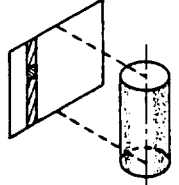
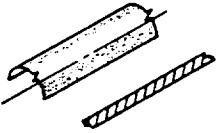
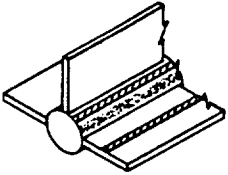
Configuration number	Geometry	Configuration	Source
B-21	Elemental strip of finite length to parallel cylinder of same length; normals at ends of strip pass through cylinder axis		Refs. 14-16, 18, 21
B-22	Strip or element on plane parallel to cylinder axis to cylinder of finite length		Refs. 18, 21
B-23	Infinitely long strip of differential width to parallel semicylinder		Ref. 22
B-24	Infinite strip on any side of any of three fins to tube or environment, and infinite strip on tube to fin or environment		Ref. 23

TABLE A-I.—TABLE OF REFERENCES FOR CONFIGURATION FACTORS—Continued
 (b) Factors for exchange between differential element and finite area—Continued

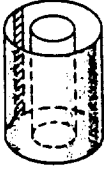
Configuration number	Geometry	Configuration	Source
B-25	Element and strip element on interior of finite cylinder to interior of cylindrical surface		Refs. 18, 21
B-26	Elemental strip on inner surface of outer concentric cylinder to surface of <u>outer</u> concentric cylinder		Refs. 14-16, 18, 21
B-27	Elemental strip on inner surface of outer concentric cylinder to either annular end		Refs. 14-16, 18, 21
B-28	Element on inside of outer finite concentric cylinder to inside cylinder or annular end		Refs. 18, 21

TABLE A-I.—TABLE OF REFERENCES FOR CONFIGURATION FACTORS—Continued
 (b) Factors for exchange between differential element and finite area—Continued

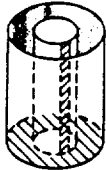
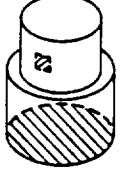
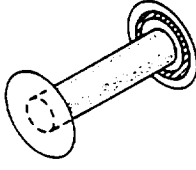
Configuration number	Geometry	Configuration	Source
B-29	Strip element on exterior of inner finite length concentric cylinder to inside of outer cylinder or to annular end		Refs. 18, 21
B-30	Strip on plane inside cylinder of finite length to inside of cylinder		Refs. 18, 21
B-31	Area element on interior of cylinder to base of second concentric cylinder; cylinders are one atop other		Refs. 18, 21
B-32	Ring element on fin to tube		Ref. 7

TABLE A-I.—TABLE OF REFERENCES FOR CONFIGURATION FACTORS—Continued
 (b) Factors for exchange between differential element and finite area—Continued

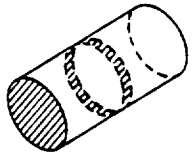
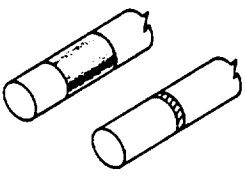
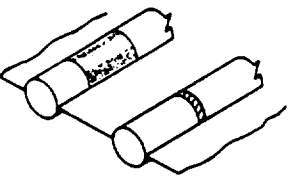
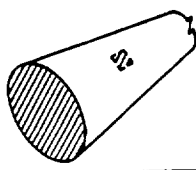
Configuration number	Geometry	Configuration	Source
B-33	Ring element on interior of right circular cylinder to end of cylinder		Ref. 4
B-34	Exterior element on tube surface to finite area on adjacent parallel tube of same diameter		Ref. 3
B-35	Exterior element on tube surface of partitioned tube to finite area on adjacent parallel tube of same diameter		Ref. 3
B-36	Element on wall of right circular cone to base of cone		Ref. 24

TABLE A-1.—TABLE OF REFERENCES FOR CONFIGURATION FACTORS—Continued
 (b) Factors for exchange between differential element and finite area—Continued

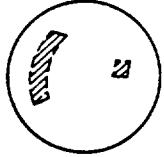
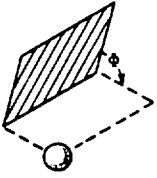
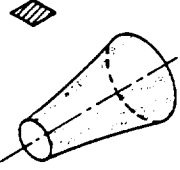
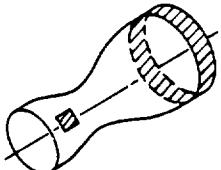
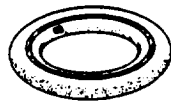
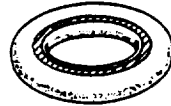
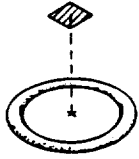
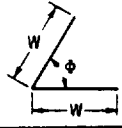
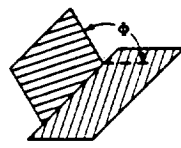
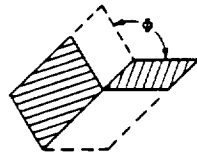
Configuration number	Geometry	Configuration	Source
B-37	Any infinitesimal element on interior of sphere to any finite element on interior of same sphere		Ref. 1 and section 3, 4, 2, 5
B-38	Spherical point source to rectangle. Point source is on one corner of rectangle that intersects with receiving rectangle at angle ϕ		Refs. 1, 14-16
B-39	Area element to sphere		Refs. 15, 25-27
B-40	Area element to axisymmetric surface - paraboloid, cone, cylinder (formulation given - factors are not evaluated)		Ref. 28

TABLE A-I.—TABLE OF REFERENCES FOR CONFIGURATION FACTORS—Continued
 (b) Factors for exchange between differential element and finite area—Concluded

Configuration number	Geometry	Configuration	Source
B-41	Element on interior (or exterior) of any axisymmetric body of revolution to band of finite length on interior (or exterior)		Refs. ^a 29, ^a 30
B-42	Element on exterior of toroid to toroidal segment of finite width		Ref. 13
B-43	Element on exterior of toroid to toroidal band of finite width		Ref. 13
B-44	Element and ring element on exterior of toroid to entire exterior of toroid		Ref. 13
B-45	Slender torus to point on perpendicular axis		Ref. 17

^aKernel of integrals and limits are formulated in terms of appropriate variables, but integrations are not carried out explicitly.

TABLE A-I.—TABLE OF REFERENCES FOR CONFIGURATION FACTORS—Continued
(c) Factors for two finite areas

Configuration number	Geometry	Configuration	Source
C-1	Two infinitely long plates of equal finite width W and one common edge of included angle ϕ		Example 2-8
C-2	Two infinitely long plates of unequal width with one common edge and included angle $\phi = 90^\circ$		Ref. 15
C-3	Finite rectangle to infinitely long rectangle of same width and with one common edge		Ref. 31
C-4	Two finite rectangles of same width with common edge and included angle ϕ		Refs. 1, 19, 20 (for $\phi = 90^\circ$ only), 5, 14-16, 18, ^b 31
C-5	Two rectangles with common edge and included angle ϕ		Ref. 15
C-6	Two rectangles with one side of each parallel, and with one corner touching; planes containing rectangles intersect at angle ϕ		Ref. 15

^bRef. 31 indicates that tabulated values for this case are incorrect in all other references. Corrected values are listed in ref. 31.

TABLE A-I.—TABLE OF REFERENCES FOR CONFIGURATION FACTORS—Continued
 (c) Factors for two finite areas—Continued

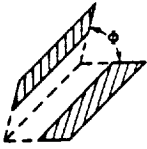
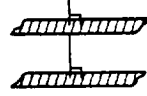
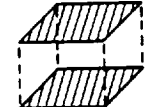
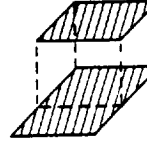
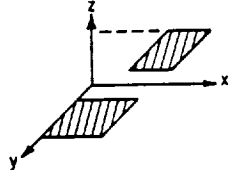
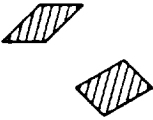
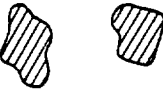
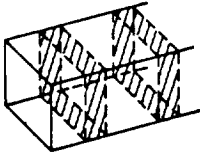
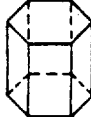
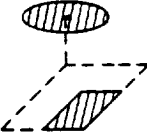
Configuration number	Geometry	Configuration	Source
C-7	Two rectangles of same width with one parallel edge; planes containing rectangles intersect at angle ϕ		Ref. 5 (for $\phi = 90^\circ$ only), 15
C-8	Two rectangles with one parallel edge; planes containing rectangles intersect at angle ϕ		Refs. 14, 15, 18
C-9	Two infinitely long directly opposed parallel strips of same finite width		Refs. 15, 19
C-10	Parallel, directly opposed rectangles of same width and length		Refs. 1, 5, 14-16, 19, 20, 32
C-11	Two rectangles in parallel planes with one rectangle directly opposite portion of other		Refs. 15, 17, 32
C-12	Two rectangles of arbitrary size in parallel planes; all sides lie parallel to x and y axes		Refs. 14, 15, 18, 32

TABLE A-I.—TABLE OF REFERENCES FOR CONFIGURATION FACTORS—Continued
(c) Factors for two finite areas—Continued

Configuration number	Geometry	Configuration	Source
C-13	Rectangle to arbitrarily oriented rectangle of arbitrary size		Ref. ^c 33
C-14	Two flat plates of arbitrary shape and arbitrary orientation		Ref. ^a 34
C-15	Finite areas on interior of square channel		Ref. 18
C-16	Factor between bases of right convex prism of regular triangular, square, pentagonal, hexagonal, or octagonal cross section		Ref. 31
C-17	Factors between various sides, and sides and bases of regular hexagonal prism		Ref. 31
C-18	Circular disk to arbitrarily placed rectangle in parallel plane (using configuration factor algebra with configuration number C-21)		Ref. 35

^aKernel of Integrals and limits are formulated in terms of appropriate variables, but Integrations are not carried out explicitly.

^cAvailable as general computer program only.

TABLE A-I.—TABLE OF REFERENCES FOR CONFIGURATION FACTORS—Continued
 (c) Factors for two finite areas—Continued

Configuration number	Geometry	Configuration	Source
C-19	Circle to arbitrarily placed rectangle in plane parallel to normal to circle (using configuration factor algebra with configuration number C-21)		Ref. 35
C-20	Disk to arbitrarily oriented rectangle or disk of arbitrary size		Ref. C33
C-21	Circular disk to parallel right triangle; normal from center of circle passes through one acute vertex		Ref. 35
C-22	Parallel, directly opposed plane circular disks		Refs. 1, 5, 9, 14-16, 18, 19, 21
C-23	Directly opposed ring and disk of arbitrary radii		Refs. 15, 21

^cAvailable as general computer program only.

TABLE A-I.—TABLE OF REFERENCES FOR CONFIGURATION FACTORS—Continued
 (c) Factors for two finite areas—Continued

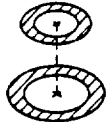
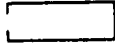
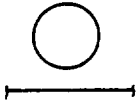
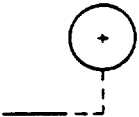
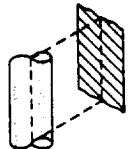
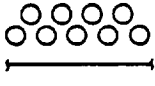
Configuration number	Geometry	Configuration	Source
C-24	Parallel, directly opposed plane ring areas		Refs. 14, 21 and example 2-10
C-25	Entire inner wall of finite cylinder to ends		Refs. 36, 37
C-26	Internal surface of cylindrical cavity to cavity opening		Refs. 15 (fig. 6-14), 38
C-27	Inner surface of cylinder to annulus on one end		Refs. 21, 37
C-28	Inner surface of cylinder to disk at one end of cylinder		Refs. 21, 37
C-29	Portion of inner surface of cylinder to remainder of inner surface		Refs. 19, 21, 37

TABLE A-I.—TABLE OF REFERENCES FOR CONFIGURATION FACTORS—Continued
 (c) Factors for two finite areas—Continued

Configuration number	Geometry	Configuration	Source
C-30	Finite ring areas on interior of right circular cylinders to separate similar areas and to ends		Refs. 18, 19, 37
C-31	Finite areas on interior of right circular cylinder		Ref. 18
C-32	Infinitely long cylinder to infinite plane; axis of cylinder parallel to plane		Refs. 14-16
C-33	Infinite cylinder to parallel infinitely long plane of finite width		Refs. 5, 14, 15 ^a
C-34	Infinitely long plane of finite width to infinitely long cylinder		Ref. 21
C-35	Infinite plane to first, second, and first plus second rows of infinitely long parallel tubes of equal diameter		Refs. 1, 19, 20

^aErroneously given in references. With the notation of ref. 5, should be

$$F_{1-2} = \frac{1}{Z - Y} \left(\tan^{-1} \frac{Z}{X} - \tan^{-1} \frac{Y}{X} \right)$$

TABLE A-I.—TABLE OF REFERENCES FOR CONFIGURATION FACTORS—Continued
 (c) Factors for two finite areas—Continued

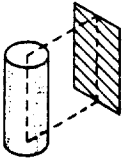
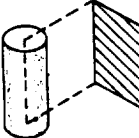
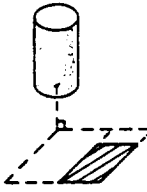
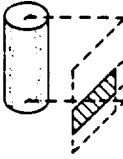
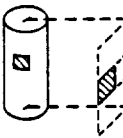
Configuration number	Geometry	Configuration	Source
C-36	Finite length cylinder to rectangle with one edge parallel to cylinder axis and of length equal to cylinder		Ref. 5
C-37	Finite cylinder to finite rectangle of same length		Ref. 39
C-38	Cylinder to any rectangle in plane perpendicular to cylinder axis (using configuration factor algebra with configuration number C-42)		Ref. 35
C-39	Cylinder to any rectangle in plane parallel to cylinder axis (using configuration factor algebra with configuration number C-42)		Ref. 35
C-40	Finite area on exterior of cylinder to finite area on plane parallel to cylinder axis		Ref. 18

TABLE A-I.—TABLE OF REFERENCES FOR CONFIGURATION FACTORS—Continued
 (c) Factors for two finite areas—Continued

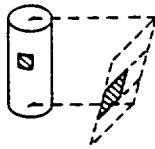
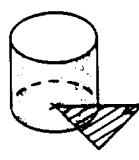
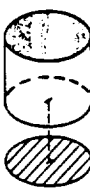
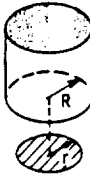
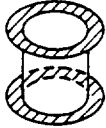
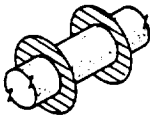
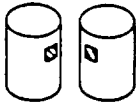
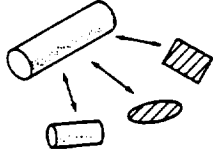
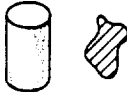
Configuration number	Geometry	Configuration	Source
C-41	Finite area on exterior of cylinder to finite area on skewed plane	 A diagram showing a cylinder on the left and a skewed rectangular plane on the right. Dashed lines indicate the projection of the plane's corners onto the cylinder's surface.	Ref. 18
C-42	Outside surface of cylinder to perpendicular right triangle; triangle is in plane of cylinder base with one vertex of triangle at center of base	 A diagram showing a cylinder on the left and a right-angled triangle on the right. The triangle is positioned such that its hypotenuse is parallel to the cylinder's base, and one of its vertices is at the center of the base.	Ref. 35
C-43	Cylinder and plane of equal length parallel to cylinder axis; plane inside cylinder; all factors between plane and inner surface of cylinder	 A diagram showing a cylinder with a vertical plane inside it. The plane is parallel to the cylinder's axis and extends from the top to the bottom of the cylinder.	Refs. 18, 21
C-44	Inner surface of cylinder to disk of same radius	 A diagram showing a cylinder on the left and a shaded disk on the right. The disk is positioned below the cylinder, and its radius is indicated as being equal to the cylinder's radius.	Refs. 18, 21
C-45	Interior surface of circular cylinder of radius R to disk of radius r where $r < R$; disk is perpendicular to axis of cylinder, and axis passes through center of disk (using configuration factor algebra with configuration number C-22)	 A diagram showing a cylinder on the left and a shaded disk on the right. The disk is positioned below the cylinder, and its radius is indicated as being smaller than the cylinder's radius. The cylinder's radius is labeled as R .	Example 2-11

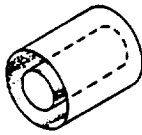
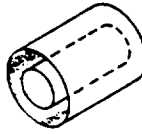
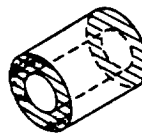
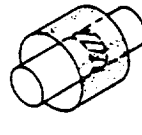
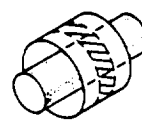
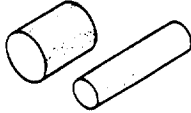
TABLE A-I.—TABLE OF REFERENCES FOR CONFIGURATION FACTORS—Continued
 (c) Factors for two finite areas—Continued

Configuration number	Geometry	Configuration	Source
C-46	Annular ring to similar annular ring each at end of cylinder		Refs. 7, 18, 21
C-47	Factors for interchange between fins and tube (given in algebraic form, untabulated)		Ref. 7
C-48	Finite area on exterior of cylinder to finite area on exterior of parallel cylinder		Ref. 18
C-49	Cylinder of arbitrary length and radius to rectangle, disk, or cylinder of arbitrary size and orientation		Ref. ^c 33
C-50	Cylinder and plate with arbitrary orientation		Ref. ^a 34
C-51	Concentric cylinders of infinite length; inner to outer cylinder; outer to inner cylinder; outer cylinder to itself		Ref. 14

^aKernel of integrals and limits are formulated in terms of appropriate variables, but integrations are not carried out explicitly.

^cAvailable as general computer program only.

TABLE A-I.—TABLE OF REFERENCES FOR CONFIGURATION FACTORS—Continued
 (c) Factors for two finite areas—Continued

Configuration number	Geometry	Configuration	Source
C-52	Inside surface of outer concentric cylinder of finite length to inner cylinder of same length		Refs. 5, 14, 19, 21, 40
C-53	Inside surface of outer concentric cylinder to itself		Refs. 5, 7, 14, 21, 40
C-54	Inside surface of outer concentric cylinder to either end of annulus		Refs. 5, 14, 21, 40
C-55	Concentric cylinders of different finite lengths - portion of inner cylinder to entire outer cylinder		Ref. 21
C-56	Concentric cylinders of different finite lengths - portion of inside of outer to outside of entire inner cylinder		Refs. 18, 21, ^a 34
C-57	Parallel cylinders of different radii and length - any portions of outer curved surfaces		Ref. ^a 34

^aKernel of integrals and limits are formulated in terms of appropriate variables, but integrations are not carried out explicitly.

TABLE A-I.—TABLE OF REFERENCES FOR CONFIGURATION FACTORS—Continued
(c) Factors for two finite areas—Continued

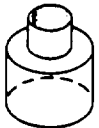
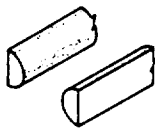
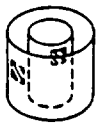
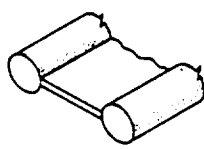
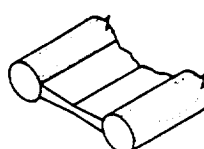
Configu- ration number	Geometry	Configuration	Source
C-58	Concentric cylinders of different radii, one atop other; factors between inside of upper cylinder and inside or base of lower cylinder		Refs. 18, 21
C-59	Infinitely long parallel semi-cylinders of same diameter		Example 2-16 and ref. 5
C-60	Finite area on exterior of inner cylinder to finite area on interior of concentric outer cylinder		Ref. 18
C-61	Two tubes connected with fin of finite thickness; length can be finite or infinite; all factors between finite surfaces formulated in terms of integrations between differential strips		Ref. 2
C-62	Two tubes connected with tapered fins of finite thickness; length can be finite or infinite; all factors between finite surfaces formulated in terms of integrations between differential strips		Ref. 2

TABLE A-I.—TABLE OF REFERENCES FOR CONFIGURATION FACTORS—Continued
 (c) Factors for two finite areas—Continued

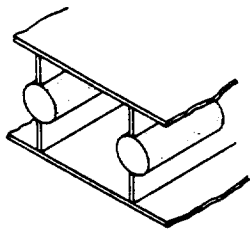
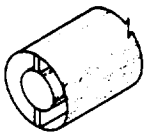
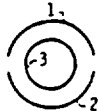
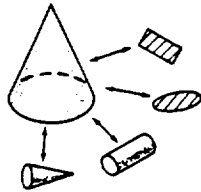
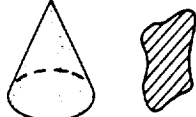
Configuration number	Geometry	Configuration	Source
C-63	Sandwich tube and fin structure of infinite or finite length; all factors between finite surfaces formulated in terms of integrations between differential strips		Ref. 2
C-64	Concentric cylinders connected by fin of finite thickness; length finite or infinite; all factors between finite surfaces formulated in terms of integrations between differential strips		Ref. 2
C-65	Exterior of infinitely long cylinder to interior of concentric semicylinder		Example 2-22
C-66	Interior of infinitely long semicylinder 1 to interior of semicylinder 2 when concentric parallel cylinder 3 is present		Example 2-22
C-67	Between axisymmetrical sections of right circular cone		Refs. 18, 37

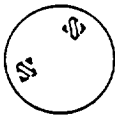
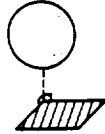
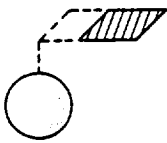
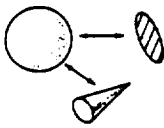
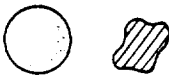
TABLE A-I.—TABLE OF REFERENCES FOR CONFIGURATION FACTORS—Continued
(c) Factors for two finite areas—Continued

Configuration number	Geometry	Configuration	Source
C-68	Between axisymmetrical sections of right circular cone and base or ring or disk on base		Refs. 19, 37
C-69	Internal surface of conical cavity to cavity opening		Refs. 15 (fig. 6-14), 37, 38
C-70	Entire inner surface of frustum of cone to ends		Refs. 36, 37
C-71	Right circular cone of arbitrary size to rectangle, disk, cylinder, or cone of arbitrary size and orientation		Ref. C33
C-72	Cone to arbitrarily skewed plate		Ref. a34
C-73	Internal surface of spherical cavity to cavity opening		Refs. 15 (fig. 6-14), 38

^aKernel of integrals and limits are formulated in terms of appropriate variables, but integrations are not carried out explicitly.

^cAvailable as general computer program only.

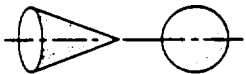
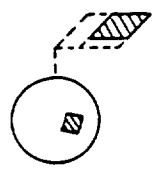
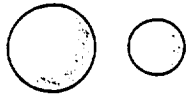
TABLE A-I.—TABLE OF REFERENCES FOR CONFIGURATION FACTORS—Continued
 (c) Factors for two finite areas—Continued

Configuration number	Geometry	Configuration	Source
C-74	Any finite area on interior of sphere to any other finite area on interior		Section 3.4.2.5 and ref. 1
C-75	Finite sphere to rectangle		Ref. 35
C-76	Sphere to arbitrary rectangle (using configuration factor algebra and configuration number C-75)		Refs. C33, 35
C-77	Sphere of arbitrary diameter to disk or cone of arbitrary size and orientation		Ref. C33
C-78	Sphere to arbitrarily skewed plate		Ref. 234
C-79	Sphere to cylinder		Refs. C33, 41

^aKernel of integrals and limits are formulated in terms of appropriate variables, but integrations are not carried out explicitly.

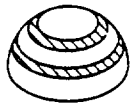
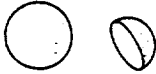
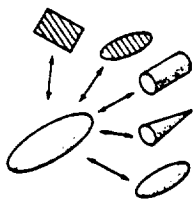
^cAvailable as general computer program only.

TABLE A-I.—TABLE OF REFERENCES FOR CONFIGURATION FACTORS—Continued
 (c) Factors for two finite areas—Continued

Configuration number	Geometry	Configuration	Source
C-80	Cone to sphere having same diameter as base of cone; axis of cone passes through center of sphere		Refs. 12, ^C 33
C-81	Concentric spheres; inner to outer sphere; outer to inner sphere; outer sphere to itself		Refs. 14, 15, and example 2-13
C-82	Area on surface of sphere to rectangle in plane perpendicular to axis of sphere		Ref. 18
C-83	Sphere to sphere		Refs. 12, ^C 33, 41, 42 (equal spheres)
C-84	Internal surface of hemispherical cavity to cavity opening		Refs. 15 (fig. 6-14), 37, 38
C-85	Between axisymmetrical section of hemisphere and base or ring or disk on base		Ref. 37

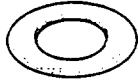
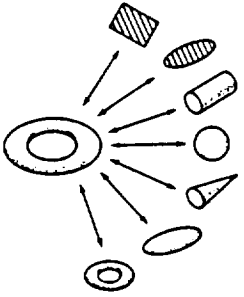
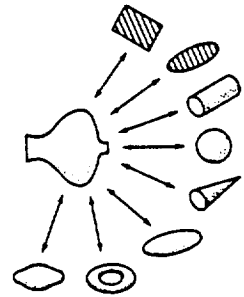
^CAvailable as general computer program only.

TABLE A-I.—TABLE OF REFERENCES FOR CONFIGURATION FACTORS—Continued
 (c) Factors for two finite areas—Continued

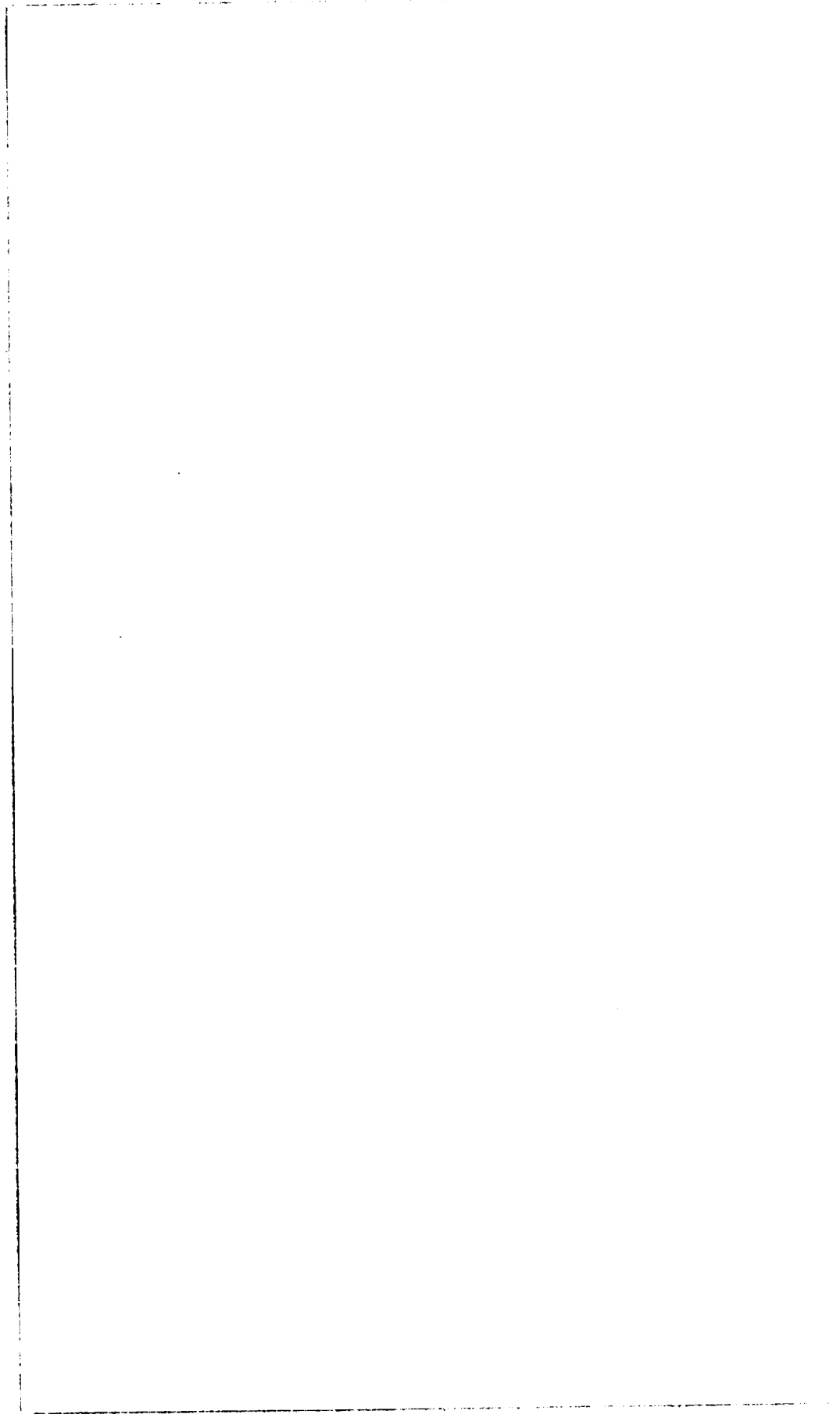
Configuration number	Geometry	Configuration	Source
C-86	Between axisymmetrical sections of hemisphere		Refs. 18, 37
C-87	Sphere to hemisphere		Ref. 41
C-88	Sphere to ellipsoid		Refs. C33, 41
C-89	Ellipsoid of arbitrary major and minor axes to rectangle, disk, cylinder, cone, or ellipsoid of arbitrary size and orientation		Ref. C33
C-90	From Moebius strip to itself		Ref. 43
C-91	Segment of finite width on toroid to exterior of toroid		Ref. 13
C-92	Toroidal band of finite width to exterior of toroid		Ref. 13

^cAvailable as general computer program only.

TABLE A-I.—TABLE OF REFERENCES FOR CONFIGURATION FACTORS—Concluded
(c) Factors for two finite areas—Concluded

Configu- ration number	Geometry	Configuration	Source
C-93	Exterior of toroid to itself		Ref. 13
C-94	Toroid of arbitrary size to rectangle, disk, cylinder, sphere, cone, ellipsoid, or toroid of arbitrary size and orientation		Ref. C33
C-95	Arbitrary polynomial of revolution to rectangle, disk, cylinder, sphere, cone, ellipsoid, toroid, or other arbitrary polynomial of revolution of arbitrary size and orientation (polynomials of fifth order or less)		Ref. C33
C-96	General plane polygon to any general plane polygon or two or more intersecting or adjoining polygons.		Ref. C44

^CAvailable as general computer program only.



PRECEDING PAGE BLANK NOT FILMED.

Appendix B

Enclosure Analysis Method of Gebhart

In chapter 3 the radiative exchange within a diffuse-gray enclosure was analyzed by the method originated by Poljak. A somewhat different viewpoint has been set forth by Gebhart and will be briefly presented here. Additional discussion can be found in references 1 to 3. The special utility in this formulation is that it yields coefficients that provide the fraction of energy emitted by a surface that is *absorbed* at another surface after reaching the absorbing surface by all possible paths. These coefficients can be of value in formulating some types of problems. After the derivation, a correspondence between the Gebhart and Poljak formulations will be indicated.

As in chapter 3, an enclosure having N diffuse-gray surfaces is considered, and the same restrictions are imposed here as in section 3.1.2. For a typical surface A_k the net energy loss is the emission from the surface minus the energy that is absorbed by the surface from all incident sources. The emitted energy is $A_k \epsilon_k \sigma T_k^4$. Let G_{jk} be the fraction of the emission from surface A_j that reaches A_k and is *absorbed*. This includes all the paths for reaching A_k ; that is, the direct path, paths by means of one reflection, and paths by means of multiple reflections. Thus $A_j \epsilon_j \sigma T_j^4 G_{jk}$ is the amount of energy emitted by A_j that is absorbed by A_k . A heat balance on A_k then gives

$$\begin{aligned}
 Q_k &= A_k \epsilon_k \sigma T_k^4 - (A_1 \epsilon_1 \sigma T_1^4 G_{1k} + A_2 \epsilon_2 \sigma T_2^4 G_{2k} + \dots + A_j \epsilon_j \sigma T_j^4 G_{jk} \\
 &\quad + \dots + A_k \epsilon_k \sigma T_k^4 G_{kk} + \dots + A_N \epsilon_N \sigma T_N^4 G_{Nk}) \\
 &= A_k \epsilon_k \sigma T_k^4 - \sum_{j=1}^N A_j \epsilon_j \sigma T_j^4 G_{jk}
 \end{aligned} \tag{B1}$$

The G_{kk} would generally not be zero since, even for a plane or convex surface, some of the emission from a surface will be returned to itself by reflection from other surfaces. Equation (B1) can be written for each surface; this will relate each of the Q 's to the surface temperatures in the enclosure. The G factors must now be found.

The quantity G_{jk} is the fraction of energy emitted by A_j that reaches A_k and is absorbed. The total emitted energy from A_j is $A_j \epsilon_j \sigma T_j^4$. The portion traveling by a direct path to A_k and then absorbed is $A_j \epsilon_j \sigma T_j^4 F_{j-k} \epsilon_k$, where for a gray surface, ϵ is equal to the absorptivity. All other radiation

from A_j arriving at A_k will first undergo one reflection. The emission from A_j that arrives at a typical surface A_n and is then reflected is $A_j \epsilon_j \sigma T_j^4 F_{j-n} \rho_n$. The fraction G_{nk} then reaches A_k and is absorbed. Then all the energy absorbed at A_k originating by emission from A_j is

$$A_j \epsilon_j \sigma T_j^4 F_{j-k} \epsilon_k + (A_j \epsilon_j \sigma T_j^4 F_{j-1} \rho_1 G_{1k} + A_j \epsilon_j \sigma T_j^4 F_{j-2} \rho_2 G_{2k} \\ + \dots + A_j \epsilon_j \sigma T_j^4 F_{j-k} \rho_k G_{kk} + \dots + A_j \epsilon_j \sigma T_j^4 F_{j-N} \rho_N G_{Nk})$$

Dividing this energy by the total emission from A_j gives the fraction

$$G_{jk} = F_{j-k} \epsilon_k + F_{j-1} \rho_1 G_{1k} + F_{j-2} \rho_2 G_{2k} \\ + \dots + F_{j-k} \rho_k G_{kk} + \dots + F_{j-N} \rho_N G_{Nk}$$

By letting j take on all values from 1 to N , the following set of equations is obtained:

$$\left. \begin{aligned} G_{1k} &= F_{1-k} \epsilon_k + F_{1-1} \rho_1 G_{1k} + F_{1-2} \rho_2 G_{2k} \\ &\quad + \dots + F_{1-k} \rho_k G_{kk} + \dots + F_{1-N} \rho_N G_{Nk} \\ G_{2k} &= F_{2-k} \epsilon_k + F_{2-1} \rho_1 G_{1k} + F_{2-2} \rho_2 G_{2k} \\ &\quad + \dots + F_{2-k} \rho_k G_{kk} + \dots + F_{2-N} \rho_N G_{Nk} \\ G_{Nk} &= F_{N-k} \epsilon_k + F_{N-1} \rho_1 G_{1k} + F_{N-2} \rho_2 G_{2k} \\ &\quad + \dots + F_{N-k} \rho_k G_{kk} + \dots + F_{N-N} \rho_N G_{Nk} \end{aligned} \right\} \quad (\text{B2})$$

Equations (B2) can be solved simultaneously for G_{1k} , G_{2k} , . . . , G_{Nk} . Equation (B1) then relates Q_k to the surface temperatures. The k index in equations (B1) and (B2) can correspond to any of the surfaces in the enclosure.

At the end of section 3.3.2, it was mentioned that matrix inversion can be applied to equations (3-19) to yield each Q as a weighted sum of T^4 's. The coefficients obtained by the matrix inversion thus correspond to those in equation (B1). This shows the correspondence between the method described here and that in chapter 3.

REFERENCES

1. GEBHART, B.: Unified Treatment for Thermal Radiation Transfer Processes—Gray, Diffuse Radiators and Absorbers. Paper No. 57-A-34, ASME, Dec. 1957.
2. GEBHART, B.: Heat Transfer. McGraw-Hill Book Co., Inc., 1961, pp. 117-122.
3. GEBHART, B.: Surface Temperature Calculations in Radiant Surroundings of Arbitrary Complexity—for Gray, Diffuse Radiation. Int. J. Heat Mass Transfer, vol. 3, no. 4, 1961, pp. 341-346.

Appendix C

Conversion Factors

Tables of conversion factors between the mks and other common systems of units are given in tables C-I to C-III of this appendix.

REFERENCE

1. MECHTLY, E. A.: The International System of Units. Physical Constants and Conversion Factors. NASA SP-7012, 1964.

TABLE C-1.—CONVERSION FACTORS FOR LENGTHS

	Mile (mi)	Kilometer (km)	Meter (m)	Foot (ft)	Inch (in.)	Centimeter (cm)	Millimeter (mm)	Micron (μm)	Millimicron ($\text{m}\mu\text{m}$)	Angstrom (\AA)
1 mile =	1	1.609	1609	5280	6.336×10^4	1.609×10^5	1.609×10^6	1.609×10^8	1.609×10^{12}	1.609×10^{13}
1 kilometer =	0.6214	1	10^3	3.281×10^3	3.937×10^4	10^5	10^6	10^8	10^{12}	10^{13}
1 meter =	6.214×10^{-4}	10^{-3}	1	3.281	39.37	10^2	10^3	10^6	10^9	10^{10}
1 foot =	1.894×10^{-4}	3.048×10^{-4}	0.3048	1	12	30.48	3.048×10^3	3.048×10^6	3.048×10^9	3.048×10^9
1 inch =	1.578×10^{-5}	2.540×10^{-5}	2.540×10^{-2}	8.333×10^{-3}	1	2.540	25.40	2.540×10^4	2.540×10^7	2.540×10^8
1 centimeter =	6.214×10^{-6}	10^{-5}	10^{-2}	3.281×10^{-2}	0.3937	1	10	10^4	10^7	10^8
1 millimeter =	6.214×10^{-7}	10^{-6}	10^{-3}	3.281×10^{-3}	0.03937	10^{-1}	1	10^3	10^6	10^7
1 micron =	6.214×10^{-10}	10^{-9}	10^{-6}	3.281×10^{-6}	3.937×10^{-5}	10^{-4}	10^{-3}	1	10^3	10^4
1 millimicron (nanometer) =	6.214×10^{-13}	10^{-12}	10^{-9}	3.281×10^{-9}	3.937×10^{-8}	10^{-7}	10^{-6}	10^{-2}	1	10
1 angstrom =	6.214×10^{-14}	10^{-13}	10^{-10}	3.281×10^{-10}	3.937×10^{-9}	10^{-8}	10^{-7}	10^{-4}	10^{-1}	1

TABLE C-II.—CONVERSION FACTORS FOR ENERGY UNITS^a

	Kilowatt-hour (kW-hr)	British thermal unit (Btu)	Gram-calorie (g-cal)	Joule (J)	Erg	Electron volt (eV)
1 kilowatt-hour =	1	3412	8.598×10^5	3.600×10^6	3.600×10^{13}	2.247×10^{23}
1 British thermal unit ^b =	2.931×10^{-4}	1	252.0	1055	1.055×10^{10}	6.585×10^{21}
1 gram-calorie ^b =	1.163×10^{-6}	3.968×10^{-3}	1	4.187	4.187×10^7	2.614×10^{19}
1 joule (W-sec) =	2.778×10^{-7}	9.479×10^{-4}	0.2388	1	10^7	6.242×10^{18}
1 erg (dyne-cm) =	2.778×10^{-14}	9.479×10^{-11}	2.388×10^{-8}	10^{-7}	1	6.242×10^{11}
1 electron volt =	4.450×10^{-28}	1.519×10^{-22}	3.826×10^{-20}	1.602×10^{-19}	1.602×10^{-12}	1

^a Values are taken from ref. 1.
^b Based on International Steam Table.

TABLE C-III. — CONVERSION FACTORS FOR ENERGY FLUX

	cal/(sec)(cm ²)	Btu/(hr)(ft ²)	W/m ²	erg/(sec)(cm ²)
1 cal/(sec)(cm ²) =	1	1.329 × 10 ⁴	4.187 × 10 ⁴	4.187 × 10 ⁷
1 Btu/(hr)(ft ²) =	7.525 × 10 ⁻⁵	1	3.152	3.152 × 10 ³
1 W/m ² =	2.388 × 10 ⁻³	0.3174	1	10 ³
1 erg/(sec)(cm ²) =	2.388 × 10 ⁻⁸	3.174 × 10 ⁻⁴	10 ⁻³	1

* Based on International Steam Table.

Index

- Absorption efficiency, 166
- Adiabatic surface, 150
- Algebra, configuration factor, 30
- Approximate separable kernel, 99
- Areas of enclosure, 67
- Band energy approximation, 156
- Black enclosure, 7, 59
- Blackbody enclosure, 95
- Bundle, energy, 4, 191
- Cavity
 - conical, 206, 207
 - spherical, 104
 - wedge, 161
- Combined modes, 4, 217, 232
 - computer programs, 237
- Combined radiation-conduction
 - coupled, 218
 - uncoupled, 217
- Concentric cylinders
 - diffuse, 114
 - specular, 112, 114
- Concentric spheres
 - diffuse, 75, 114
 - specular, 112, 114
- Conditional probability distribution, 186
- Conduction, 217
- Configuration factors, 7, 12
 - algebra, 30
 - contour integration, 46
 - crossed-string method, 43
 - differential area to differential area, 13
 - differential to finite area, 19, 47
 - differentiation, 55
 - in enclosures, 39
 - errors, 34
 - finite area to finite area, 26, 52
 - Monte Carlo method for, 204
 - reciprocity, 14, 21, 27, 35, 123
 - reciprocity, table, 29
 - specular surfaces, 117
 - table of references, 241, 244
- Conical cavity, 206, 207
- Contour integration, 46
- Convection, 227
- Convergence
 - in Monte Carlo solutions, 209
 - in numerical integration, 226
- Conversion factors, table, 279
- Coupled modes, 218
- Crossed-string method, 43
- Cumulative distribution function, 184
- Curved specular surface, 139
- Differential element
 - configuration factor, 13, 19
- Differentiation of configuration factors, 55
- Diffuse
 - enclosures, 67, 90
 - surfaces, 133
- Diffuse configuration factors, table, 241, 244
- Diffuse-gray
 - enclosures, 90
 - surfaces, 67
- Diffuse-nongray, 147, 149
- Diffuse-spectral surfaces, 149
- Directional surfaces, 5, 162
- Directional-gray surfaces, 162
- Directional-spectral surfaces, 169
- Disk, 22, 32
- Electromagnetic theory, 151
- Enclosure, 1
 - black, 7, 39, 59
 - gray-diffuse, 67, 70
 - ideal, 2
 - nonideal, 3
 - radiation exchange, 1, 7
 - with diffuse spectral surfaces, 149
 - with specular surfaces, 110
 - with specular and diffuse surfaces, 129, 144
- Enclosure equations, table, 90, 114
- Energy balance
 - diffuse-gray surface, 71
 - spectral surface, 150
- Energy bundle, 191
- Energy exchange
 - between differential areas, 10
 - between differential and finite area, 21
 - between finite areas, 29
 - summary table, 29

- Environment temperature, 92
- Errors
 - configuration factors, 34
 - Monte Carlo calculations, 188
- Exchange factors, 137, 205
- Fin, 219, 223, 235
- Fin efficiency, 221
- Finite area configuration factors, 26, 52
- Gebhart's method, 71, 277
- Geometric configuration factor, 13
- General computer programs, 237
- Gray surfaces, 67
- Grooved surfaces
 - diffuse, 168
 - specular, 121, 168
 - directional, 164, 168
- Heat flux specified on all surfaces, 89
- Herschel, Sir William, 3
- Hole, radiation from, 94
- Hottel, Hoyt C., 43, 70
 - crossed-string method, 43
- Images, 115
- Incoming radiant energy, 71
- Insulated surface, 67, 150
- Integral equation solution methods
 - numerical, 97
 - separable kernel, 99
 - Taylor series, 103
 - variational method, 102
- Integro-differential equations, 4
- Intensity, 9
- Interchange, 10
- Interference, 5
- Kernel, 86
- Laplace equation, 181
- Lunar radiation, 4, 144
- Marginal probability distribution, 186
- Markov chain, 180
- Matrix inversion, 81
- Monte Carlo
 - configuration factors, 204
 - directional and spectral surfaces, 191, 208
 - energy exchange, 191
 - table of relations, 198
- Net radiation method
 - finite areas, 70
 - infinitesimal areas, 83
 - specular and diffuse surfaces, 129
- Newton-Raphson method, 226
- Nondiffuse surfaces, 162
- Nongray surfaces, 153
- Nonisothermal surfaces, 84
- Nonlinear problems, 218
- Nonlinear simultaneous equations, 226
- Notation
 - general, 4
 - specular configuration factors, 117
- Numerical integration, 97
- Outgoing radiant energy, 71, 79
- Parallel heat transfer modes, 213
- Parallel plates
 - diffuse, 73, 114, 151
 - directional gray, 162
 - gray, 73, 95, 114
 - spectral, 151
 - specular, 110, 117
- Partial view, 119
- Prescribed surface heat flux, 89
- Prescribed surface temperature, 77, 86
- Photon bundle, 191
- Poljak, G.
 - net radiation method, 70, 71
- Probability distribution
 - conditional, 186
 - cumulative, 184
 - marginal, 186
 - normal, 193
- Probability density function, 183
- Radiosity, 72
- Random numbers, 183, 187
- Random number generation, 187
- Random walk, 180
- Ray tracing, 115
- Reciprocity
 - configuration factors, 14, 21, 29
 - specular exchange, 123, 128
- Reflectivity
 - diffuse, 68
 - specular, 110, 114
- Roughness, 168
- Restrictions for enclosure theory, 67
- Semigray approximation, 160
- Separable kernel, 99
- Series heat transfer modes, 213
- Solar, 3, 148, 161
- Solid angle, 10, 13
- Spectrally selective surfaces, 3, 69, 148
- Specular and diffuse enclosure, 129
- Specular surfaces, 69, 110
 - configuration factors, 117, 123
 - curved, 139
 - exchange factors, 137, 141
 - radiation between, 117

- Specular tube, 140
Spherical cavity, 104
Standard deviation, 190
Stratified sampling, 190
Strip, 16
Sun, 11
Surfaces
 gray, 67, 85, 109
 diffuse, 67, 85
 nongray, 153
 nondiffuse, 162
 of enclosure, 67
 specular, 109
Tables
 configuration factor references, 241, 244
 configuration factor relations, 29
 conversion factors, 279
 energy exchange in simple enclosures,
 114
 Monte Carlo relations, 198
Taylor series, 103
Temperature of heated radiating tube, 91
Total energy, 149
Transients, 4, 68, 113, 222
Tube
 radiating, 91, 140
 radiation and convection, 227
 radiation, convection, and conduction,
 233
 specular, 140
Tungsten, 151
Uncoupled modes, 217
Vacuum bottle, 112
Variance, 189
Variational method, 102
Wedge groove, 17, 24, 161